

Supplementation Strategies for Tuning Glycosylation of Monoclonal Antibodies and Enhancing  
Growth in Mammalian Cell Culture by Omics Analysis

by

Eric John McQuillan Blondeel

A thesis

presented to the University of Waterloo

in fulfillment of the

thesis requirements for the degree of

Doctor of Philosophy

in

Chemical Engineering

Waterloo, Ontario, Canada, 2018

©Eric John McQuillan Blondeel 2018

## Examining Committee Membership

The following served on the Examining Committee for this thesis. The decision of the Examining Committee is by majority vote.

External Examiner

Dr. Mario Jolicoeur

Professor

École Polytechnique de Montréal

Supervisor(s)

Dr. Marc Gordon Aucoin

Associate Professor

Internal Member

Dr. Hector Budman

Professor

Internal-external Member

Dr. Brian Dixon

Professor

Other Member(s)

Dr. Maud Gorbet

Associate Professor

## **Author's Declaration**

This thesis consists of material all of which I authored or co-authored: see Statement of Contributions included in the thesis. This is a true copy of the thesis, including any required final revisions, as accepted by my examiners.

I understand that my thesis may be made electronically available to the public.

## Statement of Contributions

The majority of the work presented in this thesis has been performed either directly by me, or directed by me as the primary researcher.

The work presented in Chapter 3 is an accepted manuscript published in the Journal of Biotechnology entitled, “An omics approach to rational feed: Enhancing growth in CHO cultures with NMR metabolomics and 2D-DIGE proteomics.” and is co-authored with Raymond Ho, Steffen Schulze, Dr. Stanislav Sokolenko, Simon R. Guillemette, Dr. Igor Slivac, Dr. Yves Durocher, Dr. Guy J. Guillemette, Dr. Brendan J. McConkey, Dr. David Chang, and Dr. Marc G. Aucoin. While I am the primary author of this manuscript, the research represents two complementary experiments conducted in collaboration with the McConkey and Durocher laboratories as part of the NSERC MAbNet antibody research network. The metabolomics experiments and necessary culturing was performed by myself, Steffen Schulze, Dr. Stanislav Sokolenko, and Simon Guillemette, while the proteomics experiments and necessary culturing was performed by Raymond Ho and Dr. Igor Slivac.

The work presented in Chapter 4 is an accepted manuscript published in the Journal of Biotechnology entitled, “Tuning a MAb glycan profile in cell culture: Supplementing N-acetylglucosamine to favour G0 glycans without compromising productivity and cell growth.” and is co-authored with Dr. Katrin Braasch, Thomas McGill, Dr. David Chang, Christina Engel, Dr. Maureen Spearman, Dr. Michael Butler, and Dr. Marc G. Aucoin. While I am the primary author of this manuscript, this research represents an experiment conducted in collaboration with the Butler laboratory as part of the NSERC MAbNet antibody research network. Myself and Thomas McGill performed the experiment and necessary culturing, while Dr. Katrin Braasch and Dr. Maureen Spearman performed intracellular metabolomic analysis of nucleotide sugar

precursors and glycan analysis of the EG2 antibody product from samples prepared by Thomas and myself. Christina Engel replicated parts the experiment on an alternative CHO cell platform.

The work presented in Chapter 5 is a manuscript submitted to the journal *Biotechnology Advances* entitled, “Supplementing Glycosylation: A Review of Applying Nucleotide-Sugar Precursors to Growth Medium to Affect Therapeutic Recombinant Protein Glycan Profiles.” and is co-authored with Dr. Marc G. Aucoin. I am the primary author of this manuscript reviewing work by several authors of this field.

## Abstract

Two fundamental objectives of bioprocess engineering are to increase productivity and improve product quality. Glycosylation is a critical and variable factor in the quality of several therapeutic proteins, particularly those with immune-system interactions such as monoclonal antibodies (mAbs). In this thesis, supplementation of nutrients to growth medium of CHO<sup>1A7</sup> mammalian cell cultures are examined towards enhancing cell growth, by increasing peak cell density, and improving product quality, by tuning glycosylation of EG2-hFc heavy-chain camelid antibodies. Targeted profiling via 1D-<sup>1</sup>H-NMR metabolomics and differential expression analysis via 2D-DIGE proteomics, elucidate factors to create a nutrient cocktail to enhance culture growth. Eight target nutrients corresponding with five identified metabolic systems for CHO cells including anaplerotic TCA-replenishment; NADH/NADPH replenishment; tetrahydrofolate cycle C1 cofactor conversions; limitations to lipid synthesis; and redox modulation; resulted in a ~75% improvement to peak cell densities. Towards improving product quality, nucleotide-sugar precursors, capable of shifting glycan distributions were supplemented to growth medium to tune glycosylation of EG2-hFc towards a single G0 glycoform. Growth inhibition from glucosamine-based precursors was mitigated given *a priori* knowledge from metabolomic analysis of the system – identifying cytosolic acetyl-CoA as a sensitive metabolic pool for CHO<sup>1A7</sup> cell growth. Additional nucleotide-sugar precursor nutrients were examined to better resolve conflicting reports of effects to glycan distributions. These conflicts are subsequently attributed to five key factors: differences across cell platforms; differences between glycan sites of expressed proteins; the fermentation and sampling timeline; glutamine levels; finally, no standardized metrics for reporting shifts in glycan distributions with respect to controls.

## Acknowledgements

I would like to express thanks to the University of Waterloo and the Department of Chemical Engineering for the opportunity to pursue graduate studies and complete my doctoral program. I would also like to thank the Government of Canada by way of NSERC and the MAbNet antibody research network for supporting my research. A major thank-you to my co-authors, as well as the Butler Lab, the McConkey Lab, the Durocher Lab, and members of MAbNet for their collaboration, help, and above all friendship. I feel privileged to be counted among these colleagues. I would further like to express my thanks to Andrew and Margaret Stevens for their scholarship to the chemical engineering department that supported me financially during my research.

An enormous thank you to my supervisor Professor Marc Aucoin for taking a chance on me to join his research group, remaining patient, and not giving up on me. Thank you for your guidance and support and always doing your best to help me. Thanks also to all my colleagues in the Aucoin Lab, Steve, Stan, Andreas, Steffen, Sandi, Megan, Jian, Zen-Zen, Altamash, and Jann – thanks for putting up with me.

Thank you to my PhD committee members Dr. Maud Gorbet, Dr Hector Budman, Dr. Brian Dixon, and Dr. Mario Jolicoeur for evaluating my thesis, and my suitability to receive a doctoral degree.

Thank you to Dr. Brendan MacDonald, Dr. Thorsten Dieckmann, Dr. Bo Cui, Dr. Bernie Dunker, for all your help, support, and encouragement; I wouldn't be here without it. I would also like to thank Dr. Marc Gibson, Dr. John Dick, and Dr. Morteza Ahmadi for commiserating with me and encouraging me to power through the hardest stretches.

Thank you to Velocity, Dean Pearl Sullivan, Jay Shah, Larry Smith, Mike Kirkup and the Faculty of Engineering for encouraging me to reach beyond my grasp. Thanks as well to Y Combinator, and my group partners Geoff Ralston and Tim Brady for encouraging me to grasp further still.

Thank you to my partner Jen for sticking with me and supporting my dreams; Mom, Dad, and my brothers for all their support and love. Thank you to all my friends who have suffered through years of pretending to listen to what my research is about.

Thanks to Moufeed, my best friend and partner on the wild adventure of the past 4 years. Thanks also to Christian, and the rest of the ExVivo gang.

Also, thank you to Jan Venne and the UWaterloo NMR Facility, as well as the administrative and support staff at the Department of Chemical Engineering: Judy, Rose, Liz, Ingrid, Bert, Tom, Ralph and Rick for helping me whenever I needed it.



## **Dedication**

To whomever should read this, I may no longer even be living, but I invite you to join me in a great conversation that was started before I got here, and will continue long after both of us have left.

Hopefully I've said something useful...

## Table of Contents

Examining Committee Membership .....	ii
Author's Declaration.....	iii
Statement of Contributions .....	iv
Abstract .....	vi
Acknowledgements.....	vii
Dedication .....	ix
Table of Contents .....	x
List of Figures .....	xv
List of Tables .....	xix
List of Abbreviations .....	xxiii
Chapter 1 Introduction.....	1
1.1 Objective of Research.....	4
1.2 Hypothesis of Research .....	5
Chapter 2 Literature Review.....	6
2.1 Antibodies <i>in vivo</i> .....	6
2.2 Antigen Binding .....	8
2.2.1 Monoclonal Antibodies (mAbs).....	9
2.2.2 Antibody Fragments and Fusion Proteins .....	10
2.3 Glycosylation.....	11
2.3.1 Eukaryotic Glycosylation .....	12
2.3.2 N-linked Glycosylation .....	13
2.3.3 Antibody Fc & Immune Effector Function .....	17

2.3.4	N-Glycoform & Immune Effector Function.....	19
2.3.5	O-linked Glycosylation .....	19
2.4	Glycan Analysis .....	20
2.5	Cell Culture Platforms and Glycoengineering.....	21
2.5.1	Mammalian.....	22
2.5.2	Prokaryotes .....	24
2.5.3	Yeast.....	25
2.5.4	Insect .....	26
2.6	Omics Methods towards Enhancing Bioprocesses.....	27
2.6.1	Proteomics .....	29
2.6.2	Metabolomics .....	31
2.6.3	Applications of Omics to Cell Culture .....	37
2.6.4	Quenching & Extraction.....	43
Chapter 3	An omics approach to rational feed: Enhancing growth in CHO cultures with NMR metabolomics and 2D-DIGE proteomics .....	46
3.1	Overview .....	46
3.2	Introduction .....	47
3.3	Materials & Methods.....	49
3.3.1	Cell Line .....	49
3.3.2	2D-DIGE Proteomics Experiments .....	50
3.3.3	NMR Metabolomics Experiments .....	55
3.4	Results .....	56
3.4.1	2D DIGE Proteomics Analysis.....	57
3.4.2	Cell Function Grouping.....	60

3.4.3	1D- <sup>1</sup> H-NMR Metabolomics Analysis .....	61
3.5	Discussion .....	68
3.5.1	Omics Methods as Tools for Rational Feed Design .....	68
3.5.2	Anaplerotic TCA Metabolism Limitations.....	68
3.5.3	Tetrahydrofolate Conversions and NADPH Regeneration.....	71
3.5.4	Limitations to Lipid Synthesis.....	72
3.5.5	Redox Modulation .....	73
3.6	Conclusions .....	74
Chapter 4	Tuning a MAb glycan profile in cell culture: Supplementing N-acetylglucosamine to favour G0 glycans without compromising productivity and cell growth.....	76
4.1	Overview .....	76
4.2	Introduction .....	78
4.3	Materials & Methods.....	80
4.3.1	Cell Culture .....	80
4.3.2	Growth Medium & Supplemented Nutrients.....	81
4.3.3	Glycan Analysis .....	81
4.3.4	mAb Quantification.....	82
4.3.5	Extracellular Metabolite Profiling.....	82
4.3.6	Intracellular Nucleotide and Nucleotide-Sugar Analysis .....	82
4.4	Results .....	83
4.4.1	Growth Effects GlcN vs. GlcNAc .....	86
4.4.2	Glycosylation Effects GlcN vs. GlcNAc.....	87
4.4.3	Glycosylation Effects GlcNAc .....	88
4.4.4	Growth and Productivity Effects from GlcNAc Supplementation .....	89

4.4.5	Intracellular Nucleotides and Nucleotide-Sugar Pools.....	92
4.5	Discussion .....	93
4.5.1	Simple Method for Affecting Glycan Distributions .....	93
4.5.2	Diversity of Reported Glycan Effects from Glucosamine.....	94
4.5.3	Growth Limitations from Glucosamine.....	95
4.6	Conclusions .....	97
Chapter 5	Supplementing Growth and Glycoform.....	99
Chapter 6	Supplementing Glycosylation: A Review of Applying Nucleotide-Sugar Precursors to Growth Medium to Affect Therapeutic Recombinant Protein Glycoform Distributions .....	101
6.1	Overview .....	101
6.2	Introduction .....	103
6.3	Glycosylation.....	105
6.3.1	Nucleotide-Sugar Metabolism.....	105
6.3.2	N-Linked Glycosylation .....	108
6.3.3	Microheterogeneity.....	109
6.4	Controlling Glycosylation by Supplementation .....	109
6.4.1	Key Factors Impacting Supplementation Results.....	111
6.4.2	Glycoform Distribution Indexes.....	115
6.4.3	Supplementation of Nucleotide-Sugar Precursors.....	117
6.5	Glycoforms: Bioefficacy and Functionality .....	133
6.5.1	Immune Effector Functions for Antibodies.....	134
6.5.2	Glycoforms and Antibody Immune Effector Functions .....	135
6.5.3	Immunogenic Glycoforms.....	141

6.6	Conclusions .....	142
	Conclusions & Recommendations .....	144
	References .....	148
	Appendix A – Chapter 3 Supplementary Data .....	163
	Appendix B – Chapter 4 Supplementary Data.....	168
	Appendix C – Chapter 6 Supplementary Data.....	172

## List of Figures

Figure 1 – Basic immunoglobulin (Ig) structure.....	7
Figure 2 – Antibodies activating two common immune effector functions to destroy an EGFR presenting cancer cell; antibody dependent cell cytotoxicity (ADCC), and complement dependent cytotoxicity (CDC). .....	8
Figure 3 – Eukaryotic 14 sugar N-linked precursor oligosaccharide .....	13
Figure 4 – Eukaryotic N-glycosylation in mammalian cells .....	15
Figure 5 – Examples of diversity of potential glycoforms .....	16
Figure 6 – Most common human N-glycoforms for IgG1&2 in blood serum according to Flynn et al. (2010) .....	16
Figure 7 – Normal phase HPLC elution profile of glycans cleaved from mAb EG2-hFc.....	21
Figure 8 – Immunogenic N-glycan moieties Neu5Gc and $\alpha$ -gal, from rodent-derived cells .....	23
Figure 9 – Prokaryote N-glycosylation from glycoengineered <i>E. coli</i> .....	25
Figure 10 – Hyper-mannosylated yeast N-glycosylation.....	26
Figure 11 – Paucimannosidic N-glycosylation in insect cells .....	27
Figure 12 – Convoluted Spectral Peaks 1D- <sup>1</sup> H-NMR .....	35
Figure 13 – Targeted Profiling of Convoluted 1D- <sup>1</sup> H-NMR Spectra by Chenomx Software.....	35
Figure 14 – Quantification by Metabolites by Chenomx Software .....	36
Figure 15 – Representative monochrome image of a 2D-DIGE Gel. CHO <sup>BRI</sup> -1 labeled with Cy5 and CHO <sup>BRI</sup> -1A7-1 labeled with Cy3.....	58
Figure 16 – Anaplerotic TCA and mitochondrial shuttle metabolism, which contribute to replenishing cytosolic acetyl-CoA, NAD <sup>+</sup> , and NADPH. ....	63
Figure 17 – Tetrahydrofolate (THF) C1 cofactors replenishing NADPH from serine, while producing glycine and formate, by cycling the THF intermediates between different oxidation states.....	64

Figure 18 – Lipid synthesis requires nutrients such as choline and several precursors observed in this work to be excreted, including phosphocholine, cytidine, glycerol and ethanol. .....	65
Figure 19 – Fully depleted nutrients under normal culture conditions (solid lines) and following additional supplementation (dashed lines) at 0 hrs (circle) and at 50 hrs (triangle) as per Table 11. ....	67
Figure 20 – Culture growth profile of CHOBRI-1A7 cells in bioreactor and flask-scale cultivations. ....	67
Figure 21 – Intracellular nucleotide sugar metabolic pathways utilizing glucose or supplemented GlcN or GlcNAc. ....	85
Figure 22 – Growth and viability of CHO cells severely impacted during supplementation of 7.5 mM glucosamine (GlcN), compared to only marginal impacts to growth and viability during supplementation of 7.5 mM N-acetylglucosamine (GlcNAc). Duplicate lines represent duplicate flasks. ....	87
Figure 23 – A similar shift to less complex glycoforms is observed from supplementing either glucosamine (GlcN) or N-acetylglucosamine (GlcNAc). ....	88
Figure 24 – Increasing the concentration of N-acetylglucosamine (GlcNAc) increases the glycan shift towards G0 glycoforms. ....	89
Figure 25 – Increasing the concentration of N-acetyleglucosamine (GlcNAc) supplemented to cultures reduces late-exponential cell growth with marginal impact to viability. Duplicate lines represent duplicate flasks. ....	90
Figure 26 – A) Final protein titers of EG2-hFc from cultures supplemented with GlcNAc. B) Final acetate concentrations from cultures supplemented with GlcNAc. Error bars represent the standard deviation between duplicate flasks. ....	91
Figure 27 – Nucleotide and nucleotide-sugar ‘per-cell’ intracellular concentrations from quenched cell samples taken at 72hrs from cultures supplemented with GlcNAc. Error bars represent the standard deviation between duplicate flasks. ....	92
Figure 28 – Glycoform distribution for EG2-hFc harvested from a bioreactor fermentation of CHO <sup>BRI</sup> -1A7 grown in BioGro-CHO medium supplemented with the cocktail of nutrients established in Chapter 3. ....	99



Figure 29 – Duplicate flasks of CHO <sup>BRI</sup> -1A7 cultured with a cocktail of supplements to improve growth, detailed in Chapter 3, as well as supplements of GlcNAc, which affect glycoform distribution, detailed in Chapter 4.....	100
Figure 30 – Metabolic pathways for the synthesis and transport of intracellular nucleotide sugars utilizing glucose (Glc), galactose (Gal), glucosamine (GlcN), acetylglucosamine (GlcNAc), and acetylmannosamine (ManNAc), towards N-glycosylation in mammalian cells. This includes the assembly of dolichol-14-sugar oligosaccharide and co-translational binding for N-glycosylation of proteins beginning in the cytosol and occurring in ER, followed by the sculpting of further monosaccharide modifications in the Golgi by pH-dependent heteromeric glycosyltransferases. ..	108
Figure 31 – A monoclonal antibody glycan distribution segmented to demonstrate the glycosylation index formulae. In each case the proportion of the glycan distribution with a particular moiety (i.e. sialic acid, terminal galactose, etc.) is divided by the proportion that could have received that particular moiety, with respect to the sequence of glycosyltransferase enzymes acting on the protein undergoing glycosylation.....	117
Figure 32 – Comparison of glycoform shifts reported for experiments employing the supplementation of glucosamine (GlcN), its acetylated form acetyl-glucosamine (GlcNAc), and the nucleoside uridine (Urd), to affect N-linked glycoforms of recombinant glycoproteins produced in mammalian cell cultures. ....	121
Figure 33 – Comparison of glycoform shifts reported for experiments employing the supplementation of glucosamine (GlcN), its acetylated form acetyl-glucosamine (GlcNAc), and the nucleoside uridine (Urd), to affect N-linked glycoforms of recombinant glycoproteins produced in mammalian cell cultures. ....	126
Figure 34 – Comparison of glycoform shifts reported for experiments employing the supplementation of acetyl-mannosamine (ManNAc), and the nucleoside cytidine (Cyt), to affect N-linked glycoforms of recombinant glycoproteins produced in mammalian cell cultures. ....	131
Figure 35 – Complete set of nutrients and metabolites tracked by 1D-1H-NMR under normal culture conditions (solid lines) and following additional supplementation (dashed lines) in batch (circle) and fed-batch (triangle).....	167
Figure 36 – Time course imaging of cell growth under GlcN and GlcNAc supplementation conditions.....	169

Figure 37 – Growth rate comparison of CHO-K1-CC1-61 cells supplemented with 7.5 mM GlcN & GlcNAc, demonstrating that the negative growth effect of glucosamine supplementation, as well as the lack of negative growth effect from GlcNAc supplementation, is independent of the CHO<sup>BR1</sup> cell line utilized in Chapter 4. ... 170

## List of Tables

Table 1 – N-Glycan distribution of IgG1&2 in human blood serum according to Flynn et al. (2010).....	17
Table 2 – Elution time, glucose units, and major glycan structures of Figure 6 .....	21
Table 3 – Examples of omics cellular domains .....	28
Table 4 – Differentially expressed proteins after transfection of CHO <sup>BRI</sup> cells to stably express EG2-hFc heavy-chain mAb, as identified by LC-MS/MS.....	59
Table 5 – Functional annotation analysis in DAVID enriched functionally related gene groups, associated with differentially expressed proteins. An enrichment score was determined by a geometric mean of all the enrichment p-values of each annotation term in the group followed by a minus log transformation applied on the averaged p-values. The enrichment score is a relative score used to rank overall importance of annotation term groups. ....	61
Table 6 – Nutrients supplemented to production growth medium with respect to their approximate initial concentrations (% increase).....	66
Table 7 – Comparison of glycoform shifts and differences between reported experiments for the supplementation of glucosamine (GlcN), its acetylated form acetyl-glucosamine (GlcNAc), and the nucleoside uridine (Urd), towards expanding intracellular nucleotide-sugar pools of UDP-GlcNAC in cultured mammalian cells to affect N-linked glycoforms of recombinant glycoproteins. Experimental differences reported include: Supplementation cocktails and concentrations with multiple bullet-points representing separate flask or bioreactor conditions; The cell line utilized and the lineage of that cell line where reported; The protein being expressed and whether it is a mutant variant or fusion; The bioprocess scale, time of supplementation, and time of harvest; The amount of glutamine (Gln) utilized in the growth medium. ....	118
Table 8 – Comparison of glycoform shifts and differences between reported experiments for the supplementation of galactose (Gal), the nucleoside uridine (Urd), and the enzyme cofactor manganese (Mn <sup>2+</sup> ), towards expanding intracellular nucleotide-sugar pools of UDP-galactose in cultured mammalian cells and affecting N-linked glycoforms of recombinant glycoproteins. Experimental differences reported include: Supplementation cocktails and concentrations with multiple bullet-points representing separate flask or bioreactor conditions; The cell line utilized and the lineage of that cell line where reported; The protein being expressed and whether it is a mutant variant or fusion; The bioprocess scale, time of supplementation, and time of harvest; The amount of glutamine (Gln) utilized in the growth medium.....	124

Table 9 – Comparison of glycoform shifts and differences between reported experiments for the supplementation of the acetylated amine sugar N-acetylmannosamine (ManNAc), and the nucleoside cytidine (Cyt), towards expanding intracellular nucleotide-sugar pools of CMP-NeuAc in cultured mammalian cells and affecting N-linked glycoforms of recombinant glycoproteins. Experimental differences reported include: Supplementation cocktails and concentrations with multiple bullet-points representing separate flask or bioreactor conditions; The cell line utilized and the lineage of that cell line where reported; The protein being expressed and whether it is a mutant variant or fusion; The bioprocess scale, time of supplementation, and time of harvest; The amount of glutamine (Gln) utilized in the growth medium.....	129
Table 10 – Therapeutic efficacy of monoclonal antibodies (mAbs) and immune effector function (IEF) with respect to fucosylation of N-glycans. A biantennary glycan with a circled region is provided to indicate the moiety. IEFs include antibody dependent cell cytotoxicity (ADCC), complement dependent cell cytotoxicity (CDC), as well as binding to the immune antibody receptor FcγRIIIa.....	136
Table 11 – Therapeutic efficacy of monoclonal antibodies (mAbs) and immune effector function (IEF) with respect to N-glycans possessing the bisecting N-acetylglucosamine (GlcNAc) moiety. A biantennary glycan with a circled region is provided to indicate the moiety. IEFs include antibody dependent cell cytotoxicity (ADCC).....	138
Table 12 – Therapeutic efficacy of monoclonal antibodies (mAbs) and immune effector function (IEF) with respect to galactosylation of N-glycans. A biantennary glycan with circled regions is provided to indicate the moieties. IEFs include antibody dependent cell cytotoxicity (ADCC), and complement dependent cell cytotoxicity (CDC).....	139
Table 13 – Therapeutic efficacy of monoclonal antibodies (mAbs) and immune effector function (IEF) with respect to sialylation of N-glycans. A biantennary glycan with circled regions is provided to indicate the moiety. IEFs include antibody dependent cell cytotoxicity (ADCC), complement dependent cell cytotoxicity (CDC), anti-inflammatory properties, as well as protein serum half-life (serum $t_{1/2}$ ).....	140
Table 14 – Therapeutic efficacy of monoclonal antibodies (mAbs) and immune effector function (IEF) with respect to high-mannose N-glycans. Two N-glycans are provided to describe this glycoform. IEFs include binding to the immune antibody receptor FcγRI, complement dependent cell cytotoxicity (CDC), and protein serum half-life (serum $t_{1/2}$ ).....	141
Table 15 – Expanded 2D-DIGE proteomics data of CHO cells expressing EG2-hFc .....	163

Table 16 – Comparison of glycoform shifts and differences between reported experiments for the supplementation of glucosamine (GlcN), its acetylated form acetyl-glucosamine (GlcNAc), and the nucleoside uridine (Urd), towards expanding intracellular nucleotide-sugar pools of UDP-GlcNAc in cultured mammalian cells to affect N-linked glycoforms of recombinant glycoproteins. N-linked glycoforms of recombinant glycoproteins. Glycoform shifts are reported as %-shifts in indices of mannosylation (MI), antennarity (AI), fucosylation (FI), galactosylation (GI), and sialylation (SI) (as per Equations 1-5, Figure 28) relative to reported control culture glycoforms. Experimental differences reported include: Supplementation cocktails and concentrations with multiple bullet-points representing separate flask or bioreactor conditions; The cell line utilized and the lineage of that cell line where reported; The protein being expressed and whether it is a mutant variant or fusion; The bioprocess scale, time of supplementation, and time of harvest; The amount of glutamine (Gln) utilized in the growth medium. .... 172

Table 17 – Comparison of glycoform shifts and differences between reported experiments for the supplementation of galactose (Gal), the nucleoside uridine (Urd), and the enzyme cofactor manganese (Mn<sup>2+</sup>), towards expanding intracellular nucleotide-sugar pools of UDP-galactose in cultured mammalian cells and affecting. Glycoform shifts are reported as %-shifts in indices of mannosylation (MI), antennarity (AI), fucosylation (FI), galactosylation (GI), and sialylation (SI) (as per Equations 1-5, Figure 28) relative to reported control culture glycoforms. Experimental differences reported include: Supplementation cocktails and concentrations with multiple bullet-points representing separate flask or bioreactor conditions; The cell line utilized and the lineage of that cell line where reported; The protein being expressed and whether it is a mutant variant or fusion; The bioprocess scale, time of supplementation, and time of harvest; The amount of glutamine (Gln) utilized in the growth medium. .... 175

Table 18 – Comparison of glycoform shifts and differences between reported experiments for the supplementation of the acetylated amine sugar acetyl-mannosamine (ManNAc), and the nucleoside cytidine (Cyt), towards expanding intracellular nucleotide-sugar pools of CMP-NeuAc in cultured mammalian cells and affecting N-linked glycoforms of recombinant glycoproteins. N-linked glycoforms of recombinant glycoproteins. Glycoform shifts are reported as %-shifts in indices of mannosylation (MI), antennarity (AI), fucosylation (FI), galactosylation (GI), and sialylation (SI) (as per Equations 1-5, Figure 28) relative to reported control culture glycoforms. Experimental differences reported include: Supplementation cocktails and concentrations with multiple bullet-points representing separate flask or bioreactor conditions; The cell line utilized and the lineage of that cell line where reported; The protein being expressed and whether it is a mutant variant or fusion; The bioprocess

scale, time of supplementation, and time of harvest; The amount of glutamine (Gln) utilized in the growth medium. .... 178

## List of Abbreviations

- $^1\text{H-NMR}$  – nuclear magnetic resonance spectroscopy of hydrogen nuclei
- 2AB – 2-aminobenzamide
- A – glycan antennarity
- ADCC – antibody dependent cell cytotoxicity
- ADP – adenosine diphosphate
- AMS – aspartate malate shuttle
- Asn - asparagine
- ATP - adenosine triphosphate
- BHK – baby hamster kidney (cell line)
- BRI – Biotechnology Research Institute of Canada
- CDC – complement dependent cytotoxicity
- CDR – complementary determining region
- CHO – Chinese hamster ovary (cells)
- CMP – cytosine monophosphate
- CQA – critical quality attribute
- CSI – chemical shape indicator
- DIGE – differential in-gel electrophoresis
- DO – dissolved oxygen
- DHFR – dihydrofolate reductase selection/amplification marker
- DSS – 2,2-Dimethyl-2-silapentane-5-sulfonate (internal NMR standard)
- EG2-hFc – single domain camelid antibody specific to EGFR fused to a human Fc region
- EGFR – epidermal growth factor receptor
- ER – endoplasmic reticulum
- F – glycan fucosylation
- Fc – crystallisable fragment (antibody)
- FID – free induction decay (NMR)
- Fv – variable fragment (antibody)
- Fab – antigen binding fragment (antibody)
- Fuc – fucose

- G – glycan galactosylation
- Gal – galactose
- GalNAc – N-acetylgalactosamine
- Glc – glucose
- GlcN - glucosamine
- GlcNAc – N-acetylglucosamine
- GnT-III – N-acetylglucosaminyltransferase III
- GPI – glycosphosphatidylinositol
- GS – glutamine synthase selection/amplification marker
- HAMA – human anti-murine antibody
- HAT – hypoxanthine-aminopterin-thymidine
- HEK293 – human embryonic kidney (cell line)
- hMT-IIA – human metallothionein IIA induced promoter
- HPLC – high performance liquid chromatography
- Ig – immunoglobulin (antibody)
- M – glycan mannose
- mAbs – monoclonal antibodies
- MAbNet – strategic NSERC monoclonal antibody research network
- Man – mannose
- ManNAc – N-acetylmannosamine
- NADH – nicotinamide adenine dinucleotide
- Neu5Ac – N-acetylneuraminic acid (sialic acid)
- Neu5Gc – N-glycolylneuraminic acid
- NK – natural killer (cells)
- NMR – nuclear magnetic resonance (spectroscopy)
- NS0 – mouse myeloma (cell line)
- NSERC – Natural Science and Engineering Research Council of Canada
- PER.C6 – human cell line derived from embryonic retinal cells
- S – glycan sialylation
- SA – sialic acid



- scFv – single chain antibody fragment
- SCLC – small cell lung cancer
- Ser - serine
- Sp2/0 – mouse hybridoma (cell line)
- TCA – tricarboxylic acid (cycle)
- Thr – threonine
- TNF – tumour necrosis factor
- UDP – uridine diphosphate
- Xyl - xylose
- YAC – yeast artificial chromosomes

## Chapter 1 Introduction

The production of recombinant therapeutic biologics in cell culture is a rapidly growing industry, creating many opportunities for bioprocess engineering research and development. Leading the products within this market are monoclonal antibodies (mAbs). Elvin et al. estimated in 2011, that global annual sales of therapeutic mAbs were approaching \$50 billion USD – over a third of all biologics – from only twenty-eight approved drugs (Elvin et al., 2011). By the end of 2014, the number of approvals had increased to forty-seven, with sales eclipsing \$75 billion USD the previous year (Ecker et al., 2015). Given the number of new products in the pipeline and the emergence of follow-on biosimilars and biobetters, i.e. nonoriginal biologics (NOBs), the size of this market is expected to nearly double by 2020 (Albrecht et al., 2014; Ecker et al., 2015). Today, biologics make up nine of the top ten global selling pharmaceutical products, and approximately 20% of all global pharmaceutical sales (Lindsley, 2017).

To meet this increasing demand for recombinant therapeutic biologics, bioprocess engineers have conventionally been tasked with the primary goal of increasing the yield of bioprocesses, either by increasing maximum cell densities of cultures, or improving their productivity. Applying emerging methods, such as metabolomics and proteomics analysis towards this primary goal is examined in Chapter 3. Compared to small-molecule pharmaceuticals, therapeutic biologics like mAbs also possess molecule-to-molecule heterogeneity directly impacting their therapeutic efficacy. Therefore a further goal of bioprocess engineers has emerged to improve the quality of therapeutic biologics. The strategy of supplementing nucleotide-sugar precursors and related components to cell cultures to affect product quality by influencing glycosylation is detailed in Chapter 4 & Chapter 6.

Regarding omics methods, these technologies are producing an unprecedented amount of information for interpreting the state of bioprocesses at various scopes (Section 2.6). Measuring the differential expression of all cellular proteins, referred to as ‘proteomics’, through methods such as two-dimensional differential in-gel electrophoresis (2D-DIGE) reveal important details of how cells are regulating to overcome stresses imposed by recombinant expression of proteins (reviewed by Lalonde and Durocher, 2017). Similarly, ‘metabolomics’, focuses upon identifying and quantifying all low molecular weight molecules being consumed and produced in both the extracellular supernatant as well as the intracellular metabolite pools; this is referred to as metabolite “footprinting” and “fingerprinting” respectively (as reviewed by Kell et al., 2005).

Omics methods far outstrip conventional metrics for bioprocesses, which limit focus solely to conventional metrics such as dissolved oxygen, temperature, pH, carbon substrates, and a selection of toxic metabolites (typically lactate and ammonia). Observing the full complement of differentially expressed proteins like in proteomics (as reviewed by J. Y. Kim et al., 2012), or the small molecular weight compounds (nutrients and excreted waste products) through metabolomics, which are the result of all cellular mechanisms during a culture (as reviewed by Cuperlović-Culf et al., 2010), offer a powerful means to characterize the phenotype of cultured cells. Omics tools and analysis applied to cell culture processes have been leveraged to produce higher overall yields, mitigate metabolic bottlenecks, and detect scaling problems (Chong et al., 2010b; Dietmair et al., 2012; Schaub et al., 2012; Sellick et al., 2011a; Zang et al., 2011). Tools such as these are demonstrated in Chapter 3 for a 75% increase in maximum cell density of CHO cultures; and to identify a metabolic bottleneck in Chapter 4 leading to growth restriction while using a supplement to modify glycan profiles.

Biotherapeutics, such as monoclonal antibodies (mAbs), require advanced cellular processes, such as glycosylation, to become biologically active (Dordal et al., 1985; Nose and Wigzell, 1983). As such, mAbs and other ‘glycoprotein’ biologics are typically manufactured using higher-order eukaryotic platforms such as mammalian cell cultures, with a significant majority by Chinese Hamster Ovary (CHO) cells, which have grown to become an industry standard (Ghaderi et al., 2012). Mammalian cells, such as CHO, are more challenging to culture compared to bacteria and yeast, and have reduced productivity, but are capable of a wide range of human-like post-translational modifications to proteins. These modifications include glycosylation, which is acknowledged in FDA guidances for industry to be a major critical quality attribute (CQA) of mAbs and other biologics (FDA, 2015). Glycosylation affects a host of drug factors including immunogenicity (Bosques et al., 2010; Padler-Karavani et al., 2008), secretion by cells (Hickman and Kornfeld, 1978), drug clearance-rate (Morell et al., 1968), protein stability (Mimura et al., 2001) and solubility (Leavitt et al., 1977), as well as effector function for mAbs for required recognition by the immune-system (Chapter 6). As such, on the subject of improving cell culture productivity, this research has focused on CHO-based mammalian cell cultures, and on the subject of product quality, this research has focused specifically on affecting glycosylation.

Glycan heterogeneity occurs naturally, but is influenced by numerous factors such as perturbations in culture conditions, including temperature, pH and dissolved oxygen, which have been widely reviewed (Butler, 2006; del Val et al., 2010; Eon-Duval et al., 2012; Hossler, 2012; Spearman et al., 2011). More directly, this heterogeneity is driven by up/down shifts in the expression of cellular enzymes and transporter proteins (Chen and Harcum, 2006; N. S. C. Wong et al., 2010), as well as bottlenecks in the substrate supply chain (McDonald et al., 2016; Nyberg

et al., 1999; Pels Rijcken et al., 1995b). With respect to commercial bioprocesses, heterogeneity implies drugs of inconsistent quality (molecule to molecule) and batch to batch variability. Tools, like emerging omics methods demonstrated in Chapter 3 & Chapter 4, empower bioprocess engineers to observe these domains directly and affect necessary actions.

Strategies to affect and control glycosylation can be grouped into three categories: 1) glycoengineering of cell platforms to alter expression of enzymes and Golgi transporters; 2) *in vitro* remodeling of glycans as a downstream process; 3) supplementation of nucleotide-sugar precursors and related components to culture medium to affect the metabolism of glycosylation. This 3<sup>rd</sup> strategy of supplementation of metabolic precursors of glycosylation to growth medium is the focus of this research (detailed in Chapter 4 & Chapter 6), and touches upon both bioprocess goals of culture growth and product quality due to its effects on cell growth (detailed in Chapter 4), as well as effects to the glycan distribution on product glycoproteins (i.e. product quality; Chapter 4 & Chapter 6). The particular problem regarding inconsistency of reported effects of glycosylation precursor supplementation strategies is analyzed and addressed in Chapter 6.

## **1.1 Objective of Research**

The purpose of this research is to demonstrate supplementation strategies to both enhance cell growth of CHO mammalian cell cultures, and tune glycosylation to improve mAb product quality with the aid of omics methods. Towards these objectives, omics methods are applied to elucidate factors at the scale of the metabolome and proteome, to create a nutrient cocktail to enhance culture growth as investigated in Chapter 3. Subsequently, strategies for tuning glycosylation by supplementing nucleotide sugar precursors to affect the intracellular metabolite pools are investigated in Chapter 4 & Chapter 6. Omics methods are also utilized to elucidate the

nature of growth effects to CHO cultures of nucleotide-sugar precursor supplementation in Chapter 4.

## **1.2 Hypothesis of Research**

Omics analysis of CHO<sup>BRI</sup>-1A7 cells expressing EG2-hFc heavy-chain chimeric camelid antibodies can be utilized to identify cell stresses and resource limitations. In turn, supplementation strategies can be designed to alleviate these stresses providing additional resources to metabolic systems to improve growth. Additionally, supplementation of precursors to intracellular nucleotide-sugars can be employed to alter the glycosylation profile of monoclonal antibodies produced in CHO<sup>BRI</sup>-1A7 cells. This shift in the glycoform is an effect caused by increase intracellular nucleotide-sugar pools. Metabolomic analysis of cells following supplementation will elucidate relationships between elevated levels of these intracellular pools and protein glycosylation, to overcome negative growth effects. This will allow for improved feeding strategies and process controls for affecting glycosylation and product quality of glycoproteins in bioprocesses.

## Chapter 2 Literature Review

### 2.1 Antibodies *in vivo*

Antibodies, referred to formally as immunoglobulins (Ig), are a diverse class glycoproteins secreted by B-cells, which form a fundamental part of the immune system (as reviewed by Jefferis, 2012). Five known types of human antibodies exist *in vivo*, characterized by differences in their constant-region “heavy chains”, and are classified as: IgA, IgM, IgD, IgE, and IgG, with Immunoglobulin G and A antibodies subdivided into four and two subtypes respectively and classified numerically (IgG1-4 and IgA1-2) (as reviewed by Jefferis, 2012). IgG1&2 are the most commercially exploited antibody types (Elvin et al., 2011), and IgG1 predominates in human blood (reviewed by Jefferis, 2009). Commonly described as having a “Y-shaped” structure, antibodies possess two sites for binding to a particular epitope of a target antigen with high specificity (reviewed by Ahmad et al., 2012).

The two antigen binding arms of the structure, Fab fragments, contain the variable binding portion (Fv), possessing the complementary determining regions (CDRs) specific to antigen epitopes (as reviewed by Schroeder and Cavacini, 2010). The portion of antibodies responsible for immune effector function is called the crystallisable fragment (Fc) (as reviewed by Spearman et al., 2011). Human IgG antibodies *in vivo* are heterodimer proteins assembled from two heavy chains and two light chains joined at various locations by disulfide bonds (as reviewed by Schroeder and Cavacini, 2010), a schematic diagram of which is shown in Figure 1.

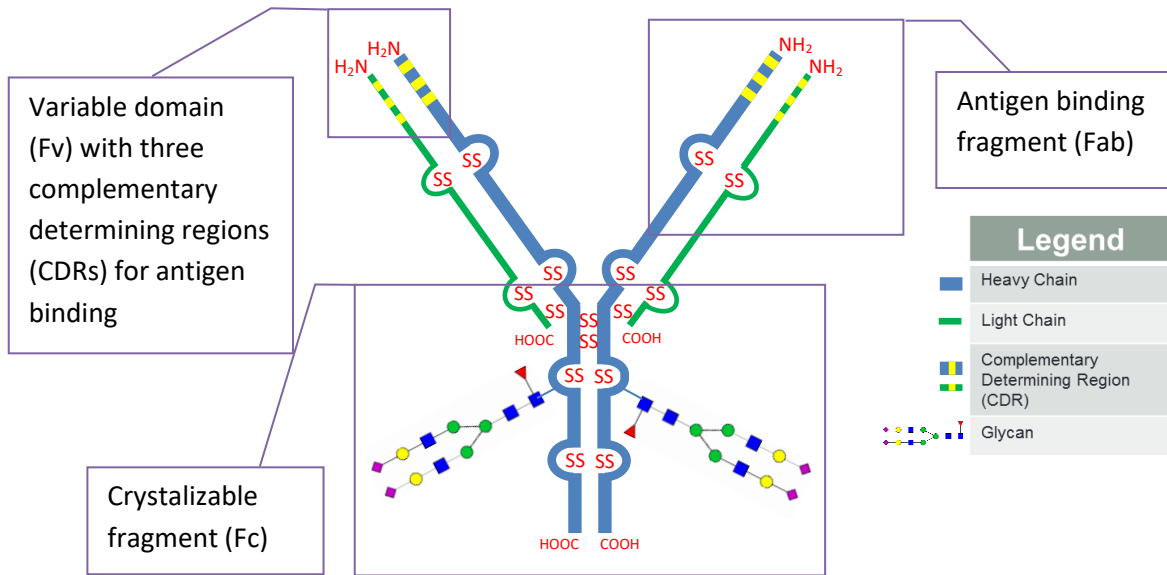


**Figure 1 – Basic immunoglobulin (Ig) structure**

The glycosylated effector region of the constant heavy-chain, shown in Figure 1, binds to Fcγ receptors of natural killer (NK) and monocyte cells of the immune system, which can trigger antibody dependent cell cytotoxicity (ADCC) for clearing pathogens (reviewed by Schroeder and Cavacini, 2010). Antibody effector regions also play a part in stimulating the complement system, triggering Complement dependent cytotoxicity (CDC) (reviewed by Jefferis, 2009). These immune effector activations are demonstrated in Figure 2, while a comprehensive review of these effector functions for antibodies is provided in Chapter 6.



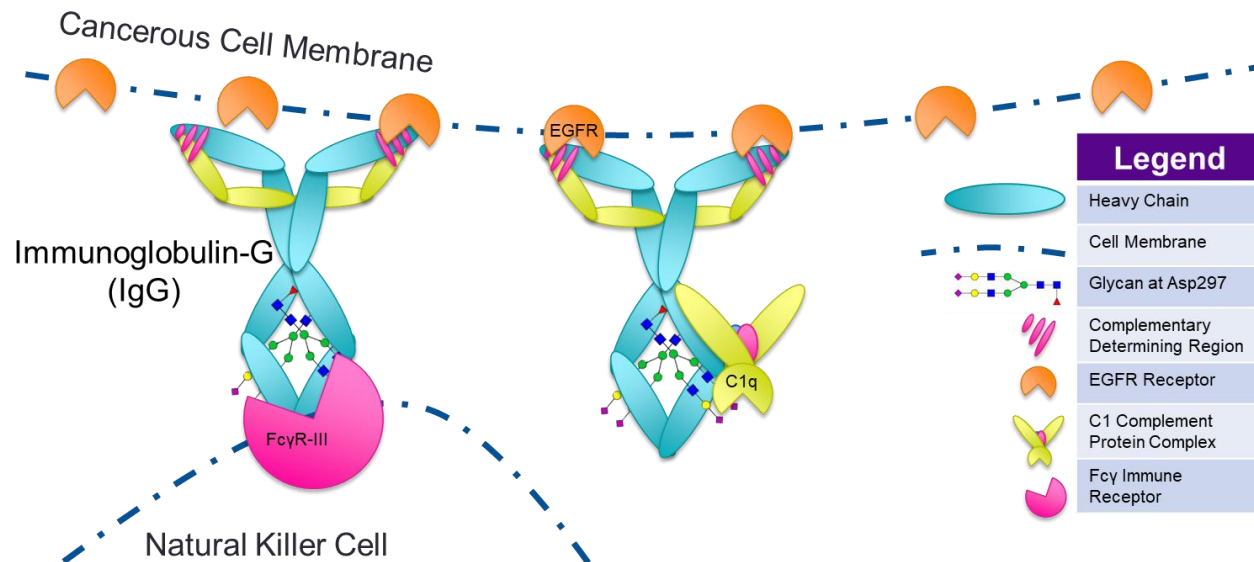


Figure 2 – Antibodies activating two common immune effector functions to destroy an EGFR presenting cancer cell; antibody dependent cell cytotoxicity (ADCC), and complement dependent cytotoxicity (CDC).

## 2.2 Antigen Binding

Antibodies bind particular epitopes of target molecules, referred to as antigens, with high specificity (as reviewed by Jefferis, 2012). This quality makes antibodies powerful tools for therapeutic applications, where antibodies can neutralize a target like a cytokine, or activate the immune system against cancerous cells, or be conjugated with a drug for targeted delivery in the body (as reviewed by Ecker et al., 2015). Similarly, an antibody's high specificity for antigen binding also makes it a valuable tool for diagnostic applications, such as detection of an analyte with a high degree of specificity – for instance, the home pregnancy test (as reviewed by Yamada et al., 2017).

Whole monoclonal antibodies (mAbs) have been favoured as an antigen-binding technology in industry, but alternatives such as antibody fragments and numerous fusion proteins have provided interesting new opportunities (reviewed by Ecker et al., 2015; reviewed by Moran, 2011).

### 2.2.1 Monoclonal Antibodies (mAbs)

The ready availability of antibodies with high specificity to any desired target are built upon the 1975 publication of Kohler and Milstein's process to create monoclonal antibodies (mAbs) *in vitro*, i.e. functionally identical immunoglobulins that bind exclusively to one epitope of a target antigen (Köhler and Milstein, 1975). The first mAbs were produced by fusing primary murine B lymphocytes producing antibodies (primary cells recovered directly from the spleen of a mouse), to a continuous strain of myeloma cells by using inactivated Sendai virus (Köhler and Milstein, 1975). Selection for fused 'hybridoma' cells was achieved by employing myeloma cells lacking an enzyme present in B-cells to metabolize hypoxanthine-aminopterin-thymidine (HAT) for purine nucleotide synthesis (Köhler and Milstein, 1975). HAT-medium eliminated unfused myeloma cells, while unfused B-cells died from poor adaptability to suspension culture (Köhler and Milstein, 1975). Single clones were then plated and observed to maintain their phenotype, thus achieving cultures producing monoclonal antibodies (Köhler and Milstein, 1975).

The first commercially approved therapeutic mAb generated from hybridoma technology was muromonab-CD3 (Orthoclone OKT3), a fully murine-derived antibody for preventing rejection of renal transplants (reviewed by Chatenoud et al., 1988). While possessing some effectiveness as an immunosuppressant for organ transplant, administration of the OKT3 and other murine-antibodies often precipitated severe flu-like symptoms in patients due to 'cytokine release syndrome' (Chatenoud et al., 1988). The non-human origins of murine-therapeutics were detected by the human immune system *in vivo* causing patients to generate human anti-murine antibodies (HAMAs) causing rapid clearance of the drugs and significantly reducing their long-term effectiveness as a treatment (Schroff et al., 1985).

The next generation of commercial mAbs was referred to as ‘chimeric’, possessing murine variable regions and human constant regions (Morrison et al., 1984). Chimeric mAbs were succeeded by ‘humanized’ mAbs, which possessed grafted complementary determining regions (CDRs, as shown in Figure 1) (Jones et al., 1986). While humanized mAbs demonstrated improved effector function, slower clearance rates, and reduced immunogenicity – chimeric and humanized antibodies possessing ~25% and ~10% murine content respectively, still elicited HAMA responses (reviewed by Spearman et al., 2011).

The latest generation of mAbs are fully human, with no murine content (reviewed by Elvin et al., 2011); however, the funnel of mAbs in clinical trials still contains humanized, chimeric, and even murine mAbs, but these are becoming fewer and fewer as the industry continues to grow rapidly (Reichert, 2017). Fully human monoclonal antibodies are actually still produced in mice; however, as this is achieved by bioengineering transgenic mice to produce human heavy and light chains from yeast artificial chromosomes (YACs) introduced to the mouse germline, and subsequently breeding them for immunodeficiency (Green et al., 1994). Similar research was simultaneously published in 1994 with an alternative method by Lonberg et al. creating a transgenic strain of mice capable of producing fully human immunoglobulins for commercial therapeutics (Lonberg et al., 1994).

### **2.2.2 Antibody Fragments and Fusion Proteins**

While a glycosylated Fc region of an antibody is essential for immune effector functions like ADCC and CDC, the treatment of several disorders rely simply on binding and neutralizing target antigens like cytokines (Ecker et al., 2015). As such, these treatments can be manufactured in higher producing cell culture platforms, such as prokaryotes and yeasts, without glycosylation

restrictions. Similarly, radioactive and toxic drug deliveries can be accomplished by fusion to antibody fragments in place of an Fc component (reviewed by Ahmad et al., 2012).

There are also fusion antigen-binding proteins that continue to possess immune effector function, such as chimeric single domain heavy-chain only camelid antibodies (HCABs), possessing enhanced tumour penetration by their reduced molecular weight and size (Zhang et al., 2009). An example of these heavy-chain mAbs is the ~80kD EG2-hFc, single domain camelid chimeric antibody produced by CHO<sup>BRI</sup>-1A7 cells utilized in this research, which binds to epidermal growth factor receptors (EGFR) towards therapeutic treatments against forms of cancer overexpressing this receptor (Agrawal et al., 2012; Bell et al., 2010; Zhang et al., 2009).

### **2.3 Glycosylation**

Glycosylation is acknowledged in several reviews of the FDAs quality by design (QbD) program to be a major critical quality attribute (CQA) of MAb and other biotherapeutics (del Val et al., 2010; Eon-Duval et al., 2012; Glassey et al., 2011). Unlike other cellular processes like transcription and translation of DNA and RNA, which follow a semi-consistent coded template, glycosylation is not coded; and as reviewed by many researchers, is influenced by numerous factors such as perturbations in culture conditions (Butler, 2006; del Val et al., 2010; Eon-Duval et al., 2012; Hossler, 2012; Spearman et al., 2011)), bottlenecks in the substrate supply chain (Nyberg et al., 1999; Pels Rijcken et al., 1995b), and the regulation of cellular processes, i.e. the up/down regulation of cellular enzymes and transporter proteins (Chen and Harcum, 2006; N. S. C. Wong et al., 2010). These factors in commercial bioprocesses contribute to variable products with direct implications to its final effectiveness for treatment. Furthermore, as reviewed by Jefferis, certain glycan structures in the resulting distribution possess superior

and inferior therapeutic qualities and as such certain glycoforms are more sought after than others (Jefferis, 2012).

A comprehensive discussion of glycosylation, its metabolism, impact on the efficacy of therapeutic glycoproteins (particularly mAbs), as well as supplementation strategies utilizing nucleotide sugar precursors and related components to affect resulting glycoforms, is available in Chapter 6.

### **2.3.1 Eukaryotic Glycosylation**

There are two main forms of glycosylation, N-linked and O-linked, which are designated by the functional group of the amino-acids where the glycans are bound; these processes have been reviewed by numerous researchers (Butler, 2006; Ghaderi et al., 2012; Hossler et al., 2009; Roy Jefferis, 2009; Moremen et al., 2012; Spearman et al., 2011; Spiro, 2002). N-glycans are bound via amide-linkages to asparagine residues, and are typically larger oligosaccharides compared to O-glycans, which are bound to serine or threonine by glycosidic bonds. O-linked glycosylation can also occur on hydroxylysine or tyrosine in the case of collagen and glycogenin respectively (reviewed by Moremen et al., 2012). Further, there are two lesser known forms of glycosylation: C-mannosylation, where mannose is affixed by carbon-carbon covalent bonds to the C2 position of tryptophan, and glypiation, where glycosylphosphatidylinositol (GPI) anchors are formed between mannose, phosphoethanolamine, and the terminal carboxyl-group of a protein, which are common in cell surface proteins of eukaryotes (reviewed by Spiro, 2002).

With respect to mAbs, N-linked glycosylation of the Fc region receives the most attention in literature, as it is a major factor in effector function and binding to Fc $\gamma$  receptors of the immune system, discussed in detail in Chapter 6.



The resulting precursor to N-linked glycosylation, shown in Figure 3, is bound to the protein at a site referred to as a 'sequon' via oligosaccharide transferase (OST) (as reviewed by Spearman et al., 2011). Failure of the oligosaccharide to attach to a sequon causes product variation referred to as macroheterogeneity for glycoprotein therapeutics, which can lead to problems of bioactivity (Dordal et al., 1985; Nose and Wigzell, 1983). The most common sequon for N-glycosylation, called the consensus sequon, is identified by a three amino-acid pattern of 'asparagine-(variable)-serine/threonine' where the variable residue must not be proline (as reviewed by Moremen et al., 2012). Non-consensus sequons have been identified, where serine/threonine are replaced with cysteine, glycine or valine; however, these are observed rarely (less than 4% cumulatively) (Zielinska et al., 2010). Once bound to its sequon, in step with protein folding, glycotransferase enzymes of the ER act upon the oligosaccharide precursor glycan shown in Figure 3, removing the three terminal glucose moieties as well as the central terminal mannose residue, as shown in Figure 4.

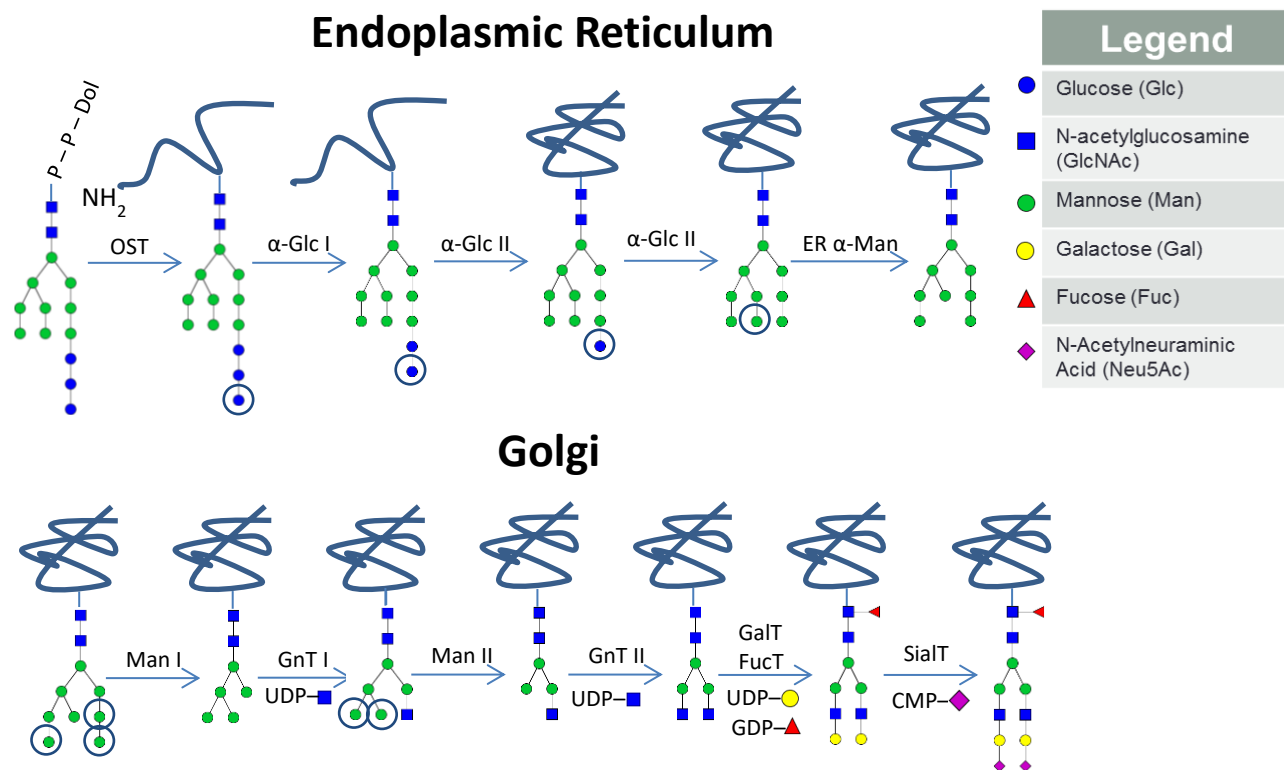


**Figure 4 – Eukaryotic N-glycosylation in mammalian cells**

Glycosylation continues into the Golgi with the removal of three more terminal mannose moieties, as per Figure 4, where an example of a possible sequence of glycosyltransferases yields a ‘complex’ glycan that is biantennary, fully galactosylated, fully sialylated, and with a core  $\alpha_{1-6}$  fucose moiety. This glycan can be represented by an abbreviated nomenclature, “FA2G2S2” for its structure, following the Oxford Glycobiology Institute convention (reviewed by Gornik et al., 2007). In this case, the ‘F’ refers to fucose bound by an  $\alpha_{1-6}$  bond, the ‘A’ to the degree of antennarity (in this case, biantennary), ‘G’ to the degree of galactosylation, and the ‘S’ for sialylation. Instead of just one glycan resulting from this process, as shown in Figure 3, glycosylation typically yields a distribution of several glycans based on partial completion or further processing beyond steps shown in Figure 3. This variation is referred to as microheterogeneity. Examples of other commonly observed glycoforms are shown in Figure 5.



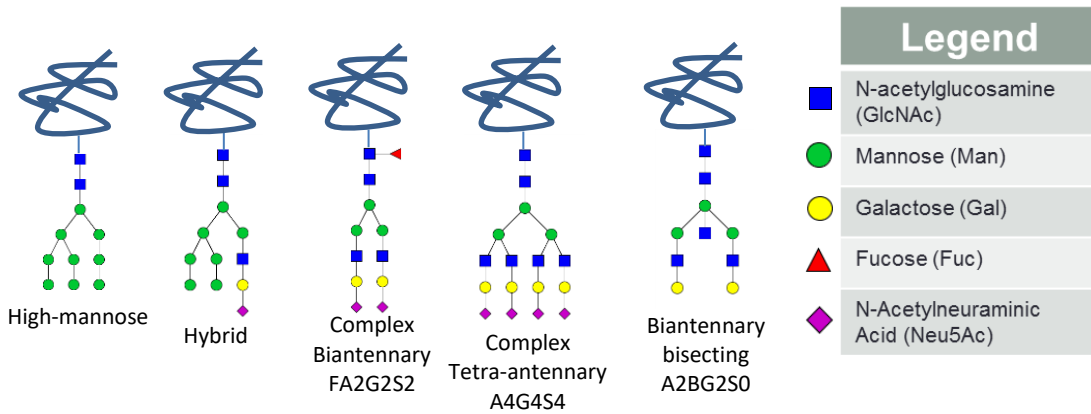


**Figure 5 – Examples of diversity of potential glycoforms**

Regarding *in vivo* human N-glycoforms for antibodies, in an examination of the prevalent glycans of IgG1&2 found in human blood serum of five healthy patients reported by Flynn and colleagues (2010), the most prevalent five glycoforms cover over 90% of the distribution; these glycans are as shown in Figure 6; their relative proportions are detailed in Table 1. An important characteristic of antibody glycoforms *in vivo*, noted by reviewer Jefferis, is their tendency to shift in response to illnesses, as such the optimal distribution of glycans on antibodies for treating a particular disorder may vary from the distribution reported by Flynn et al. (Flynn et al., 2010; Jefferis, 2012).

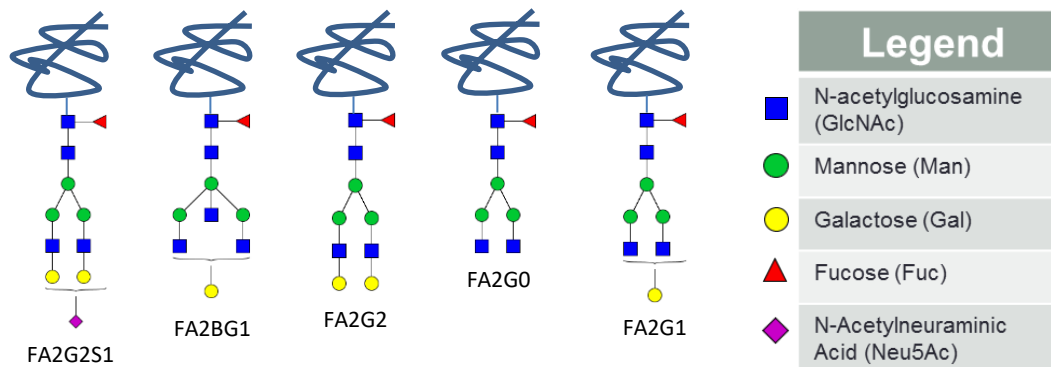


**Figure 6 – Most common human N-glycoforms for IgG1&2 in blood serum according to Flynn et al. (2010)**

Further reported by Flynn et al. for IgG1 and IgG2, as noted in Table 1, the resulting bisecting forms of IgG1&2 are approximately 12% and 9.3%, respectively (Flynn et al., 2010). This is most notable, because these glycans in particular cannot be produced in CHO mammalian cell cultures, which do not express the glycosyltransferase enzyme GnT-III (Xu et al., 2011).

**Table 1 – N-Glycan distribution of IgG1&2 in human blood serum according to Flynn et al. (2010)**

<b>N-Glycan Structure</b>	<b>IgG Type 1 (%)</b>	<b>IgG Type 2 (%)</b>
Aglycosylated	0.19 ± 0.11	0.18 ± 0.04
Hybrid	0.681 ± 0.23	1.74 ± 1.10
Bisecting	12.054 ± 2.99	9.31 ± 2.41
Afucosylated	3.66 ± 0.97	2.31 ± 0.96
Sialylated	10.533 ± 1.73	10.12 ± 2.22
<b>Most Common Glycoforms <i>in vivo</i>:</b>		
FA2G0	12.5 ± 2.7	25.1 ± 5.7
FA2G1	42.3 ± 2.4	35.6 ± 3.0
FA2G2	21.7 ± 3.7	16.1 ± 3.8
FA2BG1	7.2 ± 1.6	4.1 ± 1.1
FA2G2S1	8.6 ± 1.19	6.2 ± 1.6

### 2.3.3 Antibody Fc & Immune Effector Function

While the Fab region of antibodies allow them bind with high specificity to their target antigens, it is their glycosylated Fc regions that interact with the immune system. IgGs possess paired glycosylation sequons at ‘asparagine 297’ (Asn<sub>297</sub>) on the heavy chain CH2 domain of their Fc region, and depending on the resulting glycoform, produce varying immune response activation capability *in vivo* (as reviewed by Jefferis, 2012). N-glycosylation of the Fc region has long been understood to be essential for bioactivity of mAbs for activating immune effector

functions (Nose and Wigzell, 1983). As noted previously, the glycosylation of antibodies also affect a host of other drug factors including immunogenicity (Bosques et al., 2010; Padler-Karavani et al., 2008), secretion by cells (Hickman and Kornfeld, 1978), drug clearance-rate (Morell et al., 1968), protein stability (Mimura et al., 2001), and solubility (Leavitt et al., 1977). Therefore, this shifting in the therapeutic effect and major drug characteristics of MAbs with glycosylation forms much of the reasoning behind its status as a ‘critical quality attribute’ (CQA).

The Fc regions of antibodies interact with the immune system by binding to numerous different Fc receptors on the surfaces of white blood cells, as well as complexing with C1q of the Complement system (as reviewed by Jefferis, 2012). Fc receptors can be separated into two categories, neo-natal Fc receptors (FcRN) and Fc $\gamma$  receptors (Fc $\gamma$ R). FcRN are active in adults and play important roles in immunoglobulin serum half-life as well as transport of antibodies across epithelial membranes (as reviewed by Jefferis, 2012). Fc $\gamma$ R possess six established isotypes: Fc $\gamma$ RI (CD64), Fc $\gamma$ RIIa/b/c (CD32) and Fc $\gamma$ RIIIa/b (CD16), and are found in varying proportions on a myriad of leukocytes including macrophages, dendritic cells, neutrophils, and natural killer cells (NK) (as reviewed by Jefferis, 2012).

The interaction of Fc $\gamma$ R with an antibody-antigen complex mediates a host of immune effector functions including antibody-dependent cell phagocytosis (ADCP), cytolysis or cytotoxicity (ADCC), and the release of cytokines and chemokines spurring further cascades of immune responses within the highly regulated immune system (as reviewed by Lazar and Desjarlais, 2009).

MAb glycoforms are often characterized depending on how well they can recruit immune effector functions, particularly ADCC and CDC. Natural Killer cells (NK), a major mediator of

ADCC, typically present only Fc $\gamma$ RIIIa, which upon interaction with the glycosylated Fc region of an IgG, kill antibody-targeted cells either by lytic granule release leading to cytolysis, or induction of apoptosis by secretion of tumor necrosis factor (TNF) family (as reviewed by Lazar and Desjarlais, 2009). Complement-dependent cell cytotoxicity (CDC) is activated by the C1q component, which binds to an antibody-antigen complex, spurring on the Complement cascade, to lyse cells and also produce cytokines to recruit macrophages (as reviewed by Jefferis, 2012).

#### **2.3.4 N-Glycoform & Immune Effector Function**

While different binding sites for C1q, FcRN and Fc $\gamma$ R are employed on the Fc region of antibodies, all occur near the CH2 domain and therefore observe interaction with the major paired N-glycosylation sites at Asn<sub>297</sub> (as reviewed by Lazar and Desjarlais, 2009). As such, different glycoforms yield different binding affinities and therefore significant final effects from these three immune system triggers. A detailed discussion of this topic is available in Chapter 6, and examines the current understanding of how changes in N-glycoforms of antibody Fc regions affect their immune effector functionality.

#### **2.3.5 O-linked Glycosylation**

O-linked glycosylation occurs in the Golgi, and while some consensus binding sites have been identified, most remain unknown (as reviewed by Moremen et al., 2012). However, as reviewed by Van den Steen and colleagues, O-glycans tend to occur in locations on the protein with a higher propensity of serine, threonine and proline (Van den Steen et al., 1998). The most common form is the ‘mucin’ form, where a core N-acetylgalactosamine (GalNAc) is bound to the OH- functional group of either serine or threonine; these proteins occur ubiquitously *in vivo* in mucous secretions (reviewed by Brokhausen et al., 2009). Regarding mAbs, O-glycosylation

is not yet recognized as notably consequential to effector functions or bioefficacy; however, it will affect some basic efficacy characteristics like protein stability (Wang et al., 1996).

## **2.4 Glycan Analysis**

Methods for measuring the distribution of glycans on glycoconjugates is a burgeoning research area with a diversity of proposed techniques. The most established methods, as reviewed by Spearman and colleagues, rely on glycan isolation and fluorescent labeling, followed by quantification by various options such as chromatography, capillary electrophoresis, and mass spectroscopy (MS) (Spearman et al., 2011). Glycan isolation is achieved by cleaving glycans from proteins, using an enzyme such as N-PNGase-F, after which they are labeled with a fluorescent compound such as 2-aminobenzamide (2AB) (reviewed by Butler, 2004a). HPLC separation (normal phase) of fluorescent tagged N-glycans is compared to a reference dextran ladder creating a metric of “glucose units”, with corrections for different monosaccharides (Guile et al., 1996). Glucose units may be subsequently crosschecked against online databases such as GlycoBase, which possesses more than 350 2AB-labelled N-glycans including 117 identified in the human serum (Campbell et al., 2008). An elution profile where glucose units have been used to identify oligosaccharides cleaved from EG2-hFc chimeric heavy-chain mAb is shown in Figure 7, the retention times, glucose units, and glycan type are shown in the accompanying Table 2.

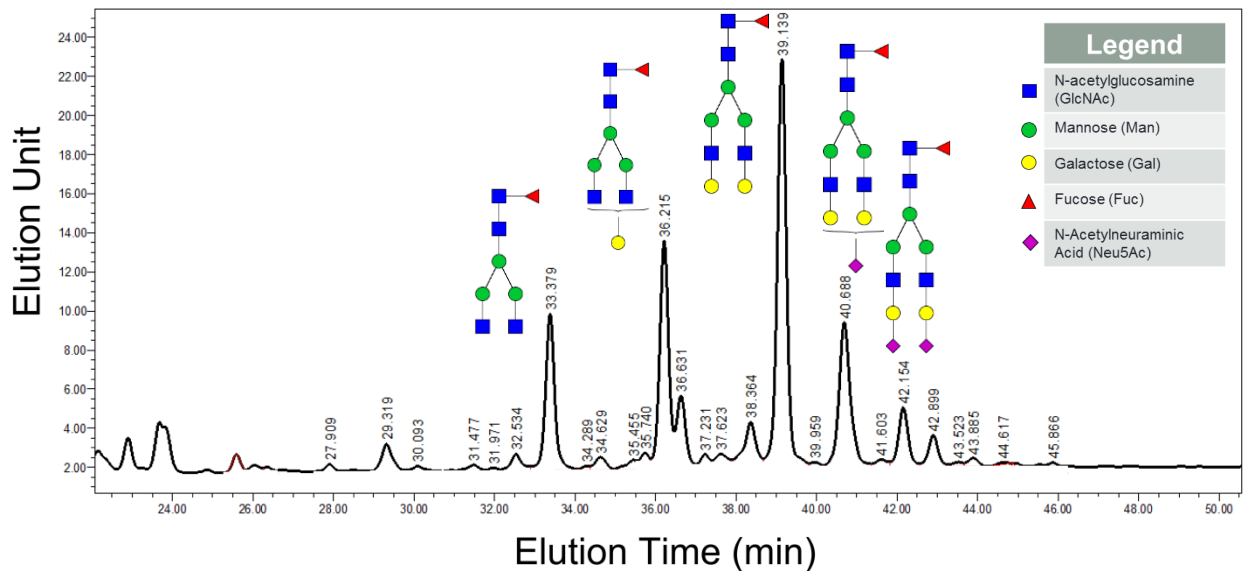


Figure 7 – Normal phase HPLC elution profile of glycans cleaved from mAb EG2-hFc

Table 2 – Elution time, glucose units, and major glycan structures of Figure 7

Elution Time (min)	Glucose Units (GU)	Glycan Structure
33.379	5.85	FA2G0
36.215	6.60	FA2G1 isomer
36.631	6.72	FA2G1 isomer
39.139	7.48	FA2G2
40.688	7.99	FA2G2S1
42.154	8.51	FA2G2S2

## 2.5 Cell Culture Platforms and Glycoengineering

Therapeutic protein biopharmaceuticals on the market today can be characterized along a gradient of complexity with respect to the cellular processing required for biological activity. Several biologics, such as mAbs and erythropoietin (EPO), require complex-type glycosylation for effector function (Dordal et al., 1985; Nose and Wigzell, 1983) and are manufactured using mammalian cell culture platforms. Other biologics like insulin and some fusion/fragment

proteins are not glycosylated and can be prepared in simpler prokaryote platforms such as *Escherichia coli* (Goeddel et al., 1979). Compared to other platforms, mammalian cell culture systems are limited by comparatively slow growth and lower product yields. Furthermore, several established rodent-derived cell lines such as NS0 and CHO form glycosylation structures immunogenic in humans (Bosques et al., 2010; Padler-Karavani et al., 2008). CHO cells, the de facto industry standard, are also incapable of forming structures like bisecting GlcNAc (Xu et al., 2011), which form ~10% of human antibody glycans *in vivo* (Flynn et al., 2010), or  $\alpha_{2-6}$  sialylation, which is present on 40% of endogenous EPO (Takeuchi et al., 1988) and the main contributor to anti-inflammatory properties of sialylated IgGs (Anthony et al., 2008). As such, fully human cell lines like HEK293 and Per.C6 have grown more popular and attempts have been made with some success to “glycoengineer” human-like glycosylation in alternative production platforms of bacteria, yeast, insect cells and improve mammalian platforms currently in use (as reviewed by Lalonde and Durocher, 2017).

### **2.5.1 Mammalian**

Complex therapeutic glycoproteins derived from recombinant technology, such as mAbs, are often manufactured in continuous rodent cell lines like Chinese hamster ovary (CHO), mouse myeloma and hybridoma (NS0 and Sp2/0), as well as baby hamster kidney (BHK) (as reviewed by del Val et al., 2010; Ghaderi et al., 2012; Hossler et al., 2009). Of these platforms, the most widely used are CHO cells, as they are the best characterized and most widely approved, making them effectively an industry standard (as reviewed by Butler and Meneses-Acosta, 2012). Although production capacity with these platforms continues to grow year by year, often exceeding 5g/L (Schaub et al., 2012), this quantity remains well below levels achieved in other systems.

The strength of mammalian cell cultures, as a production platform for biotherapeutics lies in their capacity for human-like glycosylation structures. However, it has been determined that rodent-derived cell lines can generate non-human glycoforms with implications towards immunogenicity (Bosques et al., 2010; Ghaderi et al., 2010). Shown in Figure 7, these immunogenic glycan residues include terminal glycolneuraminic acid (Neu5Gc) (Ghaderi et al., 2010) and terminal  $\alpha$ -linked galactose residues ( $\alpha$ -gal) (Bosques et al., 2010).

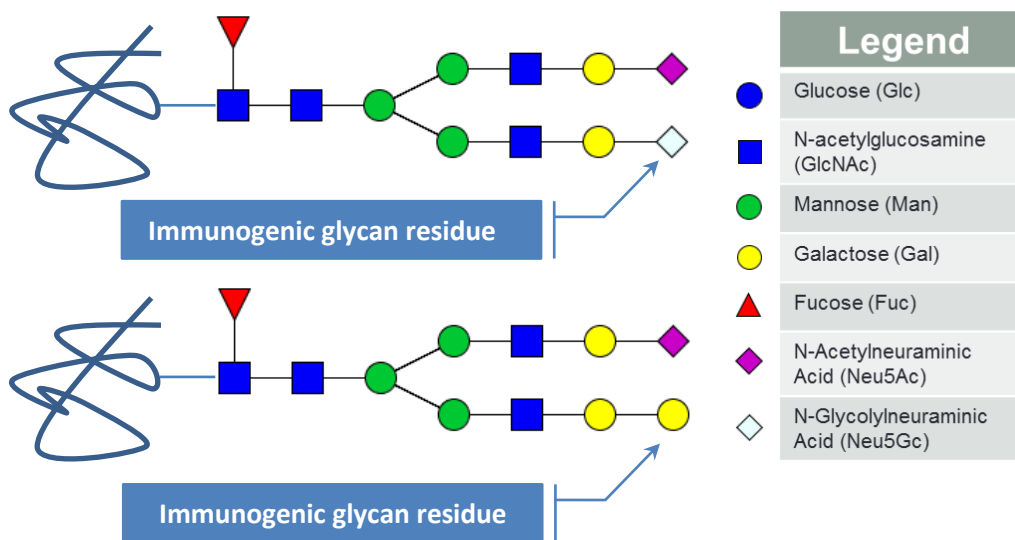


Figure 8 – Immunogenic N-glycan moieties Neu5Gc and  $\alpha$ -gal, from rodent-derived cells

The ability to add a terminal Neu5Gc moiety to glycans was lost by a mutation to the CMAH gene in hominids approximately three million years ago and the human immune system constitutively produces antibodies against this glycoform as well as  $\alpha$ -gal (as reviewed by Ghaderi et al., 2012).

Given the immunogenic glycoforms associated with rodent-originating mammalian cell lines, as well as the fact their glycosylation structures, while human-like, do not achieve the level of complexity as *de novo* human glycoforms, more attention is being directed towards fully human cell lines, such as PER.C6 derived from human embryonic retinal cells and HEK293 from human embryonic kidney cells (Butler and Meneses-Acosta, 2012; Lalonde and Durocher, 2017).



Glycoengineering of mammalian cells is seeing increasing success for altering glycan profiles, particularly as modeling of underlying glycosylation mechanics and regulation improves (McDonald et al., 2016; Spahn et al., 2016). Some common efforts by researchers include goals of increasing sialylation, and reducing immunogenic Neu5Gc. This has been accomplished by over-expression of the sialyltransferase  $\alpha_{2-6}$ -sialT in CHO (Raymond et al., 2015; Weikert et al., 1999; Zhang et al., 1998) and BHK (Schlenke et al., 1999). It has also been accomplished using silencing RNA in CHO cells, preventing expression of sialic acid-removing ‘sialidase’ enzymes (Ferrari et al., 1998). Preventing immunogenic N-glycolylneuraminic acid moieties has been accomplished with silencing RNA to block expression of CMP-Neu5Gc forming enzymes (Chenu et al., 2003). Increasing sialylation has further be improved through over-expression of transporter proteins in CHO, such as ‘CMP-SAT’ to improve sialic acid transfer into the Golgi (Wong et al., 2006). Similar strategies have been employed by other groups in CHO cells to improve galactosylation (Weikert et al., 1999), introduce the capacity for bisecting GlcNAc glycoforms to IgG (Umaña et al., 1999), and reduce fucosylation (Mori et al., 2004). Several additional examples are discussed further in Chapter 6.

### **2.5.2 Prokaryotes**

Bacteria originally were thought to lack the ability to perform complex post-translational modifications like glycosylation, until the discovery that  $\epsilon$ -proteobacterium *Campylobacter jejuni* were capable of a simplified form of protein glycosylation (Szymanski et al., 1999). This glycosylation infrastructure was subsequently transferred to *Escherichia coli* as a means to use prokaryotes to produce recombinant glycoproteins (Wacker et al., 2002). This form of glycosylation is a single step transfer of a lipid-linked heptasaccharide onto the asparagine binding site of proteins in the periplasmic region of the cell (Lizak et al., 2011). This transfer is

analogous to the dolichol lipid-linked oligosaccharide attachment to proteins co-translationally in the endoplasmic reticulum by eukaryotes discussed in Section 2.3.2 as well as Chapter 6. While this bacterial glycosylation is not human-like, one advantage to its simplicity is that all glycosylated proteins receive identical glycans (Lizak et al., 2011), of the form as shown in Figure 8.

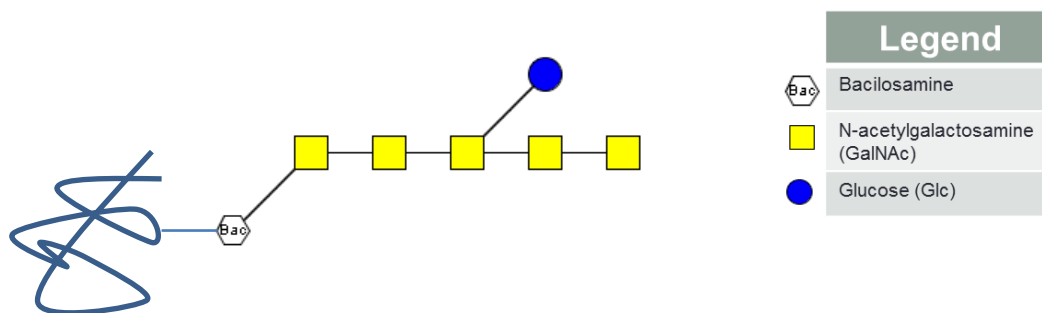
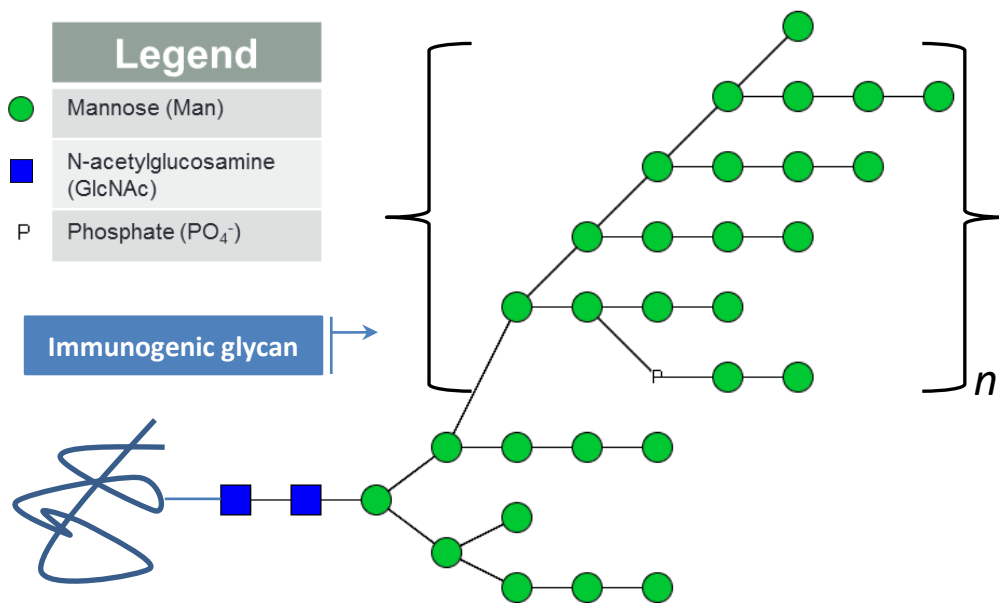


Figure 9 – Prokaryote N-glycosylation from glycoengineered *E. coli*

### 2.5.3 Yeast

Conventionally, yeasts are an attractive option for recombinant protein production and bioprocesses in general for numerous reasons: yeasts possess rapid growth rates, reach high cell densities, adapt well to suspension culture in chemically defined media, and are well-characterized for scale-up to industrial-scale production (as reviewed by Ghaderi et al., 2012). Furthermore, yeasts are eukaryotes, capable of post-translational modifications necessary for bioactivity of therapeutic proteins.

The normal glycosylation structures of yeasts, however, are very different from those found in mammals. Wild-type yeasts produce ‘hyper-mannosylated’ glycoproteins, sometimes with hundreds of mannose residues, as shown in Figure 10 (as reviewed by Gemmill and Trimble, 1999). These glycoforms tend to be immunogenic in humans with rapid clearance rates, discussed further in Chapter 6.



**Figure 10 – Hyper-mannosylated yeast N-glycosylation**

To overcome this drawback glycoengineering has been employed to create strains of *Pichia pastoris* capable of producing human-like glycosylation with upwards of 90% terminal sialylation (Hamilton et al., 2006) and removal of core fucose for enhanced ADCC (as reviewed by Lalonde and Durocher, 2017). However, no commercial examples of this technology are approved to-date.

#### 2.5.4 Insect

Insect cells offer efficient high production of protein, but yield shorter “paucimannosidic” N-glycoforms that may contain immunogenic core  $\alpha_{1-3}$  fucose residues, as shown in Figure 11 (reviewed by Ghaderi et al., 2012).

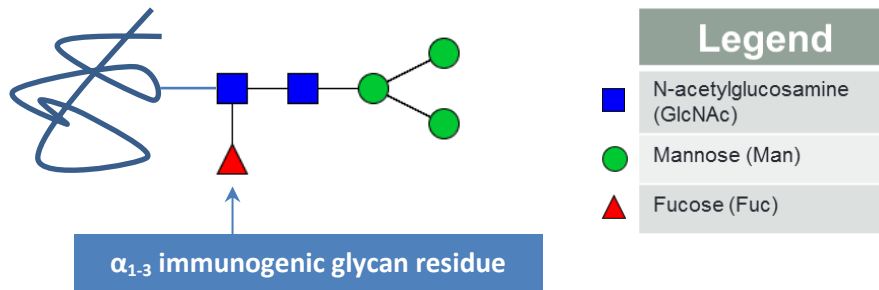


Figure 11 – Paucimannosidic N-glycosylation in insect cells

While a popular lab-scale production platform, insect cells have not historically been utilised for therapeutic protein production. However, this has changed with the approval of Cervarix™, a vaccine against forms of the human papilloma virus (HPV) from GlaxoSmithKline (GSK) (as reviewed by Palmberger et al., 2012). A major difference between insect cell platforms and others is the fact that recombinant protein production is achieved through a transient process using the baculovirus expression vector system (BEVS), rather than integrating amplified genes stably into the chromosomes of the cell line. Baculoviruses do not replicate in mammals, a safety feature for applications of BEVS towards production of therapeutics (as reviewed by Sokolenko et al., 2012).

Glycoengineering of insect cells has been pursued as a means to achieve human-like glycosylation with some success (Aumiller et al., 2012), however, no commercial examples of therapeutic glycoproteins from glycoengineered insect cells are approved to-date.

## 2.6 Omics Methods towards Enhancing Bioprocesses

Omics methods provide a holistic accounting of species within a particular domain of cellular functions, as summarized in Table 3. While genomics and transcriptomics grew out of technologies for rapid DNA and RNA sequencing, proteomics and metabolomics have been built on more conventional analytical chemistry and biochemistry techniques such as gel-

electrophoresis, chromatography, mass spectrometry (MS), and nuclear magnetic resonance spectroscopy (NMR).

**Table 3 – Examples of omics cellular domains**

<b>Cellular Function</b>	<b>Focus</b>	<b>‘Omics Method</b>
DNA Replication	DNA and Genes	Genomics
Transcription	mRNA	Transcriptomics
Translation	Proteins	Proteomics
Metabolism	Metabolites	Metabolomics

Within the realms of genomics and transcriptomics, numerous hierarchical conflicting mechanisms such as epigenetics, gene silencing, and interference produce something of a superposition of phenotype, whereas the realms of proteomics and metabolomics represent a more defined phenotype representation for characterizing cell culture bioprocesses. However, the fidelity of the sampling and analysis methodologies remain a challenge for both proteomic and metabolomic techniques. In proteomics, protocols for quenching and extraction of intracellular proteins are relatively simple to execute. However, the actual analytical protocols selected can create trade-offs for the quality of results when utilizing either a bottom-up shotgun-style proteomics method where samples are digested together without prior separation and results are dependent on mass-based labeling (e.g. isobaric tags), or a top-down method such as a gel-based separation of intact proteins prior to digestion and analysis (reviewed by Westermeier, 2016). In metabolomics on the other hand, while extracellular ‘footprinting’ of supernatant metabolites is simple to execute with just a single centrifugation step to pellet cells, intracellular ‘fingerprinting’ requires challenging quenching and extraction protocols, of which there is a limited consensus in the field for the best methods to follow (Sellick et al., 2011b). Therefore, the challenges of these protocols and methods can undermine whether a true observation of

phenotype has been achieved. Stolfa and colleagues provide a thorough accounting for the various omics methods and how they have been employed, particularly towards CHO cell bioprocesses (Stolfa et al., 2017). For the purposes of this thesis the following sections focus on proteomics and metabolomics in bioprocesses.

### **2.6.1 Proteomics**

Proteomics is the application of analytical biochemistry methods to identify and quantify the global range of proteins and peptides at the cellular level, referred to collectively as the ‘proteome’. Experiments are conducted as a quantitative detection of differential expression of species in the proteome, observing induced shifts in cellular phenotype, as well as changes regarding isoforms of proteins and differences in post-translational modifications depending on the method employed (reviewed by Westermeier, 2016).

Proteomic methodologies can be described broadly as following either a top-down, or bottom-up approach to the quantitation of sample peptides depending on the point at which trypsin digest step is implemented. For top-down methods, intact proteins are initially separated, such as in 2D-gels, by size and isoelectric focusing (IEF), after which individual spots are excised from the gel, trypsin digested and analyzed by mass spectrometry (demonstrated in Chapter 3). In the latter, or bottom-up approach, which includes methods often referred to as “shotgun” proteomics, the sample is first labelled via methods such as isobaric tagging, and then digested en masse without further discrimination, before analysis by mass spectrometry or by various forms of chromatography (reviewed by Westermeier, 2016). Shortcomings of gel-based top-down techniques include the loss of species that are very basic, hydrophobic, very large, or in very small concentrations (reviewed by Westermeier, 2016). Bottom-up techniques suffer from higher sample complexity following digestion, with the potential for misappropriation of

identical peptide sequences between different proteins, and loss of information on post-translational modifications and isoforms of species (reviewed by Westermeier, 2016). A particular advantage of bottom-up methods is that they can be fully automated, while top-down methods require the technical finesse of a trained scientist; however, top-down techniques are also generally regarded to be more reliable. Broadly, like other omics methods, hybrids or parallel analytical methods following these two approaches can minimize the limitations of one another.

#### **2.6.1.1 2D Differential In-Gel Electrophoresis (DIGE)**

Two dimensional differential in-gel electrophoresis (2D-DIGE) is a top-down gel-based proteomics method where proteins and peptides are pre-labeled fluorescently and then separated in a sodium dodecyl sulfate polyacrylamide gel via electrophoresis (SDS-PAGE) in two directions (this method is detailed in Chapter 3). Sample proteins are first separated by isoelectric focusing (IEF) by immobilized pH gradient (IPG) strips embedded in the gel, with proteins travelling to the location in the gel where they have a neutral charge. Subsequently, like a typical SDS-PAGE, the proteins are separated by molecular weight, with smaller proteins and peptides travelling faster through the polyacrylamide gel. The proteins in the gel, visible from their fluorescent tags can be identified and quantified with respect to their location on the gel, with respect to their molecular weight and isoelectric point. In a single gel, two samples are labeled with separate fluorescent dyes and run together so they can be directly compared to determine levels of differential expression (Meleady, 2018).

#### **2.6.1.2 Peptide Tagging Proteomics**

Bottom up proteomics methods function on the basis of chemically labelling peptides or amino acids in a manner to affect the mass of peptide fragments, such that following protein

digestion and subsequently mass spectrometry, the resulting spectra can be analyzed to identify and quantify the distribution of species in the proteome. Methods include stable isotope labeling with amino acids in cell culture (SILAC) utilizing light and heavy versions of amino acids; isobaric tags for relative and absolute quantitation (iTRAQ); and tandem mass tags (TMT). In these methods, the abundance of peptides (and by extension their respective proteins) from different experimental samples can be directly compared to one another for analysis of differential expression (Zhang and Elias, 2017).

### **2.6.2 Metabolomics**

Metabolomics is the application of analytical chemistry methods to identify and quantify (i.e. ‘profile’) the global range of small molecular weight compounds at the cellular level, referred to collectively as the ‘metabolome’. Observed as the cumulative result of all regulatory interactions from cellular functions, the profiled metabolome provides a time-point characterization of the cellular metabolic phenotype for a culture (reviewed by Stolfa et al., 2017)

A distinction is drawn in metabolomics between profiling the intracellular and extracellular environments, the endo and exometabolome respectively, referred to as ‘footprinting’(Allen et al., 2003) and ‘fingerprinting’(Fiehn, 2002). The distinction between these two analyses is important, for two fundamental reasons. First, differences in concentration across the cellular membrane are often characteristic of transport and regulatory actions, which may lead to deficits and bottlenecks for nutrients in the intracellular substrate supply chain of cellular functions. A clear example of this is the observed steep concentration gradient observed for glucose between the extracellular and intracellular environments reported by Ma and colleagues, where the intracellular concentration of glucose was two orders of magnitude below that of the growth medium (Ma et al., 2009). Second, footprinting and fingerprinting are separated due to the



dramatically increased difficulty of profiling the intracellular metabolite pools, or endometabolome, compared to those of the supernatant. Fingerprinting requires chemical treatments to denature enzymes and halt metabolic activity in an instant, which is referred to as “quenching”, and serves to halt enzymatic activity and preserve short-lived metabolites (Dietmair et al., 2010; Sellick et al., 2009). Quenching is subsequently followed by a chemical “extraction” process, which serves to lyse cells for recovery of metabolites (Dietmair et al., 2010; Sellick et al., 2010). Different procedures and chemical agents have been proposed for both quenching and metabolite extraction of polar and non-polar metabolites by different research groups, and are discussed in Section 2.6.4.

Metabolomics possesses several key advantages over other ‘omics platforms for elucidating bioprocess information. For instance, the capability for high throughput sample processing makes metabolomics a strong candidate for on-line process analysis. Furthermore, metabolomics requires less specialized equipment and techniques compared to other ‘omics methods, primarily utilizing conventional analytical chemistry techniques such as mass spectrometry and NMR. This also makes it the most economical omics technology for commercial applications.

A distinction is currently drawn in research between the similar fields of metabonomics and metabolomics, the latter focuses on global profiling of metabolites at the cellular level i.e. extending from cell-level regulation activities. Conversely, metabonomics has a more macroscopic focus of full biological systems, finding applications in drug pharmacokinetics and diagnostic pathology (reviewed by Chrysanthopoulos et al., 2010). The term ‘metabonomics’ was coined by Nicholson and colleagues, with a scope for observing “dynamic multiparametric metabolic responses from living systems”(Nicholson et al., 1999). Samples are typically drawn from biofluids such as urine, blood-serum or spinal-fluid, detecting metabolic patterns indicative

of disease-states and drug toxicity (reviewed by Khoo and Al-Rubeai, 2007). Therefore, the scope of metabonomics is making observations at a fundamentally larger scale (full body) compared to metabolomics (cell-level). However, given the practical similarities that these research fields both refer to quantitative metabolite analysis in biological systems, these terms are often used interchangeably.

Metabolomics is predated by several metabolic engineering tools, such as dynamic kinetic metabolic models, pathway analysis, metabolic flux analysis (MFA), and flux balance analysis (FBA). Metabolomics possesses a distinct and sometimes complementary scope to these other methods, which feature the application of predictive computational models. Since metabolic fluxes are not necessarily linearly dependent on metabolite concentrations, metabolomics does not provide direct information regarding reaction rates or fluxes through metabolic pathways (reviewed by Chrysanthopoulos et al., 2010). Rather, it provides a “snap-shot” of supernatant and intracellular pool concentrations, information which can be utilized without detailed metabolic network modeling. Computational models of intracellular metabolic networks can however be supported by data from metabolomics, as has been demonstrated (Fernandes et al., 2016; Goudar et al., 2010; Selvarasu et al., 2012) and is discussed further in Section 2.6.3.2.

#### **2.6.2.1 NMR Spectroscopy Targeted Profiling**

Numerous methods fall under the umbrella of nuclear magnetic resonance spectroscopy (NMR), and several of these are applicable for metabolic research, particularly when utilizing isotopic tracers like  $^{13}\text{C}$  and  $^{15}\text{N}$  incorporated into certain nutrients to observe their incorporation into cellular metabolism (Goudar et al., 2010). For the purposes of this thesis, discussion has been limited to simple ‘pulse-acquire’ single dimension hydrogen nuclear magnetic resonance spectroscopy (1D- $^1\text{H}$ -NMR), commonly utilized by metabolomics researchers (Aranibar et al.,

2011; Bradley et al., 2010; Rathore et al., 2015; Read et al., 2013), and demonstrated in Chapters 3&4.

In a 1D-<sup>1</sup>H-NMR experiment, the free induction decay (FID) signal is Fourier-transformed, producing a spectrum of hydrogen peaks unique to the mixture of metabolites in the sample. This spectrum is normalized against an internal standard, 2,2-Dimethyl-2-silapentane-5-sulfonate (DSS), added to the sample prior to analysis, and the area beneath the resulting peaks corresponds proportionately to the total number hydrogen nuclei sharing a particular position in a metabolite's chemical structure, and by extension the concentration of that metabolite of interest. With the aid of software and a human 'profiler', a process of "targeted profiling" can be employed to first identify metabolites by the peaks in a spectrum, and then quantify them by aligning them with the spectra of pure compounds (Sokolenko et al., 2014, 2013; Weljie et al., 2006).

1D-<sup>1</sup>H-NMR possesses advantages over other metabolomics methods including a non-destructive analysis, and a capability for observing volatile organic acid metabolites, such as formate and acetate, which are difficult to observe with some HPLC and MS methods (discussed in Chapter 3).

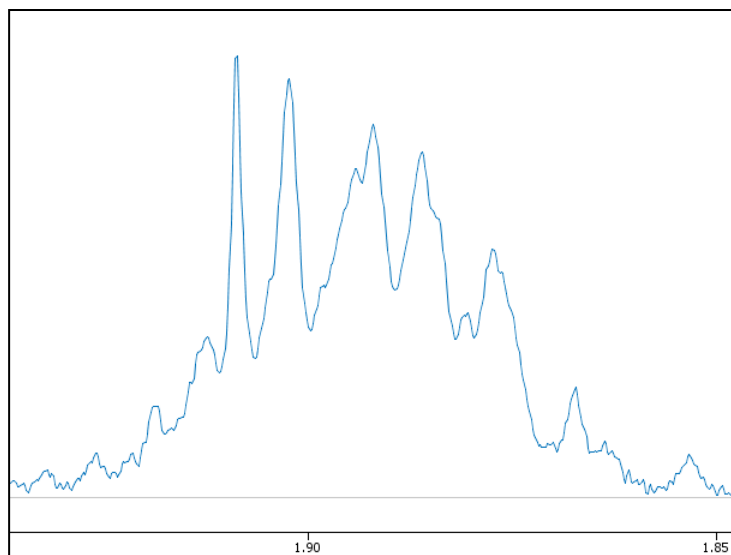


**Figure 12 – Convoluted Spectral Peaks 1D-<sup>1</sup>H-NMR**

Initially, an FID spectrum will possess areas of overlapping peaks, representing hydrogen atoms bonded to particular metabolites as shown in Figure 12. These ‘convoluted’ spectral patterns can be disentangled relatively easily by a software-assisted human profiler, as shown in Figure 13, where lysine, acetate and arginine are detected in the cluster.

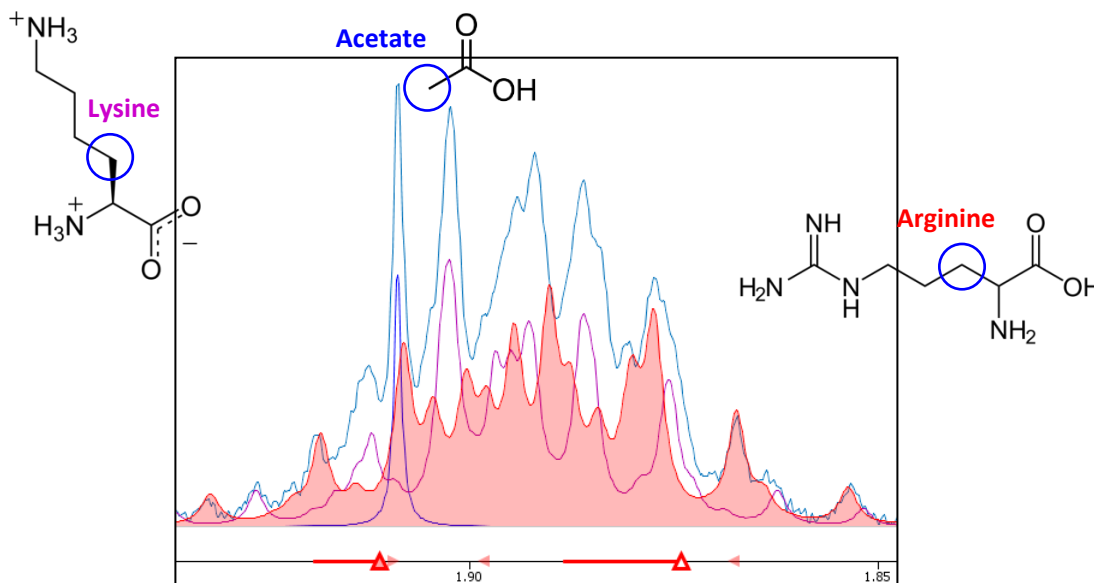


**Figure 13 – Targeted Profiling of Convoluted 1D-<sup>1</sup>H-NMR Spectra by Chemomx Software**

Quantification is achieved by nullifying the ‘subtraction line’ as shown in Figure 14, which represents area-difference between the ‘profile’ and the original spectrum.

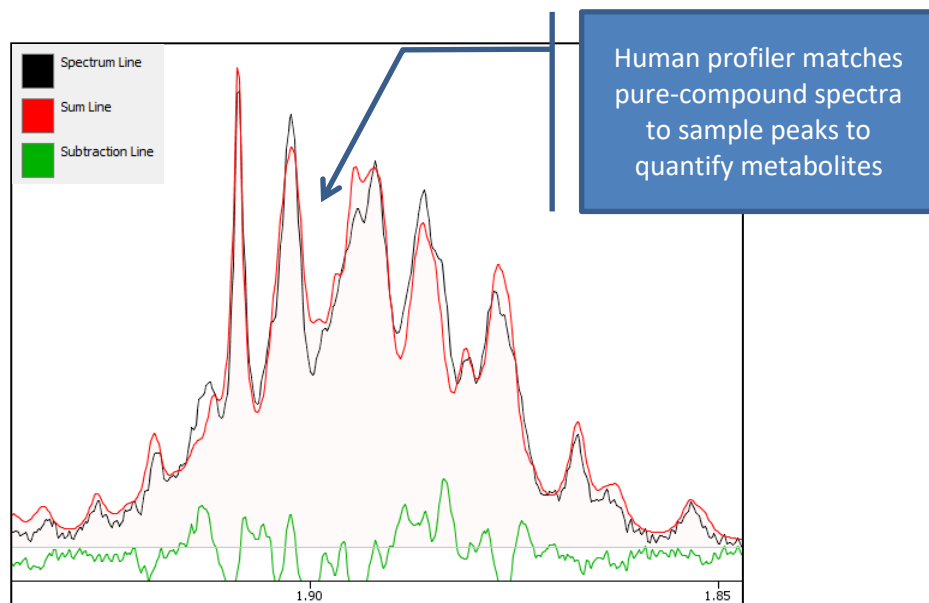


**Figure 14 – Quantification by Metabolites by Chenomx Software**

### **2.6.2.2 Mass Spectrometry (MS)**

Mass spectrometry (MS) in metabolomics, much like NMR, relies on an established library for deconvolution of species within a sample spectra for identification and quantification (as reviewed by Yi et al., 2016). MS methods generally observe a greater number of total metabolites compared to NMR; however the methods are often considered complementary and can be used together synergistically (Blondeel et al., 2015; Goudar et al., 2010). Various chromatography based MS methods have been employed by different research groups for analysis of metabolomics in mammalian cell cultures, including HPLC (Blondeel et al., 2015; Chong et al., 2009, 2010b; Dietmair et al., 2012), liquid chromatography MS (LC-MS) (Chong et al., 2012, 2010a; Goudar et al., 2010; Ma et al., 2009; Selvarasu et al., 2012; Zang et al., 2011), and gas chromatography MS (GC MS) (Chrysanthopoulos et al., 2010; Dietmair et al., 2012; Ma et al., 2009; Schaub et al., 2012; Sellick et al., 2011a).

Mass spectrometry metabolomics methods rely on various systems to ionize species, separate by mass, and subsequently analyze. Given the broad range of metabolites in any given cell culture system (i.e. aqueous, hydrophobic, volatile, etc.), different ionization and analysis schemes are necessary to observe different groups. Emwas provides a thorough comparison of different MS methods applied towards metabolomics, and compares their strengths and weaknesses against available NMR methods (Emwas, 2015).

### **2.6.3 Applications of Omics to Cell Culture**

#### **2.6.3.1 Growth Medium and Feeding Regimes**

One fundamental application of omics for mammalian cell culture is the optimization of growth medium, and post-inoculation nutrient feeding in the case of fed-batch processes. The majority of ingredients in media are detectable nutrients, and their patterns for uptake and consumption can reveal growth-limiting factors and accumulation of excreted toxic waste metabolites.

A challenge in recent decades for design of growth medium for mammalian cell culture is avoiding the practice of using ‘complex’ ingredients derived from animals or other biological systems (e.g. yeast cultures). Unlike ‘defined’ media components, complex supplements possess unquantifiable characteristics and create challenges for maintaining batch to batch consistency. Furthermore, in the case of supplements derived from animal products, there are contamination concerns from prions and viruses (as reviewed by Butler, 2004a). Despite reservations, the use of complex components in growth medium has persisted, because fully chemically defined media have historically underperformed in comparison. However, as noted in the work of Ma and colleagues, a limitation associated with complex supplements is that their digestion yields nutrients, vitamins and salts that are not optimized for the cells being cultured (Ma et al., 2009).

Therefore, as media designs improve, chemically defined options that are optimized for cultured cells will ultimately achieve better results. Ma and colleagues achieved this with metabolomics methods, creating a chemically defined medium for GS-amplified CHO and NS0 bioprocesses previously growing in non-animal derived hydrolysate-containing complex medium (Ma et al., 2009). The chemically defined medium achieved better growth and increases in protein titers of 80% and 115% for CHO and NS0 processes respectively. At the same time in applications where hydrolysates and complex components cannot be avoided, methods such as proteomics can provide a clear perspective on how these components shift phenotype (Kim et al., 2011). Such insights can provide further leads for ways to improve the growth and productivity of cultures, as well as engineer better platforms.

Another fundamental advantage of using omics methods for media design and optimization identified by Ma and colleagues was that rather than taking a conventional approach of starting at a basal medium and gradually adding nutrients, the researchers were able to perform a top-down approach. The medium design began with 90+ components, which were simultaneously monitored by metabolomics methods. Components were systematically removed until less than 40 components remained (Ma et al., 2009). Therefore, the final medium formulation was on par in terms of number of ingredients with several published basal mammalian growth media, such as modified Eagle's medium (DMEM, IMEM) (Eagle, 1955) and RPMI 1640 (Moore et al., 1967), while demonstrating fewer ingredients than other formulations such as Ham's F-12 (Ham, 1965) and 199 (Morgan et al., 1950) – as an aside, Morton provides an excellent accounting of recipes developed throughout the 20<sup>th</sup> century for defined culture medium (Morton, 1970). Ma and colleagues' 40 ingredient recipe is an important result, because the cost of growth medium is often a significant economic burden to mammalian cell culture processes, with a large expense

dedicated to complex ingredients (reviewed by Butler, 2004b). Furthermore, each additional component to a growth medium represents a possible source of vulnerability to the batch to batch consistency of commercial bioprocesses; the fewer components, the better.

A further key area for applying omics to design of media and nutrient feeds is identifying crucial growth or productivity-limiting factors. With advanced multivariate data analysis (MVDA) methods, experiments can take one very large data set to achieve significant advances in productivity (Schaub et al., 2012). Schaub and colleagues increased product titres from 5 to 8g/L in CHO cultures by applying knowledge from multivariate transcriptomics to metabolic models (Schaub et al., 2012).

Growth limiting nutrients can often be identified by observing which metabolites are depleted from the supernatant (as demonstrated in Chapter 3) or intracellular metabolite pools at major time points in the culture, such as when the cells are transitioning between exponential growth and stationary phase. Sellick and colleagues reported aspartate, asparagine and glutamate catabolism via truncated TCA interactions for a CHO culture producing IgG (Sellick et al., 2011a). By compensating for these depleting nutrients with a modified nutrient feed strategy, the system achieved an increase in biomass of 35% and more than doubled antibody titers. Culturing similar mammalian bioprocesses, Bradley and colleagues detected growth-limitations from histidine depletion (Bradley et al., 2010); Chong and colleagues detected depleted tryptophan and choline (Chong et al., 2009); and Dietmair and colleagues detected depleted CTP and UDP-glucuronic acid (Dietmair et al., 2012). While all four researchers were working with CHO cells – and, with the exception of Dietmair and colleagues, were producing an IgG protein product – the diversity of these results can be attributed to several factors, which commonly vary across mammalian cell culture bioprocesses. For instance, these experiments were all conducted with



different proprietary media, separate subtypes of CHO cell lines (i.e. K1, DG44, Dukx), different selection markers and amplification strategies (i.e. DHFR, GS, hMT-IIA), and different bioreactor scales. Determining these differences can be difficult in some cases as many publications, particularly those originating from industry research groups, routinely fail to disclose information about their expression system and cell-line origins beyond the fact that the cells are “CHO”. However, this ultimately illustrates the strength of multiple omics methods, such as metabolomics and proteomics, for optimizing cell culture bioprocesses and growth medium, because it remains capable of detecting bottlenecks in cellular infrastructure across varied production platforms.

### **2.6.3.2 Flux Modeling**

Omics methods can provide complementary tools towards flux modeling. This was well illustrated by Fernandes and colleagues, who utilized isotopic labeled  $^{13}\text{C}$  glutamine and metabolomics methods to observe a fed-batch process, developing a dynamic model of CHO major metabolic pathways (Fernandes et al., 2016). Similarly, Selvarasu and colleagues employed both footprinting and fingerprinting metabolomics data to achieve greater model complexity and better identifying growth limiting pathways linked to glutathione, and glycerophospholipid synthesis (Selvarasu et al., 2012). Given limitations to intracellular metabolomic profiling (i.e. ‘fingerprinting’), flux modeling can offer an alternative means of characterizing intracellular metabolism and potential bottlenecks. This is typified by Schaub and colleagues’ use of ‘footprinting’ for extracellular metabolomic analysis, coupled with transcriptomics and an intracellular flux model as a process-control strategy (Schaub et al., 2012). In this particular instance, flux modeling reached similar conclusions to the fingerprinting heuristic approach of Sellick and colleagues, recognizing the value of “coupling of amino acid

metabolism to the citrate cycle” (Sellick et al., 2011a). With these and similar realizations on CHO metabolism, Schaub and colleagues increased their titers from 4.9 to 7.9 g/L (Schaub et al., 2012).

### **2.6.3.3 Phenotype Consistency**

Of major concern in bioprocess engineering is maintaining phenotype consistency of cultured cells to prevent batch-to-batch variation. Phenotype refers to the observable physical characteristics resulting from gene expression and cellular responses to environmental factors. Conventionally, measuring cell phenotype was limited to factors such as cell growth, viability, productivity, and the consumption/excretion of select metabolites. However, with the advent of ‘omics methods, measuring variation in the cell phenotype of cultured cells has the potential to be extended to include the global metabolic profile and the up/down regulation of proteins (i.e. metabolomics, and proteomics). Major areas in bioprocesses vulnerable to shifts in cell phenotype producing batch-to-batch variation include: cell aging in perfusion and chemostat reactors; scaling up a bioprocess to larger volumes; process alterations; spontaneous loss of recombinant genes of interest and silencing in stable expression systems; and spontaneous mutations. Regarding batch to batch variation, cell aging and bioprocess scale-up, each of these circumstances was investigated by Chrysanthopoulos and colleagues, who successfully employed global metabolomics profiling to analyze variation in six perfusion bioreactors growing BHK cells (Chrysanthopoulos et al., 2010). Four of the reactors were “lab-scale” and two were “manufacturing-scale”, operated over a course of approximately 150 days each. Clear shifts in global metabolic phenotype were observed for all three investigated factors by observing the metabolic profile data using principle component analysis (PCA) and hierarchical clustering (HCL) (Chrysanthopoulos et al., 2010).

Similar observations of metabolomic profile shifts for a fed-batch scale-up of CHO-DG44 cells from a 7L to 5000L bioreactor process were observed by Aranibar and colleagues, with greater reliance on glycolysis in scale-up, as typified by more rapid depletion of glucose and galactose, but lower accumulation of TCA intermediates; these shifts were hypothesized to be linked to poorer DO transfer at larger scale (Aranibar et al., 2011). Regarding phenotype shifts for process changes, Aranibar and colleagues also observed whether metabolism would be significantly shifted with the introduction of the anti-apoptotic agent dextran sulfate. The researchers reported a significant shift in the metabolism of 28 separate metabolites, including amino acids, TCA intermediates and nucleotide precursors (Aranibar et al., 2011).

Regarding observations of batch-to-batch variation, Schaub and colleagues monitored a total of 45 bioreactors (9 process generations of 3 parallel fermentations), profiling the nine highest performing amongst them for correlations between productivity, metabolite consumption patterns and up/down regulation of genes (Schaub et al., 2012).

#### **2.6.3.4 Gene Overexpression**

Metabolomic analysis can reveal a lack of uptake of certain nutrients by cells, often characteristic of the cells not requiring the nutrient, or excretion and accumulation of waste metabolites. In the former case, this can be indicative of a bottleneck either in transport or metabolism caused by under-expression of necessary enzymes and transport proteins needed to properly digest the nutrient. In the latter case, it may be over-feeding of the nutrient, leading to toxic effects like apoptosis (Chong et al., 2009). Similarly to lack of nutrient consumption, it has been hypothesized that some of these excretions, particularly those of TCA intermediates such as malate, are the result of under-expressed enzymes (Chong et al., 2010a; Dietmair et al., 2012; Ma et al., 2009). Under-expression of certain enzymes can also be observed by an over-accumulation

within intracellular metabolite pools of bottlenecked intermediates, often leading to their excretion from the cell. Malate is metabolised by several enzymes including malate dehydrogenase II (MDH-II) in the mitochondrion as part of the TCA cycle (Chong et al., 2010a), and by MDH-I and malic enzyme in the cytosol (as reviewed by Schaub et al., 2012). Malic enzyme acts in the cytosol and uses malate as a substrate to regenerate pyruvate, producing NADPH in the process. MDH-I&II mediate the conversions between oxaloacetate and malate in the cytosol and mitochondria respectively. Chong and colleagues put forward the hypothesis that the excretions of malate were due to an accumulation in intracellular pools, caused by under-regulation of the MDH-II enzyme within the mitochondrion, which results in a bottleneck. By over-expressing MDH-II in CHO cultures, Chong and colleagues were able to achieve a 3-fold increase in intracellular ATP and NADH levels, a 1.9-fold increase in integral viable cell density, a 1.2-fold increase in protein titer, and a 40% reduction in malate and lactate secretions by the cells (Chong et al., 2010a).

While the approach for selection of an enzyme target by Chong et al., is a heuristic one, the selection of gene-targets for over-expression can also be achieved more systematically, as demonstrated by Schaub and colleagues, where metabolomic and transcriptomic data were correlated from high-producing batches to identify 247 deregulated genes linked to culture productivity (Schaub et al., 2012).

## **2.6.4 Quenching & Extraction**

### **2.6.4.1 Metabolites**

Metabolomic fingerprinting of the endometabolome possesses numerous challenges to ensure consistency and reliability of results. A significant concern for intracellular profiling is the issue that certain metabolites are extremely labile with rapid turnover rates (Sellick et al., 2011b).

During sampling, active enzymes in cells will deplete certain intracellular pools, and expand others, before removal of supernatant, rinsing, and conventional cell-lysing procedures can be enacted. This will result in skewed intracellular profiles with respect to the extracellular metabolites quantified from the supernatant at the matching time-point. In order to successfully extract intracellular metabolites, it is necessary to introduce a “quenching” procedure to denature these enzymes and protect intracellular metabolite pools.

Several options have been put forward for combinations of chemical and/or heat treatments to achieve this goal of reliable intracellular sampling. The two most popular options for mammalian cell culture quenching methods are those proposed by Sellick and colleagues, and Dietmair and colleagues (Dietmair et al., 2010; Sellick et al., 2009). In the former, the quenching protocol utilizes a 60% methanol solution buffered with ammonium bicarbonate (Sellick et al., 2009); however, a drawback of this method is that some cell-leakage is induced from prolonged exposure to the methanol in the solution. Indeed, 100% methanol is their proposed cell-lysing and extraction agent (Sellick et al., 2010). The researchers suggest that this can be mitigated by procedural efficiency (i.e. working faster). Dietmair and colleagues proposed an alternative quenching procedure, claiming less cell leakage, using cold 0.9% w/v NaCl saline solution (Dietmair et al., 2010). Sellick and colleagues responded reporting a direct comparison of the two methods, suggesting that despite cell-leakage, the actual quenching and denaturing of enzymes was better with their approach, citing increases in malate when profiling TCA intermediates from saline-quenched cells were due to enzymes remaining active (Sellick et al., 2011b). One clear advantage between the two procedures is that a methanol solution can be kept at far lower temperatures ( $-40^{\circ}\text{C}$ ) compared to a saline solution ( $\sim 4^{\circ}\text{C}$ ), which better halts any metabolic activity in the cells. Furthermore, this quenching protocol was demonstrated to better

preserve the intracellular metabolite pools of nucleotide sugars, the precursors for glycosylation (Braasch et al., 2015). Regarding subsequent metabolite extraction, similarly with quenching, a diverse series of procedures have been proposed by the same authors (Dietmair et al., 2010; Sellick et al., 2010). To remove the extraction solution, researchers typically apply some variation of lyophilisation treatment or evaporation on ice in a nitrogen atmosphere to capture aqueous metabolites.

Of significant concern regarding metabolomics research is a lack of standardized accepted practices, particularly with regards to quenching and extraction procedures, though acetonitrile-based extraction protocols have been demonstrated to be the most reliable of late (Lu et al., 2017). Several groups have previously employed variations of the procedures discussed in this section, some eschewing any quench at all (Aranibar et al., 2011; Goudar et al., 2010), opting instead to utilize flux modeling (Schaub et al., 2012), or selecting another omics methods for providing an intracellular perspective (demonstrated in Chapter 3).

#### **2.6.4.2 Proteins**

Unlike the metabolome, or transcriptome, the proteome doesn't suffer unduly from labile species, and halting the processes of enzymes is sufficient to preserve a sample for analysis. As such, cells can be centrifuged and pelleted, while a cell lysis and extraction protocol detailed in Chapter 3 can recover a broad range of proteins.

## **Chapter 3 An omics approach to rational feed: Enhancing growth in CHO cultures with NMR metabolomics and 2D-DIGE proteomics<sup>1</sup>**

### **3.1 Overview**

Expression of recombinant proteins exerts stress on cell culture systems, affecting the expression of endogenous proteins, and contributing to the depletion of nutrients and accumulation of waste metabolites. In this work, 2D-DIGE proteomics was employed to analyze differential expression of proteins following stable transfection of a Chinese Hamster Ovary (CHO) cell line to constitutively express a heavy-chain monoclonal antibody. Thirty-four proteins of significant differential expression were identified and cross-referenced with cellular functions and metabolic pathways to identify points of cell stress. Subsequently, 1D-<sup>1</sup>H-NMR metabolomics experiments analyzed cultures to observe nutrient depletion and waste metabolite accumulations to further examine these cell stresses and pathways. From among fifty metabolites tracked in time-course, eight were observed to be completely depleted from the production media, including: glucose, glutamine, proline, serine, cystine, asparagine, choline, and hypoxanthine, while twenty-three excreted metabolites were also observed to accumulate. The differentially expressed proteins, as well as the nutrient depletion and accumulation of these metabolites corresponded with upregulated pathways and cell systems related to anaplerotic TCA-replenishment, NADH/NADPH replenishment, tetrahydrofolate cycle C1 cofactor conversions, limitations to lipid synthesis, and redox modulation. A nutrient cocktail was

---

<sup>1</sup> This is an accepted manuscript of an article published by Elsevier in the Journal of Biotechnology on September 20, 2016, available online: <https://www.sciencedirect.com/science/article/pii/S0168165616314377>. Blondeel, E.J.M., Ho, R., Schulze, S., Sokolenko, S., Guillemette, S.R., Slivac, I., Durocher, Y., Guillemette, J.G.G., McConkey, B.J., Chang, D., Aucoin, M.G., “An omics approach to rational feed: Enhancing growth in CHO cultures with NMR metabolomics and 2D-DIGE proteomics”

assembled to improve the growth medium and alleviate these cell stresses to achieve a ~75% improvement to peak cell densities.

Keywords: CHO cells; 2D-DIGE; Proteomics; NMR; Metabolomics

## **3.2 Introduction**

The majority of recombinant therapeutic glycosylated biologics are produced in Chinese Hamster Ovary (CHO) cell lines (Ghaderi et al., 2012). Expression of these recombinant proteins draws energy and resources away from the endogenous cellular systems and infrastructure. Strategies to mitigate these stresses and maximize cell growth and productivity include optimization of growth medium and nutrient feeding (D. Y. Kim et al., 2012; Kim et al., 2005; Kim and Lee, 2009; Lee et al., 1999; Ma et al., 2009; Sellick et al., 2011a; Xing et al., 2011).

Growth medium, while historically relying on ‘complex’ components with somewhat unknown content such as serum and hydrolysates, has trended towards ‘fully chemically defined’ formulations. Switching to fully chemically defined growth medium (CDM) was motivated by high component costs, batch-to-batch ingredient variation, and most notably the potential for contamination from mycoplasma, prions, and viruses from fetal bovine serum (as reviewed by Butler, 2013). Non-animal derived complex components, such as hydrolysates derived from soy, wheat, gluten and yeast, while removing many of these concerns, remain ‘black boxes’ for process optimization. Approximately 450 commercial ‘off the shelf’ serum-free growth media are available on the market for various animal cell types (as reviewed by van der Valk et al., 2010). However, commercial growth medium can be very expensive at production scale, and for any given bioprocess, a host of factors including but not limited to: the choice of cell-line and cell-line derivative, clone selection, gene-amplification strategy, the recombinant protein



expressed, and production scale will impact cellular metabolism and how successful an ‘off the shelf’ growth medium will be, necessitating some level of tailored optimization.

Process and growth medium optimization can often be accomplished empirically in a ‘blind’ manner with multivariate methods, or by attempting to utilize simulation. However, omics methods such as proteomics and metabolomics provide an exciting opportunity to look under-the-hood of a bioprocess and make real determinations of cell stresses and system limitations for cells expressing recombinant proteins.

Omics methods have been well utilized to enhance culture growth by investigating a broad spectrum of nutrients and excreted metabolites through classical analytical chemistry methods, including liquid chromatography mass spectrometry (LC-MS) (Chong et al., 2009, 2010b; Ma et al., 2009; Selvarasu et al., 2012) and/or gas chromatography mass spectrometry (GC-MS) (Dietmair et al., 2012; Ma et al., 2009; Schaub et al., 2012; Sellick et al., 2011a) as well as NMR-based methods (Aranibar et al., 2011; Bradley et al., 2010; Carinhas et al., 2013; Goudar et al., 2010; Read et al., 2013; Sokolenko et al., 2014). NMR possesses several advantages such as ease of sampling, which is rapid and non-destructive (as reviewed by Sokolenko et al., 2014). Further, NMR is useful for detecting volatile organic acid metabolites, which are not observable by some conventional HPLC and MS methods, and have only recently been reported in CHO cells by metabolomics researchers employing NMR (Aranibar et al., 2011; Bradley et al., 2010; Carinhas et al., 2013; Sokolenko et al., 2014).

In this work, a proteomics analysis by two dimensional in-gel electrophoresis (2D-DIGE) was conducted between a parental CHO cell line and a stably transfected derivative cell line expressing a single-domain chimeric heavy chain camelid-derived antibody (EG2-hFc) (Agrawal et al., 2012) to measure differential expression of endogenous cellular proteins. Subsequently, a

metabolomics analysis of cell culture supernatant from cells stably producing EG2-hFc grown in CDM, by targeted profiling of 1D-<sup>1</sup>H-NMR spectra, was conducted to measure depleted nutrients and the accumulation of excreted metabolites. Together, these omics methods were utilized to evaluate the system stresses of the CHO cells and to tailor production growth medium to maximize the cell growth of the cultures. The production growth medium was supplemented with nutrients corresponding to four reported metabolic systems in CHO cells that were up-regulated after gaining the ability to produce EG2-hFc. These pathways related to anaplerotic TCA-replenishment, NADH/NADPH replenishment, tetrahydrofolate cycle C1 cofactor conversions, limitations to lipid synthesis, and redox modulation.

### **3.3 Materials & Methods**

#### **3.3.1 Cell Line**

DXB11-derived CHO<sup>BRI</sup>-1A7 cells, negative for dihydrofolate reductase (DHFR-), were transfected with pTT44-EG2hFc1 to stably express the 80 kDa single-domain chimeric heavy-chain monoclonal antibody EG2-hFc (Agrawal et al., 2012). Briefly, EG2-hFc cDNA was cloned into pTT44, a modified pTT5 vector (Durocher et al., 2002) containing a puromycin expression cassette, under the control of a cytomegalovirus (CMV) promoter. The parental strain of CHO<sup>BRI</sup> cells was transfected with the linearized construct pTT44-EG2hFc1 using PEI<sub>max</sub> in 2 ml of CD DG44 media (Invitrogen, ON, Canada), and puromycin selection was applied (10 µg/ml) until the pool of resistant transfectants finally reached ~80+% viability. Single cell dilution in 96-well plates was applied to isolate the best-producing clone, called CHO<sup>BRI</sup>-1A7.

### **3.3.2 2D-DIGE Proteomics Experiments**

#### **3.3.2.1 Cell Culture**

Culture supernatant samples from parental CHO<sup>BRI</sup> cells and the newly established CHO<sup>BRI</sup>-1A7 cell line that constitutively produces EG2-hFc were harvested after 8 days of batch cultivation. Six parallel cultures were carried out in 250 mL polycarbonate shaker flasks (Corning, NY, USA) for both cell lines with PowerCHO-2CD growth medium (Lonza, NY, USA). The shaker flasks, each containing 60 mL, were grown at 37°C with 5% CO<sub>2</sub>, with an agitation speed of 120 rpm for eight days. Both cell lines and their replicates were grown under the same culture conditions. On day 8, culture supernatant samples were harvested and filtered via 0.45 µm membrane. Cell pellets were collected and kept frozen until analysis.

#### **3.3.2.2 Cell Lysis & Protein Extraction**

Approximately  $2 \times 10^7$  cells were harvested from cultures after 8 days of batch cultivation and pelleted at 1000 rpm (~250 rcf) for 5 minutes and stored at -80°C. Cell pellets were subsequently resuspended and washed three times with sterile ice cold 1X PBS solution. Following washing, cell pellets were resuspended in 500 µL of lysis buffer at 4°C, containing 7M urea, 2M thiourea, 50mM Tris pH 8.0, and 4% CHAPS (Fisher, ON, Canada). The lysis buffer also included 15µL protease inhibitor cocktail (Sigma, ON, Canada). The cells in lysis buffer were subsequently vortexed and sonicated twice for 30 seconds using a Microson Ultrasonic Cell Disruptor (Misonix, NY, USA) at a power level of 4 at 4°C. Following sonication, the samples were incubated on a rotator at 4°C for 3.5 hours to ensure complete lysis. The samples were then centrifuged for 30 minutes at 14,000 rpm (22000 rcf) at 4°C to remove insoluble cell debris. Supernatant was recovered and any further interfering substances were removed via an Amersham 2-D Clean-Up Kit (GE Healthcare, Uppsala, Sweden). Protein concentrations were

determined using a Bio-Rad protein assay (Bio-Rad Laboratoris Ltd., ON, Canada) with bovine serum albumin (BSA) (Sigma, ON, Canada) utilized as the standard. Protein samples and BSA standards were measured in triplicate at an absorbance of 595 nm with a Varian Cary 50 Bio UV-Vis Spectrophotometer (Varian, QC, Canada).

### **3.3.2.3 2D Differential In-Gel Electrophoresis (2D-DIGE)**

Six biological replicate gels were prepared for comparative proteomic analysis between CHO<sup>BRI</sup>-1A7 and parental CHO<sup>BRI</sup> cell cultures. Each of six gels contained one CHO<sup>BRI</sup>-1A7 and one CHO<sup>BRI</sup> sample replicate. A dye swap procedure was employed, where gels 1-3 used a Cy5 label for CHO<sup>BRI</sup> and a Cy3 label for CHO<sup>BRI</sup>-1A7, and gels 4-6 reversed the Cy3 and Cy5 labels; CyDye DIGE Fluor minimal dye (GE Healthcare, Uppsala, Sweden). 50 µg of each protein sample was labeled with 1µL of 200 pmol/µL CyDye DIGE Fluor minimal dye. Following incubation with 10 mM lysine stop solution, samples were combined with rehydration buffer containing 7M urea, 2M thiourea, 4% CHAPS, and 20 mM dithiothreitol (DTT) (Fisher, ON, Canada), and 0.5% immobilized pH gradient buffer ampholytes (GE Healthcare, Uppsala, Sweden). Protein samples in rehydration buffer were applied to Immobiline Drystrips, pH 3-10NL; 24 cm immobilized pH gradient (IPG) gel strips (GE Healthcare, Uppsala, Sweden) with a total volume of 450 µL per strip and incubated overnight.

Isoelectric focusing (IEF) for first-dimension separation was performed using an *Ettan IPGphor II system* (GE Healthcare, Uppsala, Sweden) at 20°C for 24 hours with the following voltage program: 100V (1 h), step increase to 500V (2 h), gradient to 1000V (2 h), gradient to 3000V (3 h), gradient to 8000V (3 h), hold at 8000V (10 h), hold at 500 V prior to second dimension separation (~ 3 h). Following completion of IEF, the strips were reduced in 10 mL of pH 8.8 equilibration buffer containing 6M urea, 30% glycerol, 50 mM Tris (Fisher, ON,

Canada), and 2% SDS (BioShop Canada Inc., ON, Canada) with 1% w/v DTT (Fisher, ON, Canada) for 15 minutes. This was followed by alkylation in 10mL equilibration buffer with 2.5% w/v iodoacetamide (IAA) (Sigma, ON, Canada) for 15 minutes.

The second dimension separation was run on large format 12% SDS-PAGE gels using a *DALTSix Electrophoresis unit* (GE Healthcare, Uppsala, Sweden). IPG strips were placed on top of each of six gels with an agarose sealing solution containing 25mM Tris base, 192mM glycine (Fisher, ON, Canada), 0.1% SDS, 0.5% agarose (BioShop Canada Inc., ON, Canada), and 0.002% (w/v) bromophenol blue (Fisher, ON, Canada). The six gel plate sandwiches were placed into the cassette carrier. and the electrophoresis unit was filled with 4.5 L of 1X running buffer containing 25mM Tris base, 192mM glycine (Fisher, ON, Canada), and 0.1% SDS (BioShop Canada Inc., ON, Canada), cooled to 10°C using a MultiTemp III Thermostatic Circulator (GE Healthcare, Uppsala, Sweden). The upper buffer chamber was filled with 2X running buffer containing 50 mM Tris base, 384mM glycine (Fisher, ON, Canada), and 0.2% (w/v) SDS (BioShop Canada Inc., ON, Canada). Electrophoresis was carried out at 1 watt/gel for 30 minutes followed by an increase to 18 watts/gel until the dye front reached the bottom of the gel.

#### **3.3.2.4 Gel Scanning & Analysis**

2D-DIGE gels were scanned under fluorescence acquisition mode using a Typhoon 9400 scanner (GE Healthcare, Uppsala, Sweden). All the resulting gel images were cropped to the same size using PDQuest Advanced 2D Analysis Software v8.0.1 (Bio-Rad Laboratories LTD, ON, Canada) and then uploaded into DeCyder v7.0 software (GE Healthcare, Uppsala, Sweden). The gel images were first processed in the DeCyder Differential In-Gel Analysis (DIA) module by detecting the number of spots per gel image. Gel-to-gel matching was then performed by matching detected spots across all gel images using the DeCyder Biological Variation Analysis

(BVA) module. Only spots that matched across all six replicate gels were considered. In parallel with the DIGE labelled gels, matching preparative gels containing approximately 800 µg of protein were separated by 2D-SDS-PAGE. Gels were fixed with 50% methanol/10% acetic acid for 10 minutes and stained overnight with *GelCode® Blue Stain Reagent* (Thermo Scientific, ON, Canada), followed by destaining for 5 hours in ultrapure water.

Differences in protein abundance were assessed based on the intensity ratios of the paired samples and normalized to remove any dye-bias. Relative spot intensity levels were extracted from DeCyder v7.0 and imported into the software package R v2.12.0 for statistical analysis. Once adjusted and log-transformed, the relative spot intensity levels were subjected to a paired t-test and an initial list of p-values was produced. This list was subjected to a False Discovery Rate (FDR) test (Benjamini and Hochberg, 1995), where proteins were considered differentially expressed based on a p-value cut-off corresponding to a calculated FDR of 10%. Differential expression data is shown as fold change, with positive values representing an increase in abundance and negative values representing a decrease relative to controls. If more than one spot shared a common protein identification (e.g. where multiple isoforms were present), fold change results for the most abundant differentially expressed isoform are reported.

### **3.3.2.5 Protein Identification by Mass Spectrometry**

Protein spots that showed statistically significant differential expression between CHO<sup>BRI</sup> and CHO<sup>BRI</sup>-1A7 were excised from coomassie-stained preparative gels using an *EXQuest Spot Cutter* (Bio-Rad Laboratories LTD, ON, Canada). Excised spots were subjected to in-gel tryptic digestion followed by LC-MS/MS analysis. The gel pieces were washed twice with 50 mM ammonium bicarbonate (NH<sub>4</sub>HCO<sub>3</sub>) and destained with 50% acetonitrile (ACN)/25 mM NH<sub>4</sub>HCO<sub>3</sub>. The proteins were then reduced with 10 mM DTT for 30 minutes at 56°C followed

by alkylation with 100 mM IAA for 15 minutes in the dark at room temperature. Protein digestion was carried out with the addition of 13 ng/ $\mu$ L sequencing grade modified trypsin (Promega Corporation, Madison, Wisconsin) in 50 mM  $\text{NH}_4\text{HCO}_3$  and incubated overnight at 37°C. The peptides were extracted with 5% formic acid and 100% ACN, evaporated to dryness then reconstituted in 5  $\mu$ L of 0.1% formic acid. The digested peptides were sent to the Hospital for Sick Children Mass Spectrometry Facility (ON, Canada) for mass spectrometry (LC-MS/MS) analysis. The samples were loaded onto a 150 $\mu$ m ID Magic C18 pre-column (Michrom Biosciences, CA, USA) at 4  $\mu$ L/min and separated over a 75  $\mu$ m ID analytical column. Using an EASY n-LC nano-chromatography pump (Proxeon Biosystems, Odense, Denmark), the peptides were eluted over 60 minutes at 300 nL/min in a 0 to 40% acetonitrile gradient in 0.1% formic acid (Fisher, ON, Canada). The peptides were eluted into a LTQ linear ion trap mass spectrometer (Thermo-Fisher, CA, USA) operated in a data dependent mode. Six MS/MS scans were obtained per MS cycle.

#### **3.3.2.6 Database Protein Identification**

Protein identification was performed using PEAKS Studio v5.3 (Bioinformatics Solutions Inc., ON, Canada), which combines auto *de novo* sequencing with database searching, and the results of two search engines: PEAKS DB and X!Tandem. All mass spectra were searched against the CHO protein database (Xu et al., 2011). Search results were evaluated on a percentage score system, and FDR was also applied and estimated with decoy sequences. Protein identification was considered successful when the protein score was  $\geq 90\%$  with  $\geq 2$  unique peptides and an FDR below 1%. Additionally, at least 2 unique peptides also needed to be identified in the X!Tandem search engine. For some samples, there was more than one confident protein ID. The molecular weight (MW) and isoelectric points (pI) of these protein IDs were then

compared with their relative spot locations on the gel to manually confirm and/or reject their identification.

The resulting gene list of differentially expressed proteins was searched against DAVID (database for annotation, visualization, and integrated discovery (Huang et al., 2009a, 2009b)). The Functional Annotation Clustering tool found within DAVID was used to cluster enriched related terms for identifying related functions and pathways.

### **3.3.3 NMR Metabolomics Experiments**

#### **3.3.3.1 Cell Culture**

Flask experiments were conducted in 125 mL polycarbonate shaker flasks (Corning Inc.), while bioreactor experiments were conducted in a 3L bioreactor (Applikon Biotechnology Inc., CA, USA). All cultures were grown at 37°C, with an agitation speed of 120rpm. Samples were stored at -80°C. Cell density measurements were observed for bioreactor experiments with trypan-blue exclusion by haemocytometer and by a Coulter Counter Z2 (Beckman-Coulter, FL, USA), while flask experiments were counted exclusively via the Coulter Counter.

#### **3.3.3.2 Growth Medium & Supplemented Nutrients**

Cells were grown in serum-free BioGro-CHO (BioGro Technologies Inc., MB, Canada). Unless noted otherwise, all chemicals were purchased from Sigma-Aldrich (MT, USA). L-asparagine (Asn), choline chloride (Chol) (Alfa Aesar, Lancashire, England), L-cysteine (Cys), L-proline (Pro) and L-serine (Ser) were prepared as 100mM stock solutions. D-glucose (Glc) (Life Technologies, Carlsbad, CA, USA) was prepared as a 1M stock solution. All stock solutions were sterile filtered using a 0.2µm filter (Millipore Millex-GP, MA, USA). 200mM L-



glutamine (Gln) and 10mM hypoxanthine (Hyp) with 1.6mM thymidine, HT supplement (Life Technologies, CA, USA), were purchased as liquid stock solutions.

### 3.3.3.3 Metabolite Profiling

NMR spectra were acquired with a Bruker Avance 600MHz spectrometer with a TXI 600 probe. Following acquisition, spectra were imported into Chenomx NMR Suite 7.7 (Chenomx Inc., AB, Canada) and manually profiled (Sokolenko et al., 2014). All compounds were quantified with the software's built-in 600MHz compound library, with the exception of GlutaMAX™, which was added using the Chenomx NMR Suite 7.7's 'compound builder' tool. Ammonia measurements were taken using an Orion Star™ Plus ISE Meter (Thermo-Fisher, CA, USA).

## 3.4 Results

A combined omics approach was utilized to analyze the system stresses to CHO cells transfected to express a recombinant monoclonal antibody. A comparative proteomic analysis conducted between the EG2-hFc expressing CHO<sup>BRI</sup>-1A7 cells and the non-producing parental strain CHO<sup>BRI</sup> was conducted by 2D-DIGE (Figure 15), and a total of 34 proteins of significant differential expression were identified (Table 4). The cellular functions and metabolic pathways affected by recombinant protein expression of EG2-hFc were identified (Table 5).

Subsequently, a 1D-<sup>1</sup>H-NMR metabolomics analysis was conducted on CHO<sup>BRI</sup>-1A7 cultures and monitored for depleted nutrients and accumulated waste metabolites. Considering these metabolic trends and examining the differentially regulated metabolic enzymes of Table 4, four cellular metabolic systems were considered for potential impact to cell growth, including: anaplerotic TCA-replenishment (Figure 16), tetrahydrofolate cycle C1 cofactor conversions

(Figure 17), and limitations to lipid synthesis (Figure 18), and redox modulation. A nutrient cocktail was assembled based on the metabolic systems under stress (Table 6) and supplemented to the production growth medium (Figure 19), yielding a ~75% increase in maximum cell density of cultures (Figure 20).

### **3.4.1 2D DIGE Proteomics Analysis**

2D-DIGE gels were scanned and the relative quantities of proteins were measured by fluorescence. The gels were scanned at 580nm and 670nm corresponding to Cy3 and Cy5 channels respectively. A representative 2D-DIGE gel is shown in Figure 15. All gels showed consistent spot separation. Spot-matching was conducted both within gels, and between gels. The number of spots detected was similar across all gels, with a mean of  $1840 \pm 35$  spots. Of these, 912 protein spots were matched across all gels, and a total of 86 spots exhibited significant changes in abundance. These spots were excised and identified by LC-MS/MS. From among these 86 selected spots, 34 unique protein IDs were obtained (Table 4). The identified proteins were subsequently classified into five broad categories according to their biological function (Table 4).

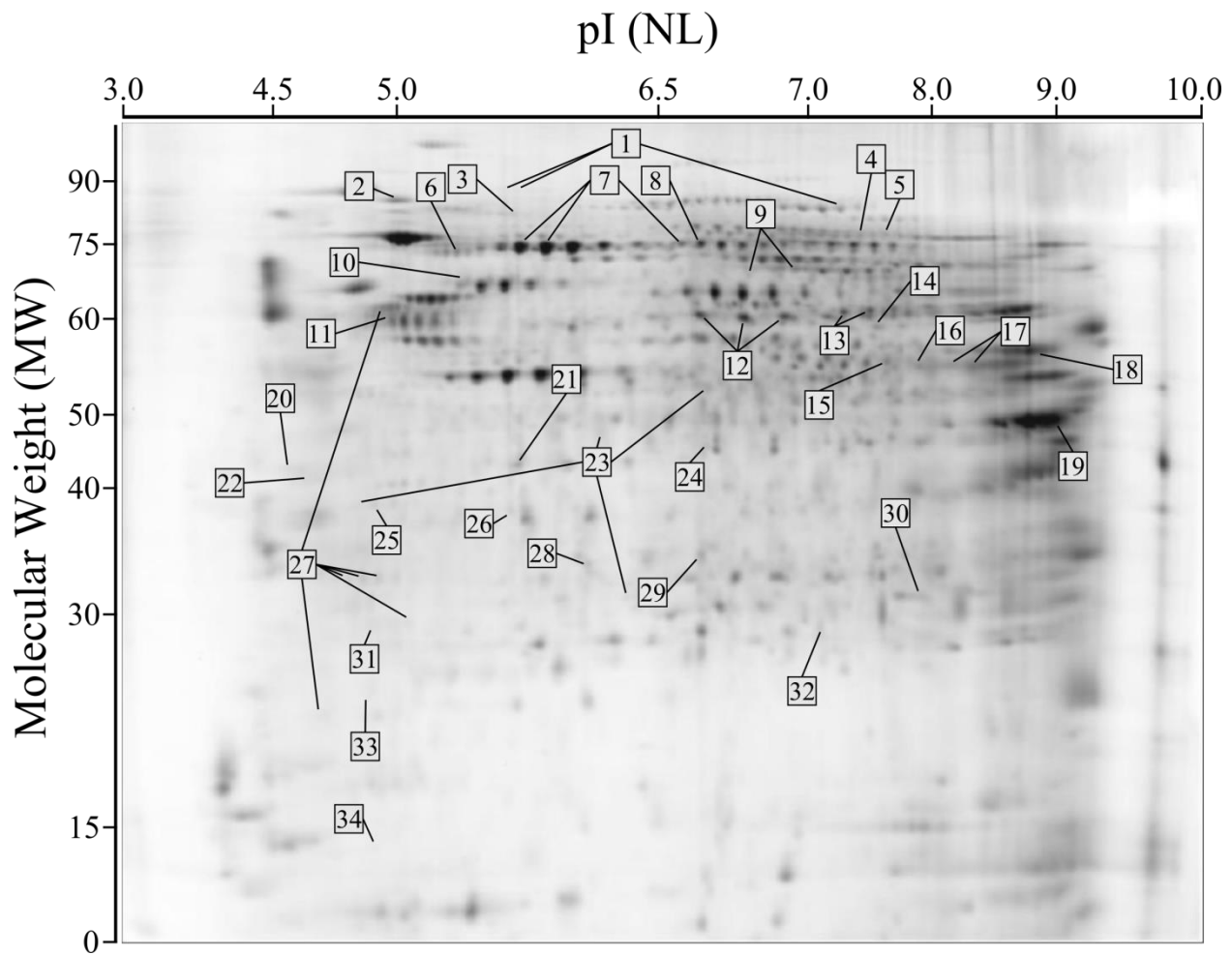


Figure 15 – Representative monochrome image of a 2D-DIGE Gel. CHO<sup>BRI</sup>-1 labeled with Cy5 and CHO<sup>BRI</sup>-1A7-1 labeled with Cy3.

Proteins were separated initially in the first dimension (x-axis) on a non-linear gradient pH 3-10 then separated in the second dimension (y-axis) on a 12% polyacrylamide gel. Green and red fluorescence were measured independently (532 nm for Cy3 and 635 nm for Cy5). From among 86 selected spots excised for LC-MS/MS analysis, 34 unique protein IDs were obtained (Table 9).

The proteins identified reflect observations of metabolic changes within the proteome of CHO<sup>BRI</sup>-1A7 as compared with that of parental cells. Enzymes involved in various metabolic processes shifted including: up-regulation of anaplerotic TCA cycle replenishment (Cs, Ast); NADH and NADPH replenishment including tetrahydrofolate conversions (Mthfd11, Aldh, Hsd17b10, Dld, Hibadh); lipid synthesis (Cs, Acot2, Gpd2); and energy metabolism (Abcg3, Ndufv1, Nfdufs3) (Table 4). Proteins involved in DNA repair, DNA replication and

transcription, apoptosis, and cellular respiration were also found to be differentially expressed. Certain heat shock proteins (Trap1, Grp75) were up-regulated whereas others (Hspd1, Hsp90aa1) were down-regulated. ER chaperones (Serpinh1, Grp94, and Pdia6) were differentially down-regulated in EG2-hFc producing cells. The up-regulation of Rplp0, a component involved in protein biosynthesis, was also observed while the majority of proteins (Actb, Vim, Lmn1, Chp) related to the structural integrity of the cell showed down-regulation.

**Table 4 – Differentially expressed proteins after transfection of CHO<sup>BRI</sup> cells to stably express EG2-hFc heavy-chain mAb, as identified by LC-MS/MS**

<b>Protein Name</b>	<b>Short Name</b>	<b>Figure 15 ID</b>	<b>Accession ID</b>	<b>Fold Change</b>	<b>Biological Process</b>
<b>Anaplerotic Replenishment &amp; TCA Cycle</b>					
Aconitate hydratase	Aco2	5	EGW13953	-1.12	TCA cycle
Citrate synthase	Cs	17	EGW12503	1.99	TCA cycle
Aspartate aminotransferase	Ast	19	EGW01755	1.21	Anaplerotic TCA metabolism
<b>NADH/NADPH Replenishment &amp; Tetrahydrofolate Conversions</b>					
Methylenetetrahydrofolate dehydrogenase	Mthfd11	1	EGV95936	1.09	Tetrahydrofolate (THF) cycle
Aldehyde dehydrogenase	Aldh	12	EGW07431	1.14	Oxidation of aldehydes to carboxylic acids
3-hydroxyacyl-CoA dehydrogenase type 2	Hsd17b10	30	EGW02330	1.11	Degradation of branched chain alpha-keto amino acids such as leucine isoleucine and valine
Dihydrolipoyl dehydrogenase	Dld	13	EGV93120	1.07	Catabolism of branch chain amino acids
3-hydroxyisobutyrate dehydrogenase	Hibadh	26	EGW08863	1.09	Amino acid catabolism
<b>Lipid Synthesis</b>					
Acyl-coenzyme A thioesterase 2	Acot2	15	EGW01631	1.21	Lipid metabolism
Procollagen-lysine, 2-oxoglutarate 5-dioxygenase 3	Plod3	4	EGW01863	-1.06	Hydroxylation of lysyl residues in collagen-like peptides
Glycerol-3-phosphate dehydrogenase	Gpd2	16	EGW05701	1.32	Lipid metabolism
<b>Energy Metabolism</b>					
ATP-binding cassette sub-family G, member 3	Abcg3	21	EGV92982	1.05	Peptide transporter
NADH dehydrogenase	Ndufv1	14	EGW12368	1.12	Oxidative phosphorylation
	Ndufs3	29	EGW03953	1.03	Oxidative phosphorylation
ATP Synthase subunit beta	Atp5b	11	EGW12490	-1.12	ATP synthesis
SPRY domain-containing protein 4	Spryd4	32	EGW12495	-1.20	Uncharacterized
<b>Apoptosis and Cell Proliferation</b>					
Proliferating cell nuclear antigen	Pcna	22	EGV92404	-1.20	Processivity factor eukaryotic DNA polymerase

Protein Name	Short Name	Figure 15 ID	Accession ID	Fold Change	Biological Process
Histone H2A type 1	Hist1h2ab	34	EGV96120	-1.25	Regulation of transcription, DNA repair, DNA replication, and chromosomal stability
DNA-directed RNA polymerase I, II, and III subunit RPABC1	Polr2e	28	EGV99483	1.17	DNA transcription
Prohibitin	Phb	3	EGW01773	1.12	Regulation of proliferation, inhibits DNA synthesis
Programmed cell death 6	Pdcd6	33	EGW09040	1.44	Induction of apoptosis by extracellular signal
<b>Chaperones &amp; Protein Synthesis</b>					
Heat shock 75 kDa protein	Trap1	8	EGV93626	1.05	Chaperone – protein folding
Heat shock 70 kDa protein 9	Grp75	7	EGW06687	1.11	Chaperone – protein folding
Heat shock 60 kDa protein	Hspd1	10	EGW00783	-1.06	Chaperone – protein folding
Heat shock protein HSP 90-alpha	Hsp90aa1	20	EGV94858	-1.38	Chaperone – protein folding
Serpin H1	Serpinh1	18	EGW02226	-1.14	Chaperone – collagen folding
Endoplasmic	GRP94	2	EGW09701	-1.57	Chaperone – protein processing and transport
60S Acidic Ribosomal protein P0	Rplp0	24	EGV93157	1.20	Protein synthesis
Protein disulfide-isomerase A6	Pdia6	25	EGW08481	-1.22	Chaperone – protein folding
<b>Structural Proteins</b>					
B-Actin	Actb	23	EGW06240	-1.25	Cytoskeleton component
Vimentin	Vim	27	EGW02055	-1.46	Intermediate filament, cell integrity
Lamin B1	Lmnb1	6	EGV92912	-1.7	Nuclear envelope framework
Lamin A	Lmna	9	EGW07066	1.10	Nuclear envelope framework
Calcium-binding protein p22	Chp	31	EGV97270	-1.18	Na <sup>+</sup> /H <sup>+</sup> ion pump regulation; intracellular pH, cytoskeletal organization

### 3.4.2 Cell Function Grouping

The compiled gene list of differentially expressed proteins identified by 2D-DIGE and LC-MS/MS was subjected to functional annotation analysis in DAVID to uncover enriched functionally related gene groups. An enrichment score was determined by a geometric mean of all the enrichment p-values of each annotation term in the group followed by a minus log transformation applied on the averaged p-values. The enrichment score is a relative score used to rank overall importance of annotation term groups. Three clusters of enriched gene ontology (EGO) terms were identified (Table 5). Cell responses to expression of EG2-hFc corresponded to

cell functions of energy generation (i.e. TCA cycle) and biosynthetic resources such as NADH/NADPH and redox activity. An expected increase in stresses related to additional protein folding and processing from EG2-hFc expression was also observed.

**Table 5 – Functional annotation analysis in DAVID enriched functionally related gene groups, associated with differentially expressed proteins. An enrichment score was determined by a geometric mean of all the enrichment p-values of each annotation term in the group followed by a minus log transformation applied on the averaged p-values. The enrichment score is a relative score used to rank overall importance of annotation term groups.**

Cluster	Enrichment Score	Cell Function	# of Genes Involved	p-value
1	3.08	NAD	6	1.40E-05
		Generation of precursor metabolites and energy	6	2.40E-04
		Oxidoreductase activity, acting on NADH or NADPH	3	5.90E-03
		Electron transport chain	3	2.50E-02
2	2.98	Chaperone	6	7.70E-06
		Unfolded protein binding	5	1.70E-05
		Stress response	4	7.70E-05
		Protein folding	5	1.70E-04
3	2.39	Generation of precursor metabolites and energy	6	2.40E-04
		Cellular respiration	3	7.50E-03
		Citrate cycle (TCA cycle)	3	7.80E-03
		Energy derivation by oxidation of organic compounds	3	2.00E-02

### 3.4.3 1D-<sup>1</sup>H-NMR Metabolomics Analysis

A metabolomic analysis by 1D-<sup>1</sup>H-NMR tracked fifty compounds in time-course for CHO cells cultivated in a 3L bioreactor (see supplementary data in Appendix A). Of these, more than forty compounds were found to have a significant correlation to time using a Spearman rank correlation coefficient at a 95% confidence level. Eight nutrients, shown in Figure 19, were observed to be fully depleted during culturing.

Metabolic enzymes identified in Table 4 involving upregulation of anaplerotic TCA cycle replenishment (+1.21 fold Cs, +1.99 fold Ast), corresponded with depletions in asparagine, proline, glutamine, aspartate and pyruvate, as well as accumulation of ammonia, lactate, citrate, and malate in the supernatant (Figure 16). Cellular processes identified in Table 5 for replenishing NADH and NADPH paralleled depletions in serine and accumulation of excreted glycine and formate via tetrahydrofolate conversions (+1.09 fold Mthfd11) (Figure 17). Upregulation of enzymes for lipid metabolism (+1.32 fold Gpd2, +1.21 fold Acot2), corresponded with depletions in choline, as well as the accumulation of excreted lipid precursors glycerol, O-phosphocholine, and cytidine (Figure 18).

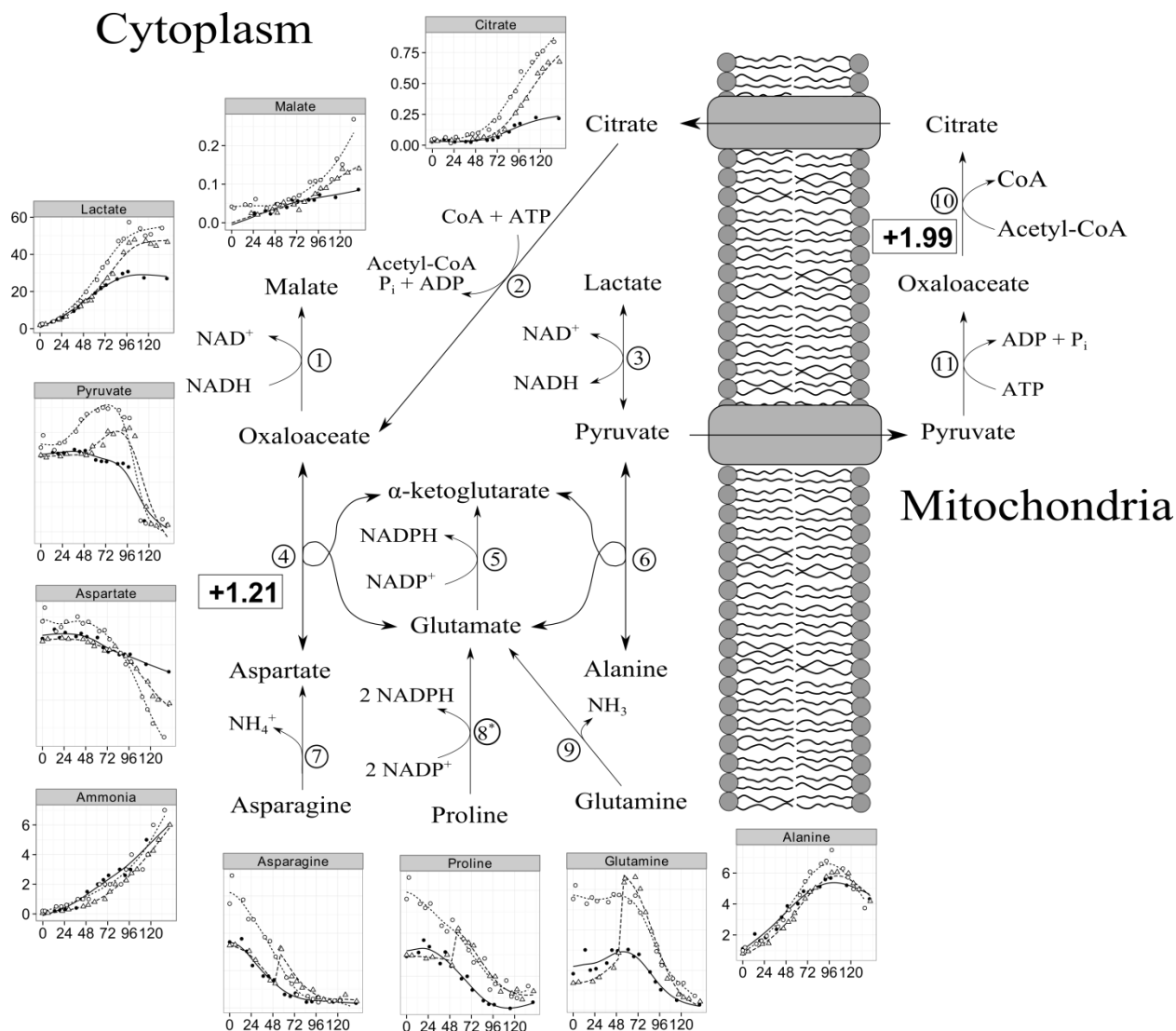


**Figure 16 – Anaplerotic TCA and mitochondrial shuttle metabolism, which contribute to replenishing cytosolic acetyl-CoA, NAD<sup>+</sup>, and NADPH.**

**Enzymes identified:** 1) malate dehydrogenase, 2) ATP citrate lyase, 3) lactate dehydrogenase, 4) aspartate aminotransferase (+1.21 fold increase), 5) glutamate dehydrogenase, 6) alanine aminotransferase 7) asparaginase 8<sup>i</sup>) proline oxidase 8<sup>ii</sup>) glutamate-5-semialdehyde dehydrogenase, 9) glutaminase, 10) citrate synthase (+1.99 fold increase), 11) pyruvate carboxylase. Metabolites concentrations are in mM (y-axis) where indicated or relative concentration, and reflect quantitation from extracellular supernatant by targeted profiling with NMR over culture time in hours (x-axis). Normal culture conditions (solid lines) and nutrient supplemented (dashed lines) at 0 hrs (circle) and at 50 hrs (triangle) as per Table 6.



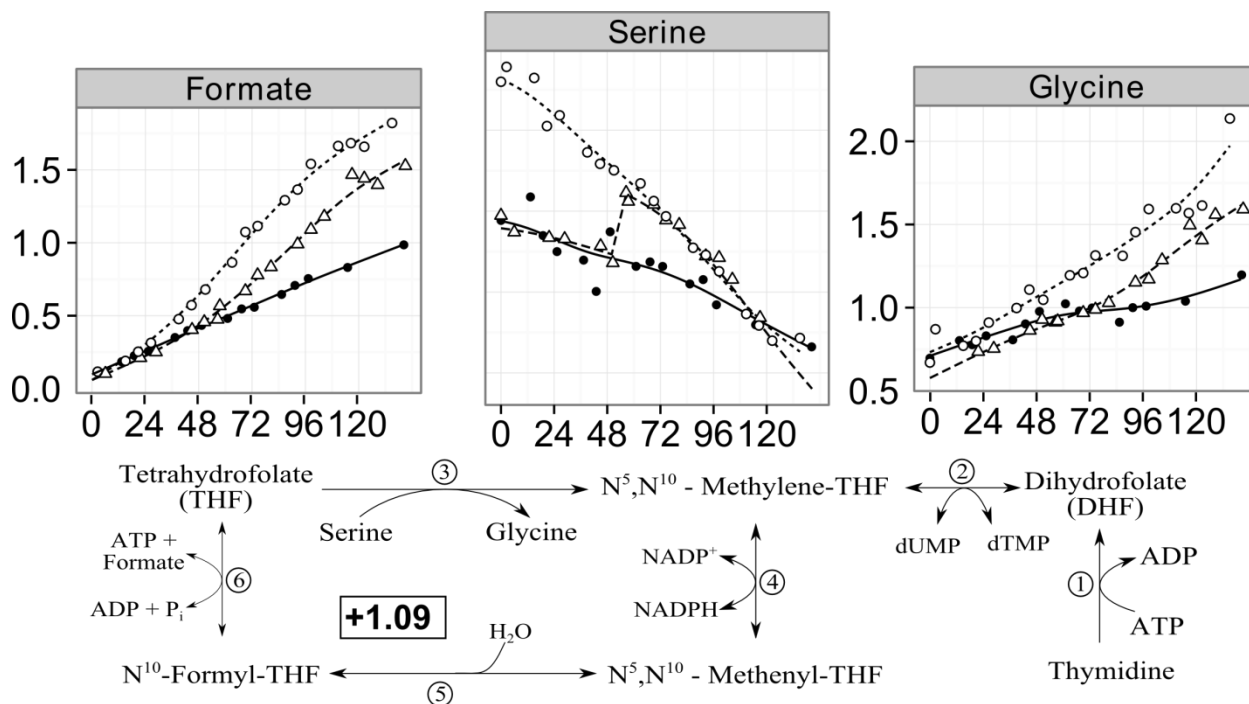


**Figure 17 – Tetrahydrofolate (THF) C1 cofactors replenishing NADPH from serine, while producing glycine and formate, by cycling the THF intermediates between different oxidation states.**

**Enzymes identified:** 1) thymidine kinase, 2) thymidylate synthase, 3) serine hydroxymethyltransferase, 4) N<sup>5</sup>,N<sup>10</sup>-methenyl-THF reductase, 5) N<sup>5</sup>,N<sup>10</sup>-methenyl-THF cyclohydrolase, 6) N<sup>10</sup>-formyl-THF synthase. Reactions 4, 5, and 6 are mediated by a single trifunctional enzyme, methylenetetrahydrofolate dehydrogenase. Metabolite concentrations are presented as relative concentration or in mM (y-axis) where indicated, and reflect quantitation from extracellular supernatant by targeted profiling with NMR over culture time in hours (x-axis). Normal culture conditions (solid lines) and nutrient supplemented (dashed lines) at 0 hrs (circle) and at 50 hrs (triangle) as per Table 6.

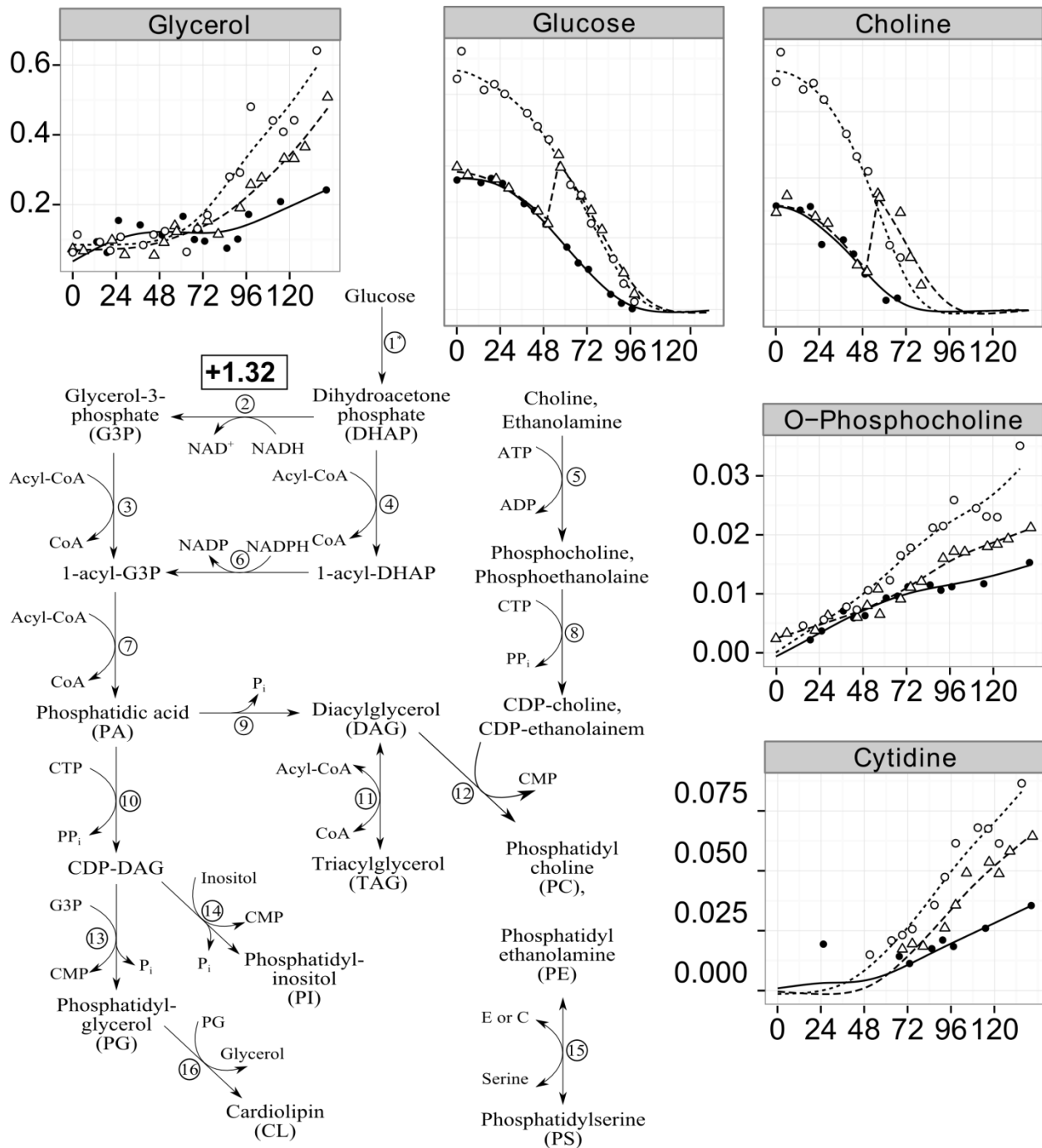


**Figure 18 – Lipid synthesis requires nutrients such as choline and several precursors observed in this work to be excreted, including phosphocholine, cytidine, glycerol and ethanol.**

Enzymes listed include: 1\*) glycolysis, 2) G3P dehydrogenase (+1.32 fold increase), 3) G3P acyltransferase, 4) DHAP acyltransferase, 5) choline kinase, ethanolamine kinase, 6) acyl-DHAP reductase, 7) acyl-G3P acyltransferase, 8) phosphocholine cytidyltransferase, phosphoethanolamine cytidyltransferase, 9) PA phosphatase, 10) CDP-DAG synthase, 11) DAG acyltransferase, 12) DAG phosphocholine transferase, DAG phosphoethanolamine transferase, 13) PG phosphate synthase, and PG phosphate phosphatase, 14) PI Synthase, 15) phosphatidyl serine synthase 1&2 16) cardiolipin synthase. Metabolite concentrations are in mM (y-axis) where indicated or shown as relative concentration, and reflect quantitation from extracellular supernatant by targeted profiling with NMR over culture time in hours (x-axis). Normal culture conditions (solid lines) and nutrient supplemented (dashed lines) at 0 hrs (circle) and at 50 hrs (triangle) as per Table 6.

**Table 6 – Nutrients supplemented to production growth medium with respect to their approximate initial concentrations (% increase).**

Component	% increase
Glucose	46%
Glutamine	50%*
Hypoxanthine	100%
Asparagine	50%
Choline	60%
Cysteine	17%
Proline	50%
Serine	50%

A nutrient cocktail was assembled based on the metabolic systems under stress (Table 6) and supplemented to the production growth medium (Figure 19), yielding a ~75% increase in maximum cell density of cultures (Figure 20). The increase in maximum cell density generally matched up well with increases in the productivity of EG2-hFc; however a tendency for precipitation of the protein (common to scFv style antibodies, as reviewed by Lee et al., 2013) prevented including these results. Even with supplementation, these compounds still became the most depleted amongst the growth medium nutrients. However, doubling the supplementation concentrations, or dosing multiple times during cultivation yielded no further improvements to peak cell density.

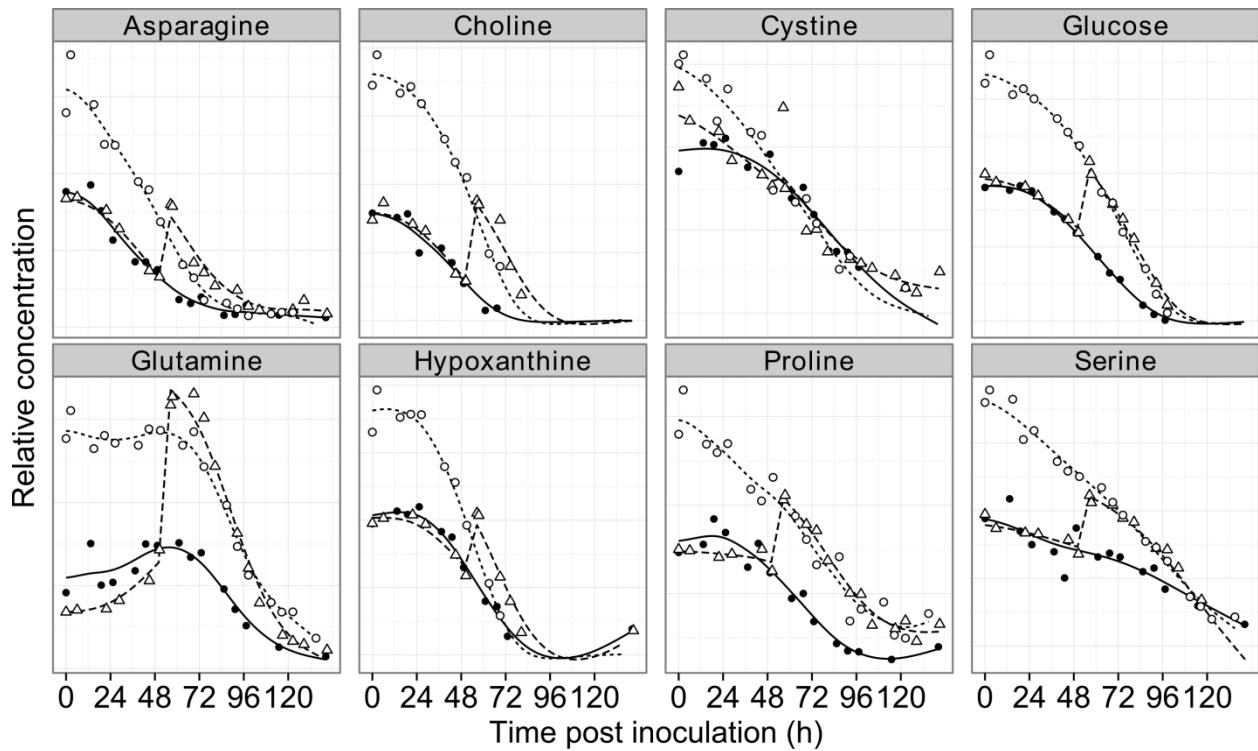


Figure 19 – Fully depleted nutrients under normal culture conditions (solid lines) and following additional supplementation (dashed lines) at 0 hrs (circle) and at 50 hrs (triangle) as per Table 6.

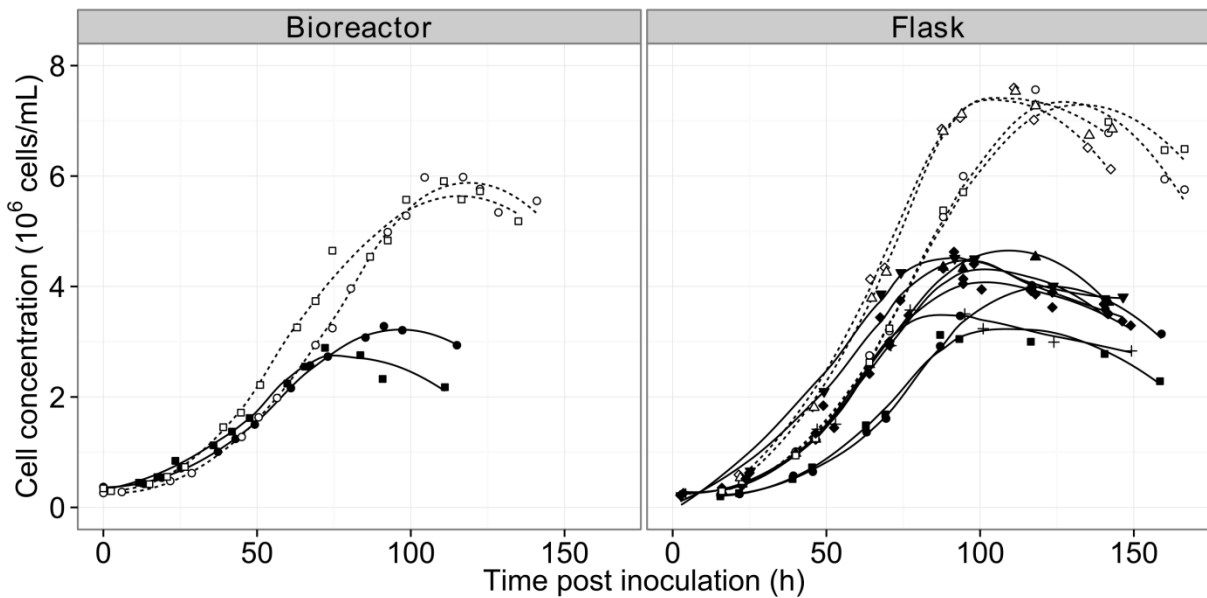


Figure 20 – Culture growth profile of CHOBRI-1A7 cells in bioreactor and flask-scale cultivations.

Control conditions (solid lines, closed points) nutrient supplementation (dashed lines, open points). Data-point shapes represent experimental repetitions.

## **3.5 Discussion**

### **3.5.1 Omics Methods as Tools for Rational Feed Design**

A proteomics analysis by two dimensional in-gel electrophoresis (2D-DIGE) was conducted between a parental CHO cell line and a progeny cell line stably expressing a single domain chimeric camelid heavy-chain antibody, to measure differential expression of endogenous cellular proteins. Subsequently, a metabolomic analysis of the supernatant of the progeny cells by targeted profiling of 1D-<sup>1</sup>H-NMR spectra, was conducted to measure depleted nutrients and the accumulation of excreted metabolites. Together, these omics methods were utilized to evaluate the system stresses of the CHO cells to rationalize a tailored production growth medium that increased cell growth, and production of EG2-hFc. The production growth medium was supplemented with nutrients corresponding to four identified metabolic systems for the CHO<sup>BRI</sup>-1A7 cells with up-regulated pathways. These pathways included anaplerotic TCA-replenishment, NADH/NADPH replenishment, tetrahydrofolate cycle C1 cofactor conversions, limitations to lipid synthesis, and redox modulation. Nutrient depletion corresponding to these pathways has also been reported by other metabolomics researchers observing CHO cell cultures and discussion of these results is included for global context of reproducibility across CHO platforms, as well as potential future targets for metabolic engineering.

### **3.5.2 Anaplerotic TCA Metabolism Limitations**

The metabolism of continuous mammalian cell lines such as CHO, as well as various cancerous cells, is shifted away from normal cellular respiration towards fermentative pathways producing lactate, termed the Warburg effect (Warburg, 1956). Glycolysis is favoured over oxidative phosphorylation, even under aerobic conditions, achieving more rapid growth rates (as reviewed by Swinnen et al., 2006). Ma et al. suggested intracellular accumulation and excretion

of TCA intermediates, such as malate and citrate, was due to a “truncated TCA cycle”, which has been observed in several CHO cultures (Chong et al., 2010a; Dietmair et al., 2012; Ma et al., 2009; Schaub et al., 2012; Sellick et al., 2011a; Selvarasu et al., 2012), and also reported here in Figure 16. The major characteristic of this truncation (Figure 16) is that citrate is transported out of mitochondria and catabolized to replenish cytosolic acetyl-CoA, a crucial pool affecting cell growth (Blondeel et al., 2015), by the action of ATP citrate lyase (Ma et al., 2009). Citrate reverts to oxaloacetate, and subsequently to malate by cytosolic malate dehydrogenase I (as reviewed by Chong et al., 2010a).

The efflux of citrate from mitochondria is hypothesized to drive anaplerotic pathways depleting amino-acids, such as asparagine and aspartate to replenish TCA intermediates (Dietmair et al., 2012; D. Y. Kim et al., 2012; Ma et al., 2009; Schaub et al., 2012; Sellick et al., 2011a) and similarly leveraged in feeding strategies (Sellick et al., 2011a) for achieving higher levels of growth and productivity. The consumption of asparagine is typically accompanied by depletion of aspartate as both are linked by a transaminase pathway (Figure 16, Pathway 7) and diverted toward cytosolic oxaloacetate (as reviewed by Ma et al., 2009). Depletion of both aspartate and asparagine was observed in this work (Figure 16) and this pathway was further observed to be upregulated in CHO<sup>BRI</sup>-1A7 (e.g. +1.21 fold Ast) (Table 5). Goudar et al., reported a considerable anaplerotic flux of aspartate accounting for 47% of total anaplerotic flux into the TCA cycle for CHO cultures grown in perfusion mode (Goudar et al., 2010). This metabolism can be recognized by the accumulation of excreted malate produced from cytosolic malate dehydrogenase (as reviewed by Chong et al., 2010a), and shown in (Figure 16). In this work, final malate concentration increased approximately three-fold during supplementation of asparagine.

The enzymes and transport-proteins of anaplerotic pathways also allow for redox balancing of  $\text{NAD}^+$  between the mitochondrion and the cytosol (mitochondrial shuttles) and have been identified as important targets for enhancing productivity, particularly with regards to shifting lactate metabolism from production to consumption (Chong et al., 2010a; Martínez et al., 2013; Zagari et al., 2013a, 2013b).

Mitochondrial shuttles and anaplerotic pathways also share an interesting benefit beyond regenerating cytosolic acetyl-CoA, helping boost cytosolic NADPH pools (Figure 16). NADPH is an essential reducing agent in most biosynthesis pathways, particularly lipid synthesis (Figure 18). The major regeneration of NADPH comes from the pentose-phosphate pathway (PPP), generating two NADPH for every glucose unit. Goudar et al. reported that as much as 41% of CHO glycolytic metabolism passes through the PPP (Goudar et al., 2010).. While the recent focus of much research regarding anaplerotic TCA-replenishing metabolism has been towards citrate and malate, it may indeed be the regeneration of NADPH as shown in Figure 16 for pathways 4, 5, 6, and as well as the catabolism of proline (Pathway 8) observed in this work, that have the larger impact on sustaining cell growth and viability near the exhaustion of glucose at the end of exponential phase.

High levels of alanine observed in this work were initially attributed primarily to the L-alanine-L-glutamine dipeptide GlutaMAX™ present in the culture medium (employed as a stable glutamine source). However, while GlutaMAX™ is exhausted in the cultures near 72hrs, alanine continues to accumulate until shifting towards uptake after 96hrs (Figure 16). This shift towards alanine consumption has similarly been reported in other GS-CHO cultures (Carinhas et al., 2013; Ma et al., 2009) and corresponds with the rapid-uptake and exhaustion of pyruvate. Therefore, it's apparent the cells are likely scavenging alanine to replenish pyruvate (Figure 16,

Pathway 6). However, it is interesting that the cells are electing to use alanine rather than lactate to accomplish this result. It may be the case that elevated levels of alanine from GlutaMAX™ are a factor in preventing the shift from production to consumption of lactate. Another potential source for the accumulation of alanine may be tryptophan, the depletion of which increased significantly following supplementation. Tryptophan is nearly fully depleted (refer to supplementary data in Appendix A), and is catabolized to alanine in order to generate quinolinate, a precursor in the synthesis of NADH and NADPH.

Regarding pyruvate, while this metabolite was observed to be fully exhausted in cultures, and has been reported by Sellick et al. (2011), as a successful component of a rational feed to support cultures transitioning from exponential to stationary phase, it was not examined as a potential additive for supplementation, as it was assumed that additional glucose provided as part of the supplemented compounds would similarly provide additional pyruvate for later uptake by the cells, which was clearly observed (Figure 16).

### **3.5.3 Tetrahydrofolate Conversions and NADPH Regeneration**

DXB11-derived CHO cells, such as CHO<sup>BRI</sup> lack the enzyme dihydrofolate reductase (DHFR-) to make tetrahydrofolate (THF) and its associated C1 cofactors; these CHO cells are “triple auxotrophs” requiring supplementation of glycine, hypoxanthine, and thymidine (GHT) in their medium (Urlaub and Chasin, 1980). Hypoxanthine was therefore considered an early candidate for further supplementation upon observing its depletion in control cultures during mid-exponential phase (Figure 19). While conferring little improvement on its own, its absence diminished the improvements of supplementing the other seven nutrients, corresponding with the hypothesis that several growth-limiting nutrients including hypoxanthine were impacting culture growth.



Serine is also a major precursor to tetrahydrofolate cofactors for the synthesis of purines and pyrimidines (as reviewed by Snell et al., 1987), and has been reported by Lee et al. (1999), as a potential growth-limiting nutrient for DHFR- CHO cultures grown in the absence of methotrexate, consistent with the culture conditions and results of this work. The enzyme forming tetrahydrofolate, serine hydroxymethyltransferase, consumes serine and produces glycine (Snell et al., 1987), and glycine was observed to accumulate consistently in all cultures (Figure 17).

The metabolic circuit for C1 tetrahydrofolate cofactors, shown in Figure 17, is mediated by a single trifunctional enzyme observed to be upregulated in CHO<sup>BRI</sup>-1A7 cells (+1.09 fold Mthfd11) (Table 4). Alongside the depletion in serine, and the excreted accumulation of glycine and formate, it becomes apparent that the CHO cultures are cycling this pathway as a means of replenishing cytosolic NADPH (Figure 17). As first reported by Bradley et al. (2010), the accumulation of excreted volatile organic acid metabolites such as formate and acetate are not observable by some conventional HPLC and MS methods, and have only recently been reported for CHO cultures by metabolomics researchers employing NMR (Aranibar et al., 2011; Bradley et al., 2010; Carinhas et al., 2013; Sokolenko et al., 2014). Therefore, the THF circuit shown in Figure 17 may present a new potential target of metabolic engineering to improve culture growth by better sustaining intracellular NADPH pools.

#### **3.5.4 Limitations to Lipid Synthesis**

Choline, a necessary B-complex vitamin in the synthesis of certain lipids, has been observed as a potentially growth limiting for CHO IgG producing cultures (Aranibar et al., 2011; Carinhas et al., 2013; Kim et al., 2005). Choline, along with the accumulating metabolites glycerol, cytidine, and O-phosphocholine, each represent precursors in the metabolism of

glycerophospholipids, specifically phosphatidylcholine (PC), as shown in Figure 18. Excretion of glycerol observed here and reported for other CHO cultures (Aranibar et al., 2011; Carinhas et al., 2013; Luo et al., 2012; Sellick et al., 2011a), as well as phosphocholine (Carinhas et al., 2013) were typically observed to accumulate more rapidly in cultures after 72hrs, corresponding to exhaustion of choline. Glycerol-3-phosphate dehydrogenase, in the pathway to produce PC, was observed to be upregulated in CHO<sup>BRI</sup>-1A7 cells (+1.32 fold Gpd2) (Figure 18, Pathway 2).

A review of glycerophospholipid synthesis by Hermansson et al., 2011, identified the formation of intracellular CDP-choline by phosphocholine cytidyltransferase (Figure 18, Pathway 8) as a potentially rate-limiting step in the production of phosphatidylcholine. Luo et al. (2012), have reported that the accumulation of glycerol and 2-hydroxybutyrate is linked with low copper containing cultures that are high-lactate producing, and do not shift to lactate consumption in later culture phases, matching the lactate profile reported in this work.

### **3.5.5 Redox Modulation**

Cystine and proline depletion impact the modulation of intracellular redox potential, as well as glutathione pools. Cysteine and its oxidized cohort cystine are essential substrates for the synthesis of glutathione, an intracellular tripeptide for regulating cellular redox potential, eliminating reactive oxygen species (ROS), and regulating intracellular thiol-disulfide protein confirmations (as reviewed by Wallace, 2012). Cystine has been reported in CHO cultures as potentially growth-limiting (D. Y. Kim et al., 2012; Kim et al., 2005; Read et al., 2013), and intracellular metabolomics analysis of IgG producing CHO cells has observed that higher producing cultures typically possess larger pools of glutathione (Chong et al., 2012). Glutathione is directly regenerated from its oxidized disulfide form by NADPH. Therefore, depleted pools of

NADPH following the loss of the pentose-phosphate-pathway metabolism, negatively impact glutathione pools and the cell's capacity to regulate ROS (Chong et al., 2012).

Uptake of cystine can be inhibited in cultures by elevated levels of glutamate (another glutathione substrate) affecting the  $x_c^-$  transport system (Broadhurst and Butler, 2000). In this work, glutamate was observed to accumulate in both control and supplemented cultures, despite being a nutrient in the growth medium (refer to supplementary data in Appendix A). Kyriakopoulos et al., 2013, determined that the  $X_{AG}^-$  system works cooperatively with the  $x_c^-$  system excreting glutamate for the uptake of cystine.

While cystine is commonly reported as growth limiting, proline (also observed in this work to be depleted) is more typically reported as either having its intracellular pool accumulate over culture when taken up (Kyriakopoulos et al., 2013; Sellick et al., 2011a), or being an excreted metabolite (Ahn and Antoniewicz, 2012; Goudar et al., 2010). Krishnan et al., 2008, reported proline to be a modulator of intracellular redox states of cells by preserving the intracellular glutathione pool. As reviewed by Kim et al., 2012, and shown in Figure 16, proline can be converted to intracellular glutamate to regenerate two NADPH units, and has been examined as an alternative to glutamine to reduce ammonia in cultures.

### **3.6 Conclusions**

A 2D-DIGE proteomics analysis between a parental CHO cell line and progeny stably producing a recombinant antibody to measure differential expression of endogenous cellular proteins, together with a metabolomics analysis of the supernatant of the progeny by targeted profiling of 1D-1H-NMR spectra, demonstrated cell stresses via upregulated metabolism, depleted nutrients and accumulated waste metabolites. Together, these omics methods were

utilized to rationalize a tailored production growth medium that enhanced cell growth. The production growth medium was supplemented with eight target nutrients corresponding with four identified metabolic systems for CHO cells with upregulated pathways related to anaplerotic TCA-replenishment, NADH/NADPH replenishment, tetrahydrofolate cycle C1 cofactor conversions, limitations to lipid synthesis, as well as redox modulation. The supplementation resulted in a ~75% improvement to peak cell densities demonstrating the potential of these metabolic subsystems in CHO cells for further optimization and metabolic engineering.

## **Chapter 4    Tuning a MAb glycan profile in cell culture: Supplementing N-acetylglucosamine to favour G0 glycans without compromising productivity and cell growth<sup>2</sup>**

### **4.1    Overview**

Glycosylation is a critical quality attribute of many therapeutic proteins, particularly monoclonal antibodies (MAbs). Nucleotide-sugar precursors supplemented to growth medium to affect the substrate supply chain of glycosylation has yielded promising but varied results for affecting glycosylation. Glucosamine (GlcN), a precursor for N-acetylglucosamine (GlcNAc), is a major component of mammalian glycans. The supplementation of GlcN to CHO cells stably-expressing a chimeric heavy-chain monoclonal antibody, EG2-hFc, reduces the complexity of glycans to favour G0 glycoforms, while also negatively impacting cell growth. Although several researchers have examined the supplementation of glucosamine, no clear explanation of its impact on cell growth has been forthcoming. In this work, the glucosamine metabolism is examined. We identified the acetylation of GlcN to produce GlcNAc to be the most likely cause for the negative impact on growth due to the depletion of intracellular acetyl-CoA pools in the cytosol. By supplementing GlcNAc in lieu of GlcN to CHO cells producing EG2-hFc we achieve the same shift in glycan complexity with marginal impacts on the cell growth and protein production.

---

<sup>2</sup> This is an accepted manuscript of an article published by Elsevier in the Journal of Biotechnology on November 20, 2015, available online: <https://www.sciencedirect.com/science/article/pii/S0168165615301206>. Blondeel, E.J.M., Braasch, K., McGill, T., Chang, D., Engel, C., Spearman, M., Butler, M., Aucoin, M.G., "Tuning a MAb glycan profile in cell culture: Supplementing N-acetylglucosamine to favour G0 glycans without compromising productivity and cell growth"

Keywords: CHO cells; Protein quality; Glycosylation; Nucleotide sugars; N-acetylglucosamine  
GlcNAc; Glucosamine GlcN

## 4.2 Introduction

Glycoprotein biotherapeutics such as monoclonal antibodies (MAbs) require sophisticated cellular processing in order to become biologically active (Dordal et al., 1985; Nose and Wigzell, 1983). As such, MAbs and other biologics have conventionally been manufactured through culturing higher-eukaryote mammalian cells. Chinese hamster ovary (CHO) cells are an industry standard and are utilized for the majority of commercial biotherapeutics (Ghaderi et al., 2012). Mammalian cells such as CHO are capable of a wide range of human-like post-translational modifications to proteins including glycosylation, which is acknowledged in several reviews of the FDAs quality by design (QbD) program to be a major critical quality attribute (CQA) of MAbs and other biologics (del Val et al., 2010; Eon-Duval et al., 2012; Glassey et al., 2011).

Glycosylation has long been known to affect a host of drug factors including immunogenicity (Bosques et al., 2010; Padler-Karavani et al., 2008), secretion by cells (Hickman and Kornfeld, 1978), drug clearance-rate (Morell et al., 1968), protein stability (Mimura et al., 2001), and solubility (Leavitt et al., 1977), as well as effector function for MAbs (Koide et al., 1977) for required recognition by the immune-system. Governed by a variable sequence of enzymes known as glycosyltransferases, which append and sculpt complex oligosaccharides, also known as ‘glycans’, onto biomolecules, glycosylation introduces heterogeneity to therapeutic products (as reviewed by Butler, 2006).

Glycan heterogeneity occurs naturally, but is influenced by numerous factors such as the up/down regulation of cellular enzymes and transporter proteins (Chen and Harcum, 2006; N. S. C. Wong et al., 2010), perturbations in culture conditions such as temperature, pH and dissolved oxygen as reviewed by several researchers (Butler, 2006; del Val et al., 2010; Eon-Duval et al., 2012; Hossler, 2012; Spearman et al., 2011); as well as bottlenecks in the substrate supply chain

(Nyberg et al., 1999; Pels Rijcken et al., 1995b). With respect to commercial bioprocesses, this implies drugs of potentially inconsistent molecule to molecule quality, as well as batch to batch variability, and challenges for biosimilars and subsequent entry biologics (SEBs) to match the structural characteristics and efficacy of their reference biologics.

The addition of glycosylation precursors, such as glucosamine (GlcN) (Baker et al., 2001; Gawlitzek et al., 1998; Grammatikos et al., 1998; Hills et al., 2001; Pels Rijcken et al., 1995b; N. S. C. Wong et al., 2010; Yang and Butler, 2002; Zanghi et al., 1998), galactose (Gal) (Clark et al., 2005; Gramer et al., 2011; Hills et al., 2001; N. S. C. Wong et al., 2010), and acetylmannosamine (ManNAc) (Baker et al., 2001; Gu and Wang, 1998; Hills et al., 2001; Pels Rijcken et al., 1995b; N. S. C. Wong et al., 2010) to growth medium has been reported to increase the intracellular pools of nucleotide-sugars – the substrates for glycosylation – and affect final glycan profiles. However, these effects are inconsistent across a range of factors including the host cell line, the recombinant protein expressed, and production scales. While galactose and ManNAc have each been reported to contribute to glycans of higher complexity, glucosamine is the only precursor reported to reduce the complexity, by affecting either by galactosylation or sialylation, of glycoforms (Hills et al., 2001; Pels Rijcken et al., 1995b; Yang and Butler, 2002; Zanghi et al., 1998). Glucosamine has also been reported in some instances to contribute to glycans of higher antennarity (Baker et al., 2001; Gawlitzek et al., 1998; Grammatikos et al., 1998); however, this effect is also often associated with elevated ammonia levels (Valley et al., 1999). While more complex glycans are often associated with enhanced efficacy (Jefferis, 2012), commercial therapeutic MAbs on the market are biased towards G0 glycoforms (Wacker et al., 2011) that must be matched by would-be biosimilars and SEBs.



Glucosamine is the only precursor from among these supplementations reported to negatively affect cell growth, an effect reported in both cultured cells expressing recombinant proteins (Baker et al., 2001; Grammatikos et al., 1998; Hills et al., 2001; N. S. C. Wong et al., 2010; Yang and Butler, 2002; Zanghi et al., 1998) and non-producing transformed cells (Bekesi and Winzler, 1970; Krug et al., 1984; Liang et al., 2010; Oh et al., 2007; Pederson et al., 1992). Historically, the negative growth effects of glucosamine were attributed to either competition with glucose transport (Yang and Butler, 2002), depletion of intracellular ATP and UTP pools, or interference with normal glycosylation, (as reviewed by Pederson et al., 1992). However, giving consideration to the metabolism of transformed mammalian cell lines that feature a truncated TCA cycle (Ma et al., 2009), it is proposed that negative growth from glucosamine is actually the result of depletion of cytosolic acetyl-CoA to convert GlcN to GlcNAc, essential for lipid biosynthesis (Goudar et al., 2010; Quek et al., 2010).

In this work, the growth medium of CHO cultures expressing a single-domain chimeric heavy chain camelid-derived antibody (EG2-hFc) (Agrawal et al., 2012) was supplemented with glucosamine (GlcN) and GlcNAc to shift the glycosylation profile toward lower complexity ‘G0’ types. While glucosamine severely restricted the cell growth of cultures, N-acetylglucosamine (GlcNAc) yielded comparatively marginal impacts to cell growth and protein productivity. Glucosamine is converted to GlcNAc, by cytosolic acetyl-CoA, an important compound in lipid biosynthetic pathways necessary for cell growth, as shown in Figure 21.

## **4.3 Materials & Methods**

### **4.3.1 Cell Culture**

DUKX-derived CHO<sup>BRI</sup> cells, negative for dihydrofolate reductase (DHFR-), stably expressing an 80 kDa chimeric heavy-chain monoclonal antibody (Agrawal et al., 2012) were

acquired from Dr. Yves Durocher (National Research Council Canada, Montreal, QC, Canada). Flask experiments were conducted in 125 mL Polycarbonate Erlenmeyer Flasks (Corning Inc.). All cultures were grown in duplicate flasks at 37°C, with an agitation speed of 120 rpm. Samples of supernatant harvested at the end of flask cultures were stored at -80°C. Cell density measurements were taken by trypan-blue exclusion via haemocytometer and by a Coulter Counter Z2 (Beckman-Coulter, Miami, USA).

#### **4.3.2 Growth Medium & Supplemented Nutrients**

Cells were grown in serum-free BioGro-CHO medium (BioGro Technologies Inc., Winnipeg, MB, Canada). Glucosamine (Sigma-Aldrich G1514) and N-acetylglucosamine (AMRESCO K250) were prepared as 120 mM stock solutions in BioGro. All stock solutions were sterile filtered using a 0.2µm filter (Millipore Millex-GP, Bedford, MA, USA).

#### **4.3.3 Glycan Analysis**

EG2-hFc antibody glycans were analyzed using normal phase HPLC (NP-HPLC) with HILIC (hydrophobic interaction liquid chromatography) separation. Supernatant containing EG2-hFc was harvested at the end of culturing and exchanged to 1X phosphate buffered saline (PBS) using a 10 kDa cut-off Ultracel® column (Merck Millipore Ltd.). Up to 100 µg of protein was bound to a Protein-A HP Spintrap column (GE Healthcare, Burlington, NC) for 15 min that was prewashed with 20 mM phosphate buffer, pH 7.4. Glycans were removed from the bound MAb protein by digesting overnight at 37°C with 1 µL of Peptide-N-Glycosidase-F (PNGaseF; Promega, Madison, WI) in 200 µL of phosphate buffer. Following incubation the glycans were eluted by washing 2X with water and dried in a Speedvac (ThermoFisher Scientific, Waltham, MA). The glycans were labelled with 2-aminobenzamide (Bigge et al., 1995) (ThermoFisher Scientific, Waltham, MA), and excess 2-AB was removed using Hypersepdiol cartridges

(ThermoFisher Scientific, Waltham, MA). Glycans were analyzed by HILIC HPLC with fluorescent detection using an X-Bridge 3.5  $\mu$ m amide column (4.6 x 250 mm) (Waters, Mississauga, ON) with the column heated to 30°C and a flow rate of 0.86 mL/min. Glycans were eluted using 50 mM ammonium formate, pH 4.4: acetonitrile starting with an initial ratio of 20:80, followed by a gradient to 50:50 over 48 minutes. Peaks were calibrated with a 2-AB labeled glucose ladder and glycan standards (Prozyme, Hayward, CA) and compared to a glycan database (GlycoBase (Campbell et al., 2008)). Glycan structures were confirmed in previous experiments by exoglycosidase enzymatic digestion.

#### **4.3.4 mAb Quantification**

Supernatant samples harvested at the end of culturing containing EG2-hFc MAb were concentrated ~10x by centrifugation through a 10 kDa cut-off Ultracel® column (Merck Millipore Ltd.). Quantification was achieved with a POROS® A20 column (Life Technologies) on a Varian Pro Star 410 HPLC (Agilent). Antibody elution was detected at a wavelength of 280 nm.

#### **4.3.5 Extracellular Metabolite Profiling**

NMR spectra were acquired with a Bruker Avance 600MHz spectrometer with a TXI 600 probe. Following acquisition, spectra were imported into Chenomx NMR Suite 7.7 (Chenomx Inc., Edmonton, Canada) and manually profiled (Sokolenko et al., 2014).

#### **4.3.6 Intracellular Nucleotide and Nucleotide-Sugar Analysis**

Cells were metabolically quenched at 72hrs of culturing as per the method of Sellick et al., 2009, in 60% methanol with 0.85% w/v ammonium bicarbonate (AMBIC) at -40°C (pH 7.4). The quenched sample was then pelleted by centrifugation (1000g for 1min), flash-frozen in

liquid nitrogen and stored at  $-80^{\circ}\text{C}$  before shipping on dry ice to the Butler Lab of the University of Manitoba. Extraction was performed as per Rabinä et al., 2001. Quenched cell pellets were reconstituted in 0.5 mL PBS and sonicated briefly on ice. Debris was subsequently removed by centrifugation at 6000g for 10 min and each extract was diluted to 1 mL with 10 mM AMBIC (pH 7.0). Nucleotide and nucleotide sugars were isolated using an ENVI-Carb™ column (Supelclean™) and eluted with 25% (v/v) acetonitrile, 50 mM TEAA buffer (pH 7). Nucleotide and nucleotide sugar samples were dried in a Speedvac and subsequently dissolved in 40  $\mu\text{L}$  of distilled water prior to analysis via HPAEC as per Tomiya et al., 2001, using a CarboPac® PA1 column (Dionex); UV absorbance for detection (260 nm).

#### 4.4 Results

The goal of this work was to utilize glucosamine to affect Mab glycan profiles, while also mitigating the negative growth effects associated with this supplementation. Glucosamine (GlcN), a precursor for N-glycans reported in many cell culture applications to reduce glycosylation, but also to hinder growth was hypothesized based on its metabolism to restrict growth by depletion of the cytosolic acetyl-CoA pool (Figure 21, reactions 5 & 11). Supplementation of 7.5mM glucosamine restricted growth, leading to an approximately 60% drop in the maximum cell density of cultures compared to controls (Figure 22). However, glucosamine also succeeded in increasing the proportion of G0 glycoforms for EG2-hFc protein produced from CHO<sup>BRI</sup> cultures by ~25% (Figure 23). To test the acetyl-CoA growth-restriction hypothesis, 7.5 mM N-acetylglucosamine (GlcNAc - the acetylated form of glucosamine) was supplemented instead of GlcN, achieving a comparable proportionate increase in G0 glycoforms (Figure 23), while achieving a maximum cell density with less than a 20% drop compared to control cultures (Figure 22). Supplementing lower concentrations of GlcNAc (2.5 mM) achieved

an equivalent maximum cell density to controls, with a ~15% increase in G0 glycoforms (Figure 24 & Figure 25). Productivity of EG2-hFc harvested at the end of cultures supplemented with GlcNAc also remained consistent with controls (Figure 26). Intracellular nucleotides and nucleotide-sugar metabolites extracted from cultures at 72 hrs following supplementation with a range of concentrations of GlcNAc, resulted in corresponding increases to intracellular UDP-GlcNAc and UDP-GalNAc metabolites (Figure 27), an effect matching those reported by researchers who supplemented GlcN.

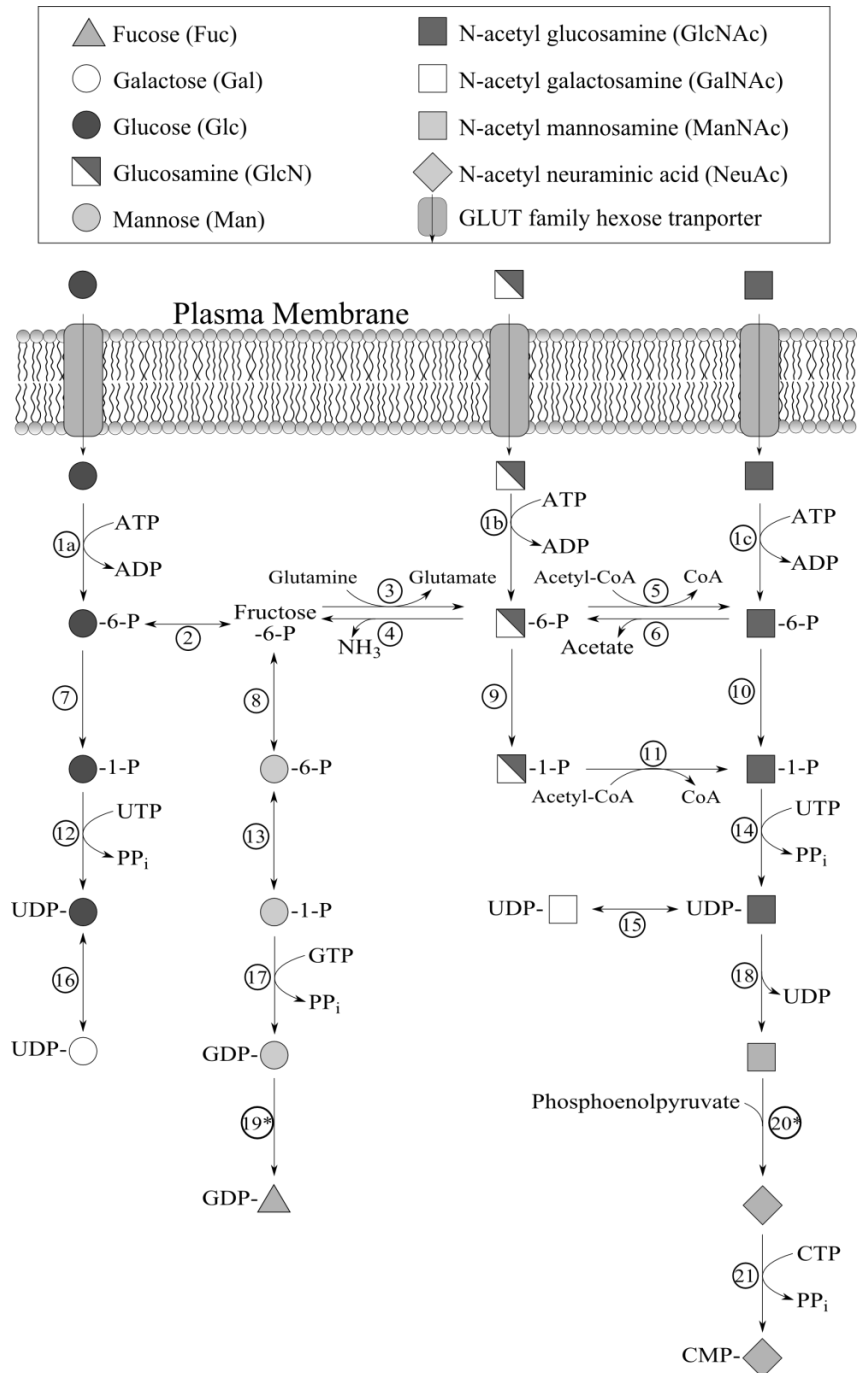


**Figure 21 – Intracellular nucleotide sugar metabolic pathways utilizing glucose or supplemented GlcN or GlcNAc.**

**Enzymes:** 1. Hexokinase, 2. Glucose-6-phosphate isomerase, 3. Glutamine-fructose-6-phosphate transaminase, 4. Glucosamine-6-phosphate deaminase, 5. Glucosamine-phosphate N-acetyltransferase, 6. N-acetylglucosamine-6-phosphate deacetylase, 7. Phosphoglucomutase, 8. Mannose-6-phosphate isomerase, 9. Phosphoglucoamine mutase, 10. Phosphoacetylglucosamine mutase, 11. Glucosamine-1-phosphate N-acetyltransferase, 12. UTP-glucose-1-phosphate uridylyltransferase, 13. Phosphomannomutase, 14. UDP-N-acetylglucosamine diphosphorylase, 15. UDP-N-acetylglucosamine 4-epimerase, 16. UDP-glucose 4-epimerase, 17. Mannose-1-phosphate guanylyltransferase, 18. UDP-N-acetylglucosamine 2-epimerase, 19\*. GDP-mannose 4,6-dehydratase and GDP-L-fucose synthase, 20\*. N-acylmannosamine kinase and N-acylneuraminate-9-phosphate synthase, 21. N-acylneuraminate cytidylyltransferase.

#### **4.4.1 Growth Effects GlcN vs. GlcNAc**

Supplementing GlcN and GlcNAc produced comparable effects to the glycan distribution (Figure 23) while the effects on cell growth were significantly different. GlcN supplemented cultures immediately presented with inhibited growth and an approximately 50% drop in growth rate during the exponential phase. GlcNAc supplemented cultures, on the other hand, maintained near equivalent growth rates compared to control cultures till the late exponential phase (Figures 2&5), with a difference in growth rate compared to control cultures of less than 5%. GlcNAc supplemented cultures also achieved comparable maximum cell density to control cultures, particularly at lower supplemented concentrations (2.5 mM). However, in all GlcNAc supplemented flasks, the cell density dropped more rapidly in the stationary phase.

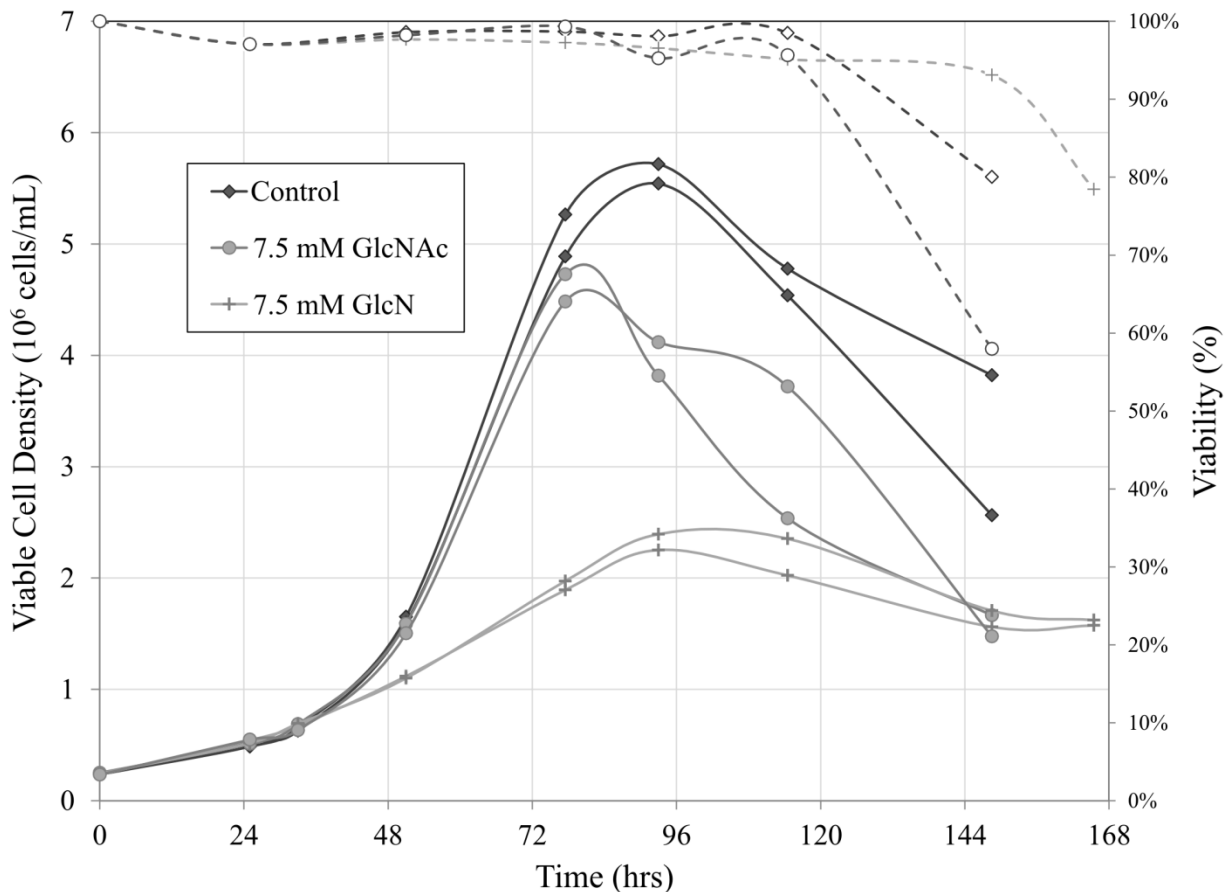


Figure 22 – Growth and viability of CHO cells severely impacted during supplementation of 7.5 mM glucosamine (GlcN), compared to only marginal impacts to growth and viability during supplementation of 7.5 mM N-acetylglucosamine (GlcNAc). Duplicate lines represent duplicate flasks.

#### 4.4.2 Glycosylation Effects GlcN vs. GlcNAc

GlcN and GlcNAc were each supplemented at 7.5mM to cultures after a cell density of  $0.5 \times 10^6$  cells/mL was reached (Figure 22). The glycan distribution of the EG2-hFc MAb harvested from the supernatant at the end of these cultures showed a shift towards the biantennary fucosylated G0 form (FA2G0) with a reduction in the galactosylated forms (FA2G1 and FA2G2) (Figure 23 and supplementary data). Supplementation of GlcN and GlcNAc each yielded a proportional increase in FA2G0 of approximately 25% to become the dominant glycoform.



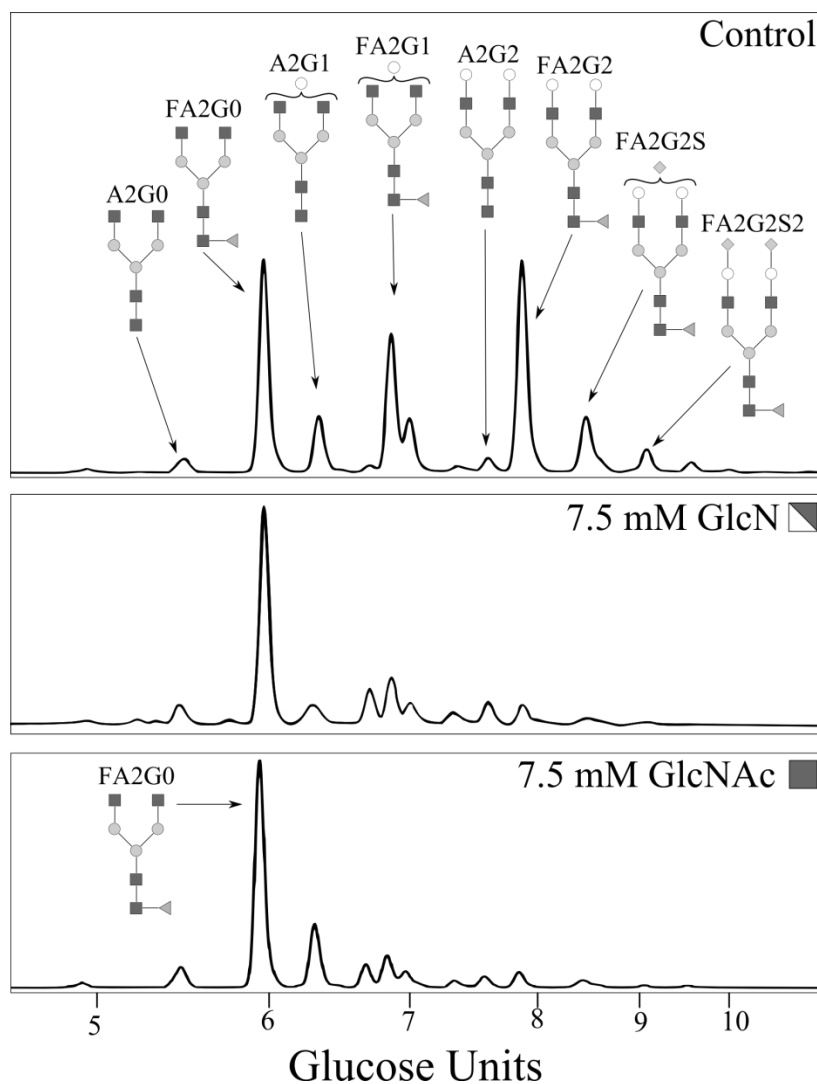


Figure 23 – A similar shift to less complex glycoforms is observed from supplementing either glucosamine (GlcN) or N-acetylglucosamine (GlcNAc).

#### 4.4.3 Glycosylation Effects GlcNAc

Supplementation of GlcNAc at increasing concentrations from 0 to 10 mM yielded corresponding increases in the proportion of G0 glycoforms from approximately 25% (control) to 50% (10 mM supplementation) (Figure 24 and supplementary data). A similar trend in the shift of the glycan distribution was also observed in previous experiments utilizing GlcN (data not shown).

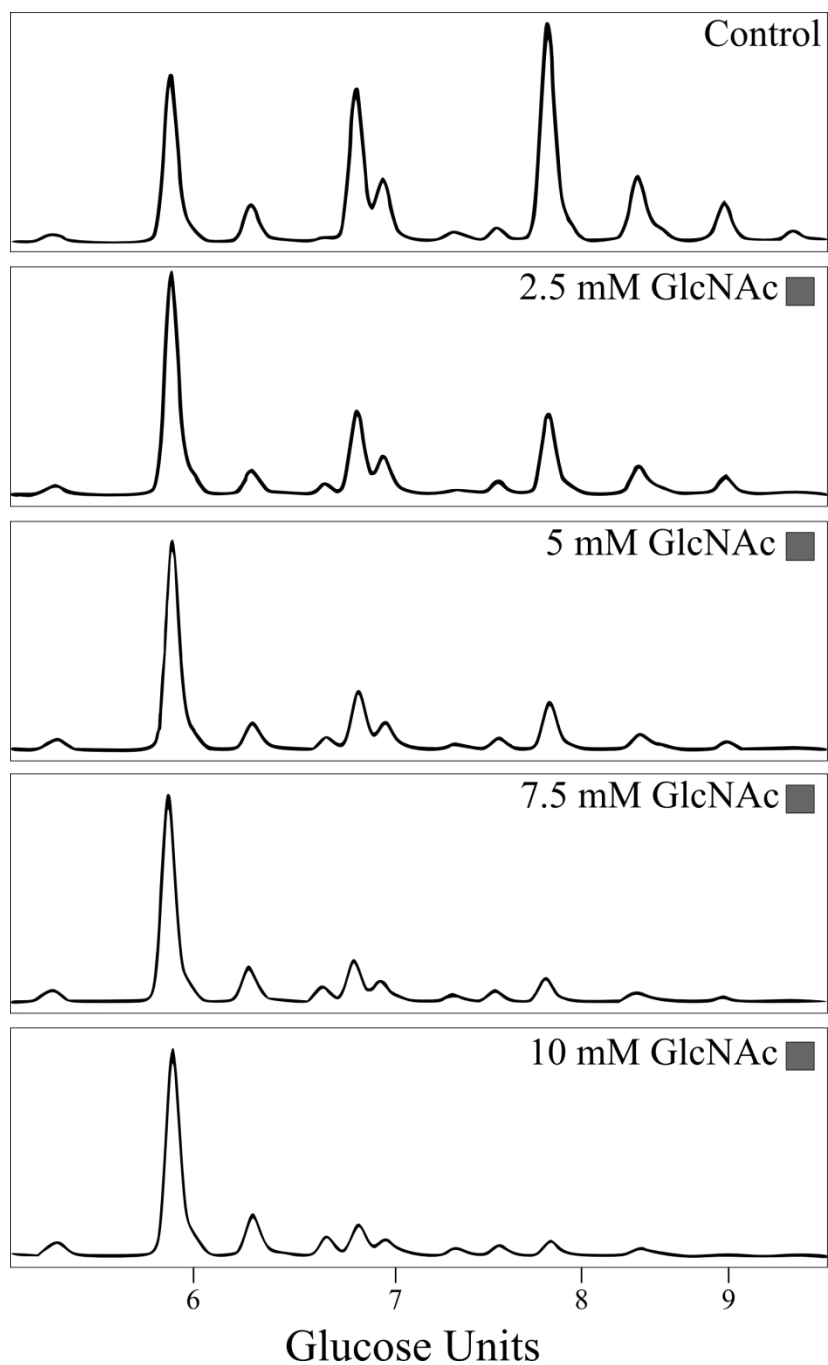


Figure 24 – Increasing the concentration of N-acetylglucosamine (GlcNAc) increases the glycan shift towards G0 glycoforms.

#### 4.4.4 Growth and Productivity Effects from GlcNAc Supplementation

Although GlcNAc had a less severe impact on cell growth compared to GlcN, it showed a concentration dependent effect on the growth of cultures (Figure 25). GlcNAc supplemented

cultures maintained near equivalent growth rates to the control cultures until late exponential phase, with less than a 5% difference from control cultures.

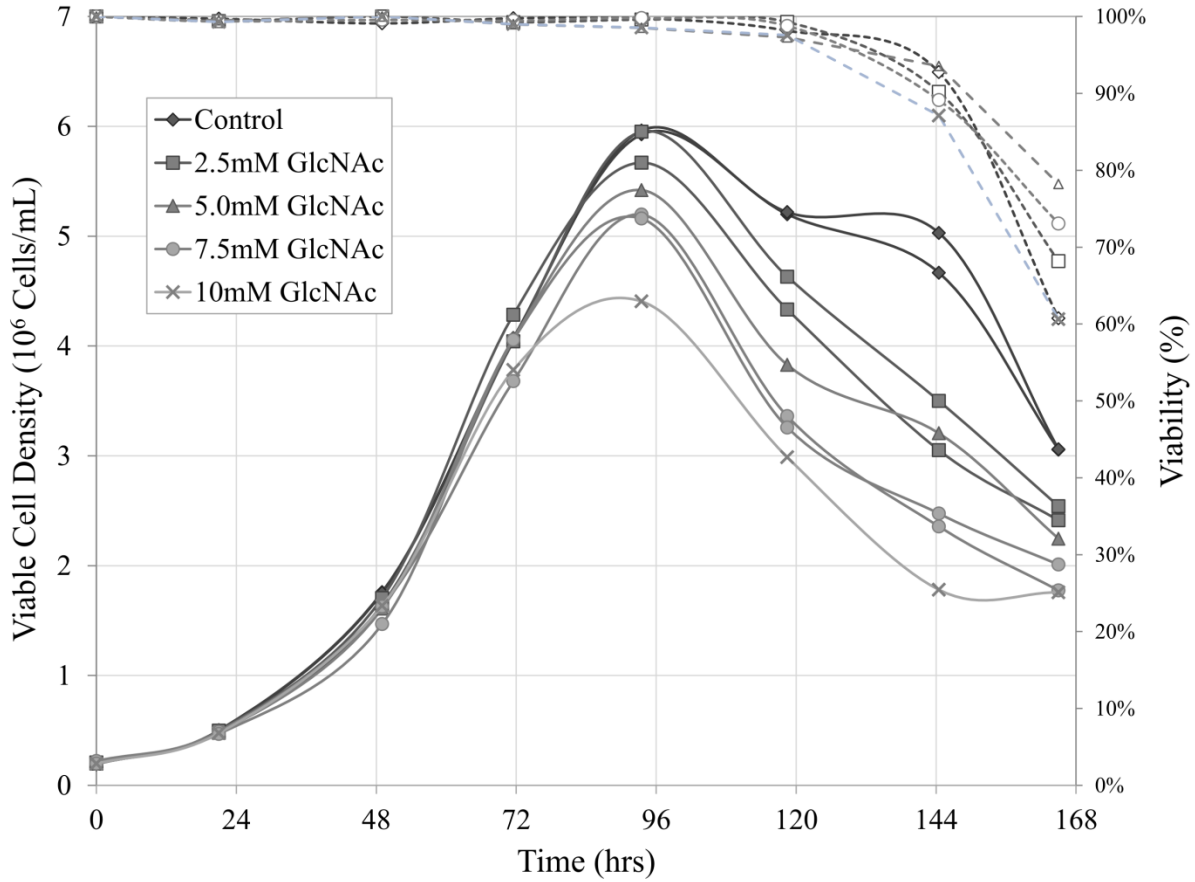
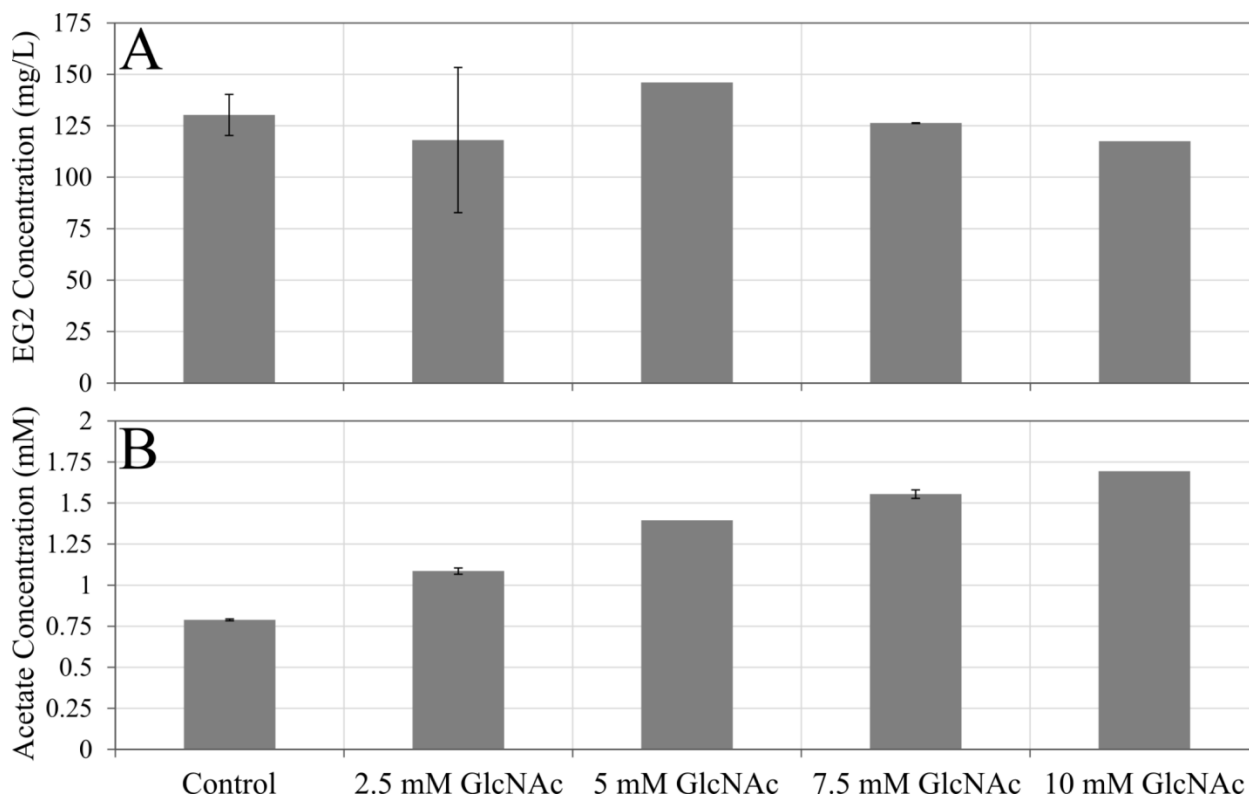


Figure 25 – Increasing the concentration of N-acetylgucosamine (GlcNAc) supplemented to cultures reduces late-exponential cell growth with marginal impact to viability. Duplicate lines represent duplicate flasks.

While cultures supplemented with GlcNAc collapsed more rapidly during stationary phase, the productivity of EG2-hFc harvested from the final time-point of the cultures remained reasonably consistent with the controls (Figure 26A).



**Figure 26 – A) Final protein titers of EG2-hFc from cultures supplemented with GlcNAc. B) Final acetate concentrations from cultures supplemented with GlcNAc. Error bars represent the standard deviation between duplicate flasks.**

1D-<sup>1</sup>H-NMR was utilized to track approximately thirty exometabolites of the cultures supplemented with GlcN and GlcNAc (refer to supplementary data). Supplementing cultures with GlcNAc produced very similar metabolite trends compared to the control cultures, with the exception of acetate. Starting at ~72hrs, prior to the end of exponential phase, a 3-fold higher concentration of acetate accumulated compared to the control cultures. This acetate accumulation trend was also observed from glucosamine supplemented cultures. Profiling the metabolites from supernatant harvested at the final time-point of GlcNAc supplemented cultures revealed a trend of increasing acetate excretion corresponding with increasing GlcNAc concentration (Figure 26B). Clipping acetate to scavenge glucose from GlcNAc is shown in Figure 21 for the activity of N-acetylglucosamine-6-phosphate deacetylase. While acetate levels increased with GlcNAc

supplementation, follow-up experiments supplementing acetate to CHO cultures did not restrict growth at these concentrations.

#### 4.4.5 Intracellular Nucleotides and Nucleotide-Sugar Pools

Extracting intracellular metabolites from cells at ~72hrs from cultures supplemented with GlcNAc revealed increases in intracellular GlcNAc, UDP-GlcNAc and UDP-GalNAc (Figure 27) corresponding to increases in the proportion of G0 glycoforms (Figure 24). Other fractions of intracellular nucleotides and nucleotide-sugars appeared stable in GlcNAc supplemented cultures, presenting no dependence or effect from GlcNAc feeding, with the exception of ATP which showed a slight dip with increasing GlcNAc concentrations.

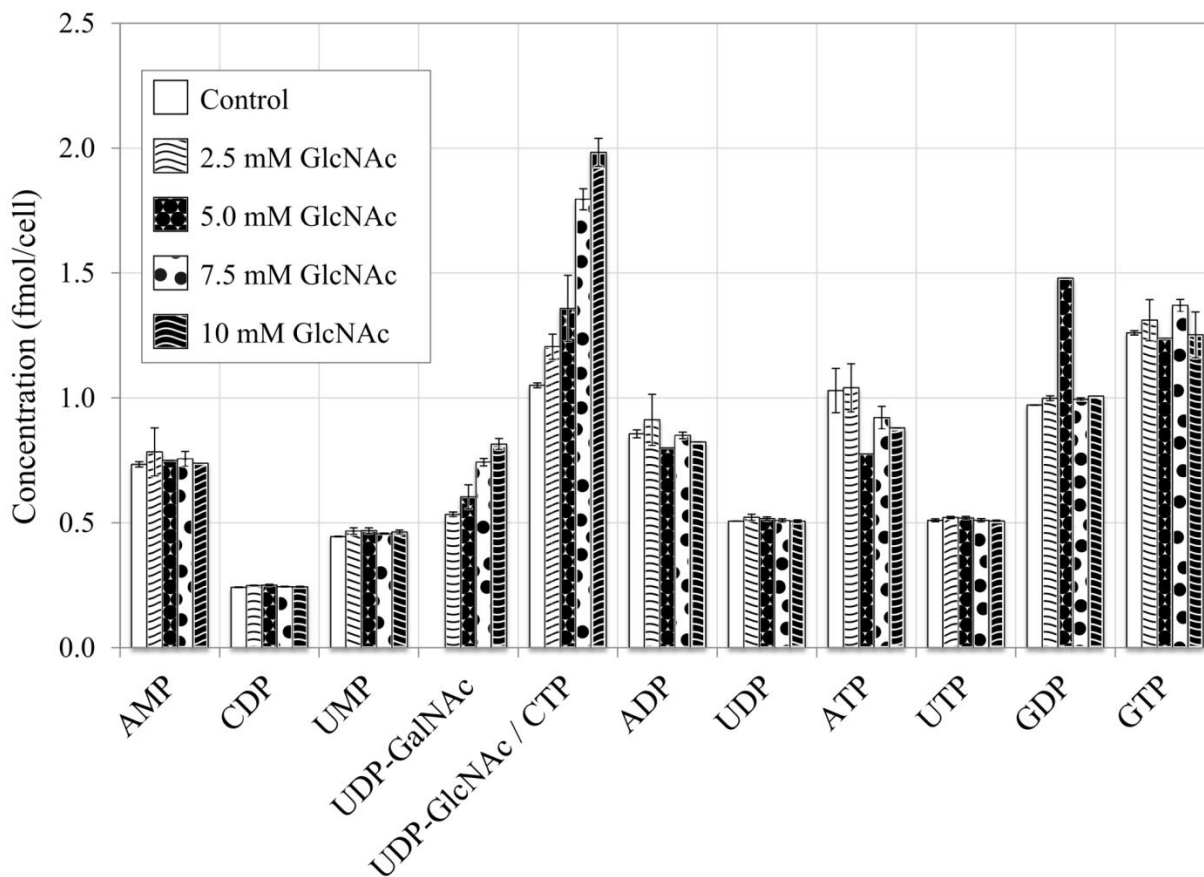


Figure 27 – Nucleotide and nucleotide-sugar ‘per-cell’ intracellular concentrations from quenched cell samples taken at 72hrs from cultures supplemented with GlcNAc. Error bars represent the standard deviation between duplicate flasks.

## 4.5 Discussion

### 4.5.1 Simple Method for Affecting Glycan Distributions

While glycoengineering of designer cell culture platforms has emerged in recent years as a means to introduce mammalian-like post-translational modifications to non-mammalian systems, it remains a fact that a significant majority of established FDA-approved therapeutic proteins are produced in Chinese hamster ovary (CHO) cells (as reviewed by Ghaderi et al., 2012). Therefore, fundamentally improving the quality of these therapeutics through systems like Quality by Design (QbD) will demand a method that can be integrated into existing bioprocesses, such as supplementing nucleotide sugar precursors (GlcNAc, ManNAc, Gal) to growth medium. Also, biosimilars, and subsequent entry biologics (SEBs) attempting to enter the market may require the means to tune glycan distributions to match glycoform distributions to approved proportions in reference biologics. Nucleotide-sugar precursor supplementation represents a promising option both for established bioprocesses and new biosimilars manufacturing because of its simplicity and its clear impact to glycan distributions.

Commercial therapeutic MABs, which are reference biologics for upcoming biosimilar products, are generally biased towards the G0 glycoform (Wacker et al., 2011). While large glycan shifts are exhibited in this work when supplementing GlcNAc at higher concentrations, partial tuning of glycoforms can be accomplished with smaller concentrations as observed by the case of 2.5mM supplementation increasing the G0 proportion by 15% (as per the results shown in Figure 24). With respect to the economics of such a supplementation; taking a conservatively estimated price of cell culture grade GlcNAc of US\$2/g, and a batch process volume of 10,000L, the additional cost per batch supplementing 2mM GlcNAc would be on the order of US\$10k per batch and therefore economically feasible.

#### 4.5.2 Diversity of Reported Glycan Effects from Glucosamine

Glucosamine has historically been associated with reducing glycosylation (as reviewed by Nyberg et al., 1999). While most often reported as reduced sialylation (Baker et al., 2001; Hills et al., 2001; Pels Rijcken et al., 1995b; Yang and Butler, 2002; Zanghi et al., 1998), due to inhibition of transport of CMP-sialic acids to the Golgi by elevated levels of UDP-GlcNAc (Pels Rijcken et al., 1995b), glucosamine supplementation has also been reported by Hills and colleagues to reduce galactosylation (Hills et al., 2001). In several instances, glucosamine supplementation has led to an increase in glycan branching producing greater proportions of tri and tetraantennary glycans (Baker et al., 2001; Gawlitzek et al., 1998; Grammatikos et al., 1998; Pels Rijcken et al., 1995b). However, the majority of these reports were made with the same BHK cell line producing interleukin-2, and these results may also be confounded by varying responses to ammonia between mammalian cell culture platforms. As reported by Valley et al., when supplementing  $^{15}\text{N}$  isotopic ammonia, up to 60% was incorporated into elevated UDP-GlcNAc pools, making glutamine and TCA metabolism important factors affecting glycosylation. D.C.F. Wong and colleagues demonstrated that glutamine levels may directly impact the up/down regulation of GnT-IV and V, the GlcNAc glycosyltransferases responsible for tri and tetraantennary glycan formation (D. C. F. Wong et al., 2010). The cell culture platform itself may be a source of variation, as reported by Baker et al. who supplemented glucosamine together with uridine in GS-CHO and GS-NS0 cultures expressing tissue inhibitor metalloproteinases 1, observing increased glycan branching in CHO, but not in NS0. While most researchers have reported either decreased sialylation or increased antennarity effects, other researchers have reported the reverse of these results, such as increasing sialylation of interferon- $\gamma$  expressed in CHO (N. S. C. Wong et al., 2010) and decreasing antennarity in EPO

expressed in CHO (Yang and Butler, 2002). Therefore, the effects of supplementation of glucosamine vary from researcher to researcher depending on cell culture platform utilized, protein being expressed, and other factors such as glutamine and ammonia concentrations.

### **4.5.3 Growth Limitations from Glucosamine**

Growth limitations from glucosamine supplementation are reported in both cultured cells expressing recombinant proteins (Baker et al., 2001; Grammatikos et al., 1998; Hills et al., 2001; N. S. C. Wong et al., 2010; Yang and Butler, 2002; Zanghi et al., 1998) and non-producing transformed cells (Bekesi and Winzler, 1970; Krug et al., 1984; Liang et al., 2010; Oh et al., 2007; Pederson et al., 1992).

As a major component in the typical mammalian glycan structure, glucosamine (GlcN) was an early candidate for research into supplementation options to affect glycosylation and was examined by many researchers (Baker et al., 2001; Gawlitzek et al., 1998; Grammatikos et al., 1998; Hills et al., 2001; Pels Rijcken et al., 1995b; N. S. C. Wong et al., 2010; Yang and Butler, 2002; Zanghi et al., 1998). GlcN was also a candidate in some early fully-defined growth medium formulations for mammalian cell culture (Evans et al., 1956). Upon being taken up by the cells, as shown in Figure 21, glucosamine is phosphorylated and acetylated, then finally activated by uridine-triphosphate to produce UDP-GlcNAc, the most common substrate of mammalian N-glycosylation.

The acetylation step to make GlcNAc (Figure 21, reactions 5 & 11) is proposed to be the cause of the growth inhibiting effects associated with GlcN supplementation. Acetyl-CoA in the mitochondria is not able to migrate out of the organelle to take part in lipid-biosynthesis in the cytosol. Citrate on the other hand will leave the mitochondria and be used to replenish the



cytosolic acetyl-CoA pool via the action of ATP-citrate lyase, a metabolic feature of transformed mammalian cell lines described as a truncated TCA cycle (Ma et al., 2009). Goudar and colleagues reported that nearly 24% of all TCA flux diverted through ATP-citrate lyase and that this was characteristic of slow-growing cells, while nearly 50% had been reported for faster growing hybridomas (Bonarius et al., 1996; Goudar et al., 2010). Quek et al. reported that during maximum growth rate, all available Acetyl-CoA will be devoted towards lipid biosynthesis (Quek et al., 2010).

Glucosamine is readily taken up by the cells, and arrives in a metabolic pathway absent of much additional regulation to produce UDP-GlcNAc (Freeze and Elbein, 2009). Several researchers have reported that supplementing glucosamine therefore leads to a ~10x (Grammatikos et al., 1998) to ~60x (Baker et al., 2001) increase in the intracellular UDP-GlcNAc pools. This acetylation of glucosamine may potentially lead to the depletion of cytosolic acetyl-CoA, necessary for many biosynthetic pathways particularly lipid synthesis, necessary for cell growth.

In this work, GlcNAc was supplemented in lieu of glucosamine to skip the acetylation step. This supplementation lead to a nearly two-fold increase in intracellular UDP-GlcNAc pools, with a negligible impact on other observed intracellular pools apart from UDP-GalNAc, which exists in equilibrium with UDP GlcNAc, and ATP, which observed a small dip in pool size. There remains some negative impact to cell growth most evident in late exponential phase with GlcNAc supplementation and the more rapid decline in stationary phase.

Historically, the negative growth effects of glucosamine were attributed to either competition with glucose transport (Yang and Butler, 2002), depletion of intracellular ATP and UTP pools,

or interference with normal glycosylation, (as reviewed by Pederson et al., 1992). Glucose, glucosamine and N-acetylglucosamine appear to share the same group of transporters on the plasma membrane, the GLUT family of hexose transporters (as reviewed by Freeze and Elbein, 2009), particularly GLUT2 in the case of glucosamine (Uldry et al., 2002), and nearly all GLUT transporters at low levels for GlcNAc (Scarcelli et al., 2012). However, glucose uptake appeared more or less unchanged between control cultures and GlcNAc supplemented cultures (supplementary data). ATP may have been slightly depleted to provide additional UDP to form UDP-GlcNAc, since as observed in Figure 27, its pool does appear somewhat declined with increasing GlcNAc concentrations. However, given that the recombinant glycoprotein expressed by the CHO<sup>BRI</sup> cells showed such a clear shift in its glycan profile from GlcNAc supplementation, it's possible that further interference with other glycan dependent cell systems might have been affected and diminished maximum cell density, leading to the more rapid decline at end of culture.

## **4.6 Conclusions**

Supplementation of nucleotide sugar precursors to the growth medium of mammalian cell cultures is a promising strategy for tuning the glycan profile of therapeutic recombinant proteins for existing bioprocesses as well as new biosimilars and SEBs. The supplementation of glucosamine (GlcN) reduces the complexity of glycan profiles of EG2-hFc expressed in CHO cells to favour the G0 glycoform, but causes a significant restriction to cell growth. Alternatively, supplementing N-acetylglucosamine (GlcNAc) yields the same affect to the glycan profile with a marginal impact to cell growth, particularly at GlcNAc concentrations of 2.5 mM. The difference in growth effects can likely be attributed to the necessary acetylation of

GlcN to become GlcNAc, which may deplete intracellular acetyl-CoA pools necessary for supporting lipid biosynthetic pathways.

## Chapter 5 Supplementing Growth and Glycoform

Supplementation of the cocktail of nutrients demonstrated in Chapter 3 to improve growth of CHO<sup>BRI</sup>-1A7 cells was repeated to examine any effects to the glycoform distribution of EG2-hFc. The cocktail did not notably affect the glycoform distribution, as shown in Figure 28. While the distribution favoured more galactosylation compared to controls, this was not considered unusual for EG2-hFc based on earlier experiments.

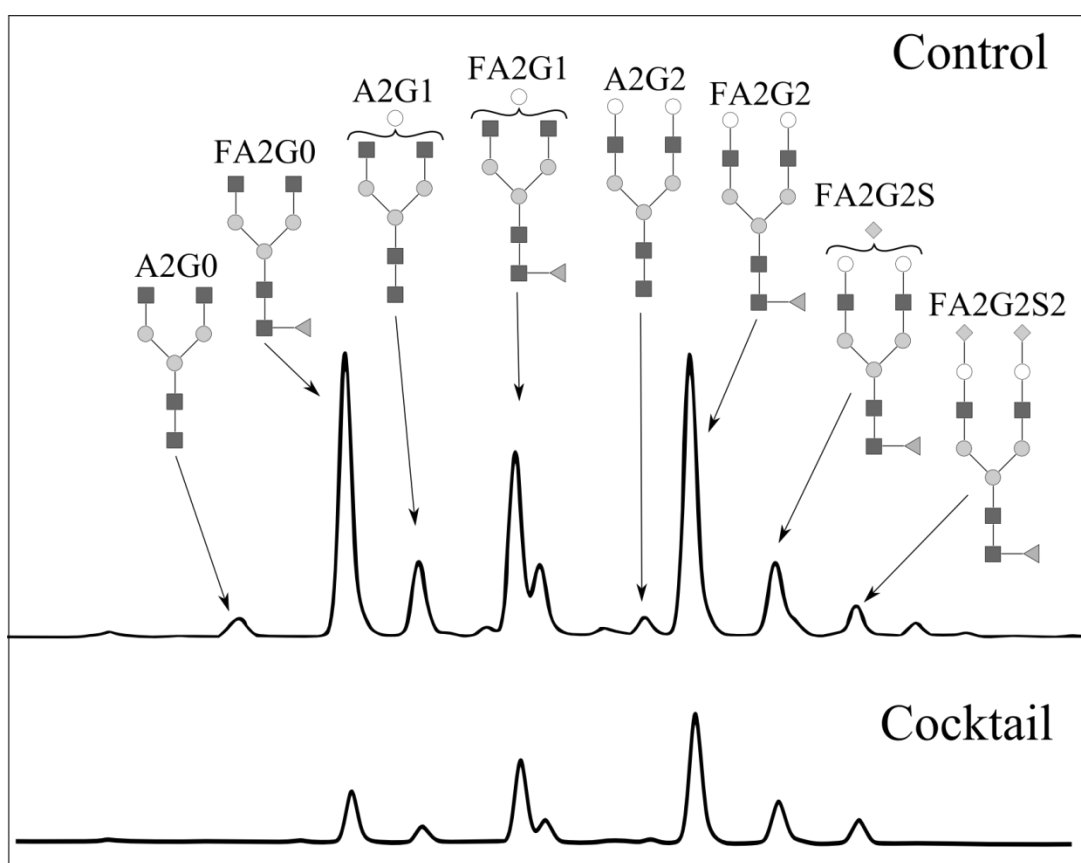


Figure 28 – Glycoform distribution for EG2-hFc harvested from a bioreactor fermentation of CHO<sup>BRI</sup>-1A7 grown in BioGro-CHO medium supplemented with the cocktail of nutrients established in Chapter 3.

Subsequently, supplementation of the cocktail was repeated together with supplementation of N-acetylglucosamine (GlcNAc), which had caused some marginal growth restriction, as demonstrated in Chapter 4. It was determined that the marginal growth limitations from GlcNAc

could be alleviated via the cocktail. As demonstrated in Figure 29, addition of the nutrient cocktail successfully improved growth for those flasks supplemented with GlcNAc compared to the control flasks. While a marginal growth restriction persisted with a similar decay rate in stationary phase, overall it was demonstrated that the cocktail and GlcNAc supplementation could be utilized together to improve growth and affect the glycan distribution of EG2-hFc.

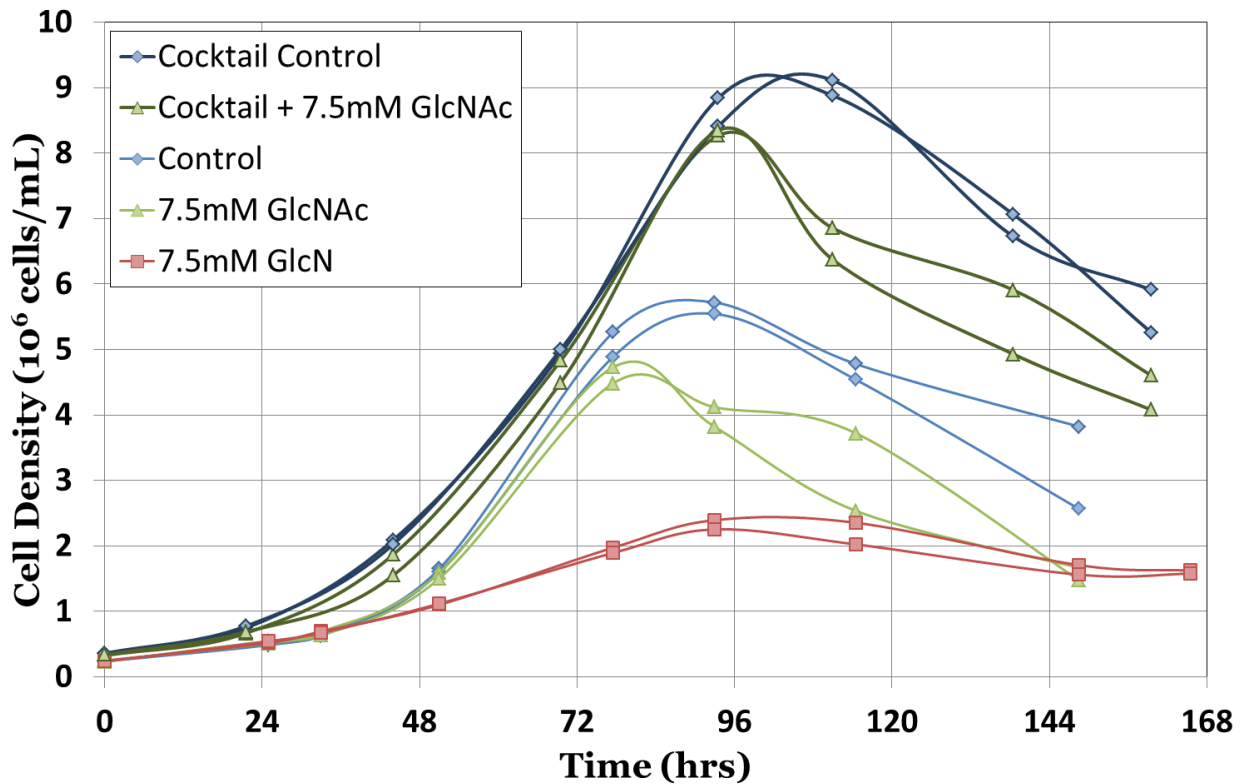


Figure 29 – Duplicate flasks of CHO<sup>BRI</sup>-1A7 cultured with a cocktail of supplements to improve growth, detailed in Chapter 3, as well as supplements of GlcNAc, which affect glycoform distribution, detailed in Chapter 4.

## **Chapter 6    Supplementing Glycosylation: A Review of Applying Nucleotide-Sugar Precursors to Growth Medium to Affect Therapeutic Recombinant Protein Glycoform Distributions<sup>3</sup>**

### **6.1    Overview**

Glycosylation is a critical quality attribute (CQA) of many therapeutic proteins, particularly monoclonal antibodies (mAbs), and is a major consideration in the approval of biosimilar biologics due to its effects to therapeutic efficacy. Glycosylation generates a distribution of glycoforms, resulting in glycoproteins with inherent molecule-to-molecule heterogeneity, capable of activating (or failing to activate) different effector functions of the immune system. Glycoforms can be affected by the supplementation of nucleotide-sugar precursors, and related components, to culture growth medium, affecting the metabolism of glycosylation. These supplementations has been demonstrated to increase nucleotide-sugar intracellular pools, and impact glycoform distributions, but with varied results. These variations can be attributed to five key factors: Differences between cell platforms (enzyme/transporter expression levels); differences between recombinant proteins produced (glycan-site accessibility); the fermentation and sampling timeline (glucose availability and exoglycosidase accumulation); glutamine levels (affecting ammonia levels, which impact Golgi pH, as well as UDP-GlcNAc pools); and finally, a lack of standardized metrics for observing shifts in glycoform distributions (glycosylation indices) across different experiments. The purpose of this review is to provide detail and clarity

---

<sup>3</sup> This manuscript was submitted [date] to the Journal of Biotechnology Advances, published by Elsevier. Blondeel, E.J.M., Aucoin, M.G., “Supplementing Glycosylation: A Review of Applying Nucleotide-Sugar Precursors to Growth Medium to Affect Therapeutic Recombinant Protein Glycoform Distributions”

on the state of the art of supplementation strategies for nucleotide-sugar precursors for affecting glycosylation in cell culture processes, and to apply glycosylation indices for standardized comparisons across the field.

Keywords: glycosylation; glycoform; nucleotide sugars; biosimilar; immune effector functions; mAbs; therapeutic protein; glutamine; ammonia; animal cell culture

## 6.2 Introduction

Glycosylation is acknowledged to be among the most important critical quality attributes (CQAs) of therapeutic biologicals, particularly for monoclonal antibodies (mAbs), which must be glycosylated for bioactivity (Dordal et al., 1985; Nose and Wigzell, 1983). Glycosylation is performed by a varying succession of enzymes, which regulate the sculpting and pruning of complex oligosaccharides, referred to broadly as ‘glycans’, onto biomolecules forming glycoconjugates. With respect to glycoprotein therapeutics, glycosylation introduces one of the major forms of molecule to molecule heterogeneity, which is broadly understood to affect a wide range of biotherapeutic efficacy metrics, including function (Dubé et al., 1988), immunogenicity (Bosques et al., 2010; Ghaderi et al., 2010; Padler-Karavani et al., 2008), drug clearance-rate (Morell et al., 1968), protein stability (Mimura et al., 2001; Wyss and Wagner, 1996), solubility (Leavitt et al., 1977), and in the case of mAbs, immune system recognition for effector function (Tao and Morrison, 1989).

Glycan heterogeneity can be influenced broadly by several process conditions including perturbations to temperature, pH and dissolved oxygen; an excellent review of which is presented by Hossler (2012). Other major factors of influence include the up/down regulation of membrane transporters and glycosyltransferases between cell platforms (Chen and Harcum, 2006; McDonald et al., 2016; N. S. C. Wong et al., 2010), and interruptions to the substrate supply chain of nucleotide-sugar metabolism and transport (Liu et al., 2014; McDonald et al., 2016; Nyberg et al., 1999; Pels Rijcken et al., 1995b). Glycan heterogeneity indicates biotherapeutics with molecule-to-molecule quality differences that will activate (or fail to activate) the immune system in different ways. This also creates a challenge for biosimilars to



match their glycan distributions with that of their reference (innovator) biologics, or at least demonstrate that any differences are not clinically significant (FDA, 2015).

Three major strategies exist to affect the glycosylation of recombinant proteins:

1. glycoengineering of cell platforms generally targeting either the addition or knock-out (including silencing) of glycosyltransferases and glycosyltransferases (Mori et al., 2004; Yamane-Ohnuki et al., 2004), or similarly targeting nucleotide-sugar Golgi transporters (Wright and Morrison, 1998);
2. downstream *in vitro* remodelling of glycans (Hodoniczky et al., 2005); or,
3. supplementation of nucleotide-sugar precursors and associated components, such as sugars and amine-sugars (Table 7-Table 9), including nucleosides like uridine and cytidine (Carvalho et al., 2003; Nyberg et al., 1999), and the metallic ion manganese (Crowell et al., 2007; St Amand et al., 2014; Surve and Gadgil, 2015).

This review will focus on the latter of these methods, providing clarity towards five key factors that have contributed to varied results for this promising method of tuning glycosylation in cell culture processes. The first of these factors are the differences in enzyme/transporter expression levels across cell platforms. Secondly, differences between recombinant proteins produced, particularly with respect to the accessibility of their glycan sites by glycosyltransferases. Thirdly, the fermentation and sampling timeline, both with respect to the glucose availability, as well as the accumulation of exoglycosidases at the latter stages of cultures. A fourth factor is the glutamine levels, as increases in ammonia alter the pH of Golgi compartments, and also increase UDP-GlcNAc intracellular pools. Finally, differences in metrics for reporting different glycan attributes (i.e. galactosylation), which prevent more standard comparisons of observed shifts in glycoform distributions between reports.

## 6.3 Glycosylation

The variability and probabilistic nature of glycosylation (Spahn et al., 2016) lends itself to a security recognition function *in vivo*, mediating countless lectin/ligand binding scenarios for sensing and signaling events, both at the molecular level as well as more broadly for cell signalling. Moremen and colleagues (2012) provide an excellent overview of glycosylation in vertebrates, and the resulting complexity of system-level interactions. From a therapeutics perspective, the significance and potential of glycosylation with respect to current and future biologics continues to grow (Dalziel et al., 2014).

Generally speaking, glycosylation comes in two main forms, N-linked and O-linked, which are designated by the functional group of the amino-acids where the glycans are bound. N-glycans are bound via amide-linkages to asparagine residues, and are typically larger oligosaccharides compared to O-glycans, which are bound to serine or threonine by glycosidic bonds. With respect to therapeutic glycoproteins, N-linked glycosylation receives the most attention in literature, particularly regarding mAbs, as glycosylation of the Fc region is a major factor in immune system effector functions, such as complement activation, and binding to Fc $\gamma$  receptors of leukocytes towards various immune responses (Tao and Morrison, 1989). O-glycosylation is not yet recognized as notably consequential to effector functions or bioefficacy for many approved glycoprotein therapeutics, but will affect some basic efficacy characteristics like protein stability (Wang et al., 1996).

### 6.3.1 Nucleotide-Sugar Metabolism

Substrates of glycosylation generally take the form of monosaccharides paired to particular nucleoside-phosphates (i.e. UDP-GlcNAc, GDP-Fucose, CMP-NeuAc, etc.), and are derived generally from glucose metabolism, as detailed in Figure 30. Nucleotide-sugars are generally

produced in the cytoplasm, with the exception of cytidine monophosphate N-acetylneuraminic acid (CMP-NeuAc), which is formed in the nucleus (Kean, 1970). Mammalian cells are able to take up a wide diversity of saccharide nutrients through the GLUT and SGLT families of cell membrane transporters. Supplementing nucleotide-sugar precursors circumvents points of regulation and feedback inhibition (Pels Rijcken et al., 1995b), leading to large fold-change increases in intracellular metabolic pools (Table 7-Table 9). Augustin and Mayoux (2014) present an excellent review of these transporter families, while Freeze and Elbein (2009) provide an exceptional review of the points of regulation controlling this metabolic network. The formation of amine-sugars like glucosamine (GlcN) require an amine donor, such as glutamine, through the action of glutamine-fructose-6-phosphate transaminase (Figure 30, Reaction 3), and these intracellular pools will be starved in glutamine's absence (Nyberg et al., 1999). However, it has also been demonstrated that ammonia can be utilized as a donor towards formation of UDP-GlcNAc and subsequent amine sugar pools (Valley et al., 1999).

With the exception of the endoplasmic reticulum (ER), where dolichol-linked monosaccharide substrates like glucose and mannose are 'flipped' from the cytosol into the organelle lumen (Figure 30, Reaction 24), nucleotide-sugars are typically transported by means of the SLC35 family of transporters, which require the respective nucleotide-monophosphate on the opposing side of the membrane to complete the exchange, as shown in Figure 30. Ishida and Kawakita (2004) have assembled a comprehensive review of the SLC35 family of transporters. Availability of particular nucleoside-monophosphates within the Golgi lumen is dependent on the activity of nucleoside diphosphatase (NDPase) to convert nucleoside-diphosphates to their monophosphate form (Figure 30); which has been identified as a potential bottleneck in glycan metabolism (McDonald et al., 2016).

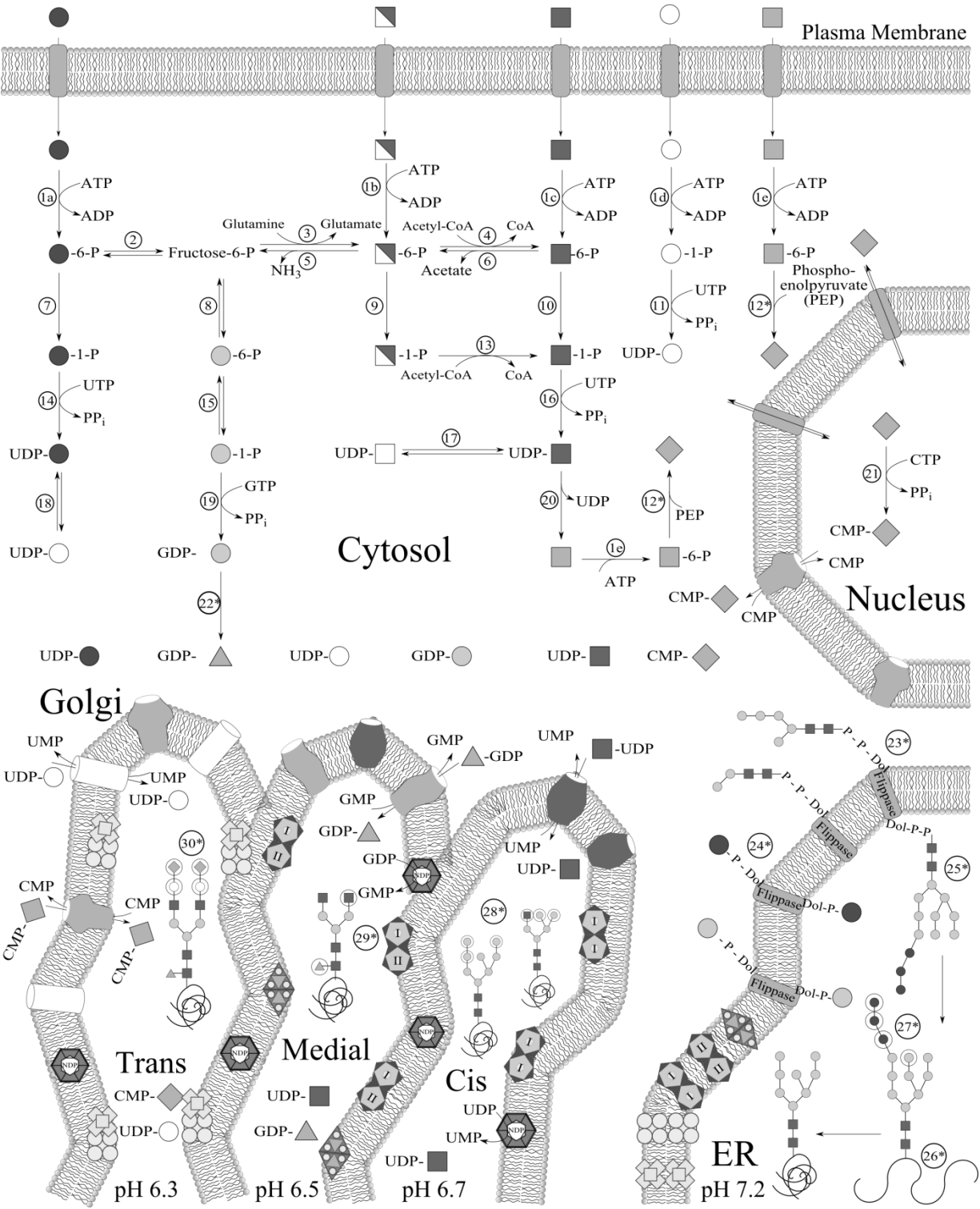
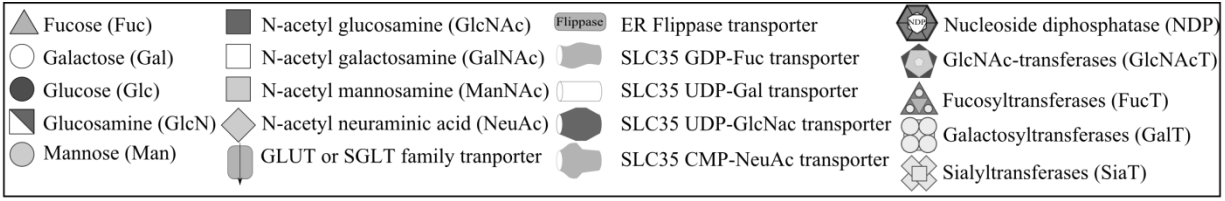


Figure 30 – Metabolic pathways for the synthesis and transport of intracellular nucleotide sugars utilizing glucose (Glc), galactose (Gal), glucosamine (GlcN), acetylglucosamine (GlcNAc), and acetylmannosamine (ManNAc), towards N-glycosylation in mammalian cells. This includes the assembly of dolichol-14-sugar oligosaccharide and co-translational binding for N-glycosylation of proteins beginning in the cytosol and occurring in ER, followed by the sculpting of further monosaccharide modifications in the Golgi by pH-dependent heteromeric glycosyltransferases.

Enzymes (asterisks\* indicate a multi-step process): (1a-e) hexokinase; (2) glucose-6-phosphate isomerase; (3) glutamine-fructose-6-phosphate transaminase; (4) glucosamine-phosphate N-acetyltransferase; (5) glucosamine-6-phosphate deaminase; (6) N-acetylglucosamine-6-phosphate deacetylase; (7) phosphoglucomutase; (8) mannose-6-phosphate isomerase; (9) phosphoglucomutase; (10) phosphoacetylglucosamine mutase; (11) UTP-galactose-1-phosphate uridylyltransferase; (12\*) N-acetylneuraminic acid-9-phosphate synthase and phosphatase; (13) glucosamine-1-phosphate N-acetyltransferase; (14) UTP-glucose-1-phosphate uridylyltransferase; (15) phosphomannomutase; (16) UDP-N-acetylglucosamine diphosphorylase; (17) UDP-N-acetylglucosamine 4-epimerase; (18) UDP-glucose 4-epimerase; (19) mannose-1-phosphate guanylyltransferase; (20) UDP-N-acetylglucosamine 2-epimerase; (21) N-acetylneuraminic acid cytidylyltransferase; (22\*) GDP-mannose 4,6-dehydratase and GDP-L-fucose synthase; (23\*) assembly at the cytoplasmic face of the endoplasmic reticulum (ER) of the dolichol diphosphate linked 7-sugar oligosaccharide of mannose and GlcNAc prior, which is flipped into the ER; (24\*) dolichol phosphate linked glucose and mannose monosaccharide, which are flipped into the ER; (25\*) dolichol diphosphate linked 14-sugar oligosaccharide precursor of N-glycosylation; (26\*) transfer of the 14-sugar oligosaccharide to an asparagine residue, part of a sequon in the amino-acid chain Asn-X-Ser/Thr where X is not proline, via the action of oligosaccharide transferase (OST); (27\*) protein folding and pruning of three terminal glucose moieties by  $\alpha$ -glucosidases I & II, as well as removal of the central terminal mannose by ER  $\alpha$ -mannosidase I, yielding Man8GlcNAc2 before transition to the Golgi; (28\*) cis-Golgi lumen, three terminal mannose residues are pruned by Golgi  $\alpha$ -mannosidase I, then acetylglucosamine transferase (GnT-I) adds a terminal GlcNAc to the  $\alpha$ 1-3 core mannose residue, finally Golgi  $\alpha$ -mannosidase II removes the final terminal  $\alpha$ 1-3 and  $\alpha$ 1-6 mannose residues yielding GlcNAcMan3GlcNAc2, the lower pH signals homomeric complexes of glycosyltransferases to reform as heteromeric dimer complexes acting sequentially on the glycan; (29\*) medial-Golgi lumen, acetylglucosamine transferase (GnT-II) adds a terminal GlcNAc to the  $\alpha$ 1-6 core mannose residue, subsequently fucosyltransferase (FucT) adds a core  $\alpha$ 1-6 fucose residue to the GlcNAc closest to the asparagine residue yielding GlcNAc2Man3GlcNAc2-Fuc, the lower pH signals homomeric complexes of glycosyltransferases to reform as heteromeric dimer complexes acting sequentially on the glycan; (30\*) trans-Golgi lumen, heteromeric dimer complexes of galactosyltransferases and sialyltransferases add terminal galactose and sialic acid moieties to the glycans.

### 6.3.2 N-Linked Glycosylation

N-linked glycosylation begins in the cytoplasm with the assembly of a seven sugar oligosaccharide onto a dolichol diphosphate anchor (Figure 30, Reaction 23). Once assembled, this oligosaccharide is flipped into the endoplasmic reticulum (ER) where dolichol phosphate linked mannose and glucose species donate the remaining four mannose residues and three glucose residues to complete the fourteen sugar N-glycosylation oligosaccharide precursor. This lipid-linked oligosaccharide is then detached from its dolichol phosphate anchor and bound to an asparagine amino acid of a protein undergoing translation by the oligosaccharyltransferase (OST) enzyme complex (Figure 30, Reaction 26). The resulting precursor to N-linked glycosylation is bound to the protein at a site referred to as a ‘sequon’. Once bound to its sequon, in step with protein folding, glycotransferase enzymes of the ER act upon the oligosaccharide

precursor glycan, removing the three terminal glucose moieties as well as the centremost terminal mannose (Figure 30, Reaction 27).

### **6.3.3 Microheterogeneity**

Glycosylation continues into the Golgi, where further glycosyltransferase activity will produce a myriad of glycans that diverge between different cell lines. With particular regards to mammalian style complex glycans, forms of microheterogeneity include whether the terminal moieties are mannose (Man) or acetyl-glucosamine (GlcNAc). The degree of GlcNAc branching is referred to as “antennarity”, which can be as many as four, plus an extra bisecting GlcNAc on the central mannose. Other forms of microheterogeneity include the binding of core  $\alpha_{1-6}$  fucose (Fuc) to the first GlcNAc bound to Asparagine (Asn); as well as the binding of galactose (Gal) to terminal GlcNAc moieties possibly followed by binding of sialic acids (NeuAc/Neu5Gc) to Gal, which are the only glycan moieties to confer a negative charge.

Differences between glycoforms can be written by abbreviated nomenclatures, such as the Oxford Glycobiology Institute convention, described by Gornik and colleagues (2007), and utilized here. In this convention, the ‘F’ refers to fucose bound by an  $\alpha_{1-6}$  bond, the ‘A’ to the degree of antennarity (i.e. GlcNAc branching), ‘B’ for the presence of a bisecting GlcNAc, ‘G’ to the degree of galactosylation, and the ‘S’ for the degree of sialylation.

## **6.4 Controlling Glycosylation by Supplementation**

Typical glycoforms observed for several commercial mAbs are under-galactosylated, hindering their therapeutic potential (Wacker et al., 2011). Research in the field of supplementing nucleotide sugar precursors for affecting glycoforms follows a hypothesis that either substrate-limitation or regulatory feedback bottlenecks prevent more complex glycoforms

with terminal galactose and sialic acid moieties, like those observed in endogenous human sera (Flynn et al., 2010). These supplementation strategies, detailed in Table 7-Table 9, and Figure 32-Figure 34, offer a simple means to adjust product glycoforms without having to completely redesign (i.e. glycoengineer) cell platforms.

Nucleotide-sugar precursors and associated components supplemented to growth media have conventionally targeted what were regarded as the most crucial glycan-moieties for mammalian N-glycosylation: N-acetylglucosamine (GlcNAc), galactose (Gal), and, N-acetylneuraminic acid (NeuAc). Precursors selected for supplementation favour intermediate species at various points in the intracellular metabolic synthesis of these nucleotide-sugars that would otherwise be synthesized from glucose, as shown in Figure 30.

The three compounds most commonly supplemented in literature include:

- Glucosamine (GlcN), and more recently N-acetylglucosamine (GlcNAc), often accompanied with uridine (Urd) – as detailed in Table 7 and Figure 32
- Galactose (Gal), often accompanied with uridine (Urd), and occasionally manganese<sup>4</sup> (Mg<sup>2+</sup>) – as detailed in Table 8 and Figure 33
- N-acetylmannosamine (ManNAc), often accompanied with cytidine (Cyt) – as detailed in Table 9 and Figure 34

These supplements have repeatedly been reported to increase the intracellular pools of nucleotide-sugars, and affect glycoform distributions. Inconsistencies in reported effects can be attributed to differences across five key factors: the host cell platform, the recombinant protein

---

<sup>4</sup> Manganese ions as a supplementation strategy has primarily been utilized in conjunction with uridine and galactose as part of the cocktail recommended by Gramer and colleagues (2011).

expressed, timeline of fermentation from supplementation to sampling/harvest, the amount of glutamine present in culture media, and a previous lack of standardized comparison via glycosylation index equations (Figure 31) for observing shifts in glycoform distribution, applied here.

## **6.4.1 Key Factors Impacting Supplementation Results**

### **6.4.1.1 Cell Platform**

Differences across cell platforms are expected to produce varying glycan distributions, as it is common even to have clones of the same cell-line that under or over-express an important enzyme or transporter, such as the YB2/0 rat hybridoma cells utilized by Shinkawa and colleagues (2003) that had low levels of fucosyltransferase-8 (FUT8), leading to low-fucose mAbs. Similarly, differences between different mammalian cell lines will commonly produce varying effects under identical nucleotide-sugar precursor supplementation strategies. This can be observed in the work of Baker and colleagues (2001), when the same TIMP-1 protein was expressed in both GS-CHO and GS-NS0 cells; 10mM glucosamine supplementation resulted in a significant antennarity index increase of 9% in the former ( $P < 0.05$ ), but no change in the latter.

### **6.4.1.2 Protein Glycan Site**

The type of protein examined is perhaps the greatest factor leading to differences in glycan profiles, as different glycan sequons will have very different solvent accessibility. A literature analysis conducted by Thaysen-Andersen and Packer (2012) determined that core  $\alpha_{1-6}$  fucosylation, glycan antennarity, and complex glycoforms vs high mannose, are all notably affected by the solvent-accessibility of glycan sites, and hypothesized the same to be true for terminal galactosylation and sialylation. Therefore, drawing a comparison between the glycans derived from EPO vs mAbs is not fundamentally direct comparison, since sequon sites on the



two proteins will have very different accessibility to the Golgi infrastructure to modify those glycans. This issue can be observed in Figure 32-Figure 34, with respect to the antennarity of different proteins. In Figure 33, the proteins are predominantly IgGs, and glycans are uniformly biantennary or lower, keeping their AI below 40%, while proteins like EPO, TIMP-1, and IL-2 shown in Figure 32 and Figure 34 can have higher levels of branching due to the accessibility of these sequons to latter N-acetylglucosyltransferases (GnT IV&V) (Thaysen-Andersen and Packer, 2012).

#### **6.4.1.3 Fermentation Sampling Timeline**

Another very important factor is the fermentation timeline, particularly the time of sampling or harvest of recombinant proteins for glycan analysis. It has been demonstrated by Gramer and colleagues (1993, 1995), that CHO cells accumulate sialidase enzymes in their supernatant, and growing cultures past exponential phase until loss of viability can diminish the total sialylation of secreted recombinant proteins. Furthermore, a clear relationship has recently been demonstrated by Liu and colleagues (2014) between availability of glucose and the level of galactosylation and sialylation of mAbs grown in CHO cells. Therefore, in experiments where recombinant proteins are harvested for glycan analysis near the peak of exponential growth compared to those harvested when viability is decreasing, proportions with terminal sialylation will be in greater proportion. This can be observed in Figure 33, comparing the experiments of both Liu and colleagues (2014) and Surve and Gadgil (2015), who sampled their cultures during exponential phase, compared against those of St Amand and colleagues (2014) and Gramer and colleagues (2011), who sampled at the end of the culture. In the case of the former, both controls and final GI levels are generally higher than the latter, despite similar supplementation regimes, cell lines, and IgG proteins. Exceptions can be observed of course in the results of Grainger and James (2013), who sampled at the end of their culture, showing high GI values for both their controls

and final galactosylation percentage; however these values might have been even higher with earlier sampling.

#### **6.4.1.4 Glutamine Level**

Glutamine is of particular interest due to its relationship with ammonia, which directly impacts glycosylation activities in two ways. First, ammonia is a weak base capable of diffusing across cellular membranes, impacting the intracellular pH of cellular organelles like the Golgi. The cis-, medial-, and trans-Golgi cisternae operate at distinct acidic pH levels, as shown in Figure 30. Glycosyltransferases form reversible homomeric and heteromeric dimers, which migrate as mobile complexes between the Golgi and the ER (Hassinen and Kellokumpu, 2014). Homodimers are favoured closer to the neutral pH of the ER, where these enzymes are synthesized, while formation of heteromeric dimers, with enhanced activity, are favoured at the reduced pH points of the respective Golgi cisternae where they operate (Hassinen and Kellokumpu, 2014). This is illustrated in the Golgi glycosyltransferase enzyme pairings in Figure 30. Higher ammonia levels will neutralize the intracellular pH of Golgi cisternae, causing heterodimer pairs to split and reform to their homodimer formats, reducing their functionality (Hassinen and Kellokumpu, 2014). Therefore, elevated supplementation of the labile nutrient glutamine, which increases intracellular ammonia levels, will in turn increase Golgi pH, and perturb the functionality of glycosyltransferases, particularly galactosyltransferase and sialyltransferase, decreasing the GI and SI of glycans. This result was demonstrated directly by Aghamohseni and colleagues (2014), who showed that supplementing increasing concentrations of glutamine to CHO cultures expressing a heavy-chain antibody (HCAb) reduced galactosylation and sialylation of these glycoproteins.

The second manner in which glutamine supplementation affects glycoform distributions is by directly increasing UDP-GlcNAc pools producing similar effects and glycoform shifts to those detailed in Table 7. Valley and colleagues (1999) supplementing ammonium ions with <sup>15</sup>N tracers to BHK-21 cells produced a significant increase in UDP-GlcNAc intracellular nucleotide sugar pools. Approximately 60% of this pool incorporated the <sup>15</sup>N tracers – a proportion approximately equivalent to the increase in the pool itself (Valley et al., 1999). As is demonstrated in Figure 32, elevated glucosamine levels will shrink levels of galactosylation and sialylation of glycoproteins. Therefore, elevated glutamine supplementations to cultures can have a similar effect as either ammonium or glucosamine supplementation, which has been demonstrated by several researchers (Gawlitzeck et al., 1998; Grammatikos et al., 1998; Yang and Butler, 2002).

CHO cells expressing glutamine synthase (GS) require little or no glutamine in their growth medium. St Amand and colleagues (2014), Kildegaard and colleagues (2015), and Surve and Gadgil (2015) all utilized glutamine nutrient in their cultures; 4mM for the former, and 8mM for the latter two respectively (Table 8). Galactose supplementation improves GI for all three of these research groups, but it's typically an increase on the order of only 10%, while researchers supplementing galactose to GS-CHO cultures achieve GI increases for mAbs of 20% or higher (Figure 33). Therefore, addition of glutamine nutrient may limit the potential improvement to GI of galactose supplementation.

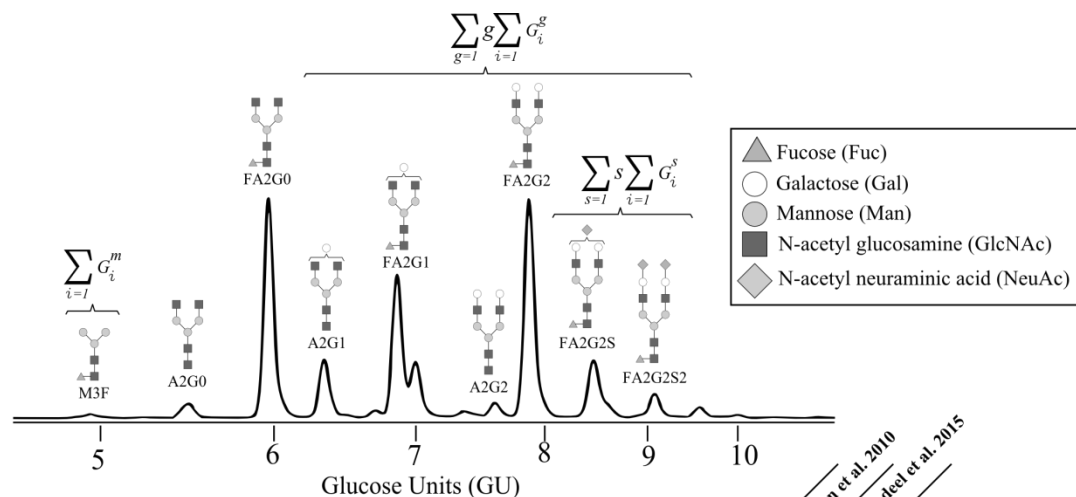
#### **6.4.1.5 Standardized Metrics for Reporting Glycan Shifts**

Lastly, given the various experimental differences across reports in literature, it is difficult to make comparisons and draw conclusions regarding the effectiveness of a particular supplementation regime without acknowledging the differences between control cultures as well.

As such, glycoform distribution index calculations have been employed, as detailed in the following section, to standardize comparisons between experimental controls and resulting shifts. These comparisons are detailed in Table 7-Table 9 and Figure 32-Figure 34.

#### **6.4.2 Glycoform Distribution Indexes**

Glycosylation indices are employed in order to provide a consistent comparison between experiments. These indices summarize the degree of glycosylation with respect to glycoform characteristics such as galactosylation (GI), sialylation (SI), core  $\alpha_{1-6}$  fucosylation (FI), antennarity (AI), and high-mannose types (MI). These equations can be described generally as a measurement of how much of an available glycan substrate has received a particular glycan moiety. This is typically calculated as the total number of a particular glycan moiety, such as a terminal galactose unit, divided by all the available sites that could have received that moiety. As an example, if half of glycans with available terminal galactose sites are sialylated, the SI will be 50%, despite whether only 5% of total glycans receive some degree of sialylation. These equations are designed to benefit tuning glycoform distributions in bioprocesses, rather than describing the distributions towards clinical applications. Figure 31 details each of the five equations, their derivation from a glycan distribution, and provides sample calculations with respect to human serum IgG1 (Flynn et al., 2010) and a recombinant HCAb (Blondeel et al., 2015). Figure 32-Figure 34 provide detailed comparisons regarding both the shifts in the glycosylation of cultures under the reported supplementation regimes, but also comparisons of the starting glycoforms of control cultures.



$$GI = \frac{\sum_{g=1}^g \sum_{i=1}^g G_i^g}{\sum_{g=0}^g \sum_{a=1}^a \sum_{j=1}^g G_j^g} \times 100 \quad (1)$$

$$SI = \frac{\sum_{s=1}^s \sum_{i=1}^s G_i^s}{\sum_{s=0}^s \sum_{g=1}^g \sum_{j=1}^s G_j^s} \times 100 \quad (2)$$

$$FI = \frac{\sum_{f=1}^f \sum_{i=1}^f G_i^f}{\sum_{f=0}^f \sum_{j=1}^f G_j^f} \times 100 \quad (3)$$

$$AI = \frac{\sum_{a=1}^a \sum_{i=1}^a G_i^a}{5 \sum_{a=0}^a \sum_{j=1}^a G_j^a} \times 100 \quad (4)$$

$$MI = \frac{\sum_{m=1}^m \sum_{i=1}^m G_i^m}{\sum_{m=0}^m \sum_{j=1}^m G_j^m} \times 100 \quad (5)$$

	<i>g</i>	<i>s</i>	<i>f</i>	<i>a</i>	<i>m</i>	hlgG1	HCAb
Complex Neutral							
FA2G0	0	0	1	2	0	12.5	12.24
FA2G1	1	0	1	2	0	42.3	25.32
FA2G2	2	0	1	2	0	21.7	29.46
A2G0	0	0	0	2	0	0.57	0.97
A2G1	1	0	0	2	0	1.309	4.12
A2G2	2	0	0	2	0	1.44	1.83
A4G1	1	0	0	4	0	-	1.60
A4G3	3	0	0	4	0	-	1.69
A4G4	4	0	0	4	0	-	0.78
FA2BG0	0	0	1	3	0	2.70	-
FA2BG1	1	0	1	3	0	7.2	-
FA2BG2	2	0	1	3	0	1.49	-
A2BG1	1	0	0	3	0	0.341	-
Complex Charged							
FA2G1S	1	1	1	2	0	1.21	-
FA2G2S	2	1	1	2	0	8.6	11.05
FA2G2S2	2	2	1	2	0	-	5.80
A2G2S	2	1	0	2	0	0.40	-
FA2BG1S	1	1	1	3	0	0.174	-
FA2BG2S	2	1	1	3	0	0.149	-
A4G3Sn	3	1*	0	4	0	-	1.95
A4G4Sn	4	1*	0	4	0	-	0.90
Hybrid & Mannose							
A1G0	0	0	0	1	1	0.064	0.12
FA1G1	1	0	1	1	1	-	0.43
M4FA2G0	0	0	1	2	1	0.138	-
M4A2G0	0	0	0	2	1	0.053	-
M4A2G1	1	0	0	2	1	0.248	-
M4A2G2	2	0	0	2	1	0.150	-
FA1G1S	1	1	1	1	1	-	-
M4A2G2S	2	2	0	2	1	0.028	-
M3F	0	0	1	0	2	-	0.09

Flynn et al. 2010  
Blondeel et al. 2015

\**I* = glycoform index (%)

*g* = number of terminal galactose moieties per glycan

*s* = number of terminal sialic acid moieties per glycan

*f* = binary number of core  $\alpha_{1-6}$  fucosylation per glycan

*a* = antennarity/branching; the number of terminal GlcNAc moieties per glycan

*m* = number per glycan indicating hybrid (1) or high-mannose type (2)

$G_i^*$  = proportion of glycoforms with a particular moiety (*g*, *s*, *a*, *f*, *m*)

$G_j^*$  = proportion of glycoforms able to receive a particular moiety (*g*, *s*, *a*, *f*, *m*)

<i>GI</i>	58.7%	69.3%
<i>SI</i>	8.8%	17.5%
<i>FI</i>	95.4%	84.4%
<i>AI</i>	39.9%	42.6%
<i>MI</i>	0.3%	0.9%

Figure 31 – A monoclonal antibody glycan distribution segmented to demonstrate the glycosylation index formulae. In each case the proportion of the glycan distribution with a particular moiety (i.e. sialic acid, terminal galactose, etc.) is divided by the proportion that could have received that particular moiety, with respect to the sequence of glycosyltransferase enzymes acting on the protein undergoing glycosylation.

Formulae are presented for Equation 1) galactosylation index (GI); Equation 2) sialylation index (SI); Equation 3) fucosylation index (FI); Equation 4) antennarity index (AI); and Equation 5) mannose index (MI). A demonstration of the calculations is provided with respect to glycan distributions from serum-derived IgG1 pooled from five healthy donors (Flynn et al., 2010) and a recombinant heavy-chain antibody (Blondeel et al., 2015).

### 6.4.3 Supplementation of Nucleotide-Sugar Precursors

#### 6.4.3.1 Glucosamine (GlcN) & Acetyl-glucosamine (GlcNAc)

Glucosamine (GlcN) supplementation is consistently reported to increase intracellular pools of UDP-HexNAc (i.e. UDP-GlcNAc & UDP-GalNAc), as detailed in Table 7. UDP-GlcNAc/GalNAc intracellular pools form in the cytoplasm and are linked by an epimerase (Figure 30, Reaction 17), which holds them in relatively fixed concentration proportions of approximately 2:1 (Blondeel et al., 2015; Glaser, 1959).

**Table 7 – Comparison of glycoform shifts and differences between reported experiments for the supplementation of glucosamine (GlcN), its acetylated form acetyl-glucosamine (GlcNAc), and the nucleoside uridine (Urd), towards expanding intracellular nucleotide-sugar pools of UDP-GlcNAc in cultured mammalian cells to affect N-linked glycoforms of recombinant glycoproteins. Experimental differences reported include: Supplementation cocktails and concentrations with multiple bullet-points representing separate flask or bioreactor conditions; The cell line utilized and the lineage of that cell line where reported; The protein being expressed and whether it is a mutant variant or fusion; The bioprocess scale, time of supplementation, and time of harvest; The amount of glutamine (Gln) utilized in the growth medium.**

Supplement	Cell	Protein	Fermentation Timeline	Gln (mM)	Effect	Researchers
<ul style="list-style-type: none"> <li>▪ 20mM GlcNAc</li> </ul>	CHO (DG44)	IgG	<ul style="list-style-type: none"> <li>▪ Bioreactor, fedbatch</li> <li>▪ 1L</li> <li>▪ Addition 48h</li> <li>▪ Harvest 336h</li> </ul>	8	<ul style="list-style-type: none"> <li>▪ Reduced glycan complexity to favour G0 and FG0 glycoforms</li> <li>▪ Reduced galactosylation</li> </ul>	(Kildegaard et al., 2015)
<ul style="list-style-type: none"> <li>▪ 7.5mM GlcN</li> <li>▪ 2.5 - 10mM GlcNAc</li> </ul>	CHO (Dukx)	IgG HCAB	<ul style="list-style-type: none"> <li>▪ Flasks</li> <li>▪ 125mL</li> <li>▪ Addition 50h</li> <li>▪ Harvest 144h-168h</li> </ul>	5	<ul style="list-style-type: none"> <li>▪ Reduced glycan complexity to favour G0 and FG0 glycoforms – both GlcN &amp; GlcNAc supplementation</li> <li>▪ ~50% drop in growth rate with GlcN supplementation</li> <li>▪ &lt;5% drop in growth rate with GlcNAc supplementation</li> <li>▪ proportional increase in UDP-GlcNAc pool up to 2x with GlcNAc supplementation</li> </ul>	(Blondeel et al., 2015)
<ul style="list-style-type: none"> <li>▪ 10mM GlcN</li> </ul>	NS0 (GS)	IgG	<ul style="list-style-type: none"> <li>▪ Flasks</li> <li>▪ 500mL</li> <li>▪ Addition 48h</li> <li>▪ Harvest 96h</li> </ul>	0.4 (GS)	<ul style="list-style-type: none"> <li>▪ 17x UDP HexNAc</li> <li>▪ -56% Galactosylation</li> <li>▪ -63% UDP-Hex</li> <li>▪ Reduced growth</li> </ul>	(Hills et al., 2001)
<ul style="list-style-type: none"> <li>▪ 10mM GlcN</li> </ul>	CHO (K1)	EPO	<ul style="list-style-type: none"> <li>▪ Flasks</li> <li>▪ 250mL</li> <li>▪ Addition 0h</li> <li>▪ Harvest day 4-5</li> </ul>	-	<ul style="list-style-type: none"> <li>▪ 18.5x UDP-GlcNAc</li> <li>▪ Increased glycan heterogeneity</li> <li>▪ -22% tetrasialylation</li> </ul>	(Yang and Butler, 2002)
<ul style="list-style-type: none"> <li>▪ 10mM GlcN, glutamine free</li> </ul>	BHK	IL-2	<ul style="list-style-type: none"> <li>▪ Perfusion</li> <li>▪ 2.5 L</li> <li>▪ Addition: day 21</li> <li>▪ Harvest: days 26-28 and 29-30</li> </ul>	0	<ul style="list-style-type: none"> <li>▪ Greater antennarity, but lower complexity of glycans</li> <li>▪ 3x UDP-HexNAc</li> <li>▪ Greater proportion of monosialylation with GlcN</li> <li>▪ +58% sialylation in std culture without glutamine</li> </ul>	(Gawlitzek et al., 1998)
<ul style="list-style-type: none"> <li>▪ 10mM GlcN + 2mM Urd</li> </ul>	CHO (GS) NS0 (GS)	TIMP-1	<ul style="list-style-type: none"> <li>▪ Flasks</li> <li>▪ 1000mL</li> <li>▪ Addition 24h</li> <li>▪ Harvest 48h</li> </ul>	0.4 (GS)	<ul style="list-style-type: none"> <li>▪ 58x UDP-HexNAc</li> <li>▪ 8x UDP-Hex</li> <li>▪ +9% antennarity</li> <li>▪ -8% sialylation</li> </ul>	(Baker et al., 2001)

Supplement	Cell	Protein	Fermentation Timeline	Gln (mM)	Effect	Researchers
<ul style="list-style-type: none"> <li>▪ 10mM GlcN + 2mM Urd</li> </ul>	BHK	IL-2 <sup>5</sup>	<ul style="list-style-type: none"> <li>▪ Perfusion</li> <li>▪ 2.5 L</li> <li>▪ Addition 10d</li> <li>▪ Harvest 14d</li> </ul>	0	<ul style="list-style-type: none"> <li>▪ 12x UDP-GlcNAc</li> <li>▪ 5x UTP</li> <li>▪ Rise antennarity</li> </ul>	(Grammatikos et al., 1998)
<ul style="list-style-type: none"> <li>▪ 10mM GlcN</li> <li>▪ +5mM Urd</li> </ul>	CHO (Dukx)	IFN- $\gamma$	<ul style="list-style-type: none"> <li>▪ Flasks (n=1)<sup>6</sup></li> <li>▪ 1000mL</li> <li>▪ Addition 48h</li> <li>▪ Harvest 96h</li> </ul>	4	<ul style="list-style-type: none"> <li>▪ Reduced growth</li> <li>▪ +28% sialylation</li> <li>▪ 6-15x increase UDP-HexNAc</li> </ul>	(N. S. C. Wong et al., 2010)
<ul style="list-style-type: none"> <li>▪ 3.5 &amp; 17.5mM GlcN + 1mM Urd</li> </ul>	CHO SCLC	NCAM	<ul style="list-style-type: none"> <li>▪ 6 &amp; 24-well plates</li> <li>▪ Addition 12-18h</li> <li>▪ Harvest 128h</li> </ul>	6	<ul style="list-style-type: none"> <li>▪ 25x UDP GlcNAc</li> <li>▪ Reduced growth</li> <li>▪ -90% polysialylation<sup>7</sup></li> </ul>	(Zanghi et al., 1998)
<ul style="list-style-type: none"> <li>▪ 1-10mM Urd</li> </ul>	CHO (Dukx)	IFN- $\gamma$	<ul style="list-style-type: none"> <li>▪ Flasks</li> <li>▪ 100mL</li> </ul>	3	<ul style="list-style-type: none"> <li>▪ Increased UTP correlated to increased UDP-HexNAc except in absence of glutamine</li> </ul>	(Nyberg et al., 1999)
<ul style="list-style-type: none"> <li>▪ 0.5mM Urd</li> </ul>	RH	N/A	<ul style="list-style-type: none"> <li>▪ Culture dish</li> <li>▪ 3 mL</li> <li>▪ Addition 16h</li> <li>▪ Harvest 24h</li> </ul>	2.4 <sup>8</sup>	<ul style="list-style-type: none"> <li>▪ Reduced sialylation</li> <li>▪ 6.7x UTP</li> <li>▪ 3.8x UDP-hexose</li> <li>▪ 4.6x UDP-HexNAc</li> </ul>	(Pels Rijcken et al., 1995b)

Glucosamine supplementation is commonly reported to reduce the complexity of N-glycan terminal moieties, favouring “G0” glycoforms featuring terminal GlcNAc (i.e with reduced galactosylation and sialylation) (Hills et al., 2001; Pels Rijcken et al., 1995b; Yang and Butler, 2002; Zanghi et al., 1998). GlcN is also reported to increase glycan antennarity (Baker et al., 2001; Gawlitzek et al., 1998; Grammatikos et al., 1998); however, this is only reported for non-IgG proteins with higher-antennarity glycans (Thaysen-Andersen and Packer, 2012), such as TIMP-1 & IL-2 to-date (Table 7, Figure 32). Conversely, Yang and Butler (2002) actually

<sup>5</sup> Modified IL-2 variant featuring an artificial N-glycan site

<sup>6</sup> Only a single flask for each experiment, and only one control flask appears to have been used

<sup>7</sup> NCAM protein glycan results reported only relative to controls

<sup>8</sup> Waymouth culture medium (Morton, 1970)



reported the opposite effect, with a reduction in antennarity of EPO from glucosamine feeding. Interestingly, Yang and Butler also reported elevated ammonia levels and increased glutamine uptake during GlcN supplementation, while Baker and colleagues (2001) reported minimal increase in ammonia in their GS cells; as such, this effect may depend on how efficiently the cell platform converts ammonia to UDP-GlcNAc (Valley et al., 1999), as opposed to harvesting the glucose from glucosamine via glucosamine-6-phosphate deaminase (Figure 30, Reaction 5). As noted in the previous section, Valley and colleagues (1999) supplementing  $^{15}\text{N}$  traced ammonium ions, determined that BHK-21 cells produced a significant increase in UDP-GlcNAc intracellular nucleotide sugar pools, and that approximately 60% of this pool incorporated  $^{15}\text{N}$  – a proportion approximately equivalent to the increase in the pool itself. Metabolomic analysis of CHO cultures producing HCABs supplemented with both GlcN and GlcNAc reported neither elevated ammonia, nor increased uptake of glutamine; however, a three-fold increase in acetate was observed after glucose exhaustion, which has been attributed to scavenging of glucose from UDP-GlcNAc pools in stationary phase (Blondeel et al., 2015). Elevated ammonia levels will raise the pH of Golgi compartments, and prevent heteromeric glycosyltransferase dimer complexes, such as GnT-IV/V from functioning properly (Hassinen and Kellokumpu, 2014). Further, increasing glutamine can produce a similar effect as supplementing GlcN and GlcNAc to mammalian cultures (Aghamohseni et al., 2014). Therefore, the effect of increasing antennarity may depend on whether the metabolism favours formation of UDP-GlcNAc pools or scavenging glucose from those same pools.

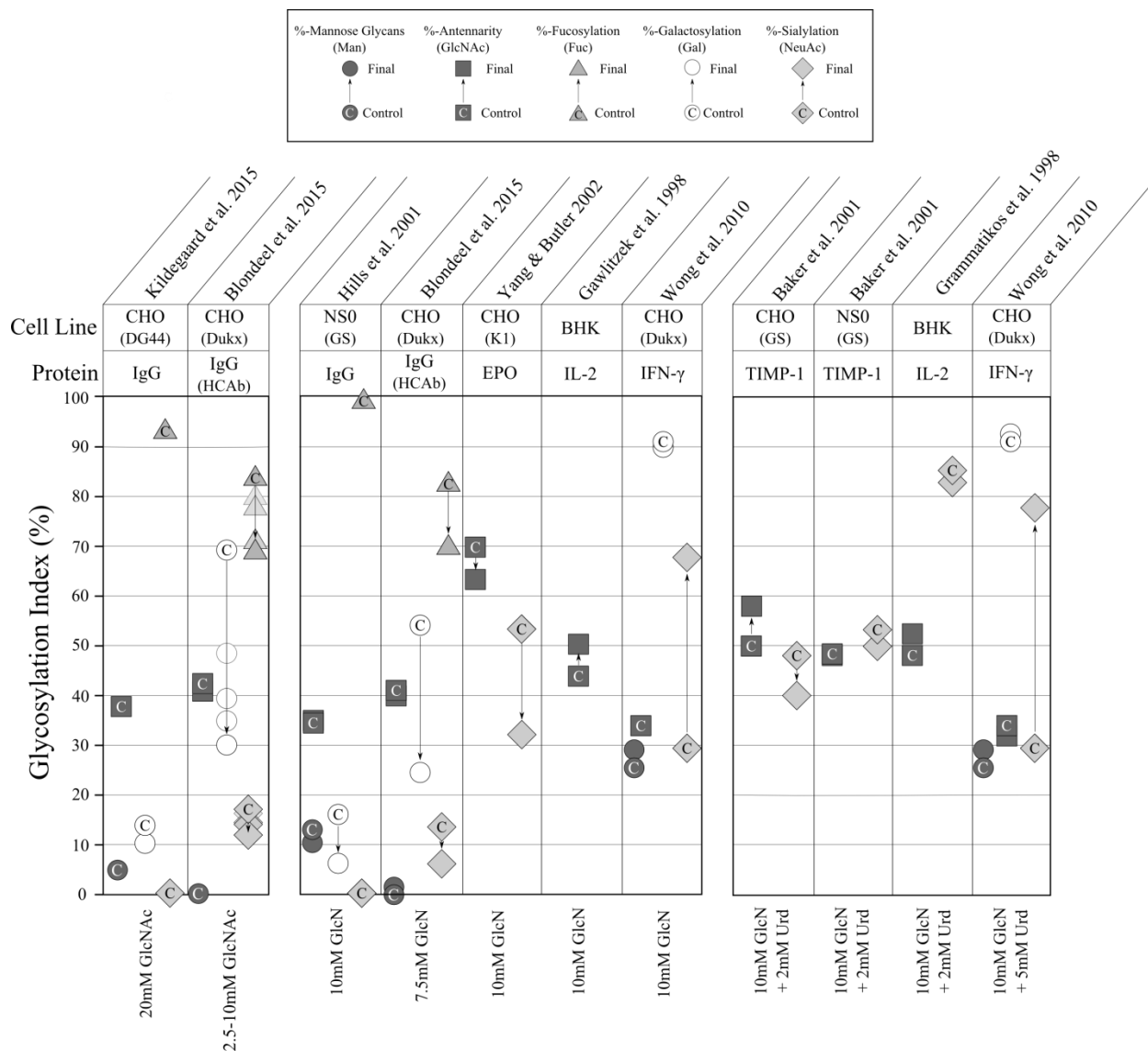


**Figure 32 – Comparison of glycoform shifts reported for experiments employing the supplementation of glucosamine (GlcN), its acetylated form acetyl-glucosamine (GlcNAc), and the nucleoside uridine (Urd), to affect N-linked glycoforms of recombinant glycoproteins produced in mammalian cell cultures.**

The %-shift in glycoforms, reported in Table 16, relative to reported control cultures is demonstrated as a shift from a starting control glycoform, indicated with a ‘C’ within the respective symbol, to a final glycoform following supplementation, as per the directional arrow between the two construction points. The glycosylation % values for mannose-type, antennarity, galactosylation, sialylation, and fucosylation are represented by their respective monosaccharide symbols.

Wong and colleagues (2010) reported the only instance where GlcN supplementation increases the complexity of N-glycans’ terminal moieties, with increased sialylation of IFN- $\gamma$ . It is worth noting that increased sialylation was observed for all of Wong et al.’s experimental conditions including supplementation with galactose and ManNAc, with and without associated

nucleosides. Furthermore, the experiment appears to be  $n=1$ , with only a single control flask. Therefore, it is possible that the control flask for this experiment is merely an outlier of reduced sialylation. Nyberg and colleagues (1999) similarly cultured CHO cells expressing IFN- $\gamma$ , and supplemented uridine rather than GlcN, reporting smaller but significant increases to intracellular UDP-GlcNAc pools (Table 7); however, no such increase in sialylation of IFN- $\gamma$  glycoforms was observed.

While more complex glycans (i.e. those possessing terminal galactose and sialic acid moieties) are therapeutically more desirable, commercial therapeutic mAbs favour terminal GlcNAc “G0” glycoforms (Wacker et al., 2011), therefore innovator biologics for biosimilars also favour G0 glycan types. Therefore, GlcN/GlcNAc supplementation has been demonstrated as a useful tool for tuning N-glycan distributions towards G0 forms in cultures (Blondeel et al., 2015). For supplementation strategies, GlcNAc should be considered more favourable compared to GlcN, which has been shown to restrict growth in mammalian cultures producing recombinant proteins (Baker et al., 2001; Blondeel et al., 2015; Grammatikos et al., 1998; Hills et al., 2001; N. S. C. Wong et al., 2010; Yang and Butler, 2002; Zanghi et al., 1998), as well as transformed cancerous cells not expressing recombinant proteins (Bekesi and Winzler, 1970; Krug et al., 1984; Oh et al., 2007; Pederson et al., 1992). A similar species to GlcN, galactosamine (GalN) also produces cytotoxic effects when supplemented to cultures (Pels Rijcken et al., 1995a). Restricted growth from supplementation of hexosamines (GlcN/GalN) have been attributed to either competition with glucose transport (Yang and Butler, 2002), or depletion of intracellular ATP and UTP pools (Pels Rijcken et al., 1995a). Pels Rijcken and colleagues (1995a) supplementing GalN to cultures hypothesized that what they considered cytotoxic effects of GalN supplementation were linked to depletion of phosphorylated pyrimidines inhibiting RNA

synthesis. However, it has more recently been demonstrated that negative growth from GlcN (and likely GalN) is actually from depleting pools of cytosolic acetyl-CoA, which convert GlcN to GlcNAc (Blondeel et al., 2015), an essential pool for lipid biosynthesis and cell division (Goudar et al., 2010; Quek et al., 2010). Supplementing GlcNAc has been demonstrated to remove this growth inhibition, while still producing an increase in intracellular UDP-GlcNAc pools (Blondeel et al., 2015; Kildegaard et al., 2015). GlcNAc supplementation may still draw phosphorylated pyrimidines away from pools for RNA synthesis leading to more rapid loss of viability in stationary phase; however, the demonstrated improved growth from avoiding acetylation by supplementing GlcNAc makes the activity of glucosamine-phosphate N-acetyltransferase the more likely source of growth inhibition for this group of glycosylation supplements.

#### **6.4.3.2 Galactose**

Galactose (Gal) supplementation represents the most successful example of nucleotide-sugar precursor feeding to affect glycoforms to-date. This strategy has been reliably reported across several different research groups, utilizing different cell platforms, expressing different proteins, to increase galactosylation (Table 8). Even beyond galactosylated glycoforms, supplementation of Gal has also been demonstrated to relieve bottlenecks towards improving the sialylation of Fc-fusion glycoproteins in GS-CHO cultures (Liu et al., 2015). Increased galactosylation is generally accepted to be of therapeutic benefit, with lack of galactosylation associated endogenously with several disease states (discussed in Section 4).

**Table 8 – Comparison of glycoform shifts and differences between reported experiments for the supplementation of galactose (Gal), the nucleoside uridine (Urd), and the enzyme cofactor manganese (Mn<sup>2+</sup>), towards expanding intracellular nucleotide-sugar pools of UDP-galactose in cultured mammalian cells and affecting N-linked glycoforms of recombinant glycoproteins. Experimental differences reported include: Supplementation cocktails and concentrations with multiple bullet-points representing separate flask or bioreactor conditions; The cell line utilized and the lineage of that cell line where reported; The protein being expressed and whether it is a mutant variant or fusion; The bioprocess scale, time of supplementation, and time of harvest; The amount of glutamine (Gln) utilized in the growth medium.**

Supplement	Cell	Protein	Fermentation Timeline	Gln (mM)	Effect	Researchers
<ul style="list-style-type: none"> <li>▪ 20mM Gal</li> </ul>	CHO (DG44)	IgG	<ul style="list-style-type: none"> <li>▪ Fed-batch bioreactor</li> <li>▪ 1L</li> <li>▪ Addition 48h</li> <li>▪ Harvest 336h</li> </ul>	8	<ul style="list-style-type: none"> <li>▪ +12% galactosylation</li> <li>▪ No reduction to cell growth or productivity</li> </ul>	(Kildegaard et al., 2015)
<ul style="list-style-type: none"> <li>▪ 10mM galactose</li> </ul>	NS0 (GS)	IgG	<ul style="list-style-type: none"> <li>▪ Flasks</li> <li>▪ 500mL</li> <li>▪ Addition 48h</li> <li>▪ Harvest 96h</li> </ul>	0.4 (GS)	<ul style="list-style-type: none"> <li>▪ 5x UDP-Gal</li> </ul>	(Hills et al., 2001)
<ul style="list-style-type: none"> <li>▪ 10mM Gal</li> <li>▪ 20mM Gal</li> <li>▪ 40mM Gal</li> </ul>	CHO (GS)	Fc-TNF fusion	<ul style="list-style-type: none"> <li>▪ Fed-batch bioreactor</li> <li>▪ 2L</li> <li>▪ Addition 120h</li> <li>▪ Harvest 288h</li> </ul>	GS	<ul style="list-style-type: none"> <li>▪ +22% galactosylation</li> <li>▪ +14% sialylation</li> <li>▪ No negative growth effects</li> <li>▪ Glycan distribution scaled well to 200L bioreactor</li> </ul>	(Liu et al., 2015)
<ul style="list-style-type: none"> <li>▪ 20mM galactose</li> </ul>	CHO	IL-4/13	<ul style="list-style-type: none"> <li>▪ Batch bioreactor</li> <li>▪ 1L</li> <li>▪ Addition 0h</li> <li>▪ Harvest 112h</li> </ul>	2	<ul style="list-style-type: none"> <li>▪ No notable effects to sialylation or gene expression</li> </ul>	(Clark et al., 2005)
<ul style="list-style-type: none"> <li>▪ 10mM Gal</li> <li>▪ +5mM Urd</li> </ul>	CHO (Dukx)	IFN- $\gamma$	<ul style="list-style-type: none"> <li>▪ Flasks (n=1)<sup>9</sup></li> <li>▪ 1000mL</li> <li>▪ Addition 48h</li> <li>▪ Harvest 96h</li> </ul>	4	<ul style="list-style-type: none"> <li>▪ 20x UDP-Gal</li> <li>▪ +12% sialylation</li> </ul>	(N. S. C. Wong et al., 2010)
<ul style="list-style-type: none"> <li>▪ 0.4, 4, 40<math>\mu</math>M Mn<sup>2+</sup></li> </ul>	CHO (dhfr-)	EPO	<ul style="list-style-type: none"> <li>▪ Roller bottles</li> <li>▪ 850cm<sup>2</sup></li> <li>▪ Media replaced every 7 days</li> <li>▪ Addition</li> <li>▪ Harvest 19d</li> </ul>	15	<ul style="list-style-type: none"> <li>▪ Reduced titres at 40<math>\mu</math>M Mn<sup>2+</sup> feed</li> <li>▪ UDP-Gal pools unchanged</li> <li>▪ Improved galactosylation and sialylation</li> </ul>	(Crowell et al., 2007)
<ul style="list-style-type: none"> <li>▪ 10, 20, 40mM Gal</li> <li>▪ 17-68mg/L Mn<sup>2+</sup></li> </ul>	CHO S	FII	<ul style="list-style-type: none"> <li>▪ Flasks</li> <li>▪ Addition 48h</li> <li>▪ Harvest 144h</li> </ul>	-	<ul style="list-style-type: none"> <li>▪ +26% sialylation from galactose addition</li> <li>▪ +30% sialylation from addition of MnSO<sub>4</sub></li> <li>▪ Temperature-shift resulted in similar sialylation improvement for final process</li> </ul>	(Lee et al., 2017)

<sup>9</sup> Only a single flask for each experiment, and only one control flask appears to have been used

Supplement	Cell	Protein	Fermentation Timeline	Gln (mM)	Effect	Researchers
<ul style="list-style-type: none"> <li>▪ 100mM Gal</li> <li>▪ 40µM Mn<sup>2+</sup></li> <li>▪ 100mM Gal + 40µM Mn<sup>2+</sup></li> </ul>	CHO (K1)	IgG	<ul style="list-style-type: none"> <li>▪ Flasks</li> <li>▪ 250mL</li> <li>▪ Addition 0h</li> <li>▪ Harvest 168h</li> </ul>	4	<ul style="list-style-type: none"> <li>▪ +9% galactosylation</li> <li>▪ -31% fucosylation and +21% high-mannose glycans for Mn+Gal</li> <li>▪ -30% fucosylation and +14% high-mannose glycans for Mn alone</li> <li>▪ 9x UDP-Gal pool</li> <li>▪ Increased expression of β-Gal II, III, IV and UDP-GalT transcripts</li> </ul>	(St Amand et al., 2014)
<ul style="list-style-type: none"> <li>▪ 4µM Mn<sup>2+</sup></li> <li>▪ 16µM Mn<sup>2+</sup></li> <li>▪ 30mM Gal<sup>10</sup></li> <li>▪ +4µM Mn<sup>2+</sup></li> <li>▪ +16µM Mn<sup>2+</sup></li> </ul>	CHO (DG44)	IgG	<ul style="list-style-type: none"> <li>▪ Flasks</li> <li>▪ 100mL</li> <li>▪ Addition 0h</li> <li>▪ Harvest 72h</li> </ul>	8	<ul style="list-style-type: none"> <li>▪ -30-50% IgG when Replacing /lowering Glc or matching Gal</li> <li>▪ +11% galactosylation</li> <li>▪ -5% fucosylation with 16µM Mn<sup>2+</sup></li> </ul>	(Surve and Gadgil, 2015)
<ul style="list-style-type: none"> <li>▪ 5-100mM Gal</li> <li>▪ +1-20mM Urd</li> <li>▪ +2-40µM Mn<sup>2+</sup></li> <li>▪ Factors: <sup>11</sup> 1,2,3,4,8,12,16,20</li> <li>▪ Factors: 8,12</li> </ul>	(2) CHO (GS)	IgG	<ul style="list-style-type: none"> <li>▪ Fed-batch bioreactor</li> <li>▪ 2L</li> <li>▪ Addition 0h</li> <li>▪ Harvest 360h</li> </ul>	GS	<ul style="list-style-type: none"> <li>▪ +20% galactosylation for 1st cell line at 100mM Gal</li> <li>▪ +24% galactosylation for 2<sup>nd</sup> cell line at 40mM Gal</li> <li>▪ Glycan distribution scaled well to 100L and 1000L bioreactors</li> </ul>	(Gramer et al., 2011)
<ul style="list-style-type: none"> <li>▪ 2.5-100mM Gal<sup>12</sup></li> <li>▪ +0.5-20mM Urd</li> <li>▪ +1-40µM Mn<sup>2+</sup></li> </ul>	CHO (GS)	IgG	<ul style="list-style-type: none"> <li>▪ Flasks</li> <li>▪ 125mL</li> <li>▪ Addition 72h</li> <li>▪ Harvest 192h</li> </ul>	GS	<ul style="list-style-type: none"> <li>▪ +21-24% galactosylation</li> <li>▪ +1.5-5% sialylation</li> <li>▪ Best overall IVCC, MAb titre and galactosylation results with low Mn<sup>2+</sup>/Urd and high Gal condition</li> <li>▪ Mab galactosylation correlated well with cell-surface Gal</li> </ul>	(Grainger and James, 2013)

<sup>10</sup> Additional experiments changed the main carbon source to fructose, glucose-free (only gal), and low-glucose delivered from a hydrogel for slow release.

<sup>11</sup> Galactose, uridine and manganese (Mn<sup>2+</sup>) fed in ratios of 5:1:0.002 mM (UMG cocktail) for two CHO-K1SV cell lines expressing two separate IgGs under GS expression system

<sup>12</sup> Face-centred DOE design for main-effects modeling of UMG cocktail developed by Gramer et al. cocktail, tested on two CHO-K1SV cell lines stably expressing IgG<sub>4</sub> under GS expression system (Gramer et al., 2011).

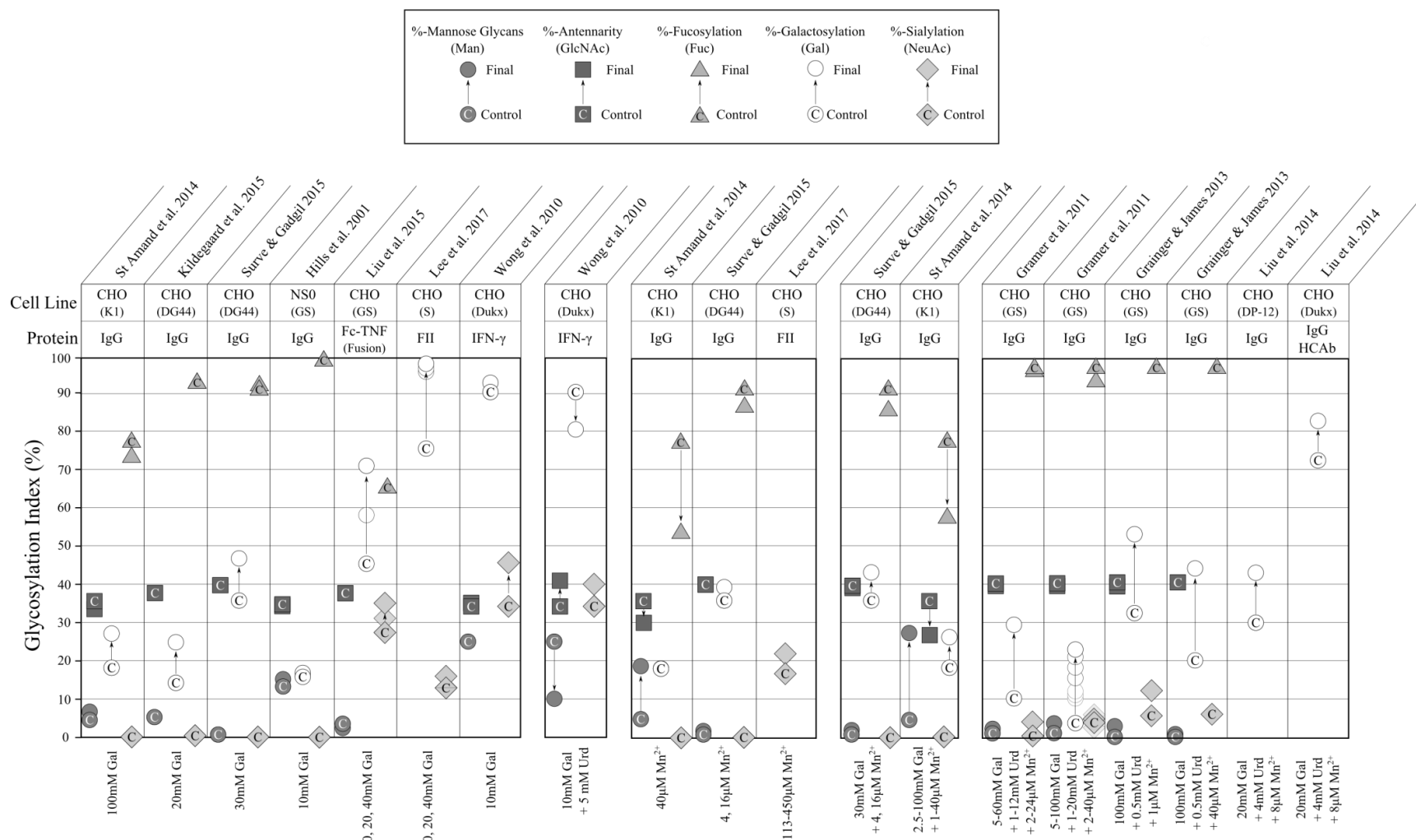


Figure 33 – Comparison of glycoform shifts reported for experiments employing the supplementation of glucosamine (GlcN), its acetylated form acetyl-glucosamine (GlcNAc), and the nucleoside uridine (Urd), to affect N-linked glycoforms of recombinant glycoproteins produced in mammalian cell cultures.

The %-shift in glycoforms, reported in Table 17, relative to reported control cultures is demonstrated as a shift from a starting control glycoform, indicated with a 'C' within the respective symbol, to a final glycoform following supplementation, as per the directional arrow between the two construction points. The glycosylation % values for mannose-type, antennarity, galactosylation, sialylation, and fucosylation are represented by their respective monosaccharide symbols.

Precursor supplementation strategies often include the complementary nucleoside for a supplemented sugar, such as uridine (Urd) for GlcN and Gal, or cytidine (Cyt) for ManNac. Galactose supplementation strategies are the first to also incorporate manganese ions ( $Mn^{2+}$ ) to enhance the activity of galactosyltransferase, demonstrated by Gramer and colleagues (2011) in GS-CHO cultures producing IgG. These researchers proposed a synergistic cocktail (in static proportions), featuring uridine, manganese ions, and galactose (UMG), and experimented with increasing concentrations up to 20mM galactose, to achieve more than a 20% increase in galactosylation (Figure 33), with improvements plateauing at 8x UMG (16 $\mu$ M  $Mn^{2+}$ , 8mM Urd, and 40mM galactose).

The results of the UMG cocktail were replicated by Grainger and James (2013) utilizing a face-centred designed experiment (i.e. varying the proportions of the UMG supplements), for main effects analysis in two CHO cell lines expressing IgG. These researchers also demonstrated more than a 20% increase in IgG galactosylation (Figure 33); however, they determined the best results overall – including growth, mAb titre, mAb galactosylation – from supplementing the low-low-high (LLH) condition (1 $\mu$ M  $Mn^{2+}$ , 0.5mM Urd, and 100mM Gal). Variations on the UMG cocktail have continued to be utilized by researchers reporting varying degrees of success for increasing glycoprotein galactosylation (Liu et al., 2014; St Amand et al., 2014; Surve and Gadgil, 2015).

Towards better understanding the main effects of supplementing Gal, Urd, and  $Mn^{2+}$ , researchers have pursued various experimental arrangements and concentrations (Table 8, Figure 33). While galactose together with uridine is reported to generate superior results (Grainger and James, 2013; Gramer et al., 2011; N. S. C. Wong et al., 2010), galactose together with manganese alone performs slightly worse (St Amand et al., 2014; Surve and Gadgil, 2015)



(Figure 33). Manganese supplementation has been reported to actually reduce fucosylation of IgG in CHO cultures (St Amand et al., 2014; Surve and Gadgil, 2015); however, St Amand and colleagues (2014) report this effect coincides with increased high-mannose type glycans and loss of antennarity (Figure 33).

#### **6.4.3.3 ManNac**

N-acetylmannosamine (ManNac), often accompanied by the nucleoside cytidine (Cyt) is supplemented to cultures to increase the intracellular nucleotide-sugar pool of CMP-acetylneuraminic acid (CMP-NeuAc) (detailed in Table 9), with the goal of improving the sialylation of glycoproteins (Figure 34). Several researchers have reported improvements in the sialylation of glycoproteins in mammalian cell culture following supplementation of ManNac (Gu and Wang, 1998; N. S. C. Wong et al., 2010; Zanghi et al., 1998). Gu and Wang reported a 15% increase in sialylation, and when supplementing 20mM radiolabelled ManNac, all of the resulting sialylation included the tracer (Gu and Wang, 1998). Interestingly, researchers that do not observe increases in sialylation typically reported a deficit of galactosylation that could be improved with galactose feeding (Hills et al., 2001; Kildegaard et al., 2015; Liu et al., 2015). Liu and colleagues (2015) supplementing galactose improved galactosylation in cultures, which subsequently also lead to increased sialylation by 14%. Synergistic supplementation of galactose and ManNac is still yet to be reported.

**Table 9 – Comparison of glycoform shifts and differences between reported experiments for the supplementation of the acetylated amine sugar N-acetylmannosamine (ManNAc), and the nucleoside cytidine (Cyt), towards expanding intracellular nucleotide-sugar pools of CMP-NeuAc in cultured mammalian cells and affecting N-linked glycoforms of recombinant glycoproteins. Experimental differences reported include: Supplementation cocktails and concentrations with multiple bullet-points representing separate flask or bioreactor conditions; The cell line utilized and the lineage of that cell line where reported; The protein being expressed and whether it is a mutant variant or fusion; The bioprocess scale, time of supplementation, and time of harvest; The amount of glutamine (Gln) utilized in the growth medium.**

Supplement	Cell	Protein	Fermentation Timeline	Gln (mM)	Effect	Researchers
▪ 20mM ManNAc <sup>13</sup>	CHO (DG44)	IgG	▪ 1L - Bioreactor, fedbatch ▪ Addition 48h ▪ Harvest 336h	8	▪ Hypothesis that increases in CMP-NeuAc lead to feedback inhibition, UDP-GlcNAc accumulation, and decrease in galactosylation.	(Kildegaard et al., 2015)
▪ 20mM ManNAc	NS0 (GS)	IgG	▪ 500mL Flasks ▪ Addition 48h ▪ Harvest 96h	0.4 (GS)	▪ 44x CMP-NeuAc ▪ No improvement to sialylation	(Hills et al., 2001)
▪ 20mM ManNAc	CHO (GS) NS0 (GS)	TIMP-1	▪ 1L - Flasks ▪ Addition 24h ▪ Harvest 48h	0.4 (GS)	▪ -22% Neu5Gc content in NS0 cultures ▪ +1% shifts in %-sialylation ▪ 12x increase in CMP-SA (CHO) ▪ 30x increase in CMP-SA (NS0)	(Baker et al., 2001)
▪ 10, 20, 40mM ManNAc	CHO S	FII	▪ Flasks ▪ Addition 48h ▪ Harvest 144h	-	▪ +20% sialylation from ManNAc addition ▪ Temperature-shift resulted in similar sialylation improvement for final process	(Lee et al., 2017)
▪ 0.2, 2, 20, 40mM ManNAc	CHO (Dukx)	IFN- $\gamma$	▪ 100mL Flasks ▪ Addition 0h ▪ Harvest 96h	-	▪ 27x increase CMP-SA ▪ +15% complete sialylation ▪ 60% & 100% of sialylation from radiolabelled supplemented ManNAc fed at 2mM & 20mM respectively ▪ No effect to cell growth or productivity	(Gu and Wang, 1998)
▪ 0.5mM Cyt	RH	N/A	▪ 3mL Culture dish ▪ Addition 16h ▪ Harvest 24h	2.4 <sup>14</sup>	▪ 3.0x CTP ▪ 3.2x UDP-HexNAc ▪ 2.6x UDP-hexose	(Pels Rijcken et al., 1995b)

<sup>13</sup> Supplementations of mannose, NeuAc, and cytidine were also attempted, but did not vary significantly from control cultures

<sup>14</sup> Waymouth culture medium (Morton, 1970)

Supplement	Cell	Protein	Fermentation Timeline	Gln (mM)	Effect	Researchers
<ul style="list-style-type: none"> <li>▪ 20mM ManNAc + 10mM Cyt</li> </ul>	CHO (GS)	Fc-TNF fusion	<ul style="list-style-type: none"> <li>▪ 2L Fed-batch bioreactor</li> <li>▪ Addition 120h</li> <li>▪ Harvest 288h</li> </ul>	GS	<ul style="list-style-type: none"> <li>▪ Statistically insignificant sialic-acid content increase (terminal galactose determined to be limiting)</li> </ul>	(Liu et al., 2015)
<ul style="list-style-type: none"> <li>▪ 20mM ManNAc</li> <li>▪ + 0.5mM Cyt</li> </ul>	CHO SCLC	NCAM	<ul style="list-style-type: none"> <li>▪ 6 &amp; 24-well plates</li> <li>▪ Addition 12-18h</li> <li>▪ Harvest 128h</li> </ul>	6	<ul style="list-style-type: none"> <li>▪ +10-20% polysialylation<sup>15</sup> in CHO</li> <li>▪ -20-30% NCAM production</li> </ul>	(Zanghi et al., 1998)
<ul style="list-style-type: none"> <li>▪ 20mM ManNAc</li> <li>▪ 10mM cytidine</li> </ul>	CHO (Dukx)	IFN- $\gamma$	<ul style="list-style-type: none"> <li>▪ 1L - Flasks (n=1)</li> <li>▪ Addition 48h</li> <li>▪ Harvest 96h</li> </ul>	4	<ul style="list-style-type: none"> <li>▪ 30-120x increase in CMP-SA</li> <li>▪ +32-36% sialylation +/- Cyt</li> <li>▪ +26-52% higher specific productivity</li> </ul>	(N. S. C. Wong et al., 2010)

Sialylation of glycoproteins by rodent-derived mammalian cell cultures comes with some risk of the immunogenic glycoform CMP-Neu5Gc, a glycan which does not occur endogenously in humans (Ghaderi et al., 2010; Padler-Karavani et al., 2008). A benefit of ManNAc supplementation reported by Baker and colleagues (2001) is that Neu5Gc moieties were reduced by 22%, making this an intelligent culture addition regardless of whether overall sialylation increases.

---

<sup>15</sup> NCAM protein glycan results reported only relative to controls

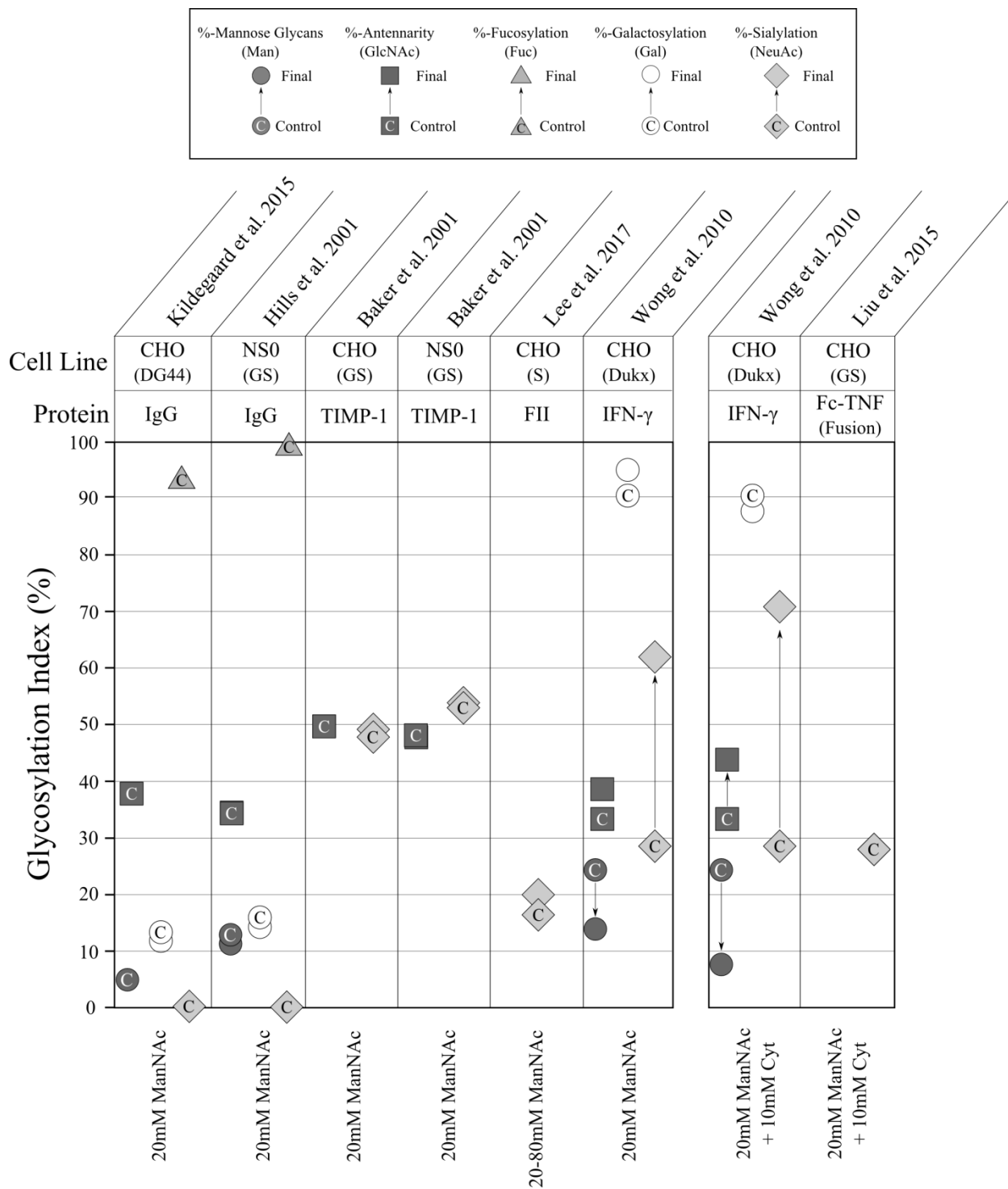


**Figure 34 – Comparison of glycoform shifts reported for experiments employing the supplementation of acetyl-mannosamine (ManNAc), and the nucleoside cytidine (Cyt), to affect N-linked glycoforms of recombinant glycoproteins produced in mammalian cell cultures.**

The %-shift in glycoforms, reported in Table 18, relative to reported control cultures is demonstrated as a shift from a starting control glycoform, indicated with a 'C' within the respective symbol, to a final glycoform following supplementation, as per the directional arrow between the two points. The glycosylation % values for mannose-type, antennarity, galactosylation, sialylation, and fucosylation are represented by their respective monosaccharide symbols.

#### **6.4.3.4 Nucleosides**

Nucleoside supplementation on its own has been considered a viable strategy for affecting glycoforms, as they have similarly been shown, if more moderately, to increase nucleotide-sugar pools (Table 7 and Table 9). Nyberg and colleagues (1999) reported that supplementing up to 10mM uridine to CHO cultures expressing IFN- $\gamma$  observed a linear correlation between increased UTP levels and UDP-GlcNAc pools. Pels Rijcken and colleagues (1995b) similarly observed corresponding increases of UTP, UDP-glucose/galactose, and UDP-GlcNAc/GalNAc upon supplementing either 0.5mM uridine or cytidine to primary cultures of rat hepatocytes. Few strategies for supplementation of nucleotides, nucleosides, or nitrogenous bases beyond the pyrimidines exist, as these have been demonstrated to produce negative growth effects (Carvalho et al., 2003).

#### **6.4.3.5 Other Exotic Sugars and Supplements**

Beyond the classic nucleotide sugar precursor supplements detailed in Table 7-Table 9, several additional supplementation strategies have been attempted to exert control over glycan distributions. Inhibitors to particular glycosyltransferases may be utilized to produce hybrid and high-mannose type glycans; however, these present little therapeutic advantage (Section 4).

Several unconventional monosaccharides have been attempted, including mannose, fucose, and N-acetylneuraminic acid (NeuAc); however, none of these produced any notable shifts to glycoforms (Kildegaard et al., 2015). Hossler and colleagues (2017) have recently reported supplementation of nine unconventional sugars to CHO cultures expressing a mAb glycoprotein. While several of these sugars produced high-mannose and hybrid type glycoforms, melezitose, turanose and to a lesser extent lactose supplemented at 1, 10, 25 and 50mM, created significant increases in galactosylation of the mAb (Hossler et al., 2016). Similarly, these researchers have

previously demonstrated that supplementing D-arabinose and L-galactose at 50 mM to CHO cultures expressing a mAb glycoprotein can achieve a complete exchange of fucose moieties for these alternate sugars producing benefits for bioactivity by antibody dependent cell cytotoxicity (ADCC) (Hossler et al., 2017).

## **6.5 Glycoforms: Bioefficacy and Functionality**

Glycoprotein biotherapeutics include mAbs, cytokines, hormones, clotting factors, and growth factors, a thorough listing of these approved by the FDA are available (Ghaderi et al., 2012). Much research has been devoted to understanding how shifts in glycoforms change effector function for mAbs, due the myriad ways IgGs activate the immune system (Table 10-Table 14). For other glycoproteins, the primary concern is generally terminal sialylation, as this has the greatest impact on extending serum half-life for most glycoprotein therapeutics like tissue plasminogen activator (tPA) and erythropoietin (EPO), and reducing how often drugs must be re-administered to patients (Cole et al., 1993; Elliott et al., 2004). Albrecht and colleagues (2014) provide an excellent examination of the impact of glycoform on commercial therapeutics, particularly Darbepoetin- $\alpha$ , a commercial therapeutic recombinant erythropoietin (EPO), which is modified to possess two additional N-glycan sites compared to the usual three in human EPO. Darbepoetin- $\alpha$  carries a much greater proportion of sialic acid moieties compared to the two other commercial forms of EPO, epoetin- $\alpha/\beta$  (Egrie et al., 2003). These additional sialylated glycan sites effectively double the half-life and bioactivity; however, Darbepoetin's higher aggregate sialylation causes a 5-fold reduced receptor binding, requiring higher dosages (Egrie et al., 2003; Elliott et al., 2004). This result corresponds to reports by Scallon and colleagues (2007), who observed that higher sialylation of mAbs impeded their binding to Fc $\gamma$ RIIIa

receptors to activate antibody dependent cell cytotoxicity (ADCC), a major bioactivity metric of mAbs (Table 13).

Serum clearance of glycoproteins is often the result of receptors for specific terminal glycans, like mannose binding receptors on liver endothelial cells, or asialoglycoprotein receptors for galactose moieties, also of the liver (Smedsrød and Einarsson, 1990). Conversely to most glycoproteins, it has been reported that sialylation does not extend serum half-life *in vivo* for mAbs (Kaneko et al., 2006; Wright and Morrison, 1998), a result possibly due to the positioning of the glycan site on the Fc region, where IgG glycans are predominantly located.

### **6.5.1 Immune Effector Functions for Antibodies**

The Fab regions of antibodies allow them to bind to their target antigens with high specificity, but it is their glycosylated Fc regions that interact with and activate immune responses. IgGs possess paired glycosylation sequons at ‘asparagine 297’ (Asn<sub>297</sub>) on the heavy chain CH2 domain of their Fc region, and produce varying immune response activation capability *in vivo* depending on their glycoform (Table 10-Table 14). Jefferis (2012) provides an excellent overview of antibody isotypes, their key features, and interactions with the immune system.

The Fc region of antibodies interacts with the immune system by binding to numerous different Fc receptors on the surfaces of immune cells, as well as complexing with C1q, which activates the Complement system cascade. Complement can also be activated by G0 and high-mannose glycans via mannose-binding lectin (MBL) activation; however, such glycoforms also observe rapid clearance from serum (Table 12) (Malhotra et al., 1995; Nimmerjahn et al., 2007). The interaction of immune cell antibody receptors (FcγR) with an antibody-antigen complex

mediates a host of immune effector functions, such as antibody-dependent cell phagocytosis (ADCP), cytolysis or cytotoxicity (ADCC), and the release of cytokines and chemokines spurring further cascades of immune responses within the highly regulated immune system. Vidarsson and colleagues (2014) provide a comprehensive review of these effector functions. Therapeutic monoclonal antibody (mAb) glycoforms are often characterized by how well they can recruit immune effector functions, particularly ADCC and Complement dependent cell cytotoxicity (CDC).

Regarding activation of ADCC and CDC endogenously, a typical glycan distribution for human serum IgG1&2 from five healthy volunteers showed a prevalence for five main glycoforms: fucosylated biantennary G0, G1, G2, G2S1, and bisecting G1 (Flynn et al., 2010). While this and similar studies provide a general conception of a “normal” glycan distribution for mAbs, an important characteristic of antibody glycoforms *in vivo*, is their tendency to shift with pathology, as evidenced by Kaneko and colleagues (2006), who reported the downregulation of sialylated antibodies *in vivo* during antigenic challenge removing their anti-inflammatory properties (Table 13). Therefore, the optimal distribution of glycans on therapeutic antibodies likely varies from the distribution reported by Flynn and colleagues for treating a particular disorder/pathology. Kapur and colleagues (2014) provide a summary of patterns of IgG-antibody glycosylation with respect to their effects in reported pathologies.

### **6.5.2 Glycoforms and Antibody Immune Effector Functions**

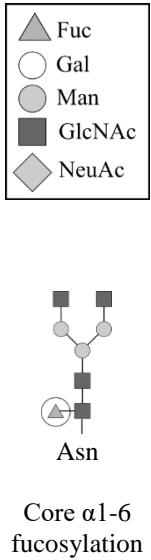
Recognition and binding of IgGs by C1q and Fc receptors are affected by glycoforms yielding different binding affinities, or steric effects (Ferrara et al., 2006), and therefore significant variation in triggering the immune system. Table 10-Table 14 demonstrate how changes in glycoforms of antibodies affect their immune effector functions (IEF).



### 6.5.2.1 Fucosylation

Core  $\alpha_{1-6}$  fucosylation on the first GlcNAc moiety of the N-glycoform is typical for the majority of human glycans both for antibodies (Flynn et al., 2010) and other secreted glycoproteins (Takeuchi et al., 1988). However, absence of fucosylation has been reported to dramatically increase affinity of IgGs for Fc $\gamma$ RIIIa receptors of NK cells, increasing ADCC responses by purified peripheral blood monocytes during *in vitro* assays (Table 10). Steric interaction between the Asn<sub>297</sub> glycan of the antibody Fc and the Asn<sub>162</sub> glycan of the Fc $\gamma$ RIIIa receptor has been proposed as the mechanism behind this improvement (Ferrara et al., 2006). This also corresponds with research linking individuals with polymorphic Fc $\gamma$ RIIIa receptors to improved clinical outcomes when treated with rituximab where core-fucosylation is still present (Cartron et al., 2002). While a clear relationship between fucosylation and ADCC has been reported, several researchers have found no relationship between the core  $\alpha_{1-6}$  fucose moiety and CDC (Chung et al., 2012; Shields et al., 2002; Yamane-Ohnuki et al., 2004).

**Table 10 – Therapeutic efficacy of monoclonal antibodies (mAbs) and immune effector function (IEF) with respect to fucosylation of N-glycans. A biantennary glycan with a circled region is provided to indicate the moiety. IEFs include antibody dependent cell cytotoxicity (ADCC), complement dependent cell cytotoxicity (CDC), as well as binding to the immune antibody receptor Fc $\gamma$ RIIIa.**

N-Glycoform	IEF	Effects	Researchers
	ADCC	<ul style="list-style-type: none"> <li>50 fold improvement in binding <i>in vitro</i> of IgGs to Fc<math>\gamma</math>RIIIa receptors enhancing ADCC</li> <li>~90% afucosylated IgGs expressed in CHO and HEK cells deficient in FucT produce IgGs with 40-60% increase ADCC</li> </ul>	(Shields et al., 2002)
	ADCC	<ul style="list-style-type: none"> <li>30% increase in ADCC for anti-CD20 IgGs produced in FUT8 mRNA deficient YB2/0 rat hybridoma produced IgGs (-91% fucosylation) compared to Rituxan™</li> <li>40% increase in ADCC for afucosylated IgGs produced YB2/0 compared to CHO (-21% fucosylation)</li> <li>Overexpression of FUT8 removes ADCC enhancement in anti-CD20 IgGs from YB2/0 cells</li> </ul>	(Shinkawa et al., 2003)
	ADCC	<ul style="list-style-type: none"> <li>~40-100% increase in ADCC from a 90% reduction in fucosylation of IgG demonstrated both via <i>in vitro</i> ADCC assays from four donors and via an <i>in vivo</i> mouse model, which prevented tumor formation in mice injected with leukemia cells for ~25 days</li> </ul>	(Niwa et al., 2004)

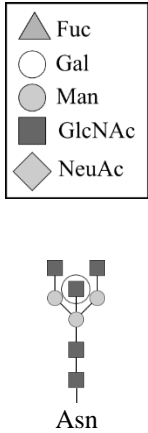
N-Glycoform	IEF	Effects	Researchers
	ADCC	<ul style="list-style-type: none"> <li>~50% increase ADCC from IgG with a 52-63% decrease in fucosylation; plasmids coding siRNA for FUT8 mRNA introduced to CHO</li> </ul>	(Mori et al., 2004)
	ADCC	<ul style="list-style-type: none"> <li>20% increase in ADCC from complete removal of fucose moiety; FUT8 mRNA knockout CHO culture producing anti-CD20 IgGs</li> </ul>	(Yamane-Ohnuki et al., 2004)
	ADCC	<ul style="list-style-type: none"> <li>~20-30% increase in ADCC reactivity with afucosylated IgG pools</li> <li>Galactosidase treated pools of IgG were 100% fucosylated or afucosylated mixed in defined proportions</li> </ul>	(Chung et al., 2012)
	CDC	<ul style="list-style-type: none"> <li>Fucose moiety on Fc glycans yields no effect to complement</li> </ul>	(Chung et al., 2012; Shields et al., 2002; Yamane-Ohnuki et al., 2004)
	Fc $\gamma$ RIIIa	<ul style="list-style-type: none"> <li>Afucosylation of just one Fc glycan (G0/G0F) sufficient to enhance ADCC because of steric hindrance between receptor glycan at Asn<sub>162</sub> and fucose moiety on Fc-glycan at Asn<sub>297</sub></li> </ul>	(Ferrara et al., 2006)

### 6.5.2.2 Bisecting N-Acetylglucosamine (biGlcNAc)

Core  $\alpha_{1-6}$  fucosylation of the N-glycoform is partially inhibited by the GnT-III enzyme, absent in the CHO genome (Xu et al., 2011). GnT-III acts to append a bisecting GlcNAc moiety to the first mannose residue of the glycan (Schachter, 1986). The higher ADCC response from NK cells via Fc $\gamma$ RIIIa binding was initially associated with antibodies bearing the bisecting N-GlcNAc (these results are detailed in Table 11); however, it was reported that *in vitro* remodelling of rituximab and trastuzumab glycans to produce antibodies with both core-fucose and bisecting GlcNAc glycoforms demonstrated little improvement (~10%) to ADCC (Hodoniczky et al., 2005). In contrast, Shinkawa and colleagues (2003) column-purified fractions of IgG produced from rat hybridoma YB2/0 cells to obtain fractions high in both bisecting GlcNAc and core  $\alpha_{1-6}$  fucosylation, and determined no improvement towards ADCC. Therefore, the benefit of the bisecting glycoform, at least with respect to ADCC mediated by NK cells is not as significant as afucosylation. However, endogenous human IgG1&2 glycoforms *in*

*in vivo* possess bisecting GlcNAc with approximately 12% and 9.3% proportions, respectively (Flynn et al., 2010). As such, this glycoform may bear some yet unknown regulatory property for antibodies.

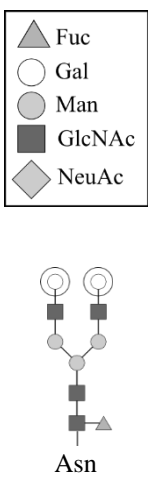
**Table 11 – Therapeutic efficacy of monoclonal antibodies (mAbs) and immune effector function (IEF) with respect to N-glycans possessing the bisecting N-acetylglucosamine (GlcNAc) moiety. A biantennary glycan with a circled region is provided to indicate the moiety. IEFs include antibody dependent cell cytotoxicity (ADCC).**

N-Glycoform	IEF	Effects	Researchers
 <p data-bbox="191 1066 305 1129">Bisecting-GlcNAc</p>	ADCC	<ul style="list-style-type: none"> <li>10% increase in ADCC of Rituxan &amp; Herceptin mAbs remodelled <i>in vitro</i> to include bisecting GlcNAc (~80% of IgG population, mAbs retained fucose)</li> </ul>	(Hodoniczky et al., 2005)
		<ul style="list-style-type: none"> <li>15-25% increase in ADCC from a 48-71% increase in bisecting GlcNAc on IgG from CHO modified to express GnT-III</li> </ul>	(Davies et al., 2001)
		<ul style="list-style-type: none"> <li>~30% increase in ADCC after GnT-III enzyme introduced to CHO, reducing fucosylation and increasing bisecting GlcNAc structures</li> </ul>	(Umaña et al., 1999)
		<ul style="list-style-type: none"> <li>No improvement in ADCC resulted from column-purified fractions of IgG1 from rat hybridoma YB2/0 possessing bisecting GlcNAc increased from 4-30%, and 0-45% (separate experiments), but constant fucosylation proportions</li> </ul>	(Shinkawa et al., 2003)

### 6.5.2.3 Galactosylation

Terminal galactosylation is not perceived to be an essential factor for stimulating ADCC responses; however, non-galactosylated IgGs have consistently been shown to have weaker C1q binding and complement-dependent cytotoxicity (CDC) responses (Table 12). Reviews of mAb effector function with respect to N-glycoforms have noted that lower galactosylation *in vivo* has been linked to aging, auto-immune disorders and disease states such as rheumatoid arthritis (Harris et al., 2010; Jefferis, 2012; Spearman et al., 2011). Therefore, increased galactosylation is viewed as therapeutically favourable; however, compared to human IgG, commercial monoclonal antibody formulations tend to be under-galactosylated (Wacker et al., 2011).

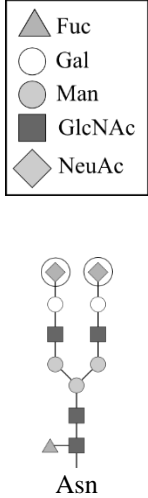
**Table 12 – Therapeutic efficacy of monoclonal antibodies (mAbs) and immune effector function (IEF) with respect to galactosylation of N-glycans. A biantennary glycan with circled regions is provided to indicate the moieties. IEFs include antibody dependent cell cytotoxicity (ADCC), and complement dependent cell cytotoxicity (CDC).**

N-Glycoform	IEF	Effects	Researchers
 <p>Asn</p> <p>Galactosylation</p>	CDC	<ul style="list-style-type: none"> <li>Reduced C1q binding <i>in vitro</i> for agalactosylated IgG from patient serum with rheumatoid arthritis</li> </ul>	(Tsuchiya et al., 1989)
		<ul style="list-style-type: none"> <li>35-50% reduction complement lysis activity <i>in vitro</i> for rIgG1 expressed in CHO treated with sialidase and galactosidase</li> </ul>	(Boyd et al., 1995)
		<ul style="list-style-type: none"> <li>3-fold reduction in CDC for rituximab treated with galactosidase</li> </ul>	(Hodoniczky et al., 2005)
		<ul style="list-style-type: none"> <li>~2-fold enhanced binding of mannose-binding-lectin (MBL) for IgGs treated with galactosidase to convert from 20% to 100% G0 Fc glycans</li> </ul>	(Malhotra et al., 1995)
		<ul style="list-style-type: none"> <li>60-70% increase in binding to mannose-binding-lectin (MBL) protein activating complement by agalactosylated IgGs</li> <li>25-45% decrease in C1Q binding for complement activation</li> </ul>	(Nimmerjahn et al., 2007)
		<ul style="list-style-type: none"> <li>G0 IgGs produced in CHO knockout cultures, without UDP-gal transport and CMP-NeuAc transport, do not to activate complement</li> </ul>	(Wright and Morrison, 1998)
	ADCC	<ul style="list-style-type: none"> <li>Limited improvement to ADCC with galactosylation</li> </ul>	(Kumpel et al., 1995, 1994)
ADCC	<ul style="list-style-type: none"> <li>No observed relationship between galactosylation and <i>in vitro</i> ADCC</li> </ul>	(Boyd et al., 1995; Shinkawa et al., 2003)	

#### 6.5.2.4 Sialylation

Terminal sialylation, unlike other glycoforms, introduces a negative charge to glycans. This glycoform has been reported to reduce binding affinity of mAbs to antigens, FcγR receptors, and reduce ADCC immune responses (Table 13). However, it does possess anti-inflammatory properties, and is credited with the success of intravenous immunoglobulin (IVIg) therapies (Kaneko et al., 2006; Scallon et al., 2007). This seems to mainly be a feature of  $\alpha_{2-6}$  linked sialic glycoforms rather than  $\alpha_{2-3}$  (Anthony et al., 2008). Unlike other therapeutic glycoproteins, mAbs with elevated sialylation have not been reported to receive improvements to serum half-life (Kaneko et al., 2006; Wright and Morrison, 1998). Raju and Lang (2014) provide a thorough examination of the effects of sialylation to a range of commercial glycoproteins.

**Table 13 – Therapeutic efficacy of monoclonal antibodies (mAbs) and immune effector function (IEF) with respect to sialylation of N-glycans. A biantennary glycan with circled regions is provided to indicate the moiety. IEFs include antibody dependent cell cytotoxicity (ADCC), complement dependent cell cytotoxicity (CDC), anti-inflammatory properties, as well as protein serum half-life (serum  $t_{1/2}$ ).**

N-Glycoform	IEF	Effects	Researchers
 <p>Asn</p> <p>Sialylation</p>	ADCC	<ul style="list-style-type: none"> <li>~20% reduced ADCC in populations fractionated to include increased sialylated glycans (~10-60% increased sialylated content) or treated with SialT to increase sialylated content.</li> <li>~40% reduced ADCC for glycoengineered glycans (~90% sialylated)</li> <li>Increased sialylation reduces affinity for Fc<math>\gamma</math>RIIIa as well as antibody-antigen affinity</li> <li>Sialylated glycans on Fc region impact hinge flexibility impeding Fc<math>\gamma</math>R binding</li> </ul>	(Scallon et al., 2007)
	Anti-inflammatory	<ul style="list-style-type: none"> <li>Terminal sialylation provides anti-inflammatory action</li> <li>Sialylated glycoform is actively downregulated <i>in vivo</i> upon antigenic challenge</li> <li>60-80-fold increase of sialylated IgGs from hybridomas purified via affinity chromatography</li> <li>40-80% reduction in IgG cytotoxicity (reversible with sialidase), and 5-10-fold reduction in FcR binding affinity</li> <li>10-fold increase in anti-inflammatory reaction when high sialic-acid fraction IgG injected into <i>in vivo</i> mouse rheumatoid arthritis model</li> </ul>	(Kaneko et al., 2006)
	CDC & ADCC	<ul style="list-style-type: none"> <li>No effect towards complement lysis activity <i>in vitro</i> for rIgG1 expressed in CHO treated with sialidase</li> </ul>	(Boyd et al., 1995)
	Serum $t_{1/2}$	<ul style="list-style-type: none"> <li>No effect for IgGs produced in galT and sialT deficient CHO cells</li> <li>No effect for high sialylated fraction (Kaneko)</li> </ul>	(Kaneko et al., 2006; Wright and Morrison, 1998)

### 6.5.2.5 High Mannose

High mannose glycans typically represent an early departure from glycosylation, either after the endoplasmic reticulum, or the cis-Golgi (Figure 30). This glycoform possesses minimal capability to activate CDC, impaired binding to Fc $\gamma$ R receptors, and rapid *in vivo* clearance (Table 14).

**Table 14 – Therapeutic efficacy of monoclonal antibodies (mAbs) and immune effector function (IEF) with respect to high-mannose N-glycans. Two N-glycans are provided to describe this glycoform. IEFs include binding to the immune antibody receptor FcγRI, complement dependent cell cytotoxicity (CDC), and protein serum half-life (serum t<sub>1/2</sub>).**

N-Glycoform	IEF	Effects	Researchers
<p>Asn Asn</p> <p>High-mannose</p>	FcγRI	<ul style="list-style-type: none"> <li>4-6-fold impairment in binding of FcγRI receptor compared to complex glycoforms</li> </ul>	(Wright and Morrison, 1998, 1994)
	CDC	<ul style="list-style-type: none"> <li>Nearly complete loss of CDC activity and C1q binding with Man5 glycoforms on GnT-I knockout CHO cells</li> </ul>	(Wright and Morrison, 1998, 1994)
	CDC	<ul style="list-style-type: none"> <li>Loss of CDC activity in IgGs with high mannose glycans from yeast cells with up to 30 mannose structures</li> </ul>	(Tao and Morrison, 1989)
	Serum t <sub>1/2</sub>	<ul style="list-style-type: none"> <li>Rapid <i>in vivo</i> clearance in mice of 80% of antibodies, significantly shorter overall serum half-life</li> </ul>	(Wright and Morrison, 1998, 1994)
	Serum t <sub>1/2</sub>	<ul style="list-style-type: none"> <li>High-mannose MAbs administered to patients cleared rapidly out of circulation before other glycoforms</li> </ul>	(Goetze et al., 2011)

### 6.5.3 Immunogenic Glycoforms

Several established rodent-derived cell lines such as NS0 and CHO form glycosylation structures immunogenic in humans such as terminal alpha-gal and a sialic acid variant, N-glycolylneuraminic acid (Neu5Gc) (Bosques et al., 2010; Ghaderi et al., 2010; Padler-Karavani et al., 2008). As such, fully human cell lines have grown more popular and attempts have been made with some success to “glycoengineer” human-like glycosylation in alternative production platforms of bacteria, yeast, insect cells, as well as making improvements to mammalian platforms currently in use. Ghaderi and colleagues provide an excellent examination of this subject from the perspective of immunogenic glycoforms (Ghaderi et al., 2012).

## 6.6 Conclusions

Glycosylation remains among the most important critical quality attributes (CQAs) of recombinant therapeutic glycoproteins, particularly regarding mAbs, where they directly impact the immune effector function of therapeutics. Galactosylation and afucosylation are the most desirable glycoforms for mAbs, while sialylation is the most desirable for other therapeutic glycoproteins.

Supplementation of nucleotide sugar precursors to tune glycan distributions for more desirable therapeutically active glycoforms continues to demonstrate strong potential as a process improvement strategy. These supplementations, while often effective, but reported with inconsistent results. This is primarily due to five key factors beyond the supplementations themselves. The first is differences across cell platforms, such as the up/down regulation of enzymes and transporters; two different cell platforms expressing the same recombinant protein can produce different effects from the same supplementation regime. Secondly, differences between expressed proteins, and by extension differences in the accessibility of the protein glycan sites, can translate to hard limits on the potential glycan complexity and effectiveness of supplementation; mAbs for instance are naturally limited to only having biantennary glycans compared to other therapeutic glycoproteins. The third factor is the fermentation and sampling timeline, specifically glucose availability, which is inversely correlated to galactosylation and sialylation of glycans. This, together with accumulation of exoglycosidases in cultures, particularly sialidase means that harvesting at the end of exponential phase will result in a different glycan distribution than during stationary phase, following a decrease in cell viability. The fourth factor is the concentration of glutamine supplemented to cultures, as the subsequent increase in ammonia will increase UDP-GlcNAc pools affecting glycoforms, as well as altering

the pH of Golgi compartments preventing the proper formation of heteromeric dimer glycosyltransferases necessary for complex terminal glycan additions such as galactosylation and sialylation. Finally, a lack of standardized glycosylation index metrics for observing shifts in glycoform distribution, which can provide better accounting for differences between control cultures and associated reported effects.

The supplementation of glucosamine (GlcN) and acetylglucosamine (GlcNAc) reduces the terminal complexity of glycans to favour the G0 glycoforms, and can increase antennarity of non-IgG proteins. GlcN causes significant restriction to cell growth, but its acetylated form GlcNAc does not. Galactose supplementation achieves increased galactosylation with the greatest reported consistency, and can be enhanced by the addition of uridine and manganese ions, with best results in a glutamine-synthase cell platform. Acetylmannosamine (ManNAc) supplementation, optionally with cytidine, has been reported to significantly increase sialylation; reports of it not succeeding tend to coincide with cell platforms that already have a deficit in galactosylation. Several other exotic sugars also have the potential to affect factors such as fucosylation in the case of D-arabinose, and galactosylation in the case of melezitose, turanose and to a lesser extent lactose.

While this field continues to present exciting new paths like to achieve more therapeutic glycoforms, there remains much opportunity for examining the synergistic supplementation of galactose and ManNAc to improve sialylation of glycoproteins. Using these supplementation methods to tune glycan distributions towards targeted glycoforms should enter the toolkit of every bioprocess engineer.



## Conclusions & Recommendations

The work presented in this thesis was intended to demonstrate supplementation strategies to both enhance cell growth of CHO mammalian cell cultures, and tune glycosylation to improve product quality with respect to protein glycosylation. Towards these objectives, omics methods were applied to elucidate factors at the scale of the metabolome and proteome, to create a nutrient cocktail to enhance culture growth. Further, supplementation of a class nutrients capable of shifting glycan distributions was subsequently examined to tune glycosylation of product monoclonal antibodies to improve quality. Fingerprinting metabolomics was also employed here to observe changes to intracellular nucleotide-sugar pools. Supplementing this class of nutrients was further examined across literature to better resolve conflicting reports of effects to glycan distributions from mammalian cell culture researchers.

In order to enhance culture growth, a multi-omics analysis was undertaken utilizing a two-dimensional differential in-gel electrophoresis (2D-DIGE) proteomics analysis between a parental CHO cell line and a daughter cell line engineered to stably express a recombinant heavy-chain antibody. Measurements of differential endogenous cellular protein expression were subsequently coupled with a metabolomics analysis of the culture supernatant of the daughter CHO cells by targeted profiling of 1D-1H-NMR spectra. Together, these omics methods demonstrated cell stresses via upregulated metabolism, depleted nutrients and accumulated waste metabolites. These results were utilized to modify the culture growth medium with a cocktail of nutrients, which enhanced cell growth. Eight target nutrients corresponding with four identified metabolic systems for CHO cells with upregulated pathways related to anaplerotic TCA-replenishment, NADH/NADPH replenishment, tetrahydrofolate cycle C1 cofactor conversions,

limitations to lipid synthesis, as well as redox modulation. The supplementation resulted in a ~75% improvement to peak cell densities.

Towards tuning glycosylation, N-acetylglucosamine (GlcNAc) and glucosamine (GlcN), nucleotide sugar precursors, were supplemented to the growth medium of CHO cell cultures. The supplementation of GlcN reduced the complexity of glycan profiles of EG2-hFc expressed in CHO cells to favour the G0 glycoform, but caused a significant restriction to cell growth. By supplementing N-acetylglucosamine (GlcNAc) instead – the acetylated form of GlcN – the same affect to the glycan profile was achieved, but with a marginal impact to cell growth, particularly at GlcNAc concentrations of 2.5 mM. The difference in growth effects were attributed to the necessary acetylation of GlcN, which depletes intracellular acetyl-CoA pools necessary for supporting lipid biosynthetic pathways, a result confirmed by the increased excretion of acetate in GlcNAc supplemented cultures by metabolomic analysis.

Supplementation of nucleotide sugar precursors to the growth medium of cell cultures is a promising strategy for tuning the glycan profile of therapeutic recombinant proteins to achieve desired glycan distributions and achieve more therapeutically active glycoforms. However, supplementation of these precursors has been reported with conflicting results. This is due to five key factors: differences across cell platforms; different solvent-accessibility of glycan sites on expressed proteins; the fermentation timeline (glucose availability runs inverse to glycan complexity) and sampling timeline (accumulation of exoglycosidases); the concentration of glutamine (ammonia alters Golgi pH and increases UDP-GlcNAc pools); and finally, a lack of standardized glycosylation index metrics for observing shifts in glycoform distribution.

The supplementation of glucosamine (GlcN) and acetylglucosamine (GlcNAc) reduces the terminal complexity of glycans to favour the G0 glycoforms, and can increase antennarity of non-IgG proteins. Galactose supplementation achieves increased galactosylation with the greatest reported consistency, and can be enhanced by the addition of uridine and manganese ions. Acetylmannosamine (ManNAc) supplementation, optionally with cytidine, has been reported to significantly increase sialylation; reports of it not succeeding tend to coincide with cell platforms that already have a deficit in galactosylation.

While the metabolomics analysis of Chapter 3 was conducted at bioreactor scale, the proteomics analysis was not. Similarly, the experiments of Chapter 4 were conducted at the flask scale. As such, the proteomics analysis, glycan analysis, and fingerprinting metabolomics analysis of intracellular metabolite pools, were all conducted at a single time-point for these cultures. It is recommended that a multi omics analysis, proteomics, glycans and intracellular fingerprinting, be conducted at bioreactor scale for time-course analysis experiments, supplementing nucleotide-sugar precursors to determine how the proteome, metabolome, and glycoform distribution shift during culturing. Of particular interest would be determining what cell stresses could be identified from glucosamine supplementation compared to N-acetylglucosamine (GlcNAc) supplementation. Given that the latter cultures did not have growth restriction, but still lost viability faster than control cultures, it would be interesting to determine whether addition of uridine could alleviate these stresses similar to the UMG cocktail utilized during galactose supplementation.

Transformed cells, such as CHO, exhibit a truncated TCA metabolism, and the growth effects of glucosamine on cytosolic acetyl-CoA pools seems an important factor in the fundamental cell density growth limitations of mammalian cultured cells. Many researchers

continue to fail to make a distinction between the intracellular acetyl-CoA pools in the mitochondrion and the cytosol, even though these two pools are not connected. It is recommended that this particular metabolic node be examined by models and experiments to elucidate its impact on cell growth. Much of the analysis and results presented in this thesis would lend well to the development of metabolic and glycan modeling.

Beyond supplementing glucosamine and GlcNAc, there is also much opportunity for examining the synergistic supplementation of galactose and ManNAc to improve sialylation of glycoproteins. While galactose cocktails of manganese and uridine are very common, inclusion of cytidine and ManNAc are not, but I suspect would yield fruitful results. Similarly, among nucleosides, only cytidine and uridine are used with regularity, generally from one report claiming cytotoxic effects from adenine, guanine and uracil. Supplementing these latter nucleosides may produce interesting results.

Additional supplementation experiments that would have been valuable include the potential for supplementation of exotic sugars to achieve more therapeutic glycoforms, particularly those that can create substitutions in glycans such as D-arabinose taking the place of the core fucose moiety, there are a large variety of natural and synthetic carbohydrates that might prove useful in similar strategies. Testing their immunogenicity would also be important. Ultimately, supplementation should continue to be explored as a key method of affecting cell culture bioprocesses, both to improve cell growth and protein quality.

## References

- Aghamohseni, H., Ohadi, K., Spearman, M., Krahn, N., Moo-Young, M., Scharer, J.M., Butler, M., Budman, H.M., 2014. Effects of nutrient levels and average culture pH on the glycosylation pattern of camelid-humanized monoclonal antibody. *J. Biotechnol.* 186, 98–109. doi:10.1016/j.jbiotec.2014.05.024
- Agrawal, V., Slivac, I., Perret, S., Bisson, L., St-Laurent, G., Murad, Y., Zhang, J., Durocher, Y., 2012. Stable expression of chimeric heavy chain antibodies in CHO cells. *Methods Mol. Biol.* 911, 287–303. doi:10.1007/978-1-61779-968-6\_18
- Ahmad, Z.A., Yeap, S.K., Ali, A.M., Ho, W.Y., Banu, N., Alitheen, M., Hamid, M., 2012. scFv Antibody : Principles and Clinical Application. *Clin. Dev. Immunol.* 2012, 15. doi:10.1155/2012/980250
- Ahn, W.S., Antoniewicz, M.R., 2012. Towards dynamic metabolic flux analysis in CHO cell cultures. *Biotechnol. J.* 7, 61–74. doi:10.1002/biot.201100052
- Albrecht, S., Hilliard, M., Rudd, P., 2014. Therapeutic proteins : facing the challenges of glycobiology. *J. Heal. Policy Outcomes Res.* 12–17. doi:10.7365/JHPOR.2014.5.2
- Allen, J., Davey, H.M., Broadhurst, D., Heald, J.K., Rowland, J.J., Oliver, S.G., Kell, D.B., 2003. High-throughput classification of yeast mutants for functional genomics using metabolic footprinting. *Nat. Biotechnol.* 21, 692–6. doi:10.1038/nbt823
- Anthony, R.M., Nimmerjahn, F., Ashline, D.J., Reinhold, V.N., Paulson, J.C., Ravetch, J. V, 2008. Recapitulation of IVIG anti-inflammatory activity with a recombinant IgG Fc. *Science* 320, 373–6. doi:10.1126/science.1154315
- Aranibar, N., Borys, M., Mackin, N. a, Ly, V., Abu-Absi, N., Abu-Absi, S., Niemitz, M., Schilling, B., Li, Z.J., Brock, B., Russell, R.J., Tymiak, A., Reily, M.D., 2011. NMR-based metabolomics of mammalian cell and tissue cultures. *J. Biomol. NMR* 49, 195–206. doi:10.1007/s10858-011-9490-8
- Augustin, R., Mayoux, E., 2014. Mammalian Sugar Transporters, in: *Glucose Homeostasis*. InTech. doi:10.5772/58325
- Aumiller, J.J., Mabashi-Asazuma, H., Hillar, A., Shi, X., Jarvis, D.L., 2012. A new glycoengineered insect cell line with an inducibly mammalianized protein N-glycosylation pathway. *Glycobiology* 22, 417–28. doi:10.1093/glycob/cwr160
- Baker, K.N., Rendall, M.H., Hills, A.E., Hoare, M., Freedman, R.B., James, D.C., 2001. Metabolic Control of Recombinant Protein N-Glycan Processing in NS0 and CHO Cells. *Biotechnol. Bioeng.* 73, 188–202. doi:10.1002/bit.1051
- Bekesi, J.G., Winzler, R.J., 1970. Inhibitory effects of D-glucosamine on the growth of Walker 256 carcinosarcoma and on protein, RNA, and DNA synthesis. *Cancer Res.* 30, 2905–2912.
- Bell, A., Wang, Z.J., Arbabi-Ghahroudi, M., Chang, T. a, Durocher, Y., Trojahn, U., Baardsnes, J., Jaramillo, M.L., Li, S., Baral, T.N., O'Connor-McCourt, M., Mackenzie, R., Zhang, J., 2010. Differential tumor-targeting abilities of three single-domain antibody formats. *Cancer Lett.* 289, 81–90. doi:10.1016/j.canlet.2009.08.003
- Benjamini, Y., Hochberg, Y., 1995. Controlling the false discovery rate: a practical and powerful approach to multiple testing. *J. R. Stat. Soc.* doi:10.2307/2346101
- Bigge, J.C., Patel, T.P., Bruce, J.A., Goulding, P.N., Charles, S.M., Parekh, R.B., 1995. Nonselective and efficient fluorescent labeling of glycans using 2-amino benzamide and anthranilic acid. *Anal. Biochem.* doi:10.1006/abio.1995.1468

- Blondeel, E.J.M., Braasch, K., McGill, T., Chang, D., Engel, C., Spearman, M., Butler, M., Aucoin, M.G., 2015. Tuning a MAb glycan profile in cell culture: Supplementing N-acetylglucosamine to favour G0 glycans without compromising productivity and cell growth. *J. Biotechnol.* 214, 105–12. doi:10.1016/j.jbiotec.2015.09.014
- Bonarius, H.P., Hatzimanikatis, V., Meesters, K.P., de Gooijer, C.D., Schmid, G., Tramper, J., 1996. Metabolic flux analysis of hybridoma cells in different culture media using mass balances. *Biotechnol. Bioeng.* 50, 299–318. doi:10.1002/(SICI)1097-0290(19960505)50:3<299::AID-BIT9>3.0.CO;2-B
- Bosques, C.J., Collins, B.E., Meador, J.W., Sarvaiya, H., Murphy, J.L., Dellorusso, G., Bulik, D.A., Hsu, I.-H., Washburn, N., Sipsey, S.F., Myette, J.R., Raman, R., Shriver, Z., Sasisekharan, R., Venkataraman, G., 2010. Chinese hamster ovary cells can produce galactose- $\alpha$ -1,3-galactose antigens on proteins. *Nat. Biotechnol.* 28, 1153–6. doi:10.1038/nbt1110-1153
- Boyd, P.N., Lines, A.C., Patel, A.K., 1995. The effect of the removal of sialic acid, galactose and total carbohydrate on the functional activity of Campath-1H. *Mol. Immunol.* 32, 1311–8.
- Braasch, K., Villacrés, C., Butler, M., 2015. Evaluation of Quenching and Extraction Methods for Nucleotide/Nucleotide Sugar Analysis. *Methods Mol. Biol.* 1321, 361–72. doi:10.1007/978-1-4939-2760-9\_24
- Bradley, S. a, Ouyang, A., Purdie, J., Smitka, T. a, Wang, T., Kaerner, A., 2010. Fermentanomics: monitoring mammalian cell cultures with NMR spectroscopy. *J. Am. Chem. Soc.* 132, 9531–3. doi:10.1021/ja101962c
- Broadhurst, E.R., Butler, M., 2000. The inhibitory effect of glutamate on the growth of a murine hybridoma is caused by competitive inhibition of the x(-) (C) transport system required for cystine utilization. *Cytotechnology* 32, 31–43. doi:10.1023/A:1008143716374
- Brokhausen, I., Schachter, H., Stanley, P., 2009. O-GalNAc Glycans, in: Varki, A., Cummings, R.D., Esko, J.D., Stanley, P., Bertozzi, C.R., Hart, G.W., Etzler, M.E. (Eds.), *Essentials of Glycobiology*. Cold Spring Harbor Laboratory Press, Cold Spring Harbor, NY.
- Burda, P., Aebi, M., 1999. The dolichol pathway of N-linked glycosylation. *Biochim. Biophys. Acta* 1426, 239–57.
- Butler, M., 2013. Serum-free media: standardizing cell culture system. *Pharm. Bioprocess.* 1, 315–318. doi:10.4155/pbp.13.45
- Butler, M., 2006. Optimisation of the cellular metabolism of glycosylation for recombinant proteins produced by Mammalian cell systems. *Cytotechnology* 50, 57–76. doi:10.1007/s10616-005-4537-x
- Butler, M., 2004a. The Glycosylation of Proteins in Cell Culture, in: *Animal Cell Culture & Technology*. BIOS Scientific Publishers, London, New York, pp. 113–134.
- Butler, M., 2004b. Growth and Maintenance of Cells in Culture, in: *Animal Cell Culture & Technology*. BIOS Scientific Publishers, London, New York, pp. 47–66.
- Butler, M., Meneses-Acosta, A., 2012. Recent advances in technology supporting biopharmaceutical production from mammalian cells. *Appl. Microbiol. Biotechnol.* 96, 885–894. doi:10.1007/s00253-012-4451-z
- Campbell, M.P., Royle, L., Radcliffe, C.M., Dwek, R.A., Rudd, P.M., 2008. GlycoBase and autoGU: tools for HPLC-based glycan analysis. *Bioinformatics* 24, 1214–6. doi:10.1093/bioinformatics/btn090
- Carinhas, N., Duarte, T.M., Barreiro, L.C., Carrondo, M.J.T., Alves, P.M., Teixeira, A.P., 2013. Metabolic signatures of GS-CHO cell clones associated with butyrate treatment and culture phase transition. *Biotechnol. Bioeng.* 110, 3244–57. doi:10.1002/bit.24983

- Cartron, G., Dacheux, L., Salles, G., Solal-Celigny, P., Bardos, P., Colombat, P., Watier, H., 2002. Therapeutic activity of humanized anti-CD20 monoclonal antibody and polymorphism in IgG Fc receptor Fcγ3 gene. *Blood* 99, 754–8. doi:10.1182/blood.V99.3.754
- Carvalho, A. V., Santos, S.S., Calado, J., Haury, M., Carrondo, M.J.T., 2003. Cell growth arrest by nucleotides, nucleosides and bases as a tool for improved production of recombinant proteins. *Biotechnol. Prog.* 19, 69–83. doi:10.1021/bp0255917
- Chatenoud, L., Ferran, C., Legendre, C., Franchimont, P., Reuter, A., Kreis, H., Bach, J.-F., 1988. Clinical use of OKT3: The role of cytokine release and xenosensitization. *J. Autoimmun.* 1, 631–640. doi:10.1016/0896-8411(88)90054-6
- Chen, P., Harcum, S.W., 2006. Effects of elevated ammonium on glycosylation gene expression in CHO cells. *Metab. Eng.* 8, 123–32. doi:10.1016/j.ymben.2005.10.002
- Chenu, S., Grégoire, A., Malykh, Y., Visvikis, A., Monaco, L., Shaw, L., Schauer, R., Marc, A., Goergen, J.-L., 2003. Reduction of CMP-N-acetylneuraminic acid hydroxylase activity in engineered Chinese hamster ovary cells using an antisense-RNA strategy. *Biochim. Biophys. Acta - Gen. Subj.* 1622, 133–144. doi:10.1016/S0304-4165(03)00137-5
- Chong, W., Goh, L., Reddy, S., 2009. Metabolomics profiling of extracellular metabolites in recombinant Chinese Hamster Ovary fed-batch culture. *Rapid Commun. Mass Spectrom.* 23, 3763–3771. doi:10.1002/rcm
- Chong, W.P.K., Reddy, S.G., Yusufi, F.N.K., Lee, D.-Y., Wong, N.S.C., Heng, C.K., Yap, M.G.S., Ho, Y.S., 2010a. Metabolomics-driven approach for the improvement of Chinese hamster ovary cell growth: overexpression of malate dehydrogenase II. *J. Biotechnol.* 147, 116–21. doi:10.1016/j.jbiotec.2010.03.018
- Chong, W.P.K., Thng, S.H., Hiu, A.P., Lee, D.-Y., Chan, E.C.Y., Ho, Y.S., 2012. LC-MS-based metabolic characterization of high monoclonal antibody-producing Chinese hamster ovary cells. *Biotechnol. Bioeng.* 109, 3103–11. doi:10.1002/bit.24580
- Chong, W.P.K., Yusufi, F.N.K., Lee, D.-Y., Reddy, S.G., Wong, N.S.C., Heng, C.K., Yap, M.G.S., Ho, Y.S., 2010b. Metabolomics-based identification of apoptosis-inducing metabolites in recombinant fed-batch CHO culture media. *J. Biotechnol.* 151, 218–224. doi:10.1016/j.jbiotec.2010.12.010
- Chrysanthopoulos, P.K., Goudar, C.T., Klapa, M.I., 2010. Metabolomics for high-resolution monitoring of the cellular physiological state in cell culture engineering. *Metab. Eng.* 12, 212–22. doi:10.1016/j.ymben.2009.11.001
- Chung, S., Quarmany, V., Gao, X., Ying, Y., Lin, L., Reed, C., Fong, C., Lau, W., Qiu, Z.J., Shen, A., Vanderlaan, M., Song, A., 2012. Quantitative evaluation of fucose reducing effects in a humanized antibody on Fcγ receptor binding and antibody-dependent cell-mediated cytotoxicity activities. *MAbs* 4, 326–40. doi:10.4161/mabs.19941
- Clark, K.J.-R., Griffiths, J., Bailey, K.M., Harcum, S.W., 2005. Gene-expression profiles for five key glycosylation genes for galactose-fed CHO cells expressing recombinant IL-4/13 cytokine trap. *Biotechnol. Bioeng.* 90, 568–77. doi:10.1002/bit.20439
- Cole, E.S., Nichols, E.H., Poisson, L., Harnois, M.L., Livingston, D.J., 1993. In vivo clearance of tissue plasminogen activator: The complex role of sites of glycosylation and level of sialylation. *Fibrinolysis and Proteolysis* 7, 15–22. doi:10.1016/0268-9499(93)90050-6
- Crowell, C.K., Grampp, G.E., Rogers, G.N., Miller, J., Scheinman, R.I., 2007. Amino acid and manganese supplementation modulates the glycosylation state of erythropoietin in a CHO culture system. *Biotechnol. Bioeng.* 96, 538–49. doi:10.1002/bit.21141
- Cuperlović-Culf, M., Barnett, D. a, Culf, A.S., Chute, I., 2010. Cell culture metabolomics: applications

- and future directions. *Drug Discov. Today* 15, 610–21. doi:10.1016/j.drudis.2010.06.012
- Dalziel, M., Crispin, M., Scanlan, C.N., Zitzmann, N., Dwek, R.A., 2014. Emerging principles for the therapeutic exploitation of glycosylation. *Science* 343, 1235681. doi:10.1126/science.1235681
- Davies, J., Jiang, L., Pan, L.Z., LaBarre, M.J., Anderson, D., Reff, M., 2001. Expression of GnTIII in a recombinant anti-CD20 CHO production cell line: Expression of antibodies with altered glycoforms leads to an increase in ADCC through higher affinity for FC gamma RIII. *Biotechnol. Bioeng.* 74, 288–94. doi:10.1002/bit.1119
- del Val, I.J., Kontoravdi, C., Nagy, J.M., 2010. Towards the implementation of quality by design to the production of therapeutic monoclonal antibodies with desired glycosylation patterns. *Biotechnol. Prog.* 26, 1505–27. doi:10.1002/btpr.470
- Dietmair, S., Hodson, M.P., Quek, L.-E., Timmins, N.E., Chrysanthopoulos, P., John, S.S., Gray, P., Nielsen, L.K., 2012. Metabolite profiling of CHO cells with different growth characteristics. *Biotechnol. Bioeng.* 109, 1404–1414. doi:10.1002/bit.24496
- Dietmair, S., Timmins, N.E., Gray, P.P., Nielsen, L.K., Krömer, J.O., 2010. Towards quantitative metabolomics of mammalian cells: development of a metabolite extraction protocol. *Anal. Biochem.* 404, 155–64. doi:10.1016/j.ab.2010.04.031
- Dordal, M.S., Wang, F.F., Goldwasser, E., 1985. The role of carbohydrate in erythropoietin action. *Endocrinology* 116, 2293–9.
- Dubé, S., Fisher, J.W., Powell, J.S., 1988. Glycosylation at specific sites of erythropoietin is essential for biosynthesis, secretion, and biological function. *J. Biol. Chem.* 263, 17516–21.
- Durocher, Y., Perret, S., Kamen, A., 2002. High-level and high-throughput recombinant protein production by transient transfection of suspension-growing human 293-EBNA1 cells. *Nucleic Acids Res.* 30, E9. doi:10.1093/nar/30.2.e9
- Eagle, H., 1955. Nutrition needs of mammalian cells in tissue culture. *Science* 122, 501–14.
- Ecker, D.M., Jones, S.D., Levine, H.L., 2015. The therapeutic monoclonal antibody market. *MAbs* 7, 9–14. doi:10.4161/19420862.2015.989042
- Egrie, J.C., Dwyer, E., Browne, J.K., Hitz, A., Lykos, M.A., 2003. Darbepoetin alfa has a longer circulating half-life and greater in vivo potency than recombinant human erythropoietin. *Exp. Hematol.* 31, 290–299. doi:10.1016/S0301-472X(03)00006-7
- Elliott, S., Egrie, J., Browne, J., Lorenzini, T., Busse, L., Rogers, N., Ponting, I., 2004. Control of rHuEPO biological activity: The role of carbohydrate. *Exp. Hematol.* 32, 1146–1155. doi:10.1016/j.exphem.2004.08.004
- Elvin, J.G., Couston, R.G., van der Walle, C.F., 2011. Therapeutic antibodies: Market considerations, disease targets and bioprocessing. *Int. J. Pharm.* 440, 83–98. doi:10.1016/j.ijpharm.2011.12.039
- Emwas, A.-H.M., 2015. The strengths and weaknesses of NMR spectroscopy and mass spectrometry with particular focus on metabolomics research., in: *Methods in Molecular Biology* (Clifton, N.J.). pp. 161–93. doi:10.1007/978-1-4939-2377-9\_13
- Eon-Duval, A., Broly, H., Gleixner, R., 2012. Quality attributes of recombinant therapeutic proteins: an assessment of impact on safety and efficacy as part of a quality by design development approach. *Biotechnol. Prog.* 28, 608–22. doi:10.1002/btpr.1548
- Evans, V.J., Bryant, J.C., Mcquilkkin, W.T., Fioramonti, M.C., Sanford, K.K., Westfall, B.B., Earle, W.R., 1956. Studies of nutrient media for tissue cells in vitro. II. An improved protein-free chemically defined medium for long-term cultivation of strain L-929 cells. *Cancer Res.* 16, 87–94.
- FDA, 2015. Scientific Considerations in Demonstrating Biosimilarity to a Reference Product - Guidance



- for Industry, Biosimilarity. Silver Spring, MD.
- Fernandes, S., Robitaille, J., Bastin, G., Jolicoeur, M., Wouwer, A. Vande, 2016. Application of Dynamic Metabolic Flux Convex Analysis to CHO-DXB11 Cell Fed-batch Cultures. *IFAC-PapersOnLine* 49, 466–471. doi:10.1016/j.ifacol.2016.07.386
- Ferrara, C., Stuart, F., Sondermann, P., Brünker, P., Umaña, P., 2006. The carbohydrate at Fcγ3a Asn-162. An element required for high affinity binding to non-fucosylated IgG glycoforms. *J. Biol. Chem.* 281, 5032–6. doi:10.1074/jbc.M510171200
- Ferrari, J., Gunson, J., Lofgren, J., Krummen, L., Warner, T.G., 1998. Chinese hamster ovary cells with constitutively expressed sialidase antisense RNA produce recombinant DNase in batch culture with increased sialic acid. *Biotechnol. Bioeng.* 60, 589–95.
- Fiehn, O., 2002. Metabolomics--the link between genotypes and phenotypes. *Plant Mol. Biol.* 48, 155–71.
- Flynn, G.C., Chen, X., Liu, Y.D., Shah, B., Zhang, Z., 2010. Naturally occurring glycan forms of human immunoglobulins G1 and G2. *Mol. Immunol.* 47, 2074–82. doi:10.1016/j.molimm.2010.04.006
- Freeze, H.H., Elbein, A.D., 2009. *Glycosylation Precursors*, 2nd ed, *Essentials of Glycobiology*. Cold Spring Harbor Laboratory Press, Cold Spring Harbor, NY.
- Gawlitzek, M., Valley, U., Wagner, R., 1998. Ammonium ion and glucosamine dependent increases of oligosaccharide complexity in recombinant glycoproteins secreted from cultivated BHK-21 cells. *Biotechnol. Bioeng.* 57, 518–528.
- Gemmill, T.R., Trimble, R.B., 1999. Overview of N- and O-linked oligosaccharide structures found in various yeast species. *Biochim. Biophys. Acta* 1426, 227–37.
- Ghaderi, D., Taylor, R.E., Padler-Karavani, V., Diaz, S., Varki, A., 2010. Implications of the presence of N-glycolylneuraminic acid in recombinant therapeutic glycoproteins. *Nat. Biotechnol.* 28, 863–7. doi:10.1038/nbt.1651
- Ghaderi, D., Zhang, M., Hurtado-Ziola, N., Varki, A., 2012. Production platforms for biotherapeutic glycoproteins. Occurrence, impact, and challenges of non-human sialylation. *Biotechnol. Genet. Eng. Rev.* 28, 147–175. doi:10.5661/bger-28-147
- Glaser, L., 1959. The biosynthesis of N-acetylgalactosamine. *J. Biol. Chem.* 234, 2801–5. doi:10.1177/036985646700400518
- Glasse, J., Gernaey, K. V., Clemens, C., Schulz, T.W., Oliveira, R., Striedner, G., Mandenius, C.-F., 2011. Process analytical technology (PAT) for biopharmaceuticals. *Biotechnol. J.* 6, 369–77. doi:10.1002/biot.201000356
- Goeddel, D. V., Kleid, D.G., Bolivar, F., Heyneker, H.L., Yansura, D.G., Crea, R., Hirose, T., Kraszewski, a, Itakura, K., Riggs, a D., 1979. Expression in *Escherichia coli* of chemically synthesized genes for human insulin. *Proc. Natl. Acad. Sci. U. S. A.* 76, 106–10.
- Goetze, A.M., Liu, Y.D., Zhang, Z., Shah, B., Lee, E., Bondarenko, P. V., Flynn, G.C., 2011. High-mannose glycans on the Fc region of therapeutic IgG antibodies increase serum clearance in humans. *Glycobiology* 21, 949–59. doi:10.1093/glycob/cwr027
- Gornik, O., Royle, L., Harvey, D.J., Radcliffe, C.M., Saldova, R., Dwek, R. a, Rudd, P., Lauc, G., 2007. Changes of serum glycans during sepsis and acute pancreatitis. *Glycobiology* 17, 1321–32. doi:10.1093/glycob/cwm106
- Goudar, C., Biener, R., Boisart, C., Heidemann, R., Piret, J., de Graaf, A., Konstantinov, K., 2010. Metabolic flux analysis of CHO cells in perfusion culture by metabolite balancing and 2D [<sup>13</sup>C, <sup>1</sup>H] COSY NMR spectroscopy. *Metab. Eng.* 12, 138–149. doi:10.1016/j.ymben.2009.10.007
- Grainger, R.K., James, D.C., 2013. CHO cell line specific prediction and control of recombinant

- monoclonal antibody N-glycosylation. *Biotechnol. Bioeng.* 110, 2970–83. doi:10.1002/bit.24959
- Gramer, M.J., Eckblad, J.J., Donahue, R., Brown, J., Shultz, C., Vickerman, K., Priem, P., van den Bremer, E.T.J., Gerritsen, J., van Berkel, P.H.C., 2011. Modulation of antibody galactosylation through feeding of uridine, manganese chloride, and galactose. *Biotechnol. Bioeng.* 108, 1591–602. doi:10.1002/bit.23075
- Gramer, M.J., Goochee, C.F., 1993. Glycosidase activities in Chinese hamster ovary cell lysate and cell culture supernatant. *Biotechnol. Prog.* 9, 366–73. doi:10.1021/bp00022a003
- Gramer, M.J., Goochee, C.F., Chock, V.Y., Brousseau, D.T., Sliwkowski, M.B., 1995. Removal of sialic acid from a glycoprotein in CHO cell culture supernatant by action of an extracellular CHO cell sialidase. *Biotechnology*. (N. Y.) 13, 692–8.
- Grammatikos, S.I., Valley, U., Nimitz, M., Conradt, H.S., Wagner, R., 1998. Intracellular UDP-N-acetylhexosamine pool affects N-glycan complexity: a mechanism of ammonium action on protein glycosylation. *Biotechnol. Prog.* 14, 410–419. doi:10.1021/bp980005o
- Green, L.L., Hardy, M.C., Maynard-Currie, C.E., Tsuda, H., Louie, D.M., Mendez, M.J., Abderrahim, H., Noguchi, M., Smith, D.H., Zeng, Y., David, N.E., Sasai, H., Garza, D., Brenner, D.G., Hales, J.F., McGuinness, R.P., Capon, D.J., Klapholz, S., Jakobovits, A., 1994. Antigen-specific human monoclonal antibodies from mice engineered with human Ig heavy and light chain YACs. *Nat. Genet.* 7, 13–21. doi:10.1038/ng0594-13
- Gu, X., Wang, D.I., 1998. Improvement of interferon-gamma sialylation in Chinese hamster ovary cell culture by feeding of N-acetylmannosamine. *Biotechnol. Bioeng.* 58, 642–8.
- Guile, G.R., Rudd, P.M., Wing, D.R., Prime, S.B., Dwek, R. a, 1996. A rapid high-resolution high-performance liquid chromatographic method for separating glycan mixtures and analyzing oligosaccharide profiles. *Anal. Biochem.* 240, 210–26. doi:10.1006/abio.1996.0351
- Ham, R.G., 1965. Clonal Growth of Mammalian Cells in a Chemically Defined, Synthetic Medium. *Proc. Natl. Acad. Sci. U. S. A.* 53, 288–93.
- Hamilton, S.R., Davidson, R.C., Sethuraman, N., Nett, J.H., Jiang, Y., Rios, S., Bobrowicz, P., Stadheim, T.A., Li, H., Choi, B.-K., Hopkins, D., Wischniewski, H., Roser, J., Mitchell, T., Strawbridge, R.R., Hoopes, J., Wildt, S., Gerngross, T.U., 2006. Humanization of yeast to produce complex terminally sialylated glycoproteins. *Science* 313, 1441–3. doi:10.1126/science.1130256
- Harris, R.J., Chin, E.T., Macchi, F., Keck, R.G., Shyong, B.-J., Ling, V.T., Cordoba, A.J., Marian, M., Sinclair, D., Battersby, J.E., Jones, A.J.S., 2010. Analytical Characterization of Monoclonal Antibodies: Linking Structure to Function, in: Shire, S.J., Gombotz, W., Bechtold-Peters, K., Andya, J. (Eds.), *Biotechnology: Pharmaceutical Aspects, Volume XI: Current Trends in Monoclonal Antibody Development and Manufacturing*. Springer, pp. 193–205. doi:10.1007/978-0-387-76643-0\_12
- Hassinen, A., Kellokumpu, S., 2014. Organizational interplay of Golgi N-glycosyltransferases involves organelle microenvironment-dependent transitions between enzyme homo- and heteromers. *J. Biol. Chem.* 289, 26937–48. doi:10.1074/jbc.M114.595058
- Hermansson, M., Hokynar, K., Somerharju, P., 2011. Mechanisms of glycerophospholipid homeostasis in mammalian cells. *Prog. Lipid Res.* 50, 240–57. doi:10.1016/j.plipres.2011.02.004
- Hickman, S., Kornfeld, S., 1978. Effect of tunicamycin on IgM, IgA, and IgG secretion by mouse plasmacytoma cells. *J. Immunol.* 121, 990–6.
- Hills, A.E., Patel, A., Boyd, P., James, D.C., 2001. Metabolic control of recombinant monoclonal antibody N-glycosylation in GS-NS0 cells. *Biotechnol. Bioeng.* 75, 239–251. doi:10.1002/bit.10022
- Hodoniczky, J., Zheng, Y.Z., James, D.C., 2005. Control of recombinant monoclonal antibody effector

- functions by Fc N-glycan remodeling in vitro. *Biotechnol. Prog.* 21, 1644–52. doi:10.1021/bp050228w
- Hossler, P., 2012. Protein glycosylation control in mammalian cell culture: past precedents and contemporary prospects. *Adv. Biochem. Eng. Biotechnol.* 127, 187–219. doi:10.1007/10\_2011\_113
- Hossler, P., Chumsae, C., Racicot, C., Ouellette, D., Ibraghimov, A., Serna, D., Mora, A., McDermott, S., Labkovsky, B., Scesney, S., Grinnell, C., Preston, G., Bose, S., Carrillo, R., 2017. Arabinosylation of recombinant human immunoglobulin-based protein therapeutics. *MAbs* 9, 1–20. doi:10.1080/19420862.2017.1294295
- Hossler, P., Khattak, S.F., Li, Z.J., 2009. Optimal and consistent protein glycosylation in mammalian cell culture. *Glycobiology* 19, 936–949. doi:10.1093/glycob/cwp079
- Hossler, P., Racicot, C., Chumsae, C., McDermott, S., Cochran, K., 2016. Cell culture media supplementation of infrequently used sugars for the targeted shifting of protein glycosylation profiles. *Biotechnol. Prog.* 30, 429–42. doi:10.1002/btpr.2429
- Huang, D.W., Sherman, B.T., Lempicki, R. a, 2009a. Systematic and integrative analysis of large gene lists using DAVID bioinformatics resources. *Nat. Protoc.* 4, 44–57. doi:10.1038/nprot.2008.211
- Huang, D.W., Sherman, B.T., Lempicki, R. a, 2009b. Bioinformatics enrichment tools: Paths toward the comprehensive functional analysis of large gene lists. *Nucleic Acids Res.* 37, 1–13. doi:10.1093/nar/gkn923
- Ishida, N., Kawakita, M., 2004. Molecular physiology and pathology of the nucleotide sugar transporter family (SLC35). *Pflugers Arch.* 447, 768–75. doi:10.1007/s00424-003-1093-0
- Jefferis, R., 2012. Isotype and glycoform selection for antibody therapeutics. *Arch. Biochem. Biophys.* 526, 159–66. doi:10.1016/j.abb.2012.03.021
- Jefferis, R., 2009. Recombinant antibody therapeutics: the impact of glycosylation on mechanisms of action. *Trends Pharmacol. Sci.* 30, 356–62. doi:10.1016/j.tips.2009.04.007
- Jefferis, R., 2009. Glycosylation as a strategy to improve antibody-based therapeutics. *Nat. Rev. Drug Discov.* 8, 226–34. doi:10.1038/nrd2804
- Jones, P.T., Dear, P.H., Foote, J., Neuberger, M.S., Winter, G., 1986. Replacing the complementarity-determining regions in a human antibody with those from a mouse. *Nature* 321, 522–5. doi:10.1038/321522a0
- Kaneko, Y., Nimmerjahn, F., Ravetch, J. V, 2006. Anti-inflammatory activity of immunoglobulin G resulting from Fc sialylation. *Science* 313, 670–3. doi:10.1126/science.1129594
- Kapur, R., Einarsdottir, H.K., Vidarsson, G., 2014. IgG-effector functions: “The Good, The Bad and The Ugly.” *Immunol. Lett.* 160, 139–144. doi:10.1016/j.imlet.2014.01.015
- Kean, E.L., 1970. Nuclear cytidine 5'-monophosphosialic acid synthetase. *J. Biol. Chem.* 245, 2301–8. doi:10.1207/s15516709cog1902
- Kell, D.B., Brown, M., Davey, H.M., Dunn, W.B., Spasic, I., Oliver, S.G., 2005. Metabolic footprinting and systems biology: the medium is the message. *Nat. Rev. Microbiol.* 3, 557–65. doi:10.1038/nrmicro1177
- Khoo, S.H.G., Al-Rubeai, M., 2007. Metabolomics as a complementary tool in cell culture. *Biotechnol. Appl. Biochem.* 47, 71–84. doi:10.1042/BA20060221
- Kildegaard, H.F., Fan, Y., Sen, J.W., Larsen, B., Andersen, M.R., 2015. Glycoprofiling effects of media additives on IgG produced by CHO cells in fed-batch bioreactors. *Biotechnol. Bioeng.* 113, 359–366. doi:10.1002/bit.25715
- Kim, D.Y., Chaudhry, M.A., Kennard, M.L., Jardon, M. a, Braasch, K., Dionne, B., Butler, M., Piret,

- J.M., 2012. Fed-batch CHO cell t-PA production and feed glutamine replacement to reduce ammonia production. *Biotechnol. Prog.* 29, 165–75. doi:10.1002/btpr.1658
- Kim, D.Y., Lee, J.C., Chang, H.N., Oh, D.J., 2005. Effects of supplementation of various medium components on chinese hamster ovary cell cultures producing recombinant antibody. *Cytotechnology* 47, 37–49. doi:10.1007/s10616-005-3775-2
- Kim, J.Y., Kim, Y.-G., Lee, G.M., 2012. CHO cells in biotechnology for production of recombinant proteins: current state and further potential. *Appl. Microbiol. Biotechnol.* 93, 917–30. doi:10.1007/s00253-011-3758-5
- Kim, J.Y., Kim, Y.G., Han, Y.K., Choi, H.S., Kim, Y.H., Lee, G.M., 2011. Proteomic understanding of intracellular responses of recombinant Chinese hamster ovary cells cultivated in serum-free medium supplemented with hydrolysates. *Appl. Microbiol. Biotechnol.* 89, 1917–1928. doi:10.1007/s00253-011-3106-9
- Kim, S.H., Lee, G.M., 2009. Development of serum-free medium supplemented with hydrolysates for the production of therapeutic antibodies in CHO cell cultures using design of experiments. *Appl. Microbiol. Biotechnol.* 83, 639–48. doi:10.1007/s00253-009-1903-1
- Köhler, G., Milstein, C., 1975. Continuous cultures of fused cells secreting antibody of predefined specificity. *Nature* 256, 495–497. doi:10.1038/256495a0
- Koide, N., Nose, M., Muramatsu, T., 1977. Recognition of IgG by Fc receptor and complement: effects of glycosidase digestion. *Biochem. Biophys. Res. Commun.* 75, 838–44.
- Krishnan, N., Dickman, M.B., Becker, D.F., 2008. Proline modulates the intracellular redox environment and protects mammalian cells against oxidative stress. *Free Radic. Biol. Med.* 44, 671–81. doi:10.1016/j.freeradbiomed.2007.10.054
- Krug, E., Zweibaum, a, Schulz-Holstege, C., Keppler, D., 1984. D-glucosamine-induced changes in nucleotide metabolism and growth of colon-carcinoma cells in culture. *Biochem. J.* 217, 701–708.
- Kumpel, B.M., Rademacher, T.W., Rook, G.A., Williams, P.J., Wilson, I.B., 1994. Galactosylation of human IgG monoclonal anti-D produced by EBV-transformed B-lymphoblastoid cell lines is dependent on culture method and affects Fc receptor-mediated functional activity. *Hum. Antibodies Hybridomas* 5, 143–51.
- Kumpel, B.M., Wang, Y., Griffiths, H.L., Hadley, A.G., Rook, G.A., 1995. The biological activity of human monoclonal IgG anti-D is reduced by beta-galactosidase treatment. *Hum. Antibodies Hybridomas* 6, 82–8.
- Kyriakopoulos, S., Polizzi, K.M., Kontoravdi, C., 2013. Comparative analysis of amino acid metabolism and transport in CHO variants with different levels of productivity. *J. Biotechnol.* 168, 543–51. doi:10.1016/j.jbiotec.2013.09.007
- Lalonde, M.-E., Durocher, Y., 2017. Therapeutic glycoprotein production in mammalian cells. *J. Biotechnol.* 251, 128–140. doi:10.1016/j.jbiotec.2017.04.028
- Lazar, G.A., Desjarlais, J.R., 2009. Engineering the Antibody Fc Region for Optimal Effector Function, in: An, Z. (Ed.), *Therapeutic Monoclonal Antibodies From Bench to Clinic*. John Wiley & Sons, pp. 349–370.
- Leavitt, R., Schlesinger, S., Kornfeld, S., 1977. Impaired intracellular migration and altered solubility of nonglycosylated glycoproteins of vesicular stomatitis virus and Sindbis virus. *J. Biol. Chem.* 252, 9018–23.
- Lee, C.C., Perchiacca, J.M., Tessier, P.M., 2013. Toward aggregation-resistant antibodies by design. *Trends Biotechnol.* 31, 612–620. doi:10.1016/j.tibtech.2013.07.002

- Lee, G.M., Kim, E.J., Kim, N.S., Yoon, S.K., Ahn, Y.H., Song, J.Y., 1999. Development of a serum-free medium for the production of erythropoietin by suspension culture of recombinant Chinese hamster ovary cells using a statistical design. *J. Biotechnol.* 69, 85–93.
- Lee, J.H., Reier, J., Heffner, K.M., Barton, C., Spencer, D., Schmelzer, A.E., Venkat, R., 2017. Production and characterization of active recombinant human factor II with consistent sialylation. *Biotechnol. Bioeng.* 114, 1991–2000. doi:10.1002/bit.26317
- Liang, C.-M., Tai, M.-C., Chang, Y.-H., Chen, Y.-H., Chen, C.-L., Chien, M.-W., Chen, J.-T., 2010. Glucosamine inhibits epidermal growth factor-induced proliferation and cell-cycle progression in retinal pigment epithelial cells. *Mol. Vis.* 16, 2559–2571.
- Lindsley, C.W., 2017. New 2016 Data and Statistics for Global Pharmaceutical Products and Projections through 2017. *ACS Chem. Neurosci.* 8, 1635–1636. doi:10.1021/acchemneuro.7b00253
- Liu, B., Spearman, M., Doering, J., Lattová, E., Perreault, H., Butler, M., 2014. The availability of glucose to CHO cells affects the intracellular lipid-linked oligosaccharide distribution, site occupancy and the N-glycosylation profile of a monoclonal antibody. *J. Biotechnol.* 170, 17–27. doi:10.1016/j.jbiotec.2013.11.007
- Liu, J., Wang, J., Fan, L., Chen, X., Hu, D., 2015. Galactose supplementation enhance sialylation of recombinant Fc-fusion protein in CHO cell : an insight into the role of galactosylation in sialylation. *World J. Microbiol. Biotechnol.* 31, 1147–1156. doi:10.1007/s11274-015-1864-8
- Lizak, C., Fan, Y., Weber, T.C., Aebi, M., 2011. N-Linked Glycosylation of Antibody Fragments in *Escherichia coli*. *Bioconjug. Chem.* 22, 488–496. doi:10.1021/bc100511k
- Lonberg, N., Taylor, L.D., Harding, F.A., Trounstine, M., Higgins, K.M., Schramm, S.R., Kuo, C.C., Mashayekh, R., Wymore, K., McCabe, J.G., 1994. Antigen-specific human antibodies from mice comprising four distinct genetic modifications. *Nature* 368, 856–9. doi:10.1038/368856a0
- Lu, W., Su, X., Klein, M.S., Lewis, I.A., Fiehn, O., Rabinowitz, J.D., 2017. Metabolite Measurement: Pitfalls to Avoid and Practices to Follow. *Annu. Rev. Biochem.* 86, 277–304. doi:10.1146/annurev-biochem-061516-044952
- Luo, J., Vijayasankaran, N., Autsen, J., Santuray, R., Hudson, T., Amanullah, A., Li, F., 2012. Comparative metabolite analysis to understand lactate metabolism shift in Chinese hamster ovary cell culture process. *Biotechnol. Bioeng.* 109, 146–56. doi:10.1002/bit.23291
- Ma, N., Ellet, J., Okediadi, C., Hermes, P., McCormick, E., Casnocha, S., 2009. A single nutrient feed supports both chemically defined NS0 and CHO fed-batch processes: Improved productivity and lactate metabolism. *Biotechnol. Prog.* 25, 1353–63. doi:10.1002/btpr.238
- Malhotra, R., Wormald, M.R., Rudd, P.M., Fischer, P.B., Dwek, R.A., Sim, R.B., 1995. Glycosylation changes of IgG associated with rheumatoid arthritis can activate complement via the mannose-binding protein. *Nat. Med.* 1, 237–43. doi:10.1038/nm0495-365
- Martínez, V.S., Dietmair, S., Quek, L.-E., Hodson, M.P., Gray, P., Nielsen, L.K., 2013. Flux balance analysis of CHO cells before and after a metabolic switch from lactate production to consumption. *Biotechnol. Bioeng.* 110, 660–6. doi:10.1002/bit.24728
- McDonald, A.G., Hayes, J.M., Davey, G.P., 2016. Metabolic flux control in glycosylation. *Curr. Opin. Struct. Biol.* 40, 97–103. doi:10.1016/j.sbi.2016.08.007
- Meleady, P., 2018. Two-Dimensional Gel Electrophoresis and 2D-DIGE. *Methods Mol. Biol.* 1664, 3–14. doi:10.1007/978-1-4939-7268-5\_1
- Mimura, Y., Church, S., Ghirlando, R., Ashton, P.R., Dong, S., Goodall, M., Lund, J., Jefferis, R., 2001. The influence of glycosylation on the thermal stability and effector function expression of human IgG1-Fc: properties of a series of truncated glycoforms. *Mol. Immunol.* 37, 697–706.

- Moore, G.E., Gerner, R.E., Franklin, H. a, 1967. Culture of normal human leukocytes. *JAMA* 199, 519–24.
- Moran, N., 2011. Boehringer splashes out on bispecific antibody platforms. *Nat. Biotechnol.* 29, 5–6. doi:10.1038/nbt0111-5
- Morell, A.G., Irvine, R.A., Sternlieb, I., Scheinberg, I.H., Ashwell, G., 1968. Physical and chemical studies on ceruloplasmin. V. Metabolic studies on sialic acid-free ceruloplasmin in vivo. *J. Biol. Chem.* 243, 155–9.
- Moremen, K.W., Tiemeyer, M., Nairn, A. V, 2012. Vertebrate protein glycosylation: diversity, synthesis and function. *Nat. Rev. Mol. Cell Biol.* 13, 448–62. doi:10.1038/nrm3383
- Morgan, J.F., Morton, H.J., Parker, R.C., 1950. Nutrition of animal cells in tissue culture; initial studies on a synthetic medium. *Proc. Soc. Exp. Biol. Med.* 73, 1–8.
- Mori, K., Kuni-Kamochi, R., Yamane-Ohnuki, N., Wakitani, M., Yamano, K., Imai, H., Kanda, Y., Niwa, R., Iida, S., Uchida, K., Shitara, K., Satoh, M., 2004. Engineering Chinese hamster ovary cells to maximize effector function of produced antibodies using FUT8 siRNA. *Biotechnol. Bioeng.* 88, 901–8. doi:10.1002/bit.20326
- Morrison, S.L., Johnson, M.J., Herzenberg, L. a, Oi, V.T., 1984. Chimeric human antibody molecules: mouse antigen-binding domains with human constant region domains. *Proc. Natl. Acad. Sci. U. S. A.* 81, 6851–5.
- Morton, H.J., 1970. A survey of commercially available tissue culture media. *In Vitro* 6, 89–108.
- Nicholson, J.K., Lindon, J.C., Holmes, E., 1999. “Metabonomics”: understanding the metabolic responses of living systems to pathophysiological stimuli via multivariate statistical analysis of biological NMR spectroscopic data. *Xenobiotica.* 29, 1181–9. doi:10.1080/004982599238047
- Nimmerjahn, F., Anthony, R.M., Ravetch, J. V, 2007. Agalactosylated IgG antibodies depend on cellular Fc receptors for in vivo activity. *Proc. Natl. Acad. Sci. U. S. A.* 104, 8433–7. doi:10.1073/pnas.0702936104
- Niwa, R., Shoji-Hosaka, E., Sakurada, M., Shinkawa, T., Uchida, K., Nakamura, K., Matsushima, K., Ueda, R., Hanai, N., Shitara, K., 2004. Defucosylated chimeric anti-CC chemokine receptor 4 IgG1 with enhanced antibody-dependent cellular cytotoxicity shows potent therapeutic activity to T-cell leukemia and lymphoma. *Cancer Res.* 64, 2127–33. doi:10.1158/0008-5472.CAN-03-2068
- Nose, M., Wigzell, H., 1983. Biological significance of carbohydrate chains on monoclonal antibodies. *Proc. Natl. Acad. Sci.* 80, 6632–6636.
- Nyberg, G.B., Balcarcel, R.R., Follstad, B.D., Stephanopoulos, G., Wang, D.I., 1999. Metabolic effects on recombinant interferon-gamma glycosylation in continuous culture of Chinese hamster ovary cells. *Biotechnol. Bioeng.* 62, 336–47.
- Oh, H.-J., Lee, J.S., Song, D.-K., Shin, D.-H., Jang, B.-C., Suh, S.-I., Park, J.-W., Suh, M.-H., Baek, W.-K., 2007. D-glucosamine inhibits proliferation of human cancer cells through inhibition of p70S6K. *Biochem. Biophys. Res. Commun.* 360, 840–845. doi:10.1016/j.bbrc.2007.06.137
- Padler-Karavani, V., Yu, H., Cao, H., Chokhawala, H., Karp, F., Varki, N., Chen, X., Varki, A., 2008. Diversity in specificity, abundance, and composition of anti-Neu5Gc antibodies in normal humans: potential implications for disease. *Glycobiology* 18, 818–30. doi:10.1093/glycob/cwn072
- Palmberger, D., Wilson, I.B.H., Berger, I., Grabherr, R., Rendic, D., 2012. SweetBac : A New Approach for the Production of Mammalianised Glycoproteins in Insect Cells. *PLoS One* 7, 1–8. doi:10.1371/journal.pone.0034226
- Pederson, N. V, Knop, R.H., Miller, W.M., 1992. UDP-N-acetylhexosamine modulation by glucosamine

- and uridine in NCI N-417 variant small cell lung cancer cells: 31P nuclear magnetic resonance results. *Cancer Res.* 52, 3782–3786. doi:10.1016/0169-5002(93)90356-3
- Pels Rijcken, W.R., Ferwerda, W., Van den Eijnden, D.H., Overdijk, B., 1995a. Influence of D-galactosamine on the synthesis of sugar nucleotides and glycoconjugates in rat hepatocytes. *Glycobiology* 5, 495–502.
- Pels Rijcken, W.R., Overdijk, B., Van den Eijnden, D.H., Ferwerda, W., 1995b. The effect of increasing nucleotide-sugar concentrations on the incorporation of sugars into glycoconjugates in rat hepatocytes. *Biochem. J.* 305 ( Pt 3, 865–70.
- Quek, L.-E., Dietmair, S., Krömer, J.O., Nielsen, L.K., 2010. Metabolic flux analysis in mammalian cell culture. *Metab. Eng.* 12, 161–71. doi:10.1016/j.ymben.2009.09.002
- Räbinä, J., Mäki, M., Savilahti, E.M., Järvinen, N., Penttilä, L., Renkonen, R., 2001. Analysis of nucleotide sugars from cell lysates by ion-pair solid-phase extraction and reversed-phase high-performance liquid chromatography. *Glycoconj. J.* 18, 799–805. doi:5108619 [pii]
- Raju, T.S., Lang, S.E., 2014. Diversity in structure and functions of antibody sialylation in the Fc. *Curr. Opin. Biotechnol.* 30, 147–152. doi:10.1016/j.copbio.2014.06.014
- Rathore, A.S., Kumar Singh, S., Pathak, M., Read, E.K., Brorson, K.A., Agarabi, C.D., Khan, M., 2015. Fermentanomics: Relating quality attributes of a monoclonal antibody to cell culture process variables and raw materials using multivariate data analysis. *Biotechnol. Prog.* 31, 1586–1599. doi:10.1002/btpr.2155
- Raymond, C., Robotham, A., Spearman, M., Butler, M., Kelly, J., Durocher, Y., 2015. Production of  $\alpha$ 2,6-sialylated IgG1 in CHO cells. *MAbs* 7, 571–83. doi:10.1080/19420862.2015.1029215
- Read, E.K., Bradley, S. a, Smitka, T. a, Agarabi, C.D., Lute, S.C., Brorson, K. a, 2013. Fermentanomics informed amino acid supplementation of an antibody producing mammalian cell culture. *Biotechnol. Prog.* 29, 745–53. doi:10.1002/btpr.1728
- Reichert, J.M., 2017. Antibodies to watch in 2017. *MAbs* 9, 167–181. doi:10.1080/19420862.2016.1269580
- Scallon, B.J., Tam, S.H., McCarthy, S.G., Cai, A.N., Raju, T.S., 2007. Higher levels of sialylated Fc glycans in immunoglobulin G molecules can adversely impact functionality. *Mol. Immunol.* 44, 1524–34. doi:10.1016/j.molimm.2006.09.005
- Scarcelli, J.J., Colussi, P. a., Fabre, A.L., Boles, E., Orlean, P., Taron, C.H., 2012. Uptake of radiolabeled GlcNAc into *Saccharomyces cerevisiae* via native hexose transporters and its in vivo incorporation into GPI precursors in cells expressing heterologous GlcNAc kinase. *FEMS Yeast Res.* 12, 305–316. doi:10.1111/j.1567-1364.2011.00778.x
- Schachter, H., 1986. Biosynthetic controls that determine the branching and microheterogeneity of protein-bound oligosaccharides. *Biochem. Cell Biol.* 64, 163–81.
- Schaub, J., Clemens, C., Kaufmann, H., Schulz, T.W., 2012. Advancing biopharmaceutical process development by system-level data analysis and integration of omics data. *Adv. Biochem. Eng. Biotechnol.* 127, 133–63. doi:10.1007/10\_2010\_98
- Schlenke, P., Grabenhorst, E., Nimtz, M., Conradt, H.S., 1999. Construction and characterization of stably transfected BHK-21 cells with human-type sialylation characteristic. *Cytotechnology* 30, 17–25. doi:10.1023/A:1008049603947
- Schroeder, H.W., Cavacini, L., 2010. Structure and function of immunoglobulins. *J. Allergy Clin. Immunol.* 125, S41-52. doi:10.1016/j.jaci.2009.09.046
- Schroff, R.W., Foon, K.A., Beatty, S.M., Oldham, R.K., Morgan, A.C., 1985. Human anti-murine

- immunoglobulin responses in patients receiving monoclonal antibody therapy. *Cancer Res.* 45, 879–85.
- Sellick, C.A., Knight, D., Croxford, A.S., Maqsood, A.R., Stephens, G.M., Goodacre, R., Dickson, A.J., 2010. Evaluation of extraction processes for intracellular metabolite profiling of mammalian cells: matching extraction approaches to cell type and metabolite targets. *Metabolomics* 6, 427–438. doi:10.1007/s11306-010-0216-9
- Sellick, C. a, Croxford, A.S., Maqsood, A.R., Stephens, G., Westerhoff, H. V, Goodacre, R., Dickson, A.J., 2011a. Metabolite profiling of recombinant CHO cells: designing tailored feeding regimes that enhance recombinant antibody production. *Biotechnol. Bioeng.* 108, 3025–31. doi:10.1002/bit.23269
- Sellick, C. a, Hansen, R., Maqsood, A.R., Dunn, W.B., Stephens, G.M., Goodacre, R., Dickson, A.J., 2009. Effective quenching processes for physiologically valid metabolite profiling of suspension cultured Mammalian cells. *Anal. Chem.* 81, 174–83. doi:10.1021/ac8016899
- Sellick, C. a, Hansen, R., Stephens, G.M., Goodacre, R., Dickson, A.J., 2011b. Metabolite extraction from suspension-cultured mammalian cells for global metabolite profiling. *Nat. Protoc.* 6, 1241–9. doi:10.1038/nprot.2011.366
- Selvarasu, S., Ho, Y.S., Chong, W.P.K., Wong, N.S.C., Yusufi, F.N.K., Lee, Y.Y., Yap, M.G.S., Lee, D.-Y., 2012. Combined in silico modeling and metabolomics analysis to characterize fed-batch CHO cell culture. *Biotechnol. Bioeng.* 109, 1415–29. doi:10.1002/bit.24445
- Shields, R.L., Lai, J., Keck, R., O'Connell, L.Y., Hong, K., Meng, Y.G., Weikert, S.H.A., Presta, L.G., 2002. Lack of fucose on human IgG1 N-linked oligosaccharide improves binding to human FcγRIII and antibody-dependent cellular toxicity. *J. Biol. Chem.* 277, 26733–40. doi:10.1074/jbc.M202069200
- Shinkawa, T., Nakamura, K., Yamane, N., Shoji-Hosaka, E., Kanda, Y., Sakurada, M., Uchida, K., Anazawa, H., Satoh, M., Yamasaki, M., Hanai, N., Shitara, K., 2003. The absence of fucose but not the presence of galactose or bisecting N-acetylglucosamine of human IgG1 complex-type oligosaccharides shows the critical role of enhancing antibody-dependent cellular cytotoxicity. *J. Biol. Chem.* 278, 3466–73. doi:10.1074/jbc.M210665200
- Smedsrød, B., Einarsson, M., 1990. Clearance of tissue plasminogen activator by mannose and galactose receptors in the liver. *Thromb. Haemost.* 63, 60–6.
- Snell, K., Natsumeda, Y., Weber, G., 1987. The modulation of serine metabolism in hepatoma 3924A during different phases of cellular proliferation in culture. *Biochem. J.* 245, 609–12.
- Sokolenco, S., Blondeel, E.J.M.M., Azlah, N., George, B., Schulze, S., Chang, D., Aucoin, M.G., 2014. Profiling convoluted single-dimension proton NMR spectra: a Plackett-Burman approach for assessing quantification error of metabolites in complex mixtures with application to cell culture. *Anal. Chem.* 86, 3330–7. doi:10.1021/ac4033966
- Sokolenco, S., George, S., Wagner, A., Tuladhar, A., Andrich, J.M.S., Aucoin, M.G., 2012. Co-expression vs. co-infection using baculovirus expression vectors in insect cell culture: Benefits and drawbacks. *Biotechnol. Adv.* 30, 766–81. doi:10.1016/j.biotechadv.2012.01.009
- Sokolenco, S., McKay, R., Blondeel, E.J.M., Lewis, M.J., Chang, D., George, B., Aucoin, M.G., 2013. Understanding the variability of compound quantification from targeted profiling metabolomics of 1D-1H-NMR spectra in synthetic mixtures and urine with additional insights on choice of pulse sequences and robotic sampling. *Metabolomics* 9, 887–903. doi:10.1007/s11306-013-0503-3
- Spahn, P.N., Hansen, A.H., Hansen, H.G., Arnsdorf, J., Kildegaard, H.F., Lewis, N.E., 2016. A Markov chain model for N-linked protein glycosylation--towards a low-parameter tool for model-driven glycoengineering. *Metab. Eng.* 33, 52–66. doi:10.1016/j.ymben.2015.10.007



- Spearman, M., Dionne, B., Butler, M., 2011. The Role of Glycosylation in Therapeutic Antibodies, in: Al-Rubeai, M. (Ed.), *Antibody Expression and Production*, Cell Engineering. Springer Netherlands, Dordrecht, pp. 251–292. doi:10.1007/978-94-007-1257-7\_12
- Spiro, R.G., 2002. Protein glycosylation: nature, distribution, enzymatic formation, and disease implications of glycopeptide bonds. *Glycobiology* 12, 43R–56R.
- St Amand, M.M., Radhakrishnan, D., Robinson, A.S., Ogunnaike, B.A., 2014. Identification of manipulated variables for a glycosylation control strategy. *Biotechnol. Bioeng.* 111, 1957–70. doi:10.1002/bit.25251
- Stolfa, G., Smonskey, M.T., Boniface, R., Hachmann, A.-B., Gulde, P., Joshi, A.D., Pierce, A.P., Jacobia, S.J., Campbell, A., 2017. CHO-Omics Review: The Impact of Current and Emerging Technologies on Chinese Hamster Ovary Based Bioproduction. *Biotechnol. J.* 1700227, 1700227. doi:10.1002/biot.201700227
- Surve, T., Gadgil, M., 2015. Manganese increases high mannose glycoform on monoclonal antibody expressed in CHO when glucose is absent or limiting: Implications for use of alternate sugars. *Biotechnol. Prog.* 31, 460–7. doi:10.1002/btpr.2029
- Swinnen, J. V, Brusselmans, K., Verhoeven, G., 2006. Increased lipogenesis in cancer cells: new players, novel targets. *Curr. Opin. Clin. Nutr. Metab. Care* 9, 358–65. doi:10.1097/01.mco.0000232894.28674.30
- Szymanski, C.M., Yao, R., Ewing, C.P., Trust, T.J., Guerry, P., 1999. Evidence for a system of general protein glycosylation in *Campylobacter jejuni*. *Mol. Microbiol.* 32, 1022–30.
- Takeuchi, M., Takasaki, S., Miyazaki, H., Kato, T., Hoshi, S., Kochibe, N., Kobata, A., 1988. Comparative study of the asparagine-linked sugar chains of human erythropoietins purified from urine and the culture medium of recombinant Chinese hamster ovary cells. *J. Biol. Chem.* 263, 3657–63.
- Tao, M.H., Morrison, S.L., 1989. Studies of aglycosylated chimeric mouse-human IgG. Role of carbohydrate in the structure and effector functions mediated by the human IgG constant region. *J. Immunol.* 143, 2595–601.
- Thaysen-Andersen, M., Packer, N.H., 2012. Site-specific glycoproteomics confirms that protein structure dictates formation of N-glycan type, core fucosylation and branching. *Glycobiology* 22, 1440–52. doi:10.1093/glycob/cws110
- Tomiya, N., Ailor, E., Lawrence, S.M., Betenbaugh, M.J., Lee, Y.C., 2001. Determination of nucleotides and sugar nucleotides involved in protein glycosylation by high-performance anion-exchange chromatography: sugar nucleotide contents in cultured insect cells and mammalian cells. *Anal. Biochem.* 293, 129–37. doi:10.1006/abio.2001.5091
- Tsuchiya, N., Endo, T., Matsuta, K., Yoshinoya, S., Aikawa, T., Kosuge, E., Takeuchi, F., Miyamoto, T., Kobata, A., 1989. Effects of galactose depletion from oligosaccharide chains on immunological activities of human IgG. *J. Rheumatol.* 16, 285–90.
- Uldry, M., Ibberson, M., Hosokawa, M., Thorens, B., 2002. GLUT2 is a high affinity glucosamine transporter. *FEBS Lett.* 524, 199–203. doi:10.1016/S0014-5793(02)03058-2
- Umaña, P., Jean-Mairet, J., Moudry, R., Amstutz, H., Bailey, J.E., 1999. Engineered glycoforms of an antineuroblastoma IgG1 with optimized antibody-dependent cellular cytotoxic activity. *Nat. Biotechnol.* 17, 176–80. doi:10.1038/6179
- Urlaub, G., Chasin, L. a, 1980. Isolation of Chinese hamster cell mutants deficient in dihydrofolate reductase activity. *Proc. Natl. Acad. Sci. U. S. A.* 77, 4216–20.
- Valley, U., Nimtz, M., Conradt, H.S., Wagner, R., 1999. Incorporation of ammonium into intracellular

- UDP-activated N-acetylhexosamines and into carbohydrate structures in glycoproteins. *Biotechnol. Bioeng.* 64, 401–17. doi:10.1002/(SICI)1097-0290(19990820)64:4<401::AID-BIT3>3.0.CO;2-M
- Van den Steen, P., Rudd, P.M., Dwek, R. a, Opdenakker, G., 1998. Concepts and principles of O-linked glycosylation. *Crit. Rev. Biochem. Mol. Biol.* 33, 151–208. doi:10.1080/10409239891204198
- van der Valk, J., Brunner, D., De Smet, K., Fex Svenningsen, a, Honegger, P., Knudsen, L.E., Lindl, T., Noraberg, J., Price, a, Scarino, M.L., Gstraunthaler, G., 2010. Optimization of chemically defined cell culture media--replacing fetal bovine serum in mammalian in vitro methods. *Toxicol. In Vitro* 24, 1053–63. doi:10.1016/j.tiv.2010.03.016
- Vidarsson, G., Dekkers, G., Rispens, T., 2014. IgG subclasses and allotypes: From structure to effector functions. *Front. Immunol.* 5, 1–17. doi:10.3389/fimmu.2014.00520
- Wacker, C., Berger, C.N., Girard, P., Meier, R., 2011. Glycosylation profiles of therapeutic antibody pharmaceuticals. *Eur. J. Pharm. Biopharm.* 79, 6–10. doi:10.1016/j.ejpb.2011.06.010
- Wacker, M., Linton, D., Hitchen, P.G., Nita-Lazar, M., Haslam, S.M., North, S.J., Panico, M., Morris, H.R., Dell, A., Wren, B.W., Aebi, M., 2002. N-linked glycosylation in *Campylobacter jejuni* and its functional transfer into *E. coli*. *Science* 298, 1790–3. doi:10.1126/science.298.5599.1790
- Wallace, D.C., 2012. Mitochondria and cancer. *Nat. Rev. Cancer* 12, 685–98. doi:10.1038/nrc3365
- Wang, C., Eufemi, M., Turano, C., Giartosio, A., 1996. Influence of the carbohydrate moiety on the stability of glycoproteins. *Biochemistry* 35, 7299–307. doi:10.1021/bi9517704
- Warburg, O.H., 1956. On the Origin of Cancer Cells. *Oncol.* 9, 75–83.
- Weikert, S., Papac, D., Briggs, J., Cowfer, D., Tom, S., Gawlitzek, M., Lofgren, J., Mehta, S., Chisholm, V., Modi, N., Eppler, S., Carroll, K., Chamow, S., Peers, D., Berman, P., Krummen, L., 1999. Engineering Chinese hamster ovary cells to maximize sialic acid content of recombinant glycoproteins. *Nat. Biotechnol.* 17, 1116–21. doi:10.1038/15104
- Weljie, A.M., Newton, J., Mercier, P., Carlson, E., Slupsky, C.M., 2006. Targeted profiling: quantitative analysis of 1H NMR metabolomics data. *Anal. Chem.* 78, 4430–42. doi:10.1021/ac060209g
- Westermeier, R., 2016. 2D gel-based Proteomics: there's life in the old dog yet. *Arch. Physiol. Biochem.* 122, 236–237. doi:10.1080/13813455.2016.1179766
- Wong, D.C.F., Wong, N.S.C., Goh, J.S.Y., May, L.M., Yap, M.G.S., 2010. Profiling of N-glycosylation gene expression in CHO cell fed-batch cultures. *Biotechnol. Bioeng.* 107, 516–528. doi:10.1002/bit.22828
- Wong, N.S.C., Wati, L., Nissom, P.M., Feng, H.T., Lee, M.M., Yap, M.G.S., 2010. An investigation of intracellular glycosylation activities in CHO cells: effects of nucleotide sugar precursor feeding. *Biotechnol. Bioeng.* 107, 321–36. doi:10.1002/bit.22812
- Wong, N.S.C., Yap, M.G.S., Wang, D.I.C., 2006. Enhancing recombinant glycoprotein sialylation through CMP-sialic acid transporter over expression in Chinese hamster ovary cells. *Biotechnol. Bioeng.* 93, 1005–16. doi:10.1002/bit.20815
- Wright, A., Morrison, S.L., 1998. Effect of C2-associated carbohydrate structure on Ig effector function: studies with chimeric mouse-human IgG1 antibodies in glycosylation mutants of Chinese hamster ovary cells. *J. Immunol.* 160, 3393–402.
- Wright, A., Morrison, S.L., 1994. Effect of altered CH2-associated carbohydrate structure on the functional properties and in vivo fate of chimeric mouse-human immunoglobulin G1. *J Exp Med* 180, 1087–1096. doi:10.1084/jem.180.3.1087
- Wyss, D.F., Wagner, G., 1996. The structural role of sugars in glycoproteins. *Curr. Opin. Biotechnol.* 7, 409–16. doi:10.1016/S0958-1669(96)80116-9

- Xing, Z., Kenty, B., Koyrakh, I., Borys, M., Pan, S.-H., Li, Z.J., 2011. Optimizing amino acid composition of CHO cell culture media for a fusion protein production. *Process Biochem.* 46, 1423–1429. doi:10.1016/j.procbio.2011.03.014
- Xu, X., Nagarajan, H., Lewis, N.E., Pan, S., Cai, Z., Liu, X., Chen, W., Xie, M., Wang, W., Hammond, S., Andersen, M.R., Neff, N., Passarelli, B., Koh, W., Fan, H.C., Wang, J., Gui, Y., Lee, K.H., Betenbaugh, M.J., Quake, S.R., Famili, I., Palsson, B.O., Wang, J., 2011. The genomic sequence of the Chinese hamster ovary (CHO)-K1 cell line. *Nat. Biotechnol.* 29, 735–41. doi:10.1038/nbt.1932
- Yamada, K., Shibata, H., Suzuki, K., Citterio, D., 2017. Toward practical application of paper-based microfluidics for medical diagnostics: state-of-the-art and challenges. *Lab Chip* 17, 1206–1249. doi:10.1039/c6lc01577h
- Yamane-Ohnuki, N., Kinoshita, S., Inoue-Urakubo, M., Kusunoki, M., Iida, S., Nakano, R., Wakitani, M., Niwa, R., Sakurada, M., Uchida, K., Shitara, K., Satoh, M., 2004. Establishment of FUT8 knockout Chinese hamster ovary cells: an ideal host cell line for producing completely defucosylated antibodies with enhanced antibody-dependent cellular cytotoxicity. *Biotechnol. Bioeng.* 87, 614–22. doi:10.1002/bit.20151
- Yang, M., Butler, M., 2002. Effects of ammonia and glucosamine on the heterogeneity of erythropoietin glycoforms. *Biotechnol. Prog.* 18, 129–38. doi:10.1021/bp0101334
- Yi, L., Dong, N., Yun, Y., Deng, B., Ren, D., Liu, S., Liang, Y., 2016. Chemometric methods in data processing of mass spectrometry-based metabolomics: A review. *Anal. Chim. Acta* 914, 17–34. doi:10.1016/j.aca.2016.02.001
- Zagari, F., Jordan, M., Stettler, M., Broly, H., Wurm, F.M., 2013a. Lactate metabolism shift in CHO cell culture: the role of mitochondrial oxidative activity. *N. Biotechnol.* 30, 238–45. doi:10.1016/j.nbt.2012.05.021
- Zagari, F., Stettler, M., Baldi, L., 2013b. High expression of the aspartate-glutamate carrier Aralar1 favors lactate consumption in CHO cell culture. *Pharm. ...* 1, 19–27.
- Zang, L., Frenkel, R., Simeone, J., Lanan, M., Byers, M., Lyubarskaya, Y., 2011. Metabolomics Profiling of Cell Culture Media Leading to the Identification of Riboflavin Photosensitized Degradation of Tryptophan Causing Slow Growth in Cell Culture. *Anal. Chem.* 83, 5422–5430. doi:10.1021/ac2009492
- Zanghi, J.A., Mendoza, T.P., Schmelzer, A.E., Knop, R.H., Miller, W.M., 1998. Role of nucleotide sugar pools in the inhibition of NCAM polysialylation by ammonia. *Biotechnol. Prog.* 14, 834–44. doi:10.1021/bp9800945
- Zhang, J., Liu, X., Bell, A., To, R., Baral, T.N., Azizi, A., Li, J., Cass, B., Durocher, Y., 2009. Transient expression and purification of chimeric heavy chain antibodies. *Protein Expr. Purif.* 65, 77–82. doi:10.1016/j.pep.2008.10.011
- Zhang, L., Elias, J.E., 2017. Relative Protein Quantification Using Tandem Mass Tag Mass Spectrometry. *Methods Mol. Biol.* 1550, 185–198. doi:10.1007/978-1-4939-6747-6\_14
- Zhang, X., Lok, S.H., Kon, O.L., 1998. Stable expression of human alpha-2,6-sialyltransferase in Chinese hamster ovary cells: functional consequences for human erythropoietin expression and bioactivity. *Biochim. Biophys. Acta* 1425, 441–52.
- Zielinska, D.F., Gnad, F., Wiśniewski, J.R., Mann, M., 2010. Precision mapping of an in vivo N-glycoproteome reveals rigid topological and sequence constraints. *Cell* 141, 897–907. doi:10.1016/j.cell.2010.04.012

## Appendix A – Chapter 3 Supplementary Data

Table 15 – Expanded 2D-DIGE proteomics data of CHO cells expressing EG2-hFc

Protein Name	Short Name	Spot ID	Accession ID	PEAKS Score	<i>p</i> -value	MW* (kDa)	pI*	% Coverage	# Matched Peptides	Fold Change	Biological Process
<b>Chaperones &amp; Protein Synthesis</b>											
Heat shock 75 kDa protein	Trap1	364	EGV93626	99.2	2.08E-03	80.3	6.64	43	22	1.05	Chaperone – protein folding
Heat shock 70 kDa protein 9	Grp75	372	EGW06687	99.2	1.32E-03	65.8	5.83	57	29	1.11	Chaperone – protein folding
		359		98.2	9.76E-04			7	3	1.08	
		369		99.2	9.66E-03			59	31	1.05	
Heat shock 60 kDa protein	Hspd1	465	EGW00783	99.2	7.70E-03	56.5	6.90	52	19	-1.06	Chaperone – protein folding
Heat shock protein HSP 90-alpha	Hsp90aa1	929	EGV94858	98.9	3.84E-03	38.1	4.58	22	5	-1.38	Chaperone – protein folding
Serpin H1	Serpinh1	635	EGW02226	99.2	4.22E-03	46.6	8.74	38	12	-1.14	Chaperone – collagen folding
Endoplasmic	GRP94	841	EGW09701	99.1	3.41E-04	92.6	4.74	15	8	-1.57	Chaperone – protein processing and transport
60S Acidic Ribosomal protein P0	Rplp0	893	EGV93157	99.2	6.40E-03	29.9	8.68	38	7	1.20	Protein synthesis
Protein disulfide-isomerase A6	Pdia6	1026	EGW08481	99.0	1.47E-03	28.4	4.80	27	5	-1.22	Chaperone – protein folding
<b>Structural Proteins</b>											
B-Actin	Actb	726	EGW06240	99.1	2.15E-03	41.7	5.29	29	7	-1.16	Cytoskeleton component
		1028		99.1	9.82E-03			27	5	-1.14	
		1228		98.9	6.74E-03			26	5	-1.25	
		837		99.1	9.79E-03			25	7	-1.08	
Vimentin	Vim	1202	EGW02055	99.2	1.56E-03	53.7	5.05	38	9	-1.31	Intermediate filament, cell integrity
		1208		99.2	3.34E-03			30	12	-1.41	

Protein Name	Short Name	Spot ID	Accession ID	PEAKS Score	p-value	MW* (kDa)	pI*	% Coverage	# Matched Peptides	Fold Change	Biological Process
		1210		99.2	4.04E-05			41	12	-1.39	
		1215		99.2	1.42E-04			34	7	-1.31	
		1301		98.6	2.35E-03			8	4	-1.32	
		1522		98.2	2.46E-03			17	5	-1.46	
		544		99.2	1.02E-02			62	25	-1.12	
Lamin B1	Lmnb1	379	EGV92912	99.1	5.64E-03	55.0	4.99	33	11	-1.7	Nuclear envelope framework
Lamin A	Lmna	410	EGW07066	99.2	6.97E-03	64.0	7.75	60	33	1.08	Nuclear envelope framework
		428		99.2	2.13E-03			64	39	1.10	
Calcium-binding protein p22	Chp	1304	EGV97270	98.7	8.49E-03	22.5	4.97	25	4	-1.18	Na <sup>+</sup> /H <sup>+</sup> ion pump regulation; intracellular pH, cytoskeletal organization
<b>Metabolic Enzymes</b>											
Aconitate hydratase	Aco2	313	EGW13953	98.8	6.07E-03	85.4	8.07	10	4	-1.12	TCA cycle
Aldehyde dehydrogenase	Aldh	543	EGW07431	99.2	2.49E-03	45.9	5.55	44	15	1.11	Oxidation of aldehydes to carboxylic acids
		545		99.2	5.96E-03			59	20	1.14	
		549		99.2	4.45E-03			44	16	1.10	
Acyl-coenzyme A thioesterase 2	Acot2	651	EGW01631	99.1	4.19E-03	49.8	8.27	25	9	1.21	Lipid metabolism
Citrate synthase	Cs	679	EGW12503	99.1	2.70E-05	51.7	8.70	32	5	1.99	TCA cycle
		663		99.0	6.85E-05			22	5	1.55	
Aspartate aminotransferase	Ast	705	EGW01755	99.1	3.92E-03	47.4	9.13	23	7	1.21	Anaplerotic TCA metabolism
3-hydroxyacyl-CoA dehydrogenase type 2	Hsd17b10	1234	EGW02330	99.2	5.68E-03	27.2	7.70	72	12	1.11	Oxidation of fatty acids, alcohols and steroids
Methylenetetrahydrofolate dehydrogenase	Mthfd11	234	EGV95936	99.1	7.31E-03	105.4	7.02	23	15	1.09	Tetrahydrofolate (THF) cycle
		187		99.1	7.71E-04						
		181		99.2	1.02E-02						

Protein Name	Short Name	Spot ID	Accession ID	PEAKS Score	p-value	MW* (kDa)	pI*	% Coverage	# Matched Peptides	Fold Change	Biological Process
Procollagen-lysine, 2-oxoglutarate 5-dioxygenase 3	Plod3	316	EGW01863	98.9	9.92E-03	37.7	5.88	20	4	-1.06	Hydroxylation of lysyl residues in collagen-like peptides
Dihydrolipoyl dehydrogenase	Dld	524	EGV93120	99.2	6.31E-04	54.1	7.96	30	12	1.07	Catabolism of branch chain amino acids
		529		99.2	2.00E-03			44	14	1.06	
3-hydroxyisobutyrate dehydrogenase	Hibadh	1027	EGW08863	99.1	4.20E-03	31.7	5.17	33	6	1.09	Amino acid catabolism
Glycerol-3-phosphate dehydrogenase	Gpd2	660	EGW05701	99.2	2.79E-03	80.7	5.92	34	17	1.32	Carbohydrate and lipid metabolism
<b>Apoptosis and Cell Proliferation</b>											
Proliferating cell nuclear antigen	Pcna	959	EGV92404	99.1	6.00E-03	28.8	4.57	41	9	-1.20	Processivity factor eukaryotic DNA polymerase
Histone H2A type 1	Hist1h2ab	1779	EGV96120	98.9	1.35E-04	28.5	11.04	24	4	-1.25	Regulation of transcription, DNA repair, DNA replication, and chromosomal stability
DNA-directed RNA polymerase I, II, and III subunit RPABC1	Polr2e	1159	EGV99483	98.3	1.86E-03	25.4	5.52	27	3	1.17	DNA transcription
Prohibitin	Phb	245	EGW01773	98.9	2.44E-03	29.8	5.57	21	4	1.12	Regulation of proliferation, inhibits DNA synthesis
Programmed cell death 6	Pcdc6	1505	EGW09040	99.0	1.10E-03	25.5	5.56	27	5	1.44	Induction of apoptosis by extracellular signal
<b>Energy Metabolism</b>											
SPRY domain-containing protein 4	Spryd4	1299	EGW12495	98.9	3.17E-04	23.1	8.85	30	5	-1.20	Uncharacterized
ATP-binding cassette sub-family G, member 3	Abcd3	918	EGV92982	99.1	1.77E-04	69.6	5.43	13	6	1.05	Peptide transporter
NADH dehydrogenase	Ndufv1	566	EGW12368	99.1	4.61E-03	50.6	7.53	21	8	1.12	Oxidative

Protein Name	Short Name	Spot ID	Accession ID	PEAKS Score	<i>p</i> -value	MW* (kDa)	pI*	% Coverage	# Matched Peptides	Fold Change	Biological Process
	Ndufs3	1138	EGW03953	99.1	1.03E-02	30.1	7.78	34	7	1.03	phosphorylation Oxidative
ATP Synthase subunit beta	Atp5b	575	EGW12490	99.2	4.63E-04	56.4	5.18	45	17	-1.12	phosphorylation ATP synthesis

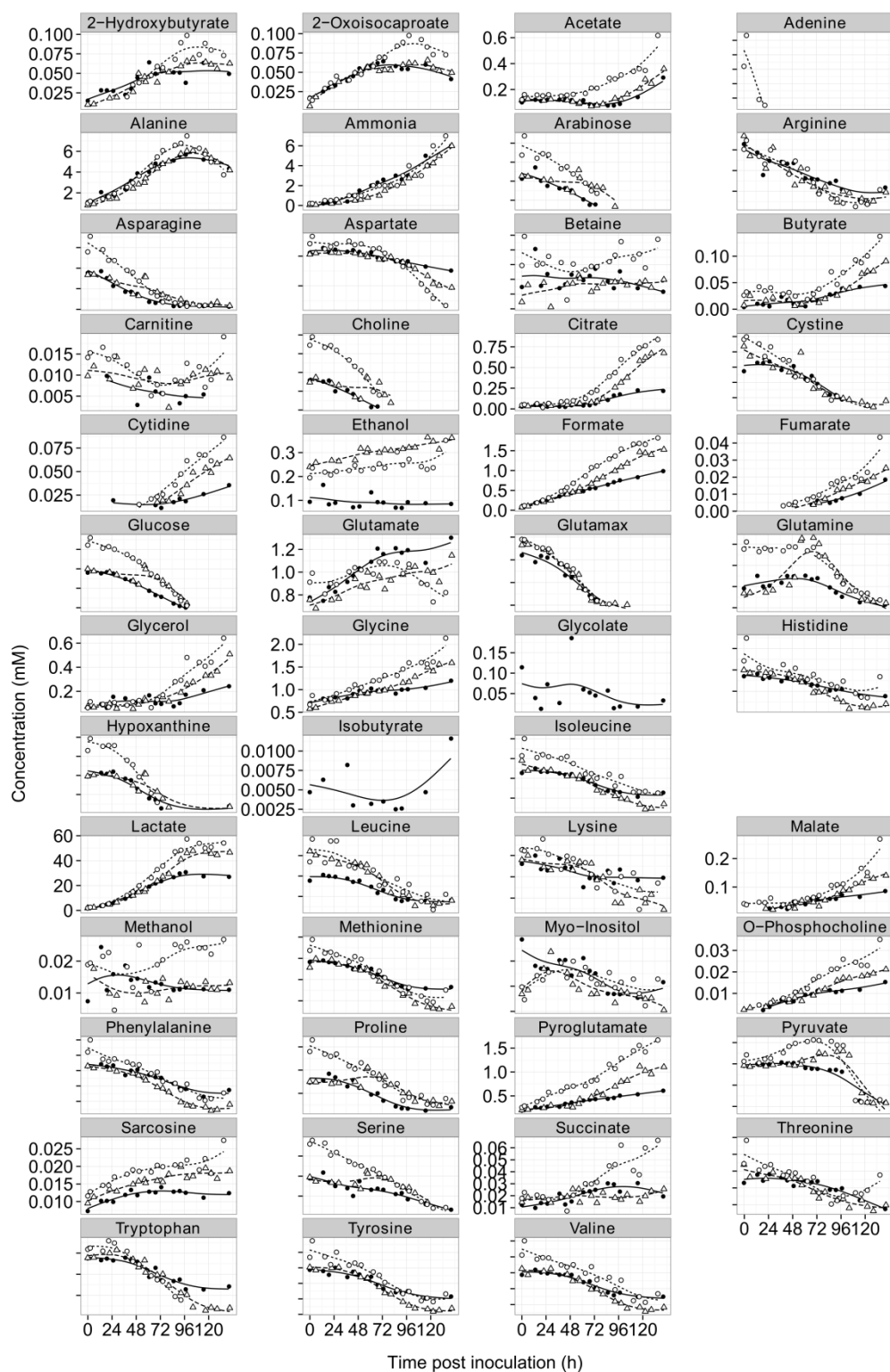
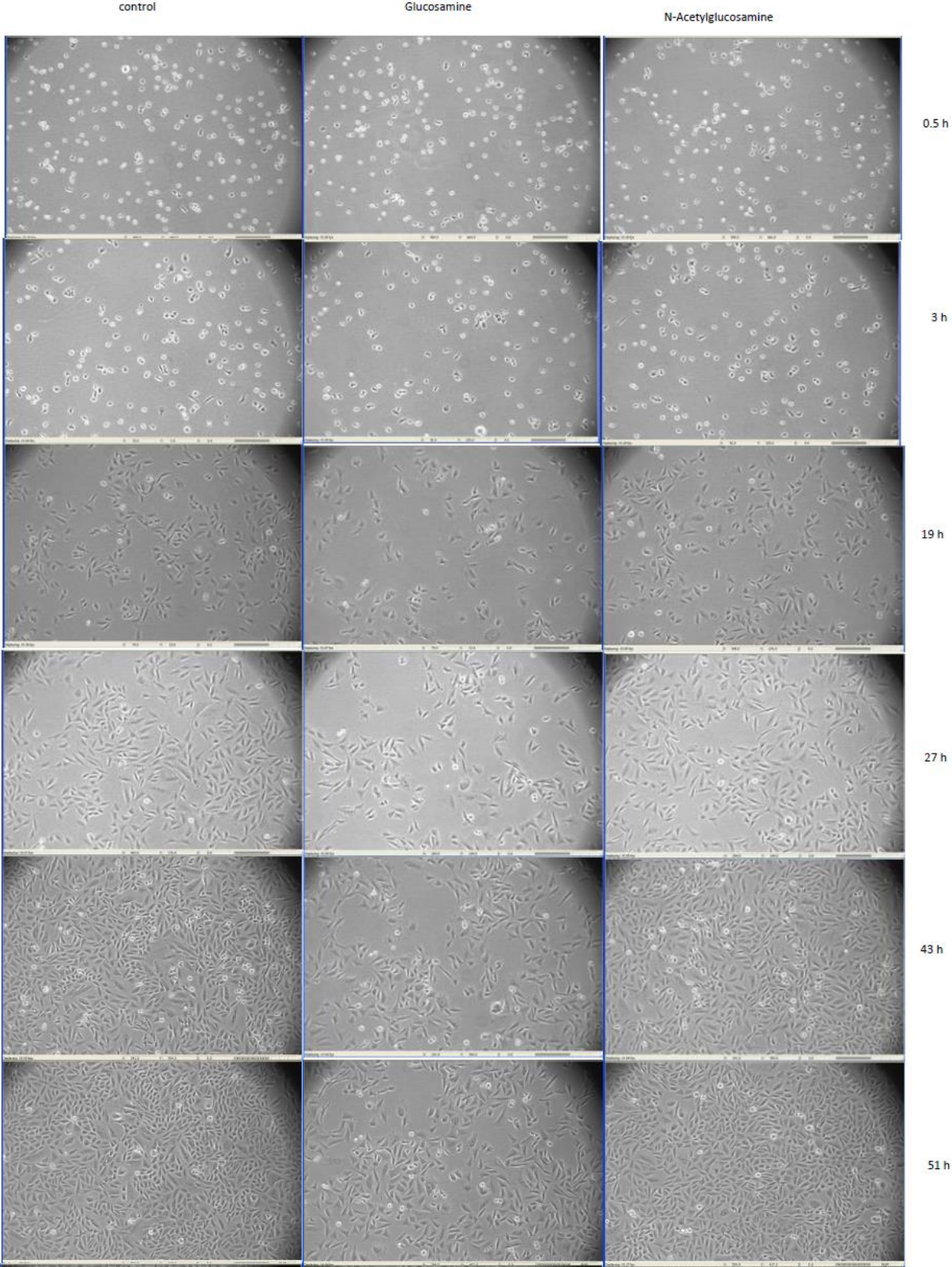
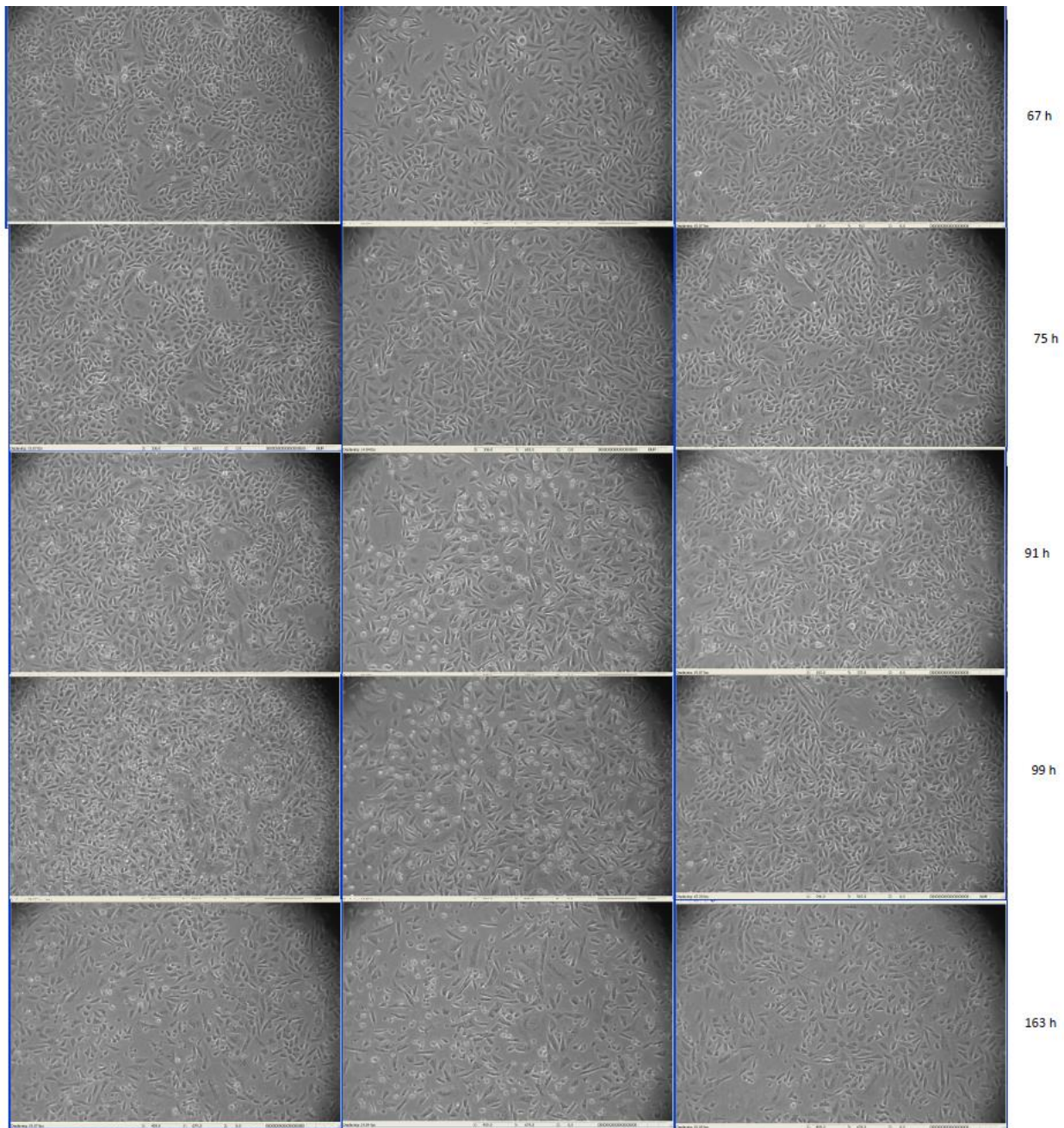


Figure 35 – Complete set of nutrients and metabolites tracked by 1D-1H-NMR under normal culture conditions (solid lines) and following additional supplementation (dashed lines) in batch (circle) and fed-batch (triangle)



# Appendix B – Chapter 4 Supplementary Data





**Figure 36 – Time course imaging of cell growth under GlcN and GlcNAc supplementation conditions**

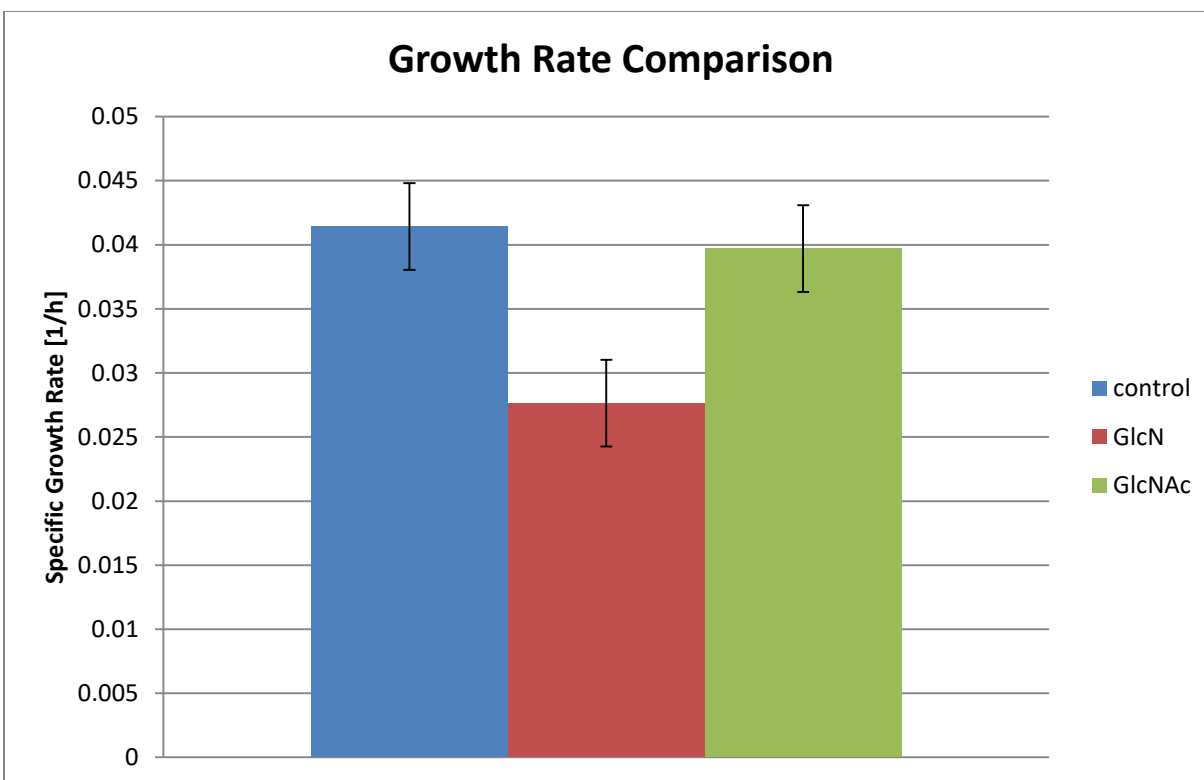


**Figure 37 – Growth rate comparison of CHO-K1-CC1-61 cells supplemented with 7.5 mM GlcN & GlcNAc, demonstrating that the negative growth effect of glucosamine supplementation, as well as the lack of negative growth effect from GlcNAc supplementation, is independent of the CHO<sup>BRI</sup> cell line utilized in Chapter 4.**

Cells of the cell line CHO-K1 CCI-61 were grown adherently in vent capped flasks in F-12 Kaighn’s modification medium (GE LifeSciences), and supplemented with 10 % FBS (Gibco Life technologies). An experiment was conducted in which the medium was supplemented with either 7.5 mM Glucosamine (GlcN) or 7.5 mM N-Acetylglucosamine (GlcNAc), with two flasks per condition; the control contained only the regular medium. To observe the cell growth two pictures of two different areas were taken per flask twice a day and cells on the pictures were counted manually. For time points 19 h, 27 h and 43 h the natural logarithm of the cell number was plotted against the time and the growth rate estimated from the slope of a linear fit. The graph shows the average growth rates estimated per condition (n=4). Errors with a 95 % confidence interval were calculated from the average variance of all slopes. Time points 19 to 43 hours were selected because the cells experienced a lag phase at the beginning of the cultivation.

The results of this growth rate comparison in CHO-K1 CCl-61, an adherent non-producing culture match the results observed with the CHO<sup>BRI</sup> cells expressing EG2-hFc camelid chimeric monoclonal antibody reported in this work. Therefore, the negative growth effect of glucosamine supplementation, as well as the lack of negative growth effect from GlcNAc supplementation is independent of the cell line utilized in Chapter 3.

## Appendix C – Chapter 6 Supplementary Data

**Table 16 – Comparison of glycoform shifts and differences between reported experiments for the supplementation of glucosamine (GlcN), its acetylated form acetylglucosamine (GlcNAc), and the nucleoside uridine (Urd), towards expanding intracellular nucleotide-sugar pools of UDP-GlcNAc in cultured mammalian cells to affect N-linked glycoforms of recombinant glycoproteins. N-linked glycoforms of recombinant glycoproteins. Glycoform shifts are reported as %-shifts in indices of mannosylation (MI), antennarity (AI), fucosylation (FI), galactosylation (GI), and sialylation (SI) (as per Equations 1-5, Figure 31) relative to reported control culture glycoforms. Experimental differences reported include: Supplementation cocktails and concentrations with multiple bullet-points representing separate flask or bioreactor conditions; The cell line utilized and the lineage of that cell line where reported; The protein being expressed and whether it is a mutant variant or fusion; The bioprocess scale, time of supplementation, and time of harvest; The amount of glutamine (Gln) utilized in the growth medium.**

Supplement	Cell	Protein	Fermentation Timeline	Gln (mM)	Control Glycoform					Affected Glycoform					Effect	Researchers
					MI (%)	AI (%)	FI (%)	GI (%)	SI (%)	MI (%)	AI (%)	FI (%)	GI (%)	SI (%)		
<ul style="list-style-type: none"> <li>▪ 20mM GlcNAc</li> <li>▪ 0.5mM Urd</li> </ul>	CHO (DG44)	IgG	<ul style="list-style-type: none"> <li>▪ Bioreactor, fedbatch</li> <li>▪ 1L</li> <li>▪ Addition 48h</li> <li>▪ Harvest 336h</li> </ul>	8	5.6	38	93.4	13.8	0.5	5.5	38	93.8	10.5	0.5	<ul style="list-style-type: none"> <li>▪ Reduced glycan complexity to favour G0 and FG0 glycoforms</li> <li>▪ Reduced galactosylation</li> </ul>	(Kildegaard et al., 2015)
					5.8	38	93.1	14.4	0.5							
<ul style="list-style-type: none"> <li>▪ 7.5mM GlcN</li> <li>▪ 2.5 - 10mM GlcNAc</li> </ul>	CHO (Dukx)	IgG HCAB	<ul style="list-style-type: none"> <li>▪ Flasks</li> <li>▪ 125mL</li> <li>▪ Addition 50h</li> <li>▪ Harvest 144h-168h</li> </ul>	5	0.2	41.2	83.0	53.8	13.0	1.6	40.4	70.8	25.9	7.2	<ul style="list-style-type: none"> <li>▪ Reduced glycan complexity to favour G0 and FG0 glycoforms – both GlcN &amp; GlcNAc supplementation</li> <li>▪ ~50% drop in growth rate with GlcN supplementation</li> <li>▪ &lt;5% drop in growth rate with GlcNAc supplementation</li> <li>proportional increase in UDP-GlcNAc pool up to 2x with GlcNAc supplementation</li> </ul>	(Blondeel et al., 2015)
					0.1	42.6	84.5	69.4	17.4	0.1	42.0	79.8	48.2	16.6		
					0.2					0.2	41.7	77.5	39.0	14.7		
					0.2					0.2	41.7	71.9	34.8	13.5		
					0.3					0.3	41.0	67.7	30.5	11.5		

Supplement	Cell	Protein	Fermentation Timeline	Gln (mM)	Control Glycoform					Affected Glycoform					Effect	Researchers
					MI (%)	AI (%)	FI (%)	GI (%)	SI (%)	MI (%)	AI (%)	FI (%)	GI (%)	SI (%)		
▪ 10mM GlcN	NS0 (GS)	IgG	▪ Flasks ▪ 500mL ▪ Addition 48h ▪ Harvest 96h	0.4 (GS)	12.8	34.9	100	16	0	10.6	35.8	100	7	0	▪ 17x UDP HexNAc ▪ -56% Galactosylation ▪ -63% UDP-Hex ▪ Reduced growth	(Hills et al., 2001)
▪ 10mM GlcN	CHO (K1)	EPO	▪ Flasks ▪ 250mL ▪ Addition 0h ▪ Harvest day 4-5	-	-	87	-	-	54 <sup>16</sup>	-	73	-	-	32	▪ 18.5x UDP-GlcNAc ▪ Increased glycan heterogeneity ▪ -22% tetrasialylation	(Yang and Butler, 2002)
▪ 10mM GlcN; free of Gln	BHK	IL-2	▪ Perfusion 2.5 L ▪ Addition: day 21 ▪ Harvest: days 26-28 and 29-30	0	-	44	-	-	-	-	50	-	-	-	▪ Greater antennarity, but lower complexity of glycans ▪ 3x UDP-HexNAc ▪ Greater proportion of monosialylation with GlcN ▪ +58% sialylation in std culture without glutamine	(Gawlitze et al., 1998)
▪ 10mM GlcN + 2mM Urd	CHO (GS) NS0 (GS)	TIMP-1	▪ Flasks ▪ 1000mL ▪ Addition 24h ▪ Harvest 48h	0.4 (GS)	-	50.2	-	-	47.8	-	57.4	-	-	39.7	▪ 58x UDP-HexNAc ▪ 8x UDP-Hex ▪ +9% antennarity ▪ -8% sialylation	(Baker et al., 2001)
▪ 10mM GlcN + 2mM Urd	BHK	IL-2 <sup>17</sup>	▪ Perfusion 2.5 L ▪ Addition 10d ▪ Harvest 14d	0	-	48	-	-	86	-	52	-	-	83	▪ 12x UDP-GlcNAc ▪ 5x UTP ▪ Rise antennarity	(Grammatikos et al., 1998)
▪ 10mM GlcN ▪ +5mM Urd	CHO (Dukx)	IFN- $\gamma$	▪ Flasks (n=1) ▪ 1000mL ▪ Addition 48h ▪ Harvest 96h	4	26	34	-	91	29	29	34	-	90	68	▪ Reduced growth ▪ +28% sialylation ▪ 6-15x increase UDP-HexNAc	(N. S. C. Wong et al., 2010)

<sup>16</sup> Measured as a proportion of tetra-sialylated glycans

<sup>17</sup> Modified IL-2 variant featuring an artificial N-glycan site

Supplement	Cell	Protein	Fermentation Timeline	Gln (mM)	Control Glycoform					Affected Glycoform					Effect	Researchers
					MI (%)	AI (%)	FI (%)	GI (%)	SI (%)	MI (%)	AI (%)	FI (%)	GI (%)	SI (%)		
<ul style="list-style-type: none"> <li>▪ 3.5 &amp; 17.5mM GlcN + 1mM Urd</li> </ul>	CHO SCLC	NCAM	<ul style="list-style-type: none"> <li>▪ 6 &amp; 24-well plates</li> <li>▪ Addition 12-18h</li> <li>▪ Harvest 128h</li> </ul>	6		-		-	-		-		-	-	<ul style="list-style-type: none"> <li>▪ 25x UDP GlcNAc</li> <li>▪ Reduced growth</li> <li>▪ -90% polysialylation</li> </ul>	(Zanghi et al., 1998)
<ul style="list-style-type: none"> <li>▪ 1-10mM Urd</li> </ul>	CHO (Dukx)	IFN- $\gamma$	<ul style="list-style-type: none"> <li>▪ Flasks</li> <li>▪ 100mL</li> </ul>	3		-		-	-		-		-	-	<ul style="list-style-type: none"> <li>▪ 18.5x UDP-GlcNAc</li> <li>▪ Increased glycan heterogeneity</li> <li>▪ -22% tetrasialylation</li> </ul>	(Nyberg et al., 1999)
<ul style="list-style-type: none"> <li>▪ 0.5mM Urd</li> </ul>	RH	N/A	<ul style="list-style-type: none"> <li>▪ Culture dish</li> <li>▪ 3 mL</li> <li>▪ Addition 16h</li> <li>▪ Harvest 24h</li> </ul>	2.4		-		-	-		-		-	-	<ul style="list-style-type: none"> <li>▪ 58x UDP-HexNAc</li> <li>▪ 8x UDP-Hex</li> <li>▪ +9% antennarity</li> <li>▪ -8% sialylation</li> </ul>	(Pels Rijcken et al., 1995b)

**Table 17 – Comparison of glycoform shifts and differences between reported experiments for the supplementation of galactose (Gal), the nucleoside uridine (Urd), and the enzyme cofactor manganese (Mn<sup>2+</sup>), towards expanding intracellular nucleotide-sugar pools of UDP-galactose in cultured mammalian cells and affecting. Glycoform shifts are reported as %-shifts in indices of mannosylation (MI), antennarity (AI), fucoylation (FI), galactosylation (GI), and sialylation (SI) (as per Equations 1-5, Figure 31) relative to reported control culture glycoforms. Experimental differences reported include: Supplementation cocktails and concentrations with multiple bullet-points representing separate flask or bioreactor conditions; The cell line utilized and the lineage of that cell line where reported; The protein being expressed and whether it is a mutant variant or fusion; The bioprocess scale, time of supplementation, and time of harvest; The amount of glutamine (Gln) utilized in the growth medium.**

Supplement	Cell	Protein	Fermentation Timeline	Gln (mM)	Control Glycoform					Affected Glycoform					Effect	Researchers
					MI (%)	AI (%)	FI (%)	GI (%)	SI (%)	MI (%)	AI (%)	FI (%)	GI (%)	SI (%)		
▪ 20mM Gal	CHO (DG44)	IgG	▪ Fed-batch bioreactor ▪ 1L ▪ Addition 48h ▪ Harvest 336h	8	5.6	38	93.4	13.8	0.5	5.9	38	93.1	25.5	0.3	▪ +12% galactosylation ▪ No reduction to cell growth or productivity	(Kildegaard et al., 2015)
▪ 10mM Gal	NS0 (GS)	IgG	▪ Flasks ▪ 500mL ▪ Addition 48h ▪ Harvest 96h	0.4 (GS)	12.8	34.9	100	16	0	15.3	33.9	100	17	0	▪ 5x UDP-Gal ▪ +6% galactosylation	(Hills et al., 2001)
▪ 10mM Gal ▪ 20mM Gal ▪ 40mM Gal	CHO (GS)	Fc-TNF fusion	▪ Fed-batch bioreactor ▪ 2L ▪ Addition 120h ▪ Harvest 288h	GS	3.9	38	66	46	28	3.3	38	68	58	32	▪ +22% galactosylation ▪ +14% sialylation ▪ No negative growth effects ▪ Glycan distribution scaled well to 200L bioreactor	(Liu et al., 2015)
▪ 20mM galactose	CHO	IL-4/13	▪ Batch bioreactor ▪ 1L ▪ Addition 0h ▪ Harvest 112h	2	-	-	-	-	-	-	-	-	-	-	▪ No notable effects to sialylation or gene expression	(Clark et al., 2005)
▪ 10mM Gal ▪ +5mM Urd	CHO (Dukx)	IFN- $\gamma$	▪ Flasks (n=1) <sup>18</sup> ▪ 1000mL ▪ Addition 48h ▪ Harvest 96h	4	26	34	-	91	34	26	35	-	94	46	▪ 20x UDP-Gal ▪ +12% sialylation	(N. S. C. Wong et al., 2010)

<sup>18</sup> Only a single flask for each experiment, and only one control flask appears to have been used.



Supplement	Cell	Protein	Fermentation Timeline	Gln (mM)	Control Glycoform					Affected Glycoform					Effect	Researchers
					MI (%)	AI (%)	FI (%)	GI (%)	SI (%)	MI (%)	AI (%)	FI (%)	GI (%)	SI (%)		
<ul style="list-style-type: none"> <li>▪ 0.4, 4, 40µM Mn<sup>2+</sup></li> </ul>	CHO (dhfr-)	EPO	<ul style="list-style-type: none"> <li>▪ Roller bottles</li> <li>▪ 850cm<sup>2</sup></li> <li>▪ Media replaced every 7 days</li> <li>▪ Addition</li> <li>▪ Harvest 19d</li> </ul>	15	-	-	-	-	-	-	-	-	-	-	<ul style="list-style-type: none"> <li>▪ Reduced titres at 40µM Mn<sup>2+</sup> feed</li> <li>▪ UDP-Gal pools unchanged</li> <li>▪ Improved galactosylation and sialylation</li> </ul>	(Crowell et al., 2007)
<ul style="list-style-type: none"> <li>▪ 10, 20, 40mM Gal</li> <li>▪ 17-68mg/L Mn<sup>2+</sup></li> </ul>	CHO S	FII	<ul style="list-style-type: none"> <li>▪ Flasks</li> <li>▪ Addition 48h</li> <li>▪ Harvest 144h</li> </ul>	-	-	-	-	75	17	-	-	-	96	15	<ul style="list-style-type: none"> <li>▪ +26% sialylation from galactose addition</li> <li>▪ +30% sialylation from addition of MnSO<sub>4</sub></li> <li>▪ Temperature-shift resulted in similar sialylation improvement for final process</li> </ul>	(Lee et al., 2017)
<ul style="list-style-type: none"> <li>▪ 20mM Gal +4mM Urd +8µM Mn<sup>2+</sup></li> </ul>	CHO (Dukx) (DP12)	IgG HCAb mAb	<ul style="list-style-type: none"> <li>▪ Flasks</li> <li>▪ 250mL</li> <li>▪ Addition 0h</li> <li>▪ Harvest 72h</li> </ul>	-	-	-	-	73	-	-	-	-	83	-	<ul style="list-style-type: none"> <li>▪ Two CHO cell lines producing two IgGs; UMG supplementation increased GI in both cases<sup>19</sup></li> </ul>	(Liu et al., 2014)
<ul style="list-style-type: none"> <li>▪ 100mM Gal</li> <li>▪ 40µM Mn<sup>2+</sup></li> <li>▪ 100mM Gal + 40µM Mn<sup>2+</sup></li> </ul>	CHO (K1)	IgG	<ul style="list-style-type: none"> <li>▪ Flasks</li> <li>▪ 250mL</li> <li>▪ Addition 0h</li> <li>▪ Harvest 168h</li> </ul>	4	5.2	36	78	18	0	8.0	34	74	27	0	<ul style="list-style-type: none"> <li>▪ +9% galactosylation</li> <li>▪ -31% fucosylation and +21% high-mannose glycans for Mn+Gal</li> <li>▪ -30% fucosylation and +14% high-mannose glycans for Mn alone</li> <li>▪ 9x UDP-Gal pool</li> <li>▪ Increased expression of β-Gal II, III, IV and UDP-GalT transcripts</li> </ul>	(St Amand et al., 2014)

<sup>19</sup> Elevated GI observed for chimeric HCAb compared to commercial IgGs attributed to Fc region mutation

Supplement	Cell	Protein	Fermentation Timeline	Gln (mM)	Control Glycoform					Affected Glycoform					Effect	Researchers
					MI (%)	AI (%)	FI (%)	GI (%)	SI (%)	MI (%)	AI (%)	FI (%)	GI (%)	SI (%)		
<ul style="list-style-type: none"> <li>▪ 4µM Mn<sup>2+</sup></li> <li>▪ 16µM Mn<sup>2+</sup></li> <li>▪ 30mM Gal<sup>20</sup></li> <li>▪ +4µM Mn<sup>2+</sup></li> <li>▪ +16µM Mn<sup>2+</sup></li> </ul>	CHO (DG44)	IgG	<ul style="list-style-type: none"> <li>▪ Flasks</li> <li>▪ 100mL</li> <li>▪ Addition 0h</li> <li>▪ Harvest 72h</li> </ul>	8	0.7	40	91	36	0.0	0.9	40	90	38	0.0	<ul style="list-style-type: none"> <li>▪ -30-50% IgG when Replacing /lowering Glc or matching Gal</li> <li>▪ +11% galactosylation</li> <li>▪ -5% fucosylation with 16µM Mn<sup>2+</sup></li> </ul>	(Surve and Gadgil, 2015)
<ul style="list-style-type: none"> <li>▪ 5-100mM Gal</li> <li>▪ +1-20mM Urd</li> <li>▪ +2-40µM Mn<sup>2+</sup></li> <li>▪ Factors: <sup>21</sup> 0,1,2,3,4,8, 12,16,20</li> <li>▪ Factors: 0,8,12</li> </ul>	(2) CHO (GS)	IgG	<ul style="list-style-type: none"> <li>▪ Fed-batch bioreactor</li> <li>▪ 2L</li> <li>▪ Addition 0h</li> <li>▪ Harvest 360h</li> </ul>	GS	1.2	40	97	2.9	3.5	0.9	40	98	10	2.0	<ul style="list-style-type: none"> <li>▪ +20% galactosylation for 1st cell line at 100mM Gal</li> <li>▪ +24% galactosylation for 2<sup>nd</sup> cell line at 40mM Gal</li> <li>▪ Glycan distribution scaled well to 100L and 1000L bioreactors</li> </ul>	(Gramer et al., 2011)
<ul style="list-style-type: none"> <li>▪ 2.5-100mM Gal<sup>22</sup></li> <li>▪ +0.5-20mM Urd</li> <li>▪ +1-40µM Mn<sup>2+</sup></li> </ul>	(2) CHO (GS)	IgG	<ul style="list-style-type: none"> <li>▪ Flasks</li> <li>▪ 125mL</li> <li>▪ Addition 72h</li> <li>▪ Harvest 192h</li> </ul>	GS	0	40	97	32	6.3	2.7	39	97	53	12	<ul style="list-style-type: none"> <li>▪ +21-24% galactosylation</li> <li>▪ +1.5-5% sialylation</li> <li>▪ Best overall IVCC, MAb titre and galactosylation results with low Mn<sup>2+</sup>/Urd and high Gal condition</li> <li>▪ Mab galactosylation correlated well with cell-surface Gal</li> </ul>	(Grainger and James, 2013)

<sup>20</sup> Additional experiments changed the main carbon source to fructose, glucose-free (only gal), and low-glucose delivered from a hydrogel for slow release.

<sup>21</sup> Galactose, uridine and manganese (Mn<sup>2+</sup>) fed in ratios of 5:1:0.002 mM (UMG cocktail) for two CHO-K1SV cell lines expressing two separate IgGs under GS expression system

<sup>22</sup> Face-centred DOE design for main-effects modeling of UMG cocktail developed by Gramer et al. cocktail, tested on two CHO-K1SV cell lines stably expressing IgG<sub>4</sub> under GS expression system (Gramer et al., 2011)

**Table 18 – Comparison of glycoform shifts and differences between reported experiments for the supplementation of the acetylated amine sugar acetyl-mannosamine (ManNAc), and the nucleoside cytidine (Cyt), towards expanding intracellular nucleotide-sugar pools of CMP-NeuAc in cultured mammalian cells and affecting N-linked glycoforms of recombinant glycoproteins. N-linked glycoforms of recombinant glycoproteins. Glycoform shifts are reported as %-shifts in indices of mannosylation (MI), antennarity (AI), fucosylation (FI), galactosylation (GI), and sialylation (SI) (as per Equations 1-5, Figure 31) relative to reported control culture glycoforms. Experimental differences reported include: Supplementation cocktails and concentrations with multiple bullet-points representing separate flask or bioreactor conditions; The cell line utilized and the lineage of that cell line where reported; The protein being expressed and whether it is a mutant variant or fusion; The bioprocess scale, time of supplementation, and time of harvest; The amount of glutamine (Gln) utilized in the growth medium.**

Supplement	Cell	Protein	Fermentation Timeline	Gln (mM)	Control Glycoform					Affected Glycoform					Effect	Researchers
					MI (%)	AI (%)	FI (%)	GI (%)	SI (%)	MI (%)	AI (%)	FI (%)	GI (%)	SI (%)		
<ul style="list-style-type: none"> <li>20mM ManNAc<sup>23</sup></li> </ul>	CHO (DG44)	IgG	<ul style="list-style-type: none"> <li>1L -Bioreactor, fedbatch</li> <li>Addition 48h</li> <li>Harvest 336h</li> </ul>	8	5.6	38	93.4	13.8	0.5	5.2	38	94.1	11.9	0.6	<ul style="list-style-type: none"> <li>Speculation that increases in CMP-NeuAc lead to feedback inhibition of UDP-GlcNAc 2-epimerase producing UDP-GlcNAc accumulation and subsequently decrease in galactosylation.</li> </ul>	(Kildegaard et al., 2015)
<ul style="list-style-type: none"> <li>20mM ManNAc</li> </ul>	NS0 (GS)	IgG	<ul style="list-style-type: none"> <li>500mL Flasks</li> <li>Addition 48h</li> <li>Harvest 96h</li> </ul>	0.4 (GS)	12.8	34.9	100	16	0	11.2	35.5	100	14.5	0	<ul style="list-style-type: none"> <li>44x CMP-NeuAc</li> <li>No improvement to sialylation</li> </ul>	(Hills et al., 2001)
<ul style="list-style-type: none"> <li>20mM ManNAc</li> </ul>	CHO (GS) NS0 (GS)	TIMP-1	<ul style="list-style-type: none"> <li>Flasks</li> <li>1000mL</li> <li>Addition 24h</li> <li>Harvest 48h</li> </ul>	0.4 (GS)	-	50.2	-	-	47.8	-	49.8	-	-	48.7	<ul style="list-style-type: none"> <li>-22% Neu5Gc content in NS0 cultures</li> <li>+1% shifts in %-sialylation</li> <li>12x increase in CMP-SA (CHO)</li> <li>30x increase in CMP-SA (NS0)</li> </ul>	(Baker et al., 2001)
<ul style="list-style-type: none"> <li>20-80mM ManNAc</li> </ul>	CHO S	FII	<ul style="list-style-type: none"> <li>Flasks</li> <li>Addition 48h</li> <li>Harvest 144h</li> </ul>	-	-	-	-	75	17	-	-	-	-	19 20 20	<ul style="list-style-type: none"> <li>+20% sialylation from ManNAc addition</li> <li>Temperature-shift resulted in similar sialylation improvement for final process</li> </ul>	(Lee et al., 2017)

<sup>23</sup> Supplementations of mannose, NeuAc, and cytidine were also attempted, but did not vary significantly from control cultures

Supplement	Cell	Protein	Fermentation Timeline	Gln (mM)	Control Glycoform					Affected Glycoform					Effect	Researchers
					MI (%)	AI (%)	FI (%)	GI (%)	SI (%)	MI (%)	AI (%)	FI (%)	GI (%)	SI (%)		
<ul style="list-style-type: none"> <li>▪ 0.2, 2, 20, 40mM ManNAc</li> </ul>	CHO (Dukx)	IFN- $\gamma$	<ul style="list-style-type: none"> <li>▪ 100mL Flasks</li> <li>▪ Addition 0h</li> <li>▪ Harvest 96h</li> </ul>	-				-	-				-	-	<ul style="list-style-type: none"> <li>▪ 27x increase CMP-SA</li> <li>▪ +15% complete sialylation</li> <li>▪ 60% &amp; 100% of sialylation from radiolabelled supplemented ManNAc fed at 2mM &amp; 20mM respectively</li> <li>▪ No effect to cell growth or productivity</li> </ul>	(Gu and Wang, 1998)
<ul style="list-style-type: none"> <li>▪ 0.5mM Cyt</li> </ul>	RH	N/A	<ul style="list-style-type: none"> <li>▪ 3mL Culture dish</li> <li>▪ Addition 16h</li> <li>▪ Harvest 24h</li> </ul>	2.4				-	-				-	-	<ul style="list-style-type: none"> <li>▪ 3.0x CTP</li> <li>▪ 3.2x UDP-HexNAc</li> <li>▪ 2.6x UDP-hexose</li> </ul>	(Pels Rijcken et al., 1995b)
<ul style="list-style-type: none"> <li>▪ 20mM ManNAc + 10mM Cyt</li> </ul>	CHO (GS)	Fc-TNF fusion	<ul style="list-style-type: none"> <li>▪ 2L Fed-batch bioreactor</li> <li>▪ Addition 120h</li> <li>▪ Harvest 288h</li> </ul>	GS	3.9	38	66	46	28	-	-	-	-	28	<ul style="list-style-type: none"> <li>▪ Statistically insignificant sialic-acid content increase (terminal galactose determined to be limiting)</li> </ul>	(Liu et al., 2015)
<ul style="list-style-type: none"> <li>▪ 20mM ManNAc</li> <li>▪ + 0.5mM Cyt</li> </ul>	CHO SCLC	NCAM	<ul style="list-style-type: none"> <li>▪ 6 &amp; 24-well plates</li> <li>▪ Addition 12-18h</li> <li>▪ Harvest 128h</li> </ul>	6				-	-				-	-	<ul style="list-style-type: none"> <li>▪ +10-20% polysialylation in CHO</li> <li>▪ -20-30% NCAM production</li> </ul>	(Zanghi et al., 1998)
<ul style="list-style-type: none"> <li>▪ 20mM ManNAc</li> <li>▪ +10mM cytidine</li> </ul>	CHO (Dukx)	IFN- $\gamma$	<ul style="list-style-type: none"> <li>▪ Flasks (n=1)</li> <li>▪ 1000mL</li> <li>▪ Addition 48h</li> <li>▪ Harvest 96h</li> </ul>	4	26	34	-	91	29	14	38	-	95	62	<ul style="list-style-type: none"> <li>▪ 30-120x increase in CMP-SA</li> <li>▪ +32-36% sialylation -/+ Cyt</li> <li>▪ +26-52% higher specific productivity</li> </ul>	(N. S. C. Wong et al., 2010)